

Dissertation zur Erlangung des Doktorgrades  
der Fakultät für Chemie und Pharmazie  
der Ludwig-Maximilians-Universität München

**Towards the Total Synthesis of Portentol**  
**A Formal Synthesis of Dimethylglutamine**  
**The Crystal Structure of the Dess-Martin**  
**Periodinane**

Albert Schröckeneder

aus Salzburg, Österreich

2012



## **Erklärung**

Diese Dissertation wurde im Sinne von §7 der Promotionsordnung vom 28. November 2011 von Herrn Prof. Dr. Dirk Trauner betreut

## **Eidesstaatliche Versicherung**

Diese Dissertation wurde eigenständig und ohne unerlaubte Hilfe erarbeitet.

München, den 3. Dezember 2012

Albert Schröckeneder

Dissertation eingereicht am

06. Dezember 2012

1. Gutachter:

Prof. Dr. Dirk Trauner

2. Gutachter:

Prof. Dr. Manfred Heuschmann

Mündliche Prüfung am

17. Januar 2013

## ACKNOWLEDGEMENTS

First, I would like to thank my advisor and mentor, Professor Dr. Dirk Trauner for the opportunity to learn and develop both as a chemist and as a person in his group. His ability to unfold complex molecules and chemical riddles as well as his inimitable enthusiasm were a constant source for motivation that was crucial for the results presented in this work.

Weiters bin ich meinen Eltern und meiner Familie unendlich dankbar, dass sie mich zu dem Menschen gemacht haben, der ich heute bin, dass sie mich immer unterstützt haben und mir die Freiheit und alle Möglichkeiten eröffneten, meine Ziele selbst zu definieren und zu erreichen.

Gleichsam danke ich meiner Verlobten Carmen, dass wir uns so sehr lieben, dass sie mir den Rücken immer frei hält und jeden Weg mit mir zusammen geht. In meiner Heimat spricht man von der „besseren Hälfte“. Ich darf wissen, wieso.

I would like to thank all my colleagues in the “UV-lab:” Katie Abole, Irina Albrecht, Pascal Ellerbrock, Christian Kuttruff, Florian Löbermann, Eddie Myers and Alwin Reiter for every inspiring discussion and piece of advice they gave me. It was fun and motivating working with them, and I thank them for their tolerance of my musical taste and singing. I also thank Dr. Ingrid Chen, Dr. Laura Salonen, Daniel Hog, and Florian Löbermann for proofreading this thesis, as well as Anastasia Hager, Dominik Hager and Pascal Ellerbrock for their very helpful input and suggestions throughout the creation of this thesis. Along with these people, my thankfulness goes to all past and present members of the Trauner group for their advice, help, discussions and good spirits. I am particularly grateful to have developed strong friendships with many of these people.

Furthermore, I am very thankful to my undergraduate students who joined me during my PhD, shared my enthusiasm and contributed to the projects: Anja Walkam, Julia Redeker,

Kolio Raltchev, David Konrad and Matthias Zwiener, as well as undergraduate students Adriana Grossmann and Oliver Richter, who contributed to the VQDA project.

In this context, I also wish to thank Florian Löbermann for the great collaboration in the VQDA project and his motivational tools when NMR experiments prolonged late into the night, as well as Desiree Stichnoth for the collaboration on the DMP project.

When things work really well, there are always a lot of helping hands involved. I wish to thank these helping hands in the group: Petra Böhler, Carry Lewis, Heike Traub, Tobias Kauer and Martin Sumser as well as LMU staff Heidi Buchholz (Chem store), Claudia Dubler (NMR department), Sonja Kosak (mass spectroscopy), Michael Geyer (Ver- & Entsorgung), Klaus Hartmann (Supply), Dr. Peter Mayer (X-ray crystallography/ his efficient help when I handed him the DMP crystals), Dr. Werner Spahl (mass spectroscopy) and Dr. David Stevenson (NMR department) and all other helping hands.

There are many things that are often missed in the rush of our every day lives but even if unseen, many thanks also for those things and to those people who have not been mentioned in this acknowledgement.



## ABBREVIATIONS

°C	degrees Celsius
Ac	acetate
aq	aqueous
atm	atmosphere
b.o.r.s.m.	based on recovered starting material
BAIB	bisacetoxyiodobenzene
Bn	benzyl
ca.	circa
calc.	calculated
CAM	ceric ammonium molybdate
CAN	ceric ammonium nitrate
cy	cyclohexane
DA	Diels-Alder
dba	dibenzylidenacetone
DCM	dichloromethane
DDQ	2,3-Dichloro-5,6-dicyano-1,4-benzoquinone
decomp.	decomposition
DHP	dihydropyran
DIPA	diisopropylamine
DIPEA	N,N-diisopropylethylamine
DMAP	dimethylaminopyridin
DMF	dimethylformamide
DMP	Dess-Martin periodinane
DMS	dimethylsulfide
eq	equivalent(s)
Et	ethyl
Et <sub>2</sub> O	diethylether
EtOAc	ethylacetate
EtOH	ethanol
FTIR	Fourier-transform-infrared spektrometer
g	gram
GC	gas chromatography
GPa	giga pascal
h	hour(s)
HMDS	hexamethyldisilazane
HOMO	highest occupied molecular orbital
HPLC	high pressure liquid chromatography
HWE	Horner-Wadsworth-Emmons
Hz	Hertz
hν	light
i-PrOH	isopropanol
im	imidazol
Ipc	isopinocampoyl
l	large

LA	Lewis acid
LUMO	lowest unoccupied molecular orbital
m	medium
M	molarity/ molar
Me	methyl
MeCN	acetonitrile
MeOH	methanol
min	minute(s)
mL	mililitre
MS	mass spectroscopy
n-BuLi	n-butyllitium
NADH	nicotinamide adenine dinucleotide
NMR	nuclear magnetic resonance
OTf	triflate
PCC	pyridinium chlorochromate
Ph	phenyl
PhH	benzene
PKS	polyketide synthase
PMB	para-methoxybenzyl
PMBTCA	para-methoxybenzyltrichloroacetamide
PMP	para-methoxyphenyl
ppm	parts per million
PPTS	pyridinium para-toluenesulfonate
py	pyridin
rt	room temperature
rxn	reaction
s	small
sat.	saturated
T	temperature
t	time
TBS	tert-butyldimethylsilyl
TBSCl	tert-butyldimethylsilylchloride
TBSOTf	tert-butyldimethylsilyltriflate
TEA	triethylamine
TESOTf	triethylsilyltriflate
THF	tetrahydrofuran
TLC	thin layer chromatography
TMSOTf	trimethylsilyltriflate
TS	transition state
TsOH	para-toluenesulfonic acid
VQDA	vinyl-quinone-Diels-Alder
µg	microgram
COSY	correlated spectroscopy
HMBC	heteronuclear multiple bond correlation

HSQC heteronuclear single quantum coherence spectroscopy  
NOESY nuclear overhauser enhancement spectroscopy

NMR:

s singlet  
d doublet  
t triplet  
q quartet  
m multiplet  
ppm parts per million

IR:

b broad  
w weak  
m medium  
s strong

# TABLE OF CONTENTS

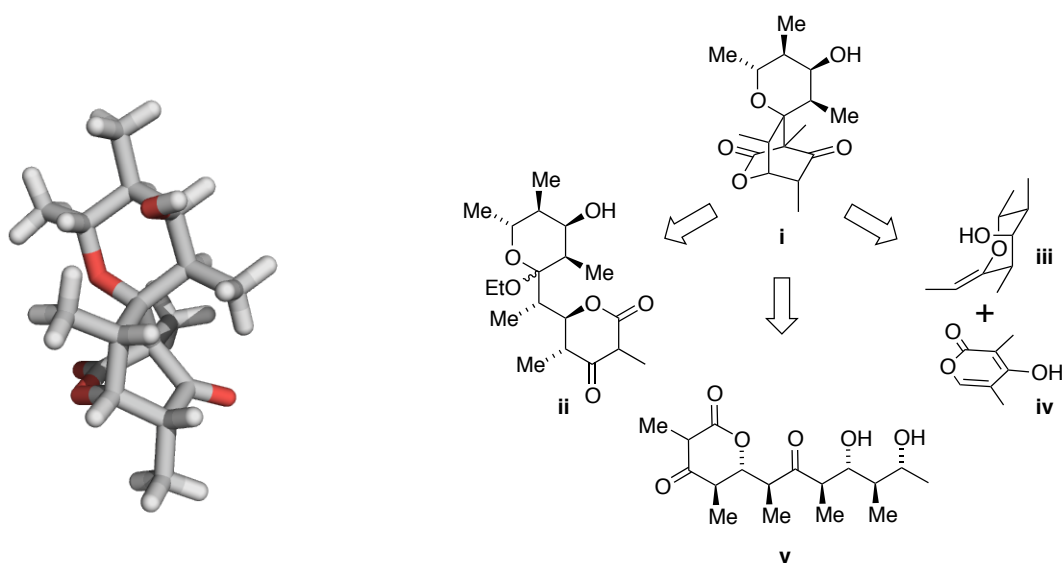
<b>Summary</b>	<b>1</b>
<b>Chapter I: Towards the Total Synthesis of Portentol</b>	<b>5</b>
<b>1 Project Aims</b>	<b>7</b>
<b>2 Introduction</b>	<b>9</b>
2.1 Isolation and Characterisation of Portentol	9
2.2 Strategic Development	12
2.2.1 The Shimalactones	12
2.2.2 Biosynthetic Hypothesis to Portentol	14
2.3 Portentol as a Synthetic Target	17
<b>3 Results and Discussion</b>	<b>19</b>
3.1 The Double-Dieckmann Approach	19
3.1.1 Retrosynthetic Analysis	19
3.1.2 Synthetic Progress	21
3.1.3 Retrosynthetic Revision and Synthetic Progress	26
3.1.4 Conclusion and Strategic Considerations	32
3.2 The Diels-Alder Approach	33
3.2.1 Retrosynthetic Analysis	33
3.2.2 Synthesis of the Southern Fragment	34
3.2.3 Diels-Alder Screenings	36
3.2.4 Synthetic Progress on the Northern Fragment	47
3.2.5 Conclusion and Strategic Considerations	50
3.3 The Chain Approach	50
3.3.1 Retrosynthetic Analysis	50
3.3.2 Synthetic Progress	52
3.3.3 Revised Retrosynthetic Analysis	59
3.3.4 Synthetic Progress	60
3.3.5 Conclusion and Strategic Considerations	65
<b>4 Summary and Outlook</b>	<b>66</b>
<b>Chapter II: Thiocarbonyl Ylid Based 1,3-Dipoles</b>	<b>71</b>
<b>1 Project Aims</b>	<b>73</b>
<b>2 Introduction</b>	<b>75</b>
2.1 [3+2] Cycloadditions: Background and Significance	75
2.2 Thiocarbonyl Ylides: Formation and Reactivity	76
2.3 Dimethylglutamine: Background and Synthetic Approaches	79
<b>3 Results and Discussion</b>	<b>83</b>

3.1	Thiocarbonyl Ylids from Horner-Wadsworth-Emmons-Type Reactions	83
3.2	Revisiting Sakurai's Reagent	89
3.3	Formal Synthesis of Dimethyl-L-glutamine	94
<b>4</b>	<b>Summary and Outlook</b>	<b>101</b>
<b>Chapter III: Vinyl-Quinone-Diels-Alder Reactions</b>		<b>103</b>
<b>1</b>	<b>Project Aims</b>	<b>105</b>
<b>2</b>	<b>Introduction</b>	<b>107</b>
<b>3</b>	<b>Results and Discussion</b>	<b>113</b>
3.1	Strategical Considerations	113
3.2	Scope of VQDA Reactions: Synthetic Progress	113
3.3	Alternative Precursors and Oxidation Methods	124
3.4	Catalysis attempts	129
<b>4</b>	<b>Conclusion</b>	<b>135</b>
<b>Chapter IV: The Crystal Structure of the Dess-Martin Periodinane</b>		<b>137</b>
<b>1</b>	<b>Project Aims</b>	<b>139</b>
<b>2</b>	<b>Background and Significance</b>	<b>140</b>
<b>3</b>	<b>The Crystal Structure of the Dess-Martin Periodinane (Manuscript)</b>	<b>142</b>
3.1	Introduction	142
3.2	Results and Discussion	143
3.3	Unpublished Results and Discussion	148
<b>4</b>	<b>Conclusion</b>	<b>149</b>
<b>Experimental Procedures and Analytical Data</b>		<b>151</b>
<b>General Experimental Section</b>		<b>151</b>
General Experimental Details		152
Instrumentation		152
<b>Experimental Data</b>		<b>154</b>
Portentol		154
Thiocarbonyl Ylid Based 1,3-Dipoles		178
VQDA		193
DMP		197
<b>X-ray Crystallographic Data</b>		<b>199</b>
<b>References</b>		<b>226</b>
<b>Appendix</b>		<b>231</b>

## SUMMARY

### Chapter I: Towards the Total Synthesis of Portentol

The first chapter of this dissertation describes synthetic studies towards a total synthesis of the naturally occurring polyketide portentol (**i**), which is a structurally unique and highly complex molecule with unprecedented structural features.<sup>[1]</sup>



**Scheme I:** X-ray crystal structure of portentol (**i**) and three retrosynthetic disconnections representing investigated routes

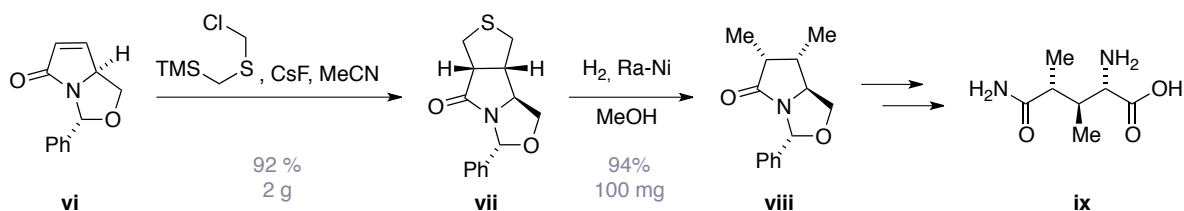
On three major retrosynthetic routes, interesting intermediates and detailed investigations on state of the art, highly stereoselective C-C bond formation reactions were carried out and discussed. The first route, represented in Scheme I by intermediate **ii** focussed on two DIECKMANN cyclisations as key reactions.<sup>[2]</sup> The second retrosynthetic disconnection interpreted portentol (**i**) as a DIELS-ALDER cycloadduct<sup>[3-6]</sup> (represented by intermediates **iii** and **iv** in Scheme I) while a third retrosynthetic plan, represented by intermediate **v**, was based on asymmetric EVANS-METTERNICH<sup>[7]</sup> aldol chemistry or a recently described crostannylation protocol introduced by the ROUSH group.<sup>[8]</sup>

Though a total synthesis of portentol (**i**) was not accomplished, key intermediates were successfully prepared and fully characterised. In addition, thorough research on the reactivity

and intrinsic stereochemical bias delivered crucial insights for future synthetic work on highly challenging, double mismatched aldol chemistry.

## Chapter II: Thiocarbonyl Ylid Based 1,3- Dipoles

The second chapter of this thesis discusses synthetic efforts regarding thiocarbonyl ylid based 1,3-dipoles, which, in contrast to other dipolar species, appear underrepresented in synthetic chemistry. Imbedded in thorough studies on existing thiocarbonyl ylid precursors and potent novel sources of such highly reactive species, a formal synthesis of non proteinogenic amino acid dimethyl-(L)-glutamine is presented,<sup>[9]</sup> underscoring the potential of thiocarbonyl ylide based 1,3- dipoles.

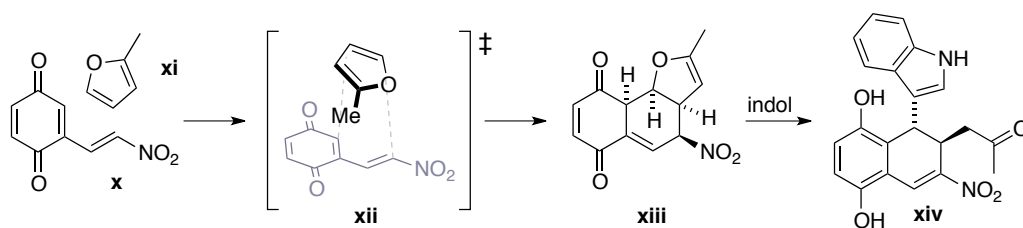


**Scheme II:** Key synthetic sequence to synthesise dimethylglutamine ix

Starting from literature known intermediate **vi**,<sup>[9]</sup> a two-step sequence was established, wherein a 1,3- dipolar cycloaddition furnished tricycle **vii** in excellent yield and stereoselectivity. Subsequently, a carefully optimised RANEY nickel reduction yielded literature known key intermediate **viii**.<sup>[9]</sup> This protocol not only represents a shorter and more efficient access to dimethyl-(L)-glutamine, but may also be seen as the synthetic equivalent of an addition of ethane over a double bond.

## Chapter III: Vinyl-Quinone-Diels-Alder Reactions

In the third chapter of this thesis, methodological studies towards vinyl-quinone-DIELS-ALDER (VQDA) reactions are presented. In the course of this coproduction with FLORIAN LÖBERMANN, the synthetic scope, asymmetric catalysis and subsequent reactivity of literature known VQDA reaction products between quinones such as compound **x** and dienophiles such as **xi**, were studied.

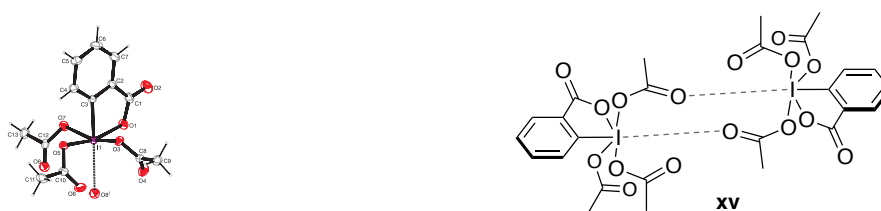


**Scheme III:** VQDA reaction to isoquinonemethide **xiii** and further reactivity

While notorious instability of most precursors and DIELS-ALDER adducts limited further studies on model systems, novel reactivity was observed when reacting isoquinonemethide **xiii** with indol, representing an unprecedented furan opening to give **xiv** upon nucleophilic attack of indol.

## Chapter IV: The Crystal Structure of the Dess-Martin Periodinane

The fourth chapter of this dissertation reports all efforts regarding the first X-ray crystal structure of the popular oxidising agent DESS-MARTIN periodinane (**xv**/ DMP).<sup>[10-12]</sup> In the course of a large scale synthesis of this well established reagent, it was found that despite thorough studies on structure and reactivity of DMP (**xv**), no X-ray crystal structure of this iodine-(V) species has ever been reported. Consequently, efforts were made to establish the first crystal structure, nearly 30 years after this reagent had been introduced to the chemical community.



**Scheme IV:** The crystal structure of DMP (**xv**)

Suitable crystals for X-ray diffraction analysis were obtained from a saturated solution in diethyl ether and acetic anhydride. The first crystal structure of DMP (**xv**) largely confirmed DFT-calculations, that have been reported in literature<sup>[13]</sup> and provides further insight into physical and chemical behaviour of this potent reagent.



**Chapter I:**  
**Towards the Total Synthesis of Portentol**



# 1 PROJECT AIMS

The biosynthetic assembly of complex molecules in nature is an inspiration to synthetic chemists, notably due to the ability of generating multiple stereogenic centres in single transformations. Clearly, it is an important task to not only study and understand the biosynthetic chemical reactivity, but to ultimately exploit this knowledge in the synthesis of complex molecules in a laboratory. In this context, biomimetic synthesis attempts to reproduce such biosynthetic pathways by utilizing elegant synthetic methodology to generating substantial molecular complexity in the absence of the enzymatic machinery found in nature.<sup>[14,15]</sup> The preparation of proposed or actual biosynthetic building blocks and the application of efficient reaction cascades as powerful key steps may form the target natural products. This not only increases our understanding of biosynthetic pathways but also opens up exciting avenues for the development of synthetic methodology, providing access to a vast number of natural products and their analogues. In this context the polyketide portentol (**1**, Figure 1), a structurally unique and remarkable molecule, was chosen to investigate acid-catalysed, biomimetic cyclisation cascades. It is highly and densely functionalised, featuring four ring systems and nine adjacent stereogenic centres, one of which is quaternary. This molecule is thus a fascinating and challenging target for modern organic synthesis.

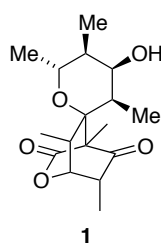


**Figure 1.** Molecular structure of portentol (**1**)

Isolated in the late 1960s, no total synthesis of this small but complex molecule has been achieved to date. The aim of this project was the total synthesis of this exceptional target using highly stereoselective C–C bond formation strategies, which push the scope of state of the art organic synthesis. Following biomimetic or bio inspired strategies, this highly complex molecule is meant to be built up by means of an acid-catalysed cyclisation.



## 2 INTRODUCTION

### 2.1 Isolation and Characterisation of Portentol

The naturally occurring polyketide portentol (**1**) was first reported in 1967 and has been isolated from lichens *Roccella luteola*,<sup>[16]</sup> *Roccolla portentosa*,<sup>[1]</sup> lending its name to portentol (**1**), *Roccella fuciformis*<sup>[17]</sup> and *Dirina repanda*<sup>[18]</sup>. Further reisolations of this natural product were reported from *Dirina stenhammari* in 1982,<sup>[19]</sup> *Lobodirina cerebriformes* during a screening of Chilean lichens for bioactive compounds by GARBARINO and co-workers in 1983<sup>[20]</sup> as well as in 2004 from Brazilian nut tree *Gustavia hexapetala*.<sup>[21]</sup> Alongside the last isolation reported, portentol (**1**) was tested for biological activity, revealing moderate growth inhibition against the cancer cell lines: DU-145 ( $GI_{50} = 1.3 \mu\text{g/mL}$ ), SF-268 ( $4.7 \mu\text{g/mL}$ ), NCI-H460 ( $4.7 \mu\text{g/mL}$ ) and BXP-3 ( $7.0 \mu\text{g/mL}$ ).<sup>[21]</sup>

The structure elucidation of portentol (**1**) commenced with a proposal by ABERHART and OVERTON in 1969,<sup>[1]</sup> wherein the accurate connectivity to the empirical formula  $C_{17}H_{26}O_5$  was established. However, ambiguity about the stereogenic centre at C4 (Figure 2) remained. Further studies on portentol (**1**) and its acetate derivative “portentol acetate” (**2**), which has been co-isolated with portentol (**1**) from some of the species mentioned above, were carried out. In 1970, the correct relative stereochemistry of portentol (**1**) was annotated on the basis of  $^1\text{H}$  NMR data along with IR band characteristics, mass spectrometry fragmentation and derivatisation experiments.<sup>[22]</sup> Shortly thereafter, both relative and absolute stereochemistry were confirmed unambiguously by X-ray crystal structures of samples of the natural product (Figure 2 and Figure 3) and a bromobenzoate derivative.<sup>[23]</sup>

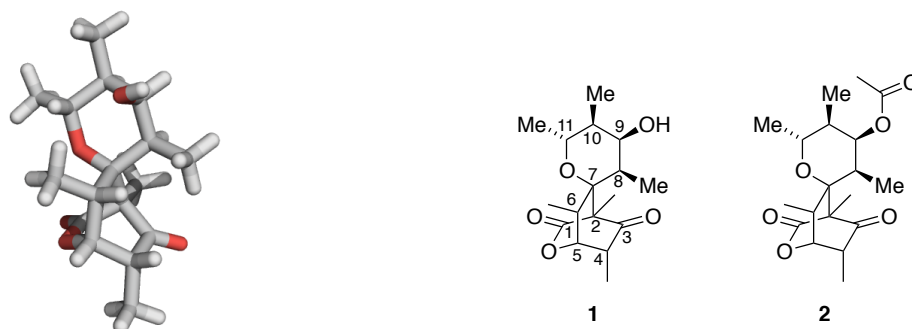


**Figure 2.** X-ray crystal structure of portentol (**1**) (colour code: grey: carbon, red: oxygen, white: hydrogen), portentol (**1**) with numbering scheme of the carbon backbone and naturally occurring portentol acetate (**2**)

The unique structural features of portentol (**1**) might originate from an unprecedented *anti* relationship of all stereogenic centres in the carbon backbone. This rich substitution pattern with six methyl- and one hydroxyl substituent creates a large steric demand. If portentol (**1**) is formed upon cyclisation of a linear precursor, which will be discussed in more detail in section 2.2.2 (*vide supra*), the particular stereochemistry may prearrange the backbone to cyclise in such manner to obtain the portentol scaffold. The complex polycyclic structure may be divided into a “northern” pyrane fragment, which is fused to a “southern” oxabicyclo[2.2.2]octane moiety in a spiro fashion.

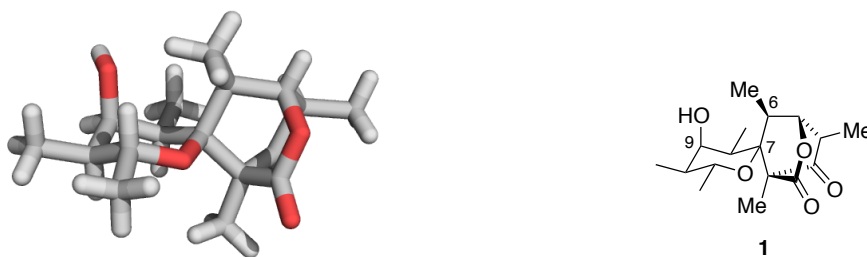


**Figure 3.** Rotated X-ray structure of portentol (**1**) (colour code: grey: carbon, red: oxygen, white: hydrogen)

As can be seen in Figure 3, the pyrane moiety is in an almost perfect chair conformation with all methyl substituents in equatorial position. In contrast, the hydroxyl group at C9 is found in axial position on the 6-membered ring, keeping the “all-*anti*” motive of portentol (**1**). The carbon–carbon bond, connecting spiro-centre C6 and C7 deviates from a perfectly axial position, due to the steric demand of the C7 methyl group on the bridgehead of

the [2.2.2] tricycle. Due to the steric demand of the substituents in northern pyrane cycle, the 6-membered ring is fixed in this conformation, as severe transannular repulsion of three methyl groups would be generated in a flipped chair conformation.

Based on thorough literature search, the “southern” oxabicyclo[2.2.2]octane with its substitution pattern is uniquely found in portentol (**1**) and its corresponding acetate **2** in the vastness of polyketide natural products. However, some polyketides feature a structurally related oxabicyclo[2.2.1] moiety and may stem from a similar biosynthetic formation as portentol (**1**). Representative examples of such oxabicyclo[2.2.1]heptane moieties are the highly bioactive coccidiostatin (**10**),<sup>[24]</sup> or the fungal polyketide natural products prugosenes A1 (**3**), A2 (**4**) and A3 (**5**).<sup>[25]</sup> A screening for NADH-fumarate reductase inhibitors lead to isolation of ukulactones A (**6**) and B (**7**),<sup>[26]</sup> which are closely related to the prugosene family, but feature an additional methyl group in the pentaene moiety. Two further representatives of polyketide natural products with a [2.2.1] tricyclic unit are shimalactones A (**8**) and B (**9**)<sup>[27,28]</sup> (Figure 4). These latter two natural products were successfully prepared in a bio inspired synthetic approach by TRAUNER and co-workers in 2008<sup>[29]</sup> and thus, inspired the strategic outline of the project described herein.

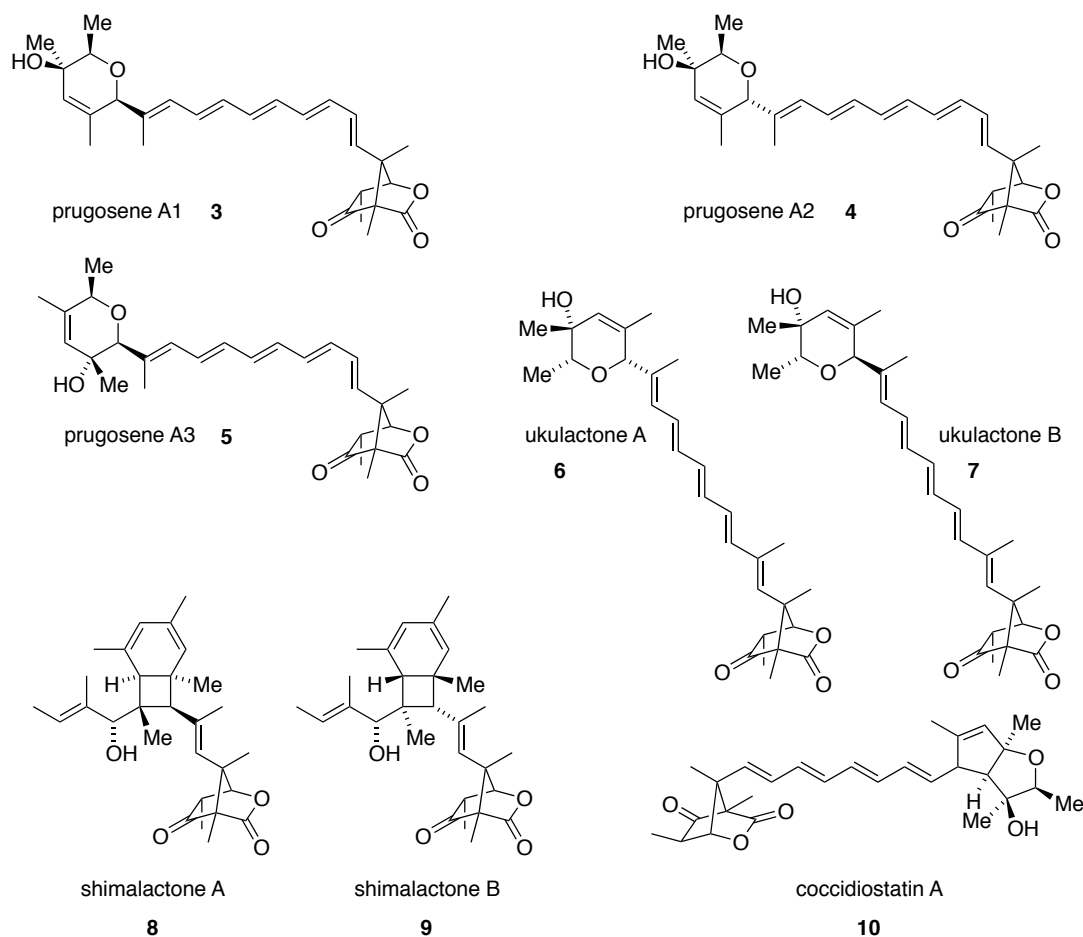
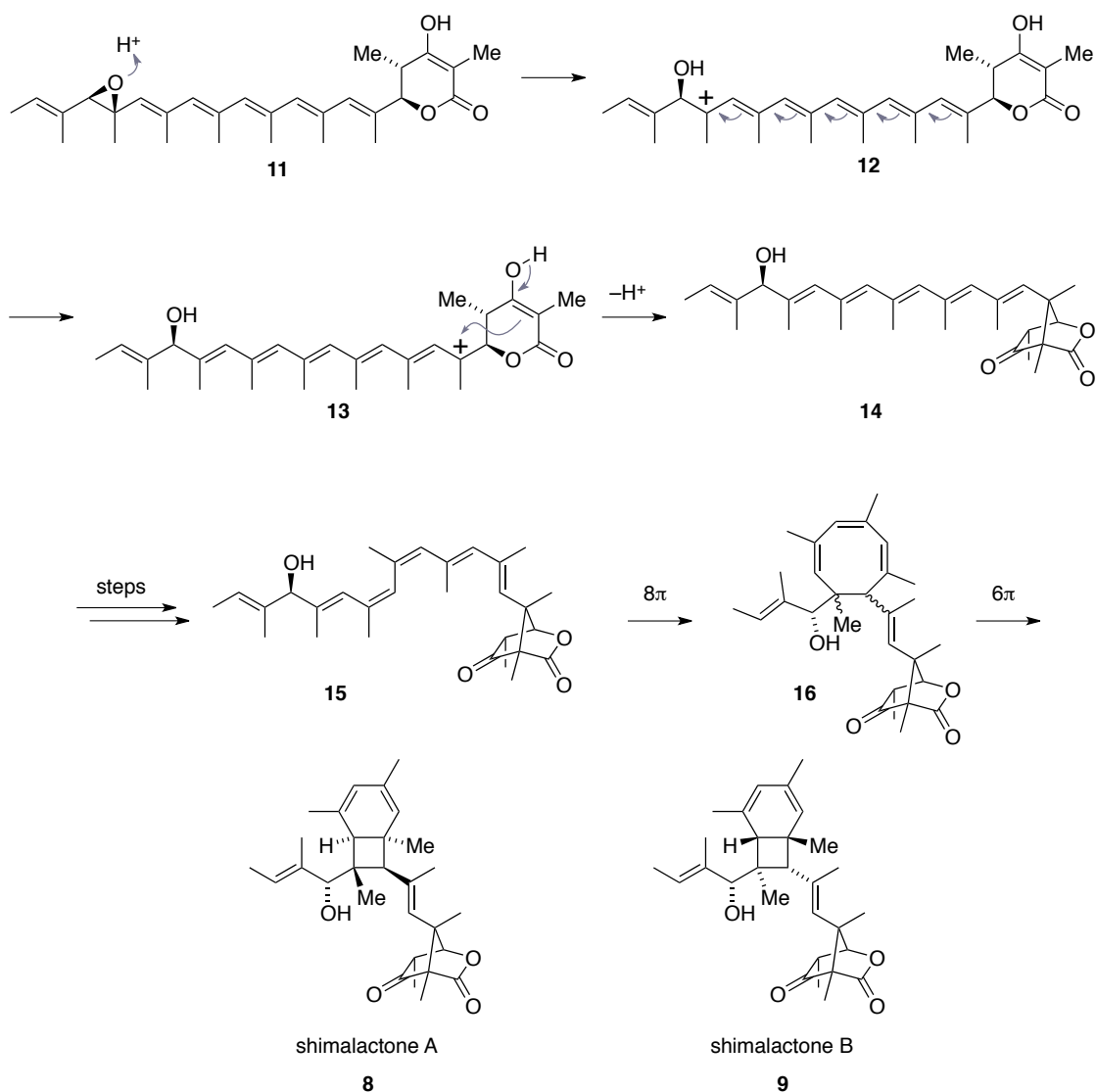


**Figure 4.** Selected polyketide natural products with an oxabicyclo[2.2.1]heptane moiety

## 2.2 Strategic Development

### 2.2.1 The Shimalactones

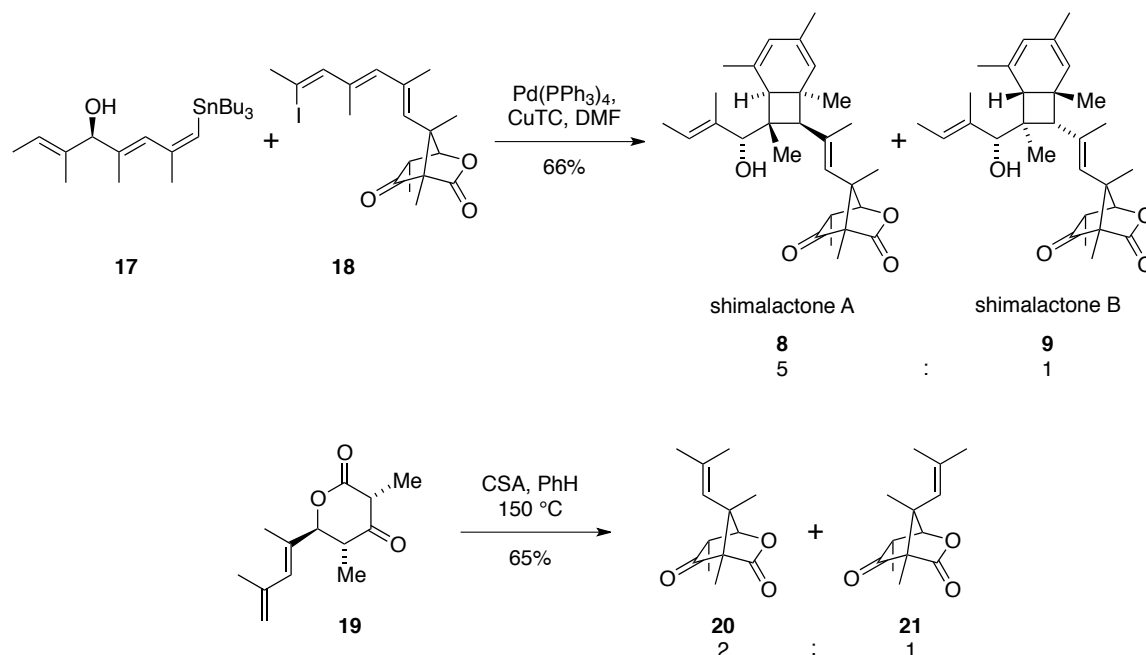
Acid-catalysed cascades play a key role in the formation of complex polyketide natural products. To investigate the hypothesis that acidic catalysis leads to the formation of the [2.2.1] oxabicyclo, the shimalactones (**8** and **9**) were explored as synthetic target in the TRAUNER research group.<sup>[29]</sup> It was hypothesised that this tricyclic is biosynthetically formed upon an acid-catalysed epoxide opening, as depicted in Scheme 1.



**Scheme 1.** Proposed biosynthetic formation of the shimalactones<sup>[29]</sup>

In this sequence, epoxide **11** opens upon protic catalysis to generate cation **12**, which is converted into isomeric cation **13** as the positive charge “travels” along the pentaene fragment. Notably, cations **12** and **13** are not resonance structures, as the numerous methyl groups prevent the  $\pi$ -system from being planar due to A 1,3-strain.<sup>[29,30]</sup> Thus, no delocalisation of the charge is evident. Reaching the end of the polyene chain, the cation can now be intercepted by the enol double-bond of the lactone moiety, forming the [2.2.1] tricyclic in **14**. Further double bond isomerisation leads to intermediate **15**. Subsequent  $8\pi$ - $6\pi$  electrocyclisation then provides the shimalactones. Herein, the  $8\pi$  electrocyclisation may delivers two diastereoisomers on the two newly formed stereogenic centres of the 8 membered ring in intermediate **16**. As a consequence, the final  $6\pi$  electrocyclisation leads to two diastereoisomers: shimalactone A (**8**) and shimalactone B (**9**).

In the course of synthetic studies on the shimalactones in the TRAUNER research group, a biomimetic synthesis of the shimalactones was accomplished.<sup>[29]</sup> As depicted in Scheme 2, both natural products were obtained after instantaneous  $8\pi$ – $6\pi$  electrocyclicisation when coupling stannane **17** and iodide **18**. The latter was derived from precursor **19**, which was successfully transferred into tricycles **20** and **21**, upon biomimetic, acid-catalysed cyclisation with camphorsulphonic acid (CSA).



**Scheme 2.** Acid catalysed, biomimetic cyclisation in the total synthesis of the shimalactones

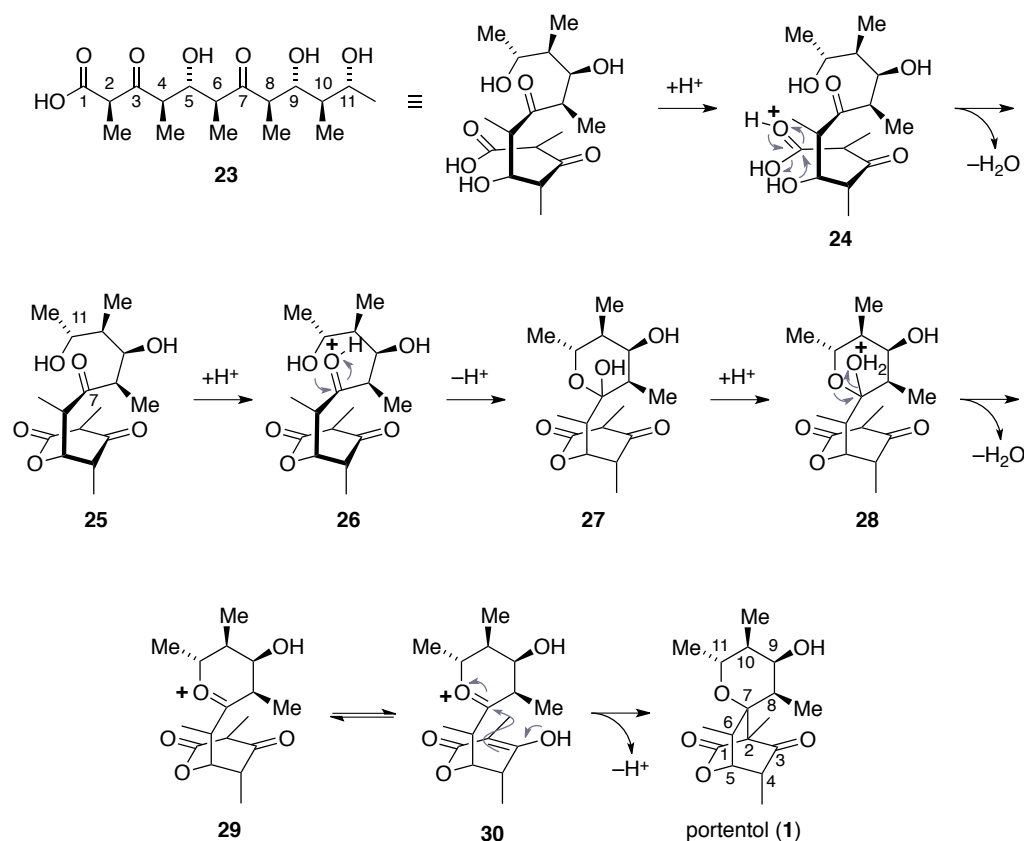
This elegant way to form complex tricycles **20** and **21** by setting two quaternary stereocentres in the course of one reaction incited further interest in acid catalysed biomimetic synthesis. Consequently, we embarked on the synthesis of the oxabicyclo[2.2.2]octane fragment of portentol (**1**).

## 2.2.2 Biosynthetic Hypothesis to Portentol

Polyketides are secondary metabolites produced by animals, plants, bacteria or, as in the case of portentol (**1**), fungi.<sup>[31]</sup> Depending on the polyketide-synthase (PKS) generating polyketides similar to the fatty acid synthesis *via* CLAISEN-condensation, these natural products may be classified as type I or type II. Type I polyketides mostly feature macrolide structures and are generated in one multifunctional enzyme complex. In contrast, type II



again to give cation **26**, activating the C-7 carbonyl moiety for a nucleophilic attack of C-11 hydroxy group. The corresponding hemiacetal **27** may then, under acidic conditions be protonated to form cation **28**, which eliminates water to form cyclic carboxonium ion **29**. Upon tautomerisation to corresponding intermediate **30**, the double-bond of the enol may now intercept the carboxonium ion to form the spiro centre at the C-7 position yielding portentol (**1**).

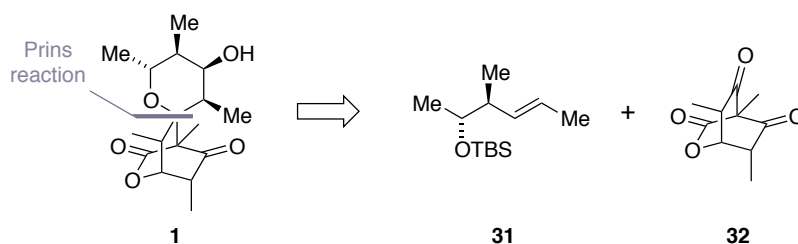


**Scheme 3.** Proposed biosynthetic formation of portentol (**1**) with numbering scheme

It is debateable if described lactonisation or formation of the pyrane moiety occurs first or possibly all at once. Either way, the above mentioned, bio inspired synthesis of the shimalactones convincingly supports the theory, that an acid-catalysed cyclisation forming the respective quaternary stereocentre concludes the biosynthetic formation of [2.2.1] and [2.2.2]oxabicyclo-moieties.

## 2.3 Portentol as a Synthetic Target

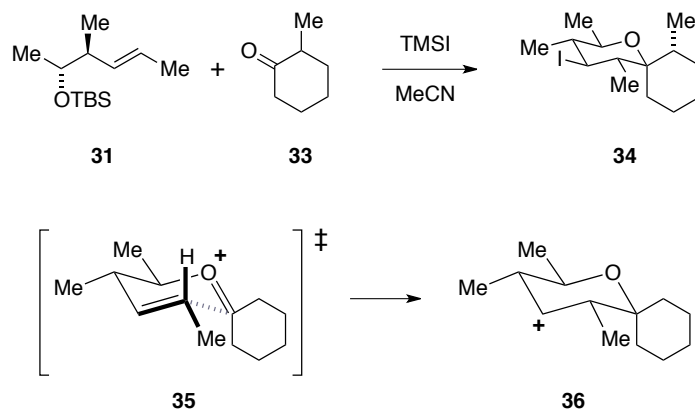
Despite its structural complexity, portentol (**1**) has only once been reported as target for synthetic chemists, in context of a methodological investigation conducted by VAN DE WEGHE and co-workers.<sup>[33]</sup> The conceptual background for this approach was based on a highly diastereoselective PRINS<sup>[34]</sup> reaction with cyclic ketones. The corresponding retrosynthetic disconnection of portentol (**1**) is depicted in Scheme 4.



**Scheme 4.** Retrosynthetic disconnection of portentol (**1**) by means of an asymmetric PRINS reaction

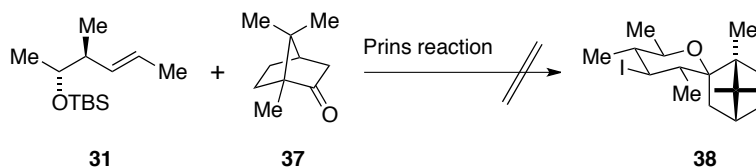
To build up the skeleton of portentol (**1**), an asymmetric PRINS reaction of intermediate **31** and symmetrical tricyclic ketone **32** was envisaged. While synthetic approaches to the tricyclic system were not discussed, VAN DE WEGHE and co-workers focused on the development of novel methodologies to conduct PRINS reactions on a variety of cyclic ketones.<sup>[33]</sup>

Extensive screenings of reaction partners, such as racemic ketone **33**, revealed that best yields and higher stereoselectivity were obtained, promoting this reaction with trimethylsilyl iodide (TMSI) in acetonitrile (Scheme 5). Upon these conditions, the *trans*-configuration of the double-bond in precursor **31** leads to the desired all equatorial configuration of the methyl substituents in the relevant pyran moiety of achieved intermediate **34**, following the logic depicted in transition state **35** (Scheme 5).



**Scheme 5.** Optimised PRINS reaction with cyclic ketone **33** and chair like transition state with stereochemical outcome

Thus obtained cation **36** may now be trapped by hydroxide or iodide. In all reported cases trapping with iodide resulted in higher yields, with the iodide substituent lining up in equatorial position. Bearing the stereochemistry of portentol (**1**) in mind, this is a useful handle to introduce the axial hydroxyl group in portentol at a later stage of a total synthesis. Although high diastereoselectivity regarding conversion with racemic ketones such as **33** could be reported, yields decreased significantly using sterically more demanding and rigid, bicyclic ketones. In fact, all attempts to obtain a PRINS reaction product with model ketone **37** (Scheme 6) failed.



**Scheme 6.** Unsuccessful attempt of PRINS reaction with sterically demanding ketone **37**

Considering the findings of VAN DE WEGHE's highly convergent synthetic approach and also acknowledging the chemical attractiveness of a highly symmetrical, yet synthetically challenging reaction partner **32** it appears unlikely that this approach may be used to obtain portentol (**1**).

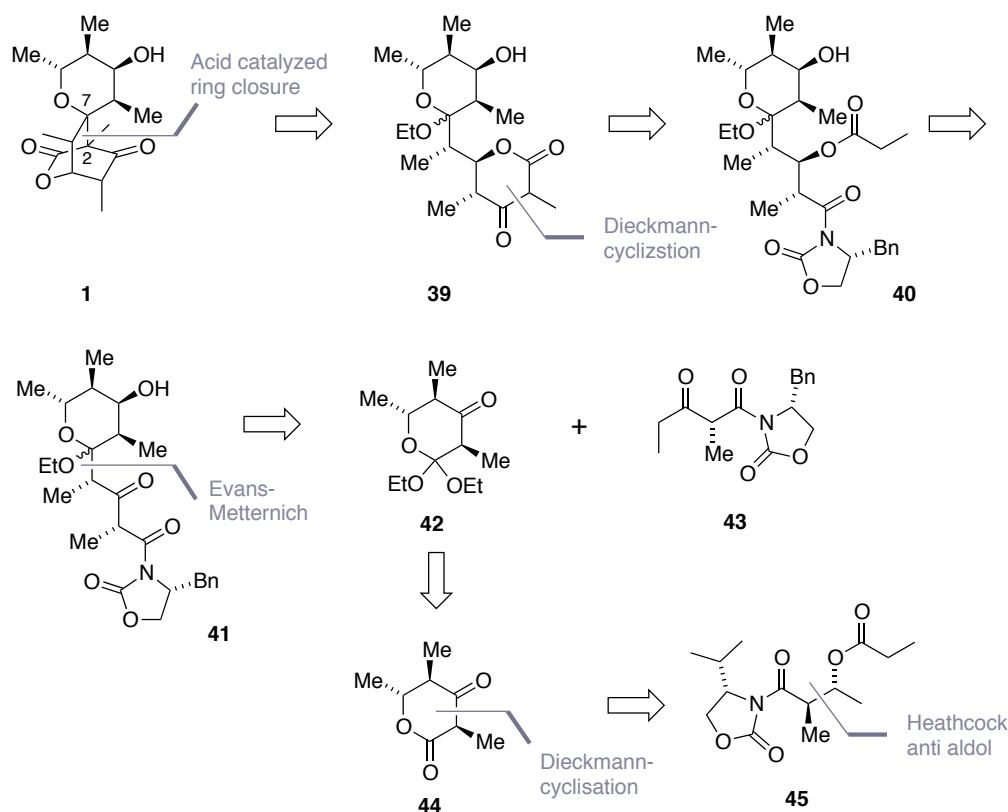
## 3 RESULTS AND DISCUSSION

We were intrigued by the idea that although structurally unique in nature, portentol (**1**) could be synthesised in such a biomimetic fashion using a final, acid-catalysed cascade reaction. This would trigger the formation of key stereogenic centres in a one pot reaction and the cascade would be terminated by formation of the C2–C7 bond. Overall, one quaternary and one tetrasubstituted carbon centre may be generated in a highly selective and elegant fashion. All synthetic strategies described in this section reflect this conceptual approach towards the total synthesis of portentol (**1**).

### 3.1 The Double-Dieckmann Approach

#### 3.1.1 Retrosynthetic Analysis

The first strategy towards the total synthesis of portentol (**1**), discussed in this work, took a convergent approach, wherein two components **42** and **43** would be combined by means of an EVANS-METTERNICH aldol reaction,<sup>[7]</sup> as outlined in the retrosynthetic analysis in Scheme 7. Retrosynthetically, the two key carbon–carbon bonds in this approach were envisioned to be formed *via* a DIECKMANN cyclisation,<sup>[2]</sup> rendering this the “double DIECKMANN approach”.



**Scheme 7.** Retrosynthetic analysis of portentol (**1**) according to the "Double-DIECKMANN approach"

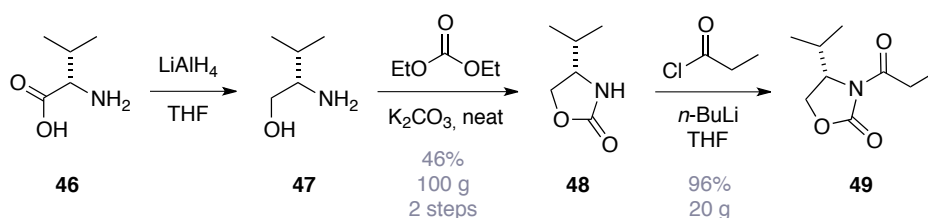
As depicted in Scheme 7, and in accordance with our biosynthetic hypothesis, a biomimetic approach was developed. The spiro centre of portentol (**1**) was envisaged to be formed by means of a BRØNSTED acid catalysed, and intramolecular reaction of intermediate **39**, which may be obtained *via* DIECKMANN cyclisation of compound **40**. The latter was to be assembled from acetal **42** and known building block **43** using METTERNICH's modification of EVANS aldol chemistry and following functional group modification.<sup>[7]</sup> It was shown that this highly diastereoselective aldol chemistry could not only be applied to aldehydes, but also could be effected using ortho esters.<sup>[35,36]</sup> The synthetic challenge of this reaction would not only introduce a highly convergent approach to a total synthesis of portentol (**1**) but also push the boundaries of this methodology.

Building block **42** was envisaged to be obtained from  $\beta$ -ketolactone **44**, which was to be generated by another DIECKMANN cyclisation from intermediate **45**. This protocol would not only facilitate two key carbon-carbon bond formations in the envisioned total synthesis of portentol (**1**), but also feature elegant and concomitant removal of the chiral oxazolidinone auxiliaries. Therefore, a highly complex molecule with immensely high functional group

density would be synthesised in a step economic and convergent manner, investigating the biosynthetic hypothesis and pushing the limits of modern organic chemistry.

### 3.1.2 Synthetic Progress

To elaborate  $\beta$ -ketolactone **44**, EVANS auxiliary **48** was synthesized following standard procedures.<sup>[37,38]</sup> Thus, (L)-valine (**46**) was reduced to (L)-valinol (**47**), and then converted to auxiliary **48** upon treatment with diethyl carbonate (Scheme 8). Subsequent acylation with propionic acid chloride yielded intermediate **49**,<sup>[39]</sup> which could be prepared on decigram scale starting from 100 g (L)-valine (**46**).



**Scheme 8.** Synthetic route towards first diastereoselective C–C bond formation

With large quantities of propionate **49** in hand, the focus was turned on the installation of the first two stereogenic centres, exploiting the diastereoselectivity of HEATHCOCK'S modification of EVANS- aldol chemistry.<sup>[40,41]</sup> In contrast to a standard EVANS- *syn*-aldol reaction<sup>[42]</sup> wherein the preferred ZIMMERMAN–TRAXLER transition state<sup>[43]</sup> governs the outcome of the aldol addition, a second equivalent of the LEWIS acid promotes the *anti*-product with high diastereoselectivity.

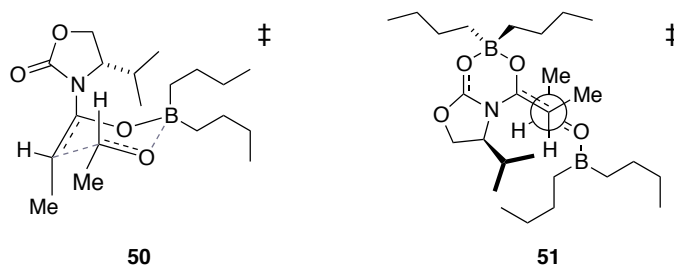
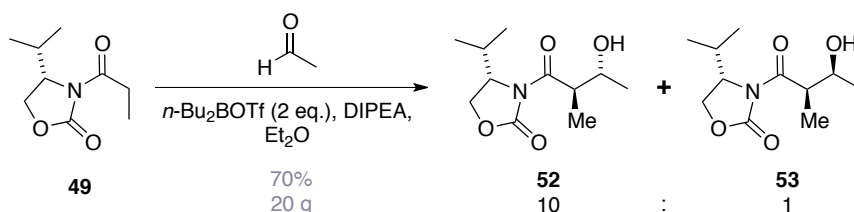


**Figure 6.** Transition states for EVANS *syn* and HEATHCOCK *anti* aldol additions

As illustrated in Figure 6, the stereochemical outcome in the *syn*-case (transition state **50**) is governed by three effects. Firstly, the preferred equatorial orientation of the aldehyde residue in the six- membered ring sets the stereocentre of the resulting hydroxyl group. Given

the absolute stereochemistry of the auxiliary, a *si*-face attack on the aldehyde is effected. Secondly, the *Z*-conformation of the boron-enolate, which is selectively obtained in EVANS-systems, sets the stereocentre of the methyl group in the given transition state. Finally, the bulky isopropyl group shields the opposed side of the enolate, allowing for the aldehyde to approach the complex from only one side. The orientation of the auxiliary is governed by electronic repulsion of the two carbonyl groups.

By contrast, an open transition state has been proposed for the *anti*- addition by HEATHCOCK and co-workers in 1991.<sup>[41]</sup> This open transition state **51** of the *anti*-selective addition overrides the repulsive dipolar interactions between the two imide-carbonyl groups by coordination of a LEWIS acid. The bulky residue of the auxiliary thus shields the opposite side of the *Z*-enolate in comparison to ZIMMERMAN–TRAXLER transition state **50**. Due to this fact, two “non-EVANS”- adducts, the desired *anti*- and the undesired *syn*- adduct may be obtained depending on the steric demand of the aldehyde and the LEWIS acid in question. In this context, an asymmetric aldol reaction with acetic aldehyde poses a significant synthetic challenge, as this substrate is not sterically demanding. The work of HEATHCOCK and co-workers clearly indicates that diastereoselectivity in favour of the non-EVANS-*anti* over the non-EVANS-*syn* product, increases with steric demand of the aldehyde.<sup>[41]</sup> However, selectivity may be increased, by using sterically demanding LEWIS acids such as dibutyl borontriflate.<sup>[41]</sup>



**Scheme 9.** Diastereoselective HEATHCOCK *anti*-aldol reaction

In agreement with literature, a diastereomeric non-EVANS-*anti* (**52**)/ non-EVANS-*syn* (**53**) ratio of 10:1 was obtained (Scheme 9). A reaction scales above 20 g is not recommended as insufficient mixing of the heterogeneous reaction mixture decreased diastereoselectivity to a 5:1 ratio. Initial diastereomeric ratios could be enhanced by repetitive recrystallization.

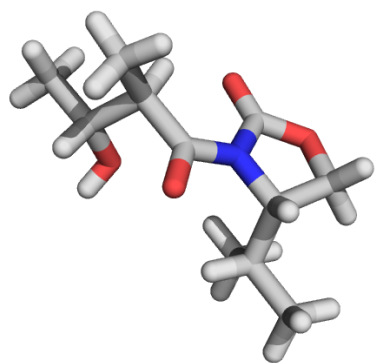
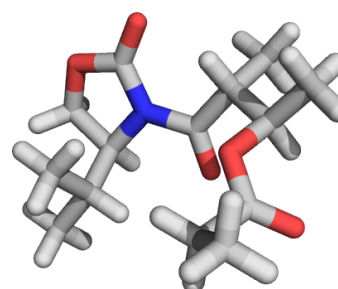
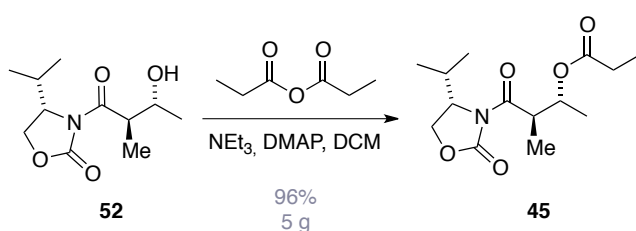


**Figure 7.** X-ray structure and single crystals (with 1€-cent) of anti aldol adduct **52** (colour code: grey: carbon, red: oxygen, blue: nitrogen, white: hydrogen)

During this process, single crystals of **52** suitable for X-ray crystallographic analysis were obtained. The structure confirms the desired *anti*- configuration of the stereocentres. Furthermore the through space orientation of the auxiliary, which avoids repulsive dipolar interactions of the carbonyl groups can be seen clearly (**Figure 7**).

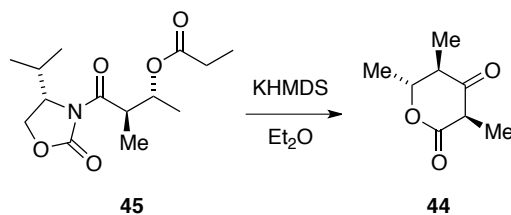
With large quantities of adduct **52** in hand, the corresponding propionate **45** could be prepared in excellent yield upon treatment with propionic anhydride in the presence of triethylamine and catalytic amounts of DMAP, following a protocol which had also been used in the shimalactone total synthesis.<sup>[29]</sup> Thereby, compound **45** could be prepared in almost quantitative yield. Upon recrystallization, an X-ray crystal structure could also be obtained from this intermediate.



**Scheme 10.** Preparation and X-ray crystal structure of propionate **45** (colour code: grey: carbon, red: oxygen, blue: nitrogen, white: hydrogen)

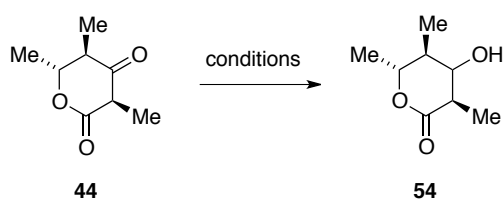
Notably, in this crystal structure, a distinct orientation of the ester fragment is evident, which may lead to a preferred nucleophilic attack of a corresponding ester-enolate on the *re*-face of the amide in the envisaged DIECKMANN cyclisation. However, the steric demand of the

chiral auxiliary might indeed promote the attack from the *si*-face, which would lead to the desired stereochemistry of resulting  $\beta$ -ketolactone **44**. Thus, the auxiliary could in fact be used to set three stereogenic centres in this synthetic sequence.



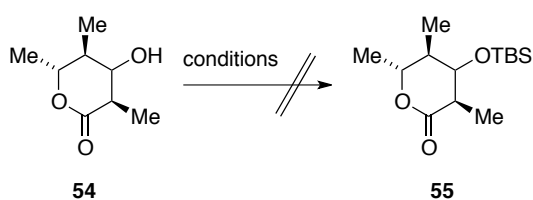
**Scheme 11.** First DIECKMANN cyclisation on this synthetic route

As depicted in Scheme 11, the first key step by means of the first DIECKMANN cyclisation<sup>[2]</sup> was attempted using KHMDS in THF at  $-78^{\circ}\text{C}$ . After careful optimisation, it was found that a reaction time of 2 hours was required for full conversion as indicated by TLC analysis. The more polar product could be unambiguously identified as recovered EVANS- auxiliary **48**, whilst  $^1\text{H}$  NMR analysis of the less polar product indicated formation of a  $\beta$ -ketolactone as single diastereoisomer. Unfortunately, all attempts to further purify and characterise this compound failed due to its extreme sensitivity. Consequently, different mild reducing agents were screened to directly convert the obtained product to the corresponding  $\beta$ -hydroxylactone **54**. Suitable reducing agents and conditions, which were found in literature on similar systems were screened and are summarised in Table 1.<sup>[44-48]</sup> For test reactions on 10 mg scales, **44** was freshly prepared, directly subjected to a short column of deactivated, neutral aluminium oxide (hexanes/ EtOAc = 1/1) concentrated *in vacuo*, re-dissolved in the appropriate solvent system and exposed to reduction conditions.

**Table 1.** Screening of reduction methods

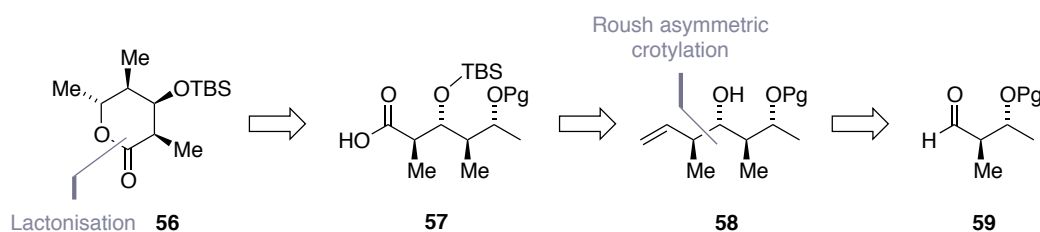
entry	reducing agents	solvent	T [°C]	time [h]	observation
1	NaBH <sub>4</sub>	MeOH	23	0.1	decomposition
2	NaBH <sub>4</sub>	MeOH	0	0.1	decomposition
3	NaBH <sub>4</sub> , CeCl <sub>3</sub> <sup>[48]</sup>	MeOH	0	0.5	decomposition
4	BH <sub>3</sub> * <i>t</i> -BuNH <sub>2</sub> / citric acid <sup>[44,45]</sup>	MeOH	23	2	decomposition
5	[ <i>n</i> -Bu <sub>4</sub> N][BH <sub>4</sub> ] <sup>[47]</sup>	DCM	23	0.5	decomposition
6	BH <sub>3</sub> * <i>t</i> -BuNH <sub>2</sub> / citric acid <sup>[44,45]</sup>	MeOH	reflux	1	conversion
7	BH <sub>3</sub> * <i>t</i> -BuNH <sub>2</sub> / citric acid <sup>[44,45]</sup>	THF/H <sub>2</sub> O	reflux	1	conversion
8	BH <sub>3</sub> *NH <sub>3</sub> / citric acid <sup>[46]</sup>	THF/H <sub>2</sub> O	23	2	conversion

Initial attempts to reduce lactone **44** were unsuccessful. While the use of sodium borohydride and LUCHE<sup>[48]</sup> conditions (entries 1 and 2) lead to immediate decomposition of the starting material, slow decomposition was observed upon treatment according to entries 3 to 5. Stability studies without reagents revealed however, that lactone **44** did not react with the corresponding reducing agents but slowly decomposed in solution. Upon heating, conversion of the starting material to a more polar compound was observed according to TLC analysis. Using a sterically less demanding reducing agent in entry 8 even provided the more polar product at ambient temperature. However, it was not possible to isolate the novel compound that had been formed. It was therefore envisaged that an *in situ* TBS protection could facilitate isolation of the assumed  $\beta$ -hydroxylactone **54** as intermediate **55** (Scheme 12).

**Scheme 12.** Envisaged TBS protection of **54**

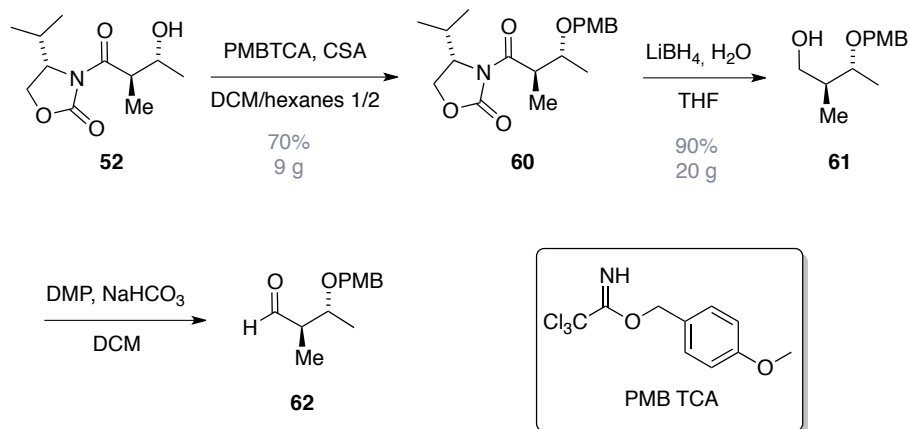
Unfortunately, neither trapping with TBSCl in the presence of imidazole in DMF, nor TBSOTf with 2,6-lutidine in DCM yielded the desired protected lactone **55**. Due to the intractability of these intermediates, an alternative route to the desired building block was considered. Specifically the alcohol in C9 position would be established and protected in the correct absolute configuration prior to lactonisation. An according retrosynthetic analysis is shown in Scheme 13.

### 3.1.3 Retrosynthetic Revision and Synthetic Progress



**Scheme 13.** Revised retrosynthetic analysis of lactone **56**

As outlined in Scheme 13, final lactonisation leads to linear precursor **57**, which upon functional group modification may be traced back to homoallylic alcohol **58**. This intermediate could be derived from corresponding aldehyde precursor **59**. As *anti*-aldol adduct **52** needed to be protected with a suitable group, differentiable from TBS *p*-methoxybenzyl- (PMB) was chosen. This protecting group also provides the advantage of adding significant mass to early intermediates such as alcohol **61**, which would otherwise be volatile.



**Scheme 14.** Synthetic sequence to aldehyde **62**

As depicted in Scheme 14 the synthetic sequence commenced with protection of the secondary alcohol in *anti*-aldol adduct **52**, utilizing BUNDLE's reagent<sup>[49]</sup> PMBTCA, following a literature procedure by SMITH III and co-workers.<sup>[50]</sup> This protocol was used after initial attempts using PMBCl proved ineffective. Subsequent removal of the chiral auxiliary was accomplished by treatment of **60** with lithiumborohydride in the presence of a stoichiometric amount of water. With alcohol **61** in hand, aldehyde **62** was readily available upon DESS-MARTIN oxidation<sup>[10,11]</sup> which set the stage for the next C–C bond formation by means of ROUSH asymmetric crotylation.<sup>[51-53]</sup> When purifying aldehyde **62** with flash column chromatography on silica, epimerisation of the system was observed. This effect could not be counteracted with deactivation of silica with triethyl amine or by using aluminium oxide. Consequently, this aldehyde (and further, similar compounds which will be discussed in following sections) was taken on crude in the following reactions. The unusual sensitivity of the  $\alpha$ -stereocentre may be considered a first indication of the synthetic challenge apparent by the *anti*- relationship of  $\beta$ -branched aldehydes. In addition, such aldehydes also display a strong intrinsic diastereofacial selectivity. Considering the FELKIN-ANH model,<sup>[54,55]</sup> established aldehyde **62** would trigger a nucleophilic attack along the BÜRGI-DUNITZ angles<sup>[56,57]</sup> indicated in Figure 8. Therefore, the envisioned all *anti*- configuration of desired homoallylic alcohol **68** may be considered a mismatched case.

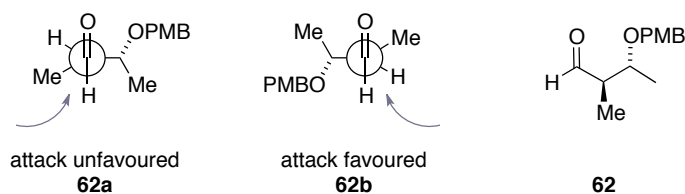
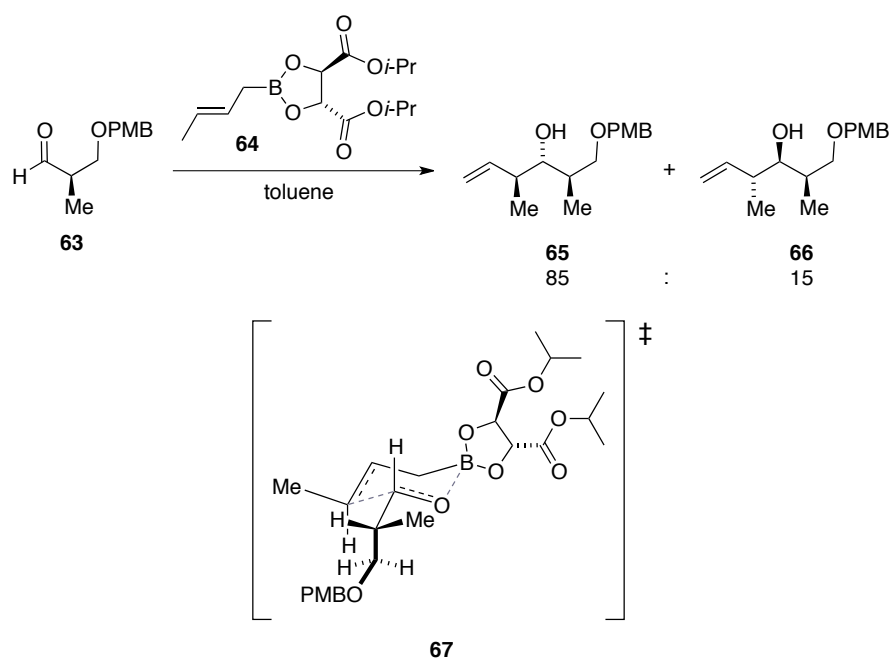


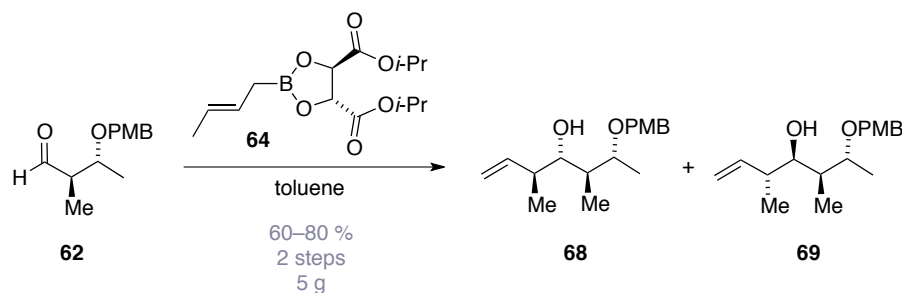
**Figure 8.** FELKIN-ANH model and favoured BÜRGI-DUNITZ trajectory for a nucleophilic attack on aldehyde **62**

The synthetic challenge of enantioselective allylations of aldehydes utilising boronic esters was first addressed and studied by HOFFMANN and co-workers.<sup>[58]</sup> To date, several potent, asymmetric methodologies for asymmetric and double asymmetric allylations and crotylations with chiral boronic ester derivatives are known, most prominently those of BROWN<sup>[59-63]</sup> and ROUSH<sup>[51-53]</sup> are established. The latter surely belongs to the most widely used reactions in polyketide syntheses due to its efficiency and versatility. Asymmetric crotylation of aldehyde **63**, derived from the respective ROCHE ester, represents a typical opening step for many polyketide syntheses.



**Scheme 15.** Successful mismatched double asymmetric crotylboration of aldehyde **63** and proposed transition state **67**.

The conversion of aldehyde **63** to homoallylic alcohol **65** using crotylation agent **64** is known to be a highly stereoselective reaction, delivering the depicted diastereoisomer in a d.r. of 85:15. The major isomer **65** is obtained *via* transition state **67**.<sup>[64]</sup> In analogy to this example, a double asymmetric crotylation of aldehyde **62** was envisioned (Scheme 16).



**Scheme 16.** Asymmetric crotylation of aldehyde **62**

When aldehyde **62** was treated with **64**, an inseparable product mixture of a 15:1 diastereomeric ratio was obtained. As homoallylic alcohol **68** was not described in literature, the obtained product mixture was carried on through subsequent reaction steps to obtain intermediates, which could be identified unambiguously. Respective intermediates will be discussed in detail in corresponding subsections and revealed that in this case, the minor product in fact had the desired stereochemistry.

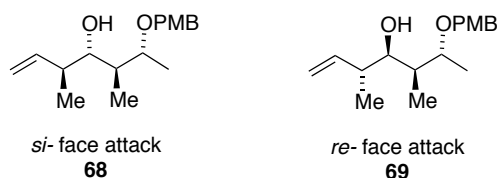
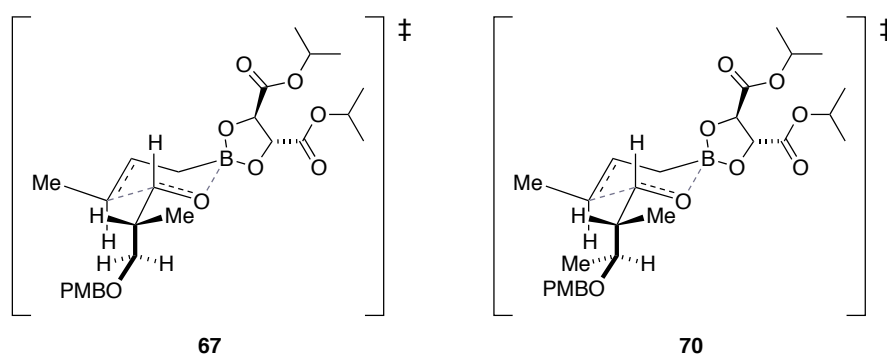


**Figure 9.** Outcome of crotylboration of aldehyde **62** after *re*- and *si*- face attack

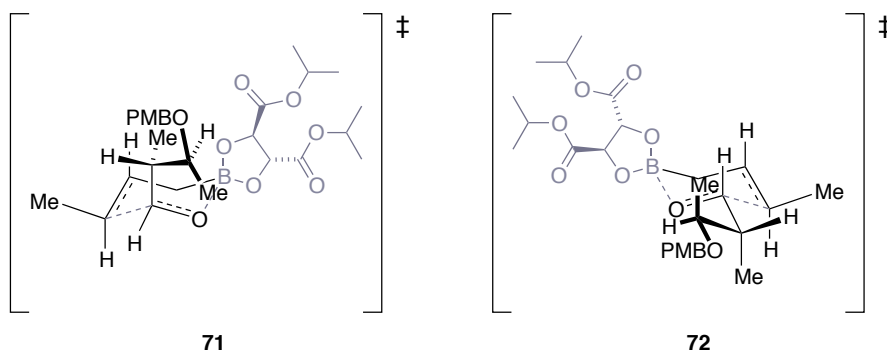
This issue may be understood considering the ZIMMERMAN–TRAXLER transition state<sup>[43]</sup> **67** wherein the full side chain of reacting aldehyde **63** is shown too. Similar to the above discussed EVANS logic (*vide supra*) three factors determine the stereochemical outcome of this reaction. The (*E*)-conformation of butenylboronate **64** determines an equatorial position of the terminal methyl group in the transition state. Again, the aldehyde side chain preferably arranges in a pseudo-equatorial position in the 6-membered ring system, determining the facial selectivity towards the aldehyde (*si*-face). Asymmetric induction of the chiral tartaric acid ester may be explained with unfavourable repulsive interaction of the non-bonding orbitals of reacting aldehyde **63** and the respective ester carbonyl group. Thus, **67** represents the favoured transition state.

It is not until considering the full aldehyde side chain however, before the limitations of this method become evident. In the assumed equatorial position of the aldehyde side chain, the smallest substituent of the aldehyde's  $\alpha$ -carbon (hydrogen) is oriented nearest to the methyl group of the crotylboronate to avoid steric clash. Consequently, the  $C\alpha$ – $C\beta$  bond is oriented parallel to the axial substituents of the chair. Both transition states **67** and **70** may accommodate the respective aldehydes in this manner, but in case of transition state **70** the additional methyl group leads to *gauche* pentane interactions, or a steric clash with pseudoaxial hydrogen.



**Scheme 17.** Proposed transition states to give the mismatched *anti*- products

With the intrinsic stereochemical bias of  $\beta$ -branched aldehydes, the *re*-attack is favoured (see Figure 8). As reaction rates are comparable with aldehydes without branching, a ZIMMERMAN–TRAXLER transition state, with boron activating the carbonyl, appears likely. Thus, two different transition states **71** and **72** may be considered.



**Scheme 18.** Alternative transition states yielding matched–case products

As depicted in Scheme 18, transition state **71** represents a coordination of the carbonyl oxygen on the sterically favoured side of the boronic ester, avoiding repulsive steric interactions upon pseudoaxial alignment of the side chain. This way, the mostly observed *re*-attack may occur. Alternatively, **72** may explain a *re*-attack on aldehyde **62** upon coordination on the less favoured face of the boronic ester. Now the side chain lines up in pseudoaxial configuration again, absolute stereochemistry on the  $\alpha$ -carbon does allow an alignment wherein *gauche* pentane interactions may be minimised. However, this transition state would yield an all-*syn* adduct. To date, literature does not discuss the possibility or characteristics of transition state **72**.

For further synthetic progress towards a total synthesis of portentol (**1**) and homoallylic alcohols **68** and **69** in hand, separation of the mixture was attempted by means of flash column chromatography and HPLC. However, separation of the mixture could not be accomplished. In fact, both reversed and normal phase HPLC yielded an additional set of two products, presumably upon migration of the PMB group, as suggested in Figure 10.

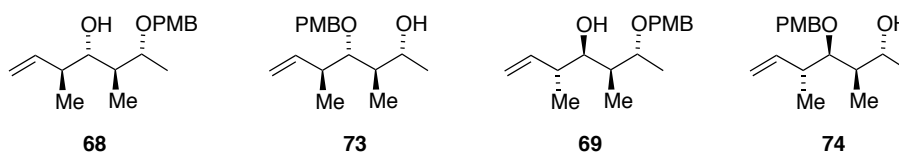
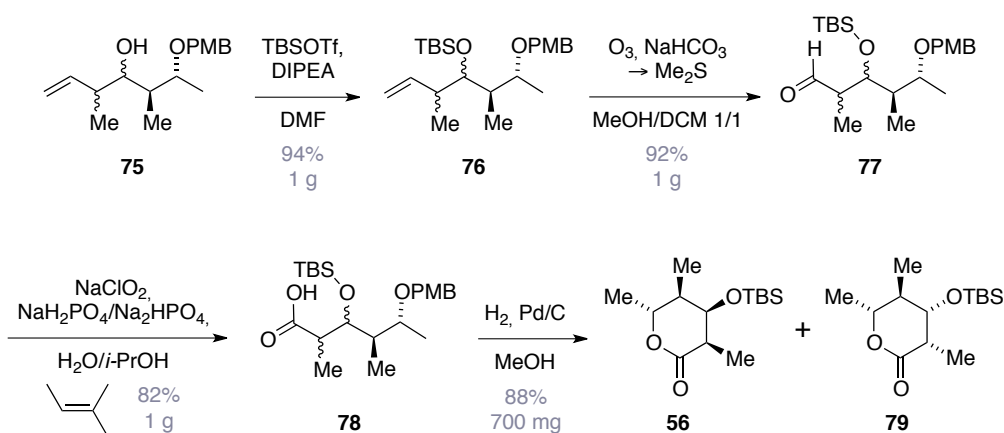


**Figure 10.** Further isomerisation upon PMB group migration

As separation of diastereoisomers was not possible at this stage, the mixture obtained from the crotoallylation was carried on through the synthetic sequence to elaborate envisaged lactone **56**. At the lactone stage, separation and full characterisation was envisaged.



**Scheme 19.** Final synthetic sequence to lactone **56**

Homoallylic alcohols **75** were protected upon treatment with TBSOTf and DIPEA yielding corresponding TBS ethers **76**. Ozonolysis of the terminal double bond, followed by reductive treatment with dimethylsulfide gave aldehyde **77**, which was further oxidised by means of PINNICK<sup>[65]</sup> oxidation to yield acid **78**. Notably, a direct conversion of the secondary ozonide with hydrogen peroxide gave only trace amounts of desired acid, along with decomposition products. Cleavage of the PMB ether then required some optimization, as initial attempts to remove the protecting group with cerammonium nitrate (CAN) failed. Hydrogenolysis conditions with Pd/C and hydrogen atmosphere were thus screened. When using EtOAc as a solvent, decomposition occurred. In EtOH, no reaction was observed. Performing hydrogenolysis in MeOH however, led to clean conversion, not only removing the protecting group but also promoting immediate lactonisation. Unfortunately, also at this stage, the diastereomeric mixture could not be fully separated. Crude NMR analysis revealed a diastereomeric ratio of **56**: **79** of ca. 1:15. The minor fraction could be obtained as clean material, however. <sup>1</sup>H and <sup>13</sup>C NMR analysis confirmed the isolated species as TBS protected  $\beta$ -hydroxylactones.

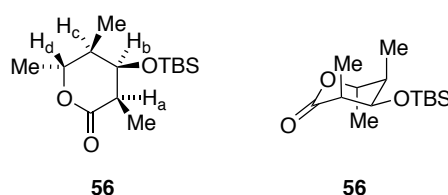


**Figure 11.** Configurational analysis of **56**

With the expected all *anti*-configuration anticipated from previous ROUSH crotylation, ring protons H<sub>a</sub>, H<sub>b</sub>, H<sub>c</sub> and H<sub>d</sub> were closely examined. Found coupling constants were:  $J(\text{H}_a\text{--H}_b) = 3.7$  Hz,  $J(\text{H}_b\text{--H}_c) = 3.7$  Hz and  $J(\text{H}_c\text{--H}_d) = 3.1$  Hz. Coupling constants of 3.7 Hz suggest coupling between an axial and an equatorial proton, whereas a coupling constant of 3.1 Hz would account for the coupling of two equatorial protons. Considering the KARPLUS curve<sup>[66]</sup> a chair confirmation as in Figure 11 may be considered.

Albeit the three methyl substituents in this chair conformation are placed in equatorial position, the sterically most demanding OTBS group would be accommodated in the equatorial position. Notably, the chair model does not fully account for six membered ring systems with heteroatoms and sp<sup>2</sup> centres, such as in lactone **56**. In the course of further synthetic studies, which will be discussed in following sections, we propose, that the major product of the ROUSH crotylation has the undesired stereochemistry. Therefore, the minor lactone diastereoisomer was used for further studies.

### 3.1.4 Conclusion and Strategic Considerations

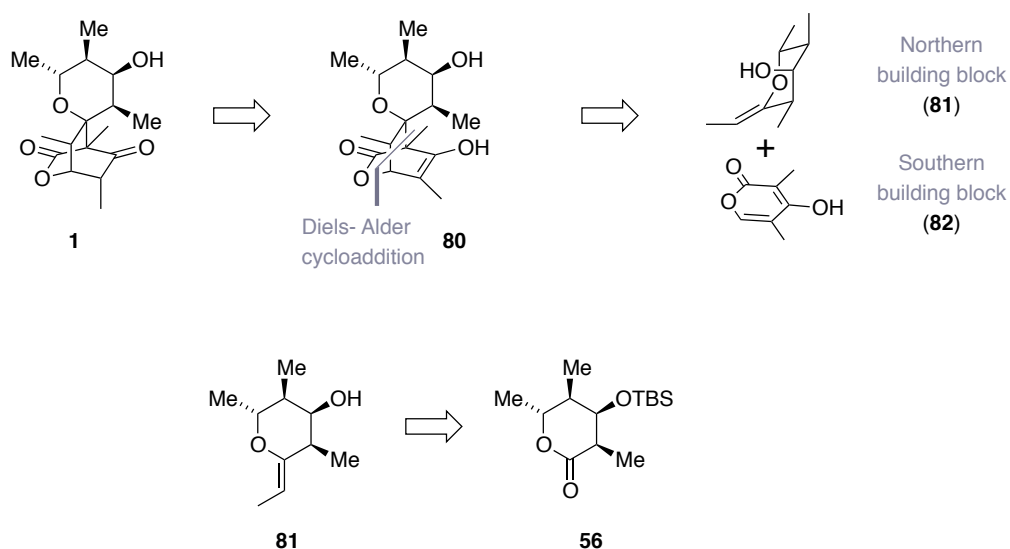
Whilst the EVANS-HEATHCOCK reaction proved effectively set the first two stereogenic centres in potential portentol-precursors, and derivatisation of the resulting adduct **52** was possible, the initial plan to elaborate a lactone building block from a DIECKMANN cyclisation<sup>[2]</sup> proved unsuccessful as the obtained product was highly unstable and could not be converted to isolable species. Building up envisaged lactone **56** could be achieved upon use of a linear sequence with a terminal lactonisation upon removal of respective PMB-protecting group. ROUSH asymmetric crotylation was a key step in this synthetic approach but delivered a diastereomeric mixture. Separation of the diastereomeric mixture at the lactone stage was not possible and NMR studies of the clean, minor product suggested that in fact this minor product displayed the desired stereochemistry.

As a large scale synthesis of **56** was not possible, a more convergent synthesis was envisaged, reducing the step count between lactonisation and formation of portentol (**1**). A retrosynthetic disconnection interpreting portentol (**1**) as a DIELS-ALDER adduct, was therefore considered.

## 3.2 The Diels-Alder Approach

### 3.2.1 Retrosynthetic Analysis

As a consequence of findings discussed in section 3.1, we were increasingly intrigued by a retrosynthetic disconnection of portentol (**1**) by means of a DIELS-ALDER cycloaddition<sup>[3-5,67]</sup> (Scheme 20).

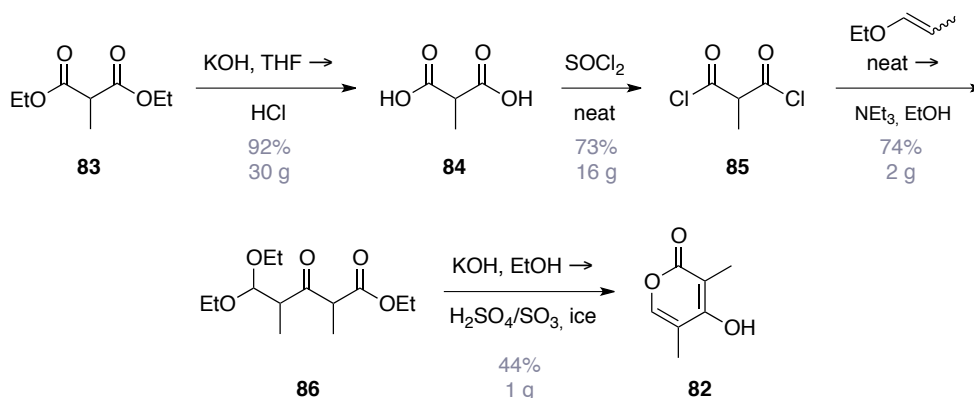


**Scheme 20.** DIELS-ALDER retrosynthetic disconnection

Bearing in mind that key building block **56** would not be feasibly synthesised in large quantities, a more convergent strategy leading directly to an advanced intermediate would be advantageous. A retrosynthetic analysis of portentol (**1**) and its corresponding tautomer **80** according to a DIELS-ALDER cycloaddition<sup>[3-5,67]</sup> leads to two building blocks. A “northern” pyrane dienophile (**81**) may be derived from discussed lactone **56** and a “southern” pyrone building block **82**, which was a literature known compound described by EFFENBERGER and co-workers,<sup>[68]</sup> could deliver portentol (**1**) in a highly convergent fashion.

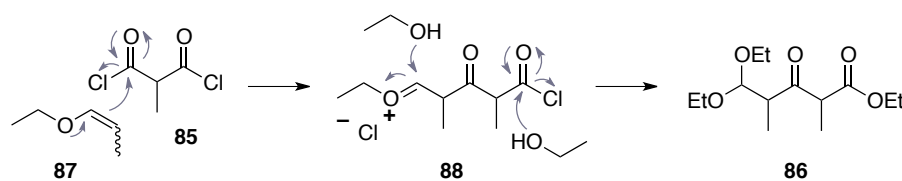
### 3.2.2 Synthesis of the Southern Fragment

In 1985 EFFENBERGER and co-workers<sup>[68]</sup> described an elegant synthesis of  $\beta$ -hydroxypyrones derived from corresponding ketals. Following this short sequence, **82** could be prepared in sufficient quantities starting from commercially available diethylmalonate **83** as depicted in Scheme 21.



**Scheme 21.** Synthesis of pyrone **82**

According to standard literature procedures,<sup>[69]</sup> diester **83** was converted to corresponding diacid upon treatment with potassium hydroxide and subsequently, aqueous HCl. Conversion of the thus prepared diacid **84** with thionyl chloride yielded acid chloride **85**. According to the carefully optimised protocol developed by EFFENBERGER and co-workers, ketal **86** was obtained in good yields.

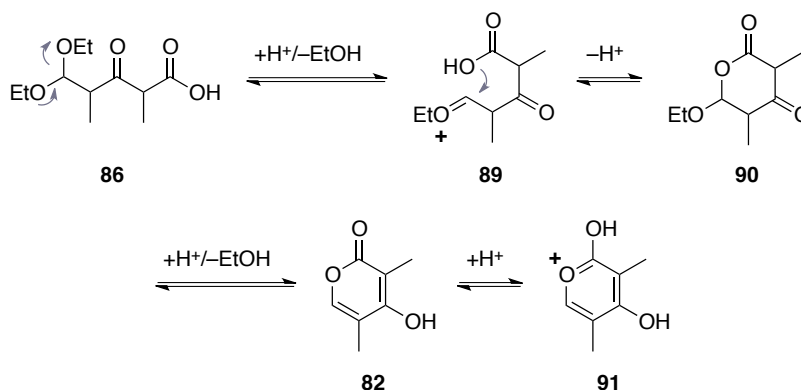


**Scheme 22.** Formation of ketal **86**

As depicted in Scheme 22, nucleophilic attack of the double-bond in ethylpropenyl ether (**87**) occurs only once on diacid chloride **85**, forming carboxonium ion **88**. After addition of EtOH and base, this reactive intermediate is intercepted, forming ketal **86**.

*In situ* conversion of ketal **86** to its corresponding potassium salt followed by treatment with oleum gave pyrone **82**. EFFENBERGER and co-workers formulated a mechanism for this cyclisation, as depicted in Scheme 23. Commencing with an acid-catalysed extrusion of EtOH, intermediate **89** is generated. Interception of the carboxonium ion by the hydroxyl

group of the carboxylic acid moiety then delivers cyclic intermediate **90**, which, upon further acid-catalysed extrusion of EtOH delivers pyrone **82**. Due to the highly acidic environment, in the reaction mixture, the equilibrium may be pushed to the side of pyryllium ion **91**.



**Scheme 23.** Acid-catalysed cyclisation of ketal **86** to pyrone **82**

It was observed, that the last two steps in this sequence could not be arbitrarily scaled up beyond 2 g of **85**. Thus, repeating the two final steps of EFFENBERGER's sequence, sufficient amounts of pyrone **86** were obtained. Upon repeated column chromatography and recrystallization from ethyl acetate, the first X-ray crystal structure of **86** was obtained.

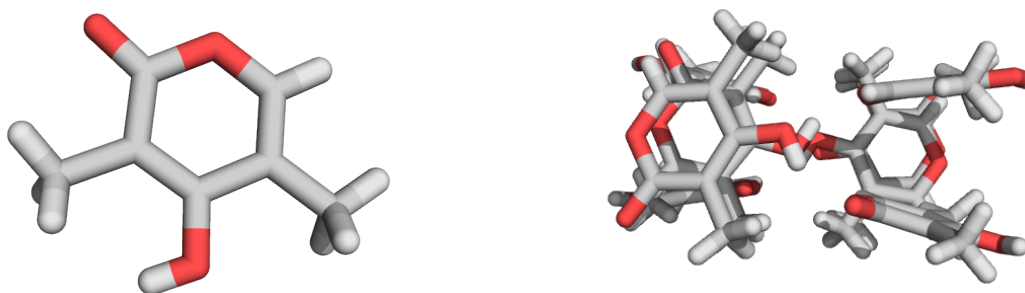
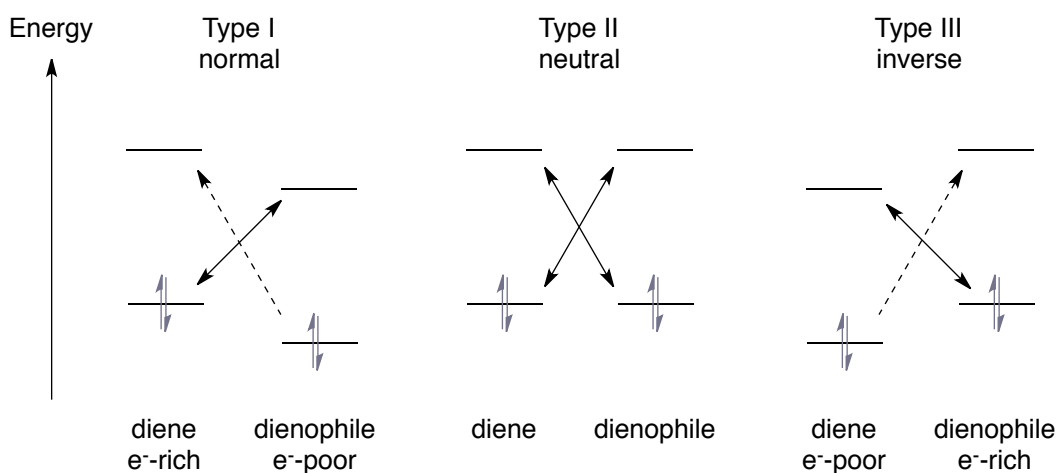


**Figure 12.** X-ray structure of pyrone **82** as single molecule and in the asymmetric unit. (colour code: grey: carbon, red: oxygen, white: hydrogen)

As can be seen in Figure 12, hydrogen bonding between a carbonyl oxygen and a hydroxyl- group of a neighbouring molecule contributes to the high crystallinity of **82**. In the crystal lattice, two molecules at a time are oriented almost parallel with respect to the planar six-membered ring system. However, steric demand of the two methyl- substituents obviates a perfectly parallel orientation of those pairs.

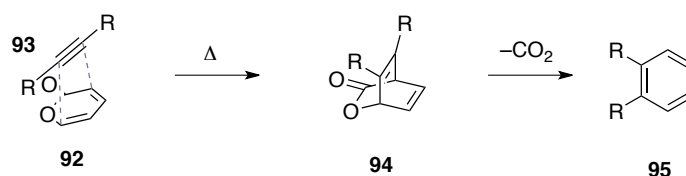
### 3.2.3 DIELS-ALDER SCREENINGS

Pyrones as dienophiles in [4+2] cycloadditions have already been introduced by DIELS and ALDER themselves in 1931<sup>[6]</sup> with maleic anhydride as dienophile. According to SUSTMANN's classification of DIELS-ALDER reactions accounting their corresponding HOMO-LUMO interactions (see Scheme 24) this first example of a pyrone DIELS-ALDER thus is a normal electron demand, type I DA-reaction.<sup>[70]</sup>



**Scheme 24.** SUSTMANN's classification of DIELS-ALDER reactions according to electron demand and resulting HOMO-LUMO interactions<sup>[70]</sup>

However, due to their remarkable ambiphilic character, 2-pyrones may also undergo inverse electron demand DA-reactions with electron rich dienophiles thus representing type III DA-reactions. In both cases, early investigations limited the use of  $\alpha$ -pyrones as dienes to the preparation of aromatic systems, as extrusion of CO<sub>2</sub> through a retro DA-mechanism occurs readily (Scheme 25).



**Scheme 25.** DA reaction of 2-pyrone (**92**) with generic, symmetric alkyne **93**

As depicted in Scheme 25, reaction of pyrone **92** with an alkyne **93** initially leads to compound **94**, but spontaneously extrudes  $\text{CO}_2$ , elevating the entropy of the system and reducing the ring strain evident in **94** and giving aromatic system **95**.

However, in 1992 MARKÓ and co-workers published the first X-ray crystal structure of a 2-pyrone DIELS-ALDER adduct, which had been achieved upon reaction of 2-pyrone (**92**) with methyl acrylate under high pressure.<sup>[71]</sup> To avoid the extrusion of  $\text{CO}_2$ , yet be able to use more benign conditions, base- or acid catalysis have led to a vast variety of isolable pyrone-DA adducts. It should be noted though, that to date no successful pyrone DA with pyrone **82** or derivatives thereof has been reported.

To synthesise portentol (**1**) by means of a 2-pyrone DIELS-ALDER reaction, pyrone **82** would be reacted with an electron rich dienophile similar to vinyl ethers in terms of electron demand, representing a type III DA reaction. For this cycloaddition, eight transition states may be discussed.

Considering the relative stereochemistry of envisaged dienophile **81** (synthetic studies towards which will be discussed in 3.2.4), the steric demand of the methyl substituents dictate a clearly favoured chair like conformation (**81a**), putting the methyl substituents in equatorial positions to avoid *trans*-annular repulsion as in **81b** (Figure 13).

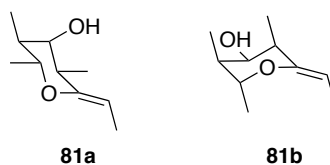
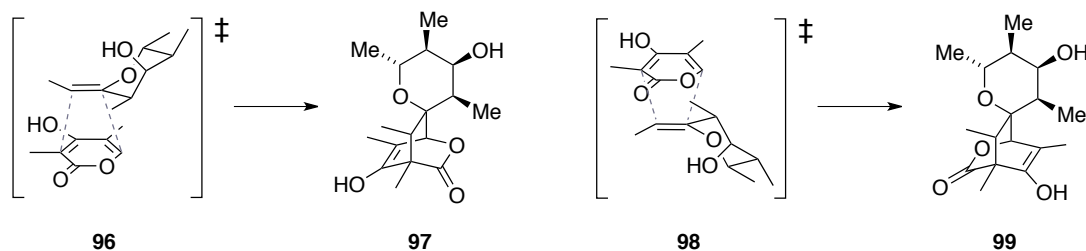


**Figure 13.** Different chair conformations of envisaged dienophile **81**

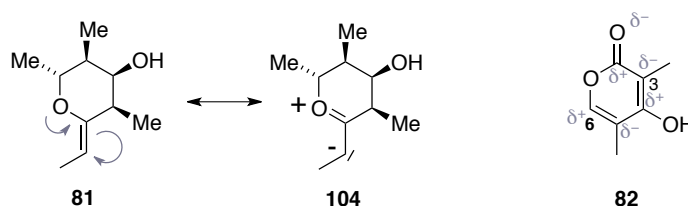
Additionally, this conformation of **81a** displays a distinct convex and concave face with respect to the double bond. The envisaged DIELS-ALDER reaction with sterically quite

demanding pyrone **82** would thus occur preferably from the convex side, avoiding repulsive interaction with the hydroxyl group of dienophile **81**. Considering this distinct facial bias, four potential transition states may be conceivable.



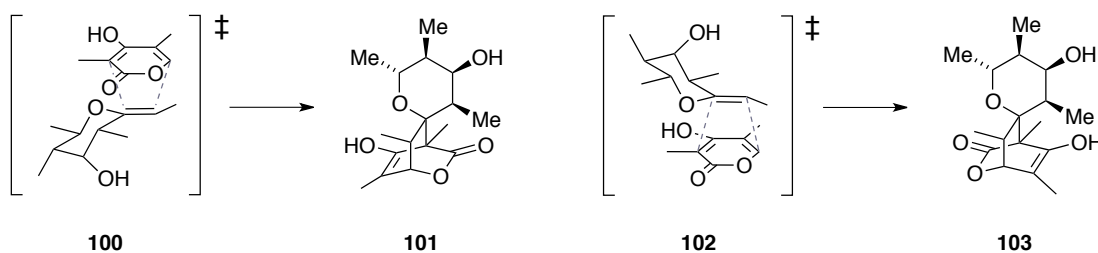
**Scheme 26.** Electronically disfavoured transition states and outcomes of a portentol DIELS-ALDER

Evaluating the first two imaginable transition states **96** and **98** for a “portentol DIELS-ALDER” it appears quite unlikely to achieve a reaction pathway *via* these two intermediates to products **97** and **99**. Electron density disfavours the regioselectivity in both cases. As emphasised in Scheme 27, displaying relevant mesomeric structures of dienophile **81** and electronic situation in pyrone **82**, the regioselectivity within transition states **96** and **98** is electronically mismatched.



**Scheme 27.** Resonance structures of **81** and partial charges in **82**

Considering mesomeric structure **104** and electronic density in pyrone **82**, the anionic  $\text{CH}_2$  fragment of **104** would prefer orbital overlap with C-6 of pyrone **82** as this carbon atom bears a positive partial charge. In contrast, C-3 bears a negative partial charge, as it is in  $\alpha$ -position to the carbonyl moiety of pyrone **82**. Consequently, transition states **100** and **102**, depicted in Scheme 28, may be considered the preferred transition states of a portentol-DIELS-ALDER reaction.

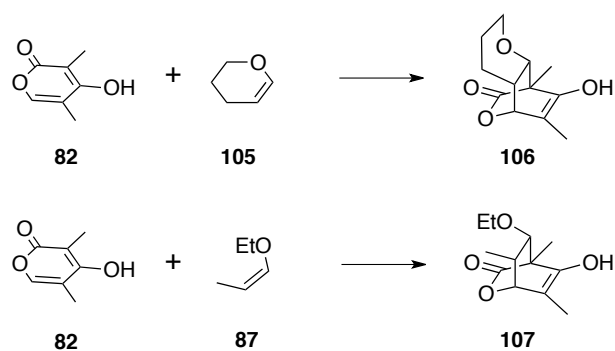


**Scheme 28.** Electronically favoured transition states **100** and **102** in a portentol-DIELS-ALDER

In these two electronically matched transition states portentol (**1**) may be obtained upon tautomerisation of enol **103**. Isomer **101** may also be obtained upon DIELS-ALDER conditions. Although it is difficult to clearly differentiate an *exo* and *endo* case in this particularly challenging DA-reaction, lone pair orbitals of the ether oxygen in **102** may yield a more constructive secondary orbital overlap with pyrone **82**, leading to a more stabilised transition state and faster product formation. In addition, a chiral catalyst, coordinating to pyrone **82** could be envisaged to solve this matter.

Keen to investigate the potential scope of the envisaged pyrone DIELS-ALDER reaction, suitable model dienophiles were picked for initial screenings. Dihydropyran (DHP, **105**) and ethylpropenyl ether (*cis/trans* mixture, **87**) were chosen, as these compounds resemble electronic demands for a type III DA reaction. Sterically, the propenyl moiety of ether **87** additionally models the steric features of envisaged northern building block **81**.

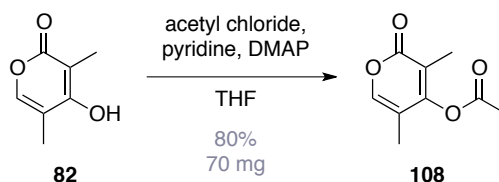
A first screening for reference conditions was designed to give a basis for further investigations, focussing on the behaviour of both diene and dienophiles as well as molarity and temperature. Findings regarding these initial test reactions are summarised in Table 2.

**Table 2.** Preliminary DA screenings with DHP (**105**) and ethylpropenyl ether (here *cis*-form, **87**)

entry	diene [mmol]/ 1eq.	dienophile [mmol]/ eq.	solvent [mL]	T [°C]	t [h]	observation
1	0.076	<b>105</b> / 0.076/ 1	toluene/ 0.4	rt.	12	no rxn
2	0.076	<b>105</b> / 0.076/ 1	toluene/ 0.4	100	24	no rxn
3	0.076	<b>105</b> / 0.21/ 3	toluene/ 0.2	100	24	decomp.
4	0.076	<b>105</b> / 2.2/ 30	neat/ MW	100	1	decomp.
5	0.078	<b>87</b> / 1.8/ 23	neat/ MW	100	1	decomp.

Whilst equimolar set ups of a 2M toluene solution neither reacted at ambient temperature nor 100°C (entries 1 and 2) a threefold excess of dienophile **105** in a 4M solution stirred at 100°C for 24 hours (entry 3) as well as neat reactions in microwave with the respective dienophiles (**105** and **87**) as solvent, lead to decomposition. Polymerisation of respective dienophiles was observed, whilst the pyrone could not be re-isolated anymore. Neither <sup>1</sup>H NMR analysis of isolated fractions nor GC/MS analysis indicated the formation of desired adducts **106** and **107**. These findings lead to the following strategic considerations: a high pressure set up, which would have seemed to be an appropriate tool to prevent CO<sub>2</sub> extrusion, would most likely decompose the southern building block, pyrone **82**. More benign conditions were required to achieve envisaged pyrone DIELS-ALDER reactions. To increase stability of **82** a suitable protecting group should be chosen. Moreover, solvents and catalysts should be screened thoroughly.

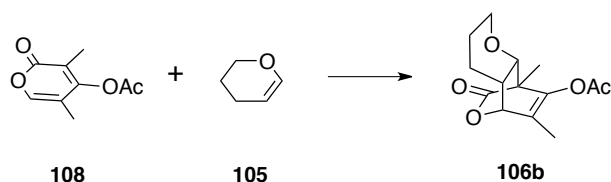
To remain close to the envisaged, protecting group free DIELS-ALDER reaction of compounds **81** and **82**, a protecting group was envisaged, which would not influence the electron demand of the pyrone. Whilst notably it was not possible to introduce a TBS group (most likely due to the steric bulk of adjacent methyl groups), conversion to the corresponding acetate proceeded smoothly upon treatment of **82** with acetyl chloride and pyridine with catalytic amounts of DMAP. As depicted in Scheme 29 acylation of **82** was accomplished in 80% yield on a 0.5 mmol scale.



**Scheme 29.** Acylation of pyrone **82**

With protected pyrone **108** in hand, different solvents were screened next. In this screening, pyrone acetate **108** and respective dienophiles were reacted at different temperatures. Also, another attempt of a neat reaction in microwave with a 30 fold excess of dienophile **105** for solvent was attempted. Findings of this screening are summarised in Table 3.

**Table 3.** First solvent screening for model pyrone-DA reactions with diene **108** and DHP (**105**)

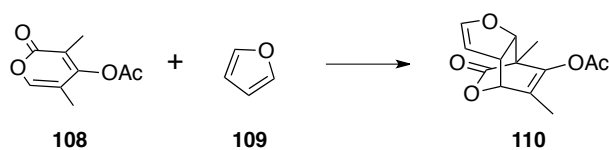


entry	diene <b>108</b> [mmol]/ eq	dienophile <b>105</b> [mmol]/ eq	solvent [0.1 mL]	T [°C]	t [h]	observation
1	0.055/ 1	0.162/ 3	DMSO	60	0.5	no rxn
2	0.055/ 1	0.162/ 3	DMSO	60	3	no rxn
3	0.055/ 1	0.162/ 3	DMSO	120	1	no rxn
4	0.055/ 1	0.162/ 3	benzene	60	0.5	no rxn
5	0.055/ 1	0.162/ 3	benzene	60	3	no rxn
6	0.055/ 1	0.162/ 3	benzene	120	1	no rxn
7	0.055/ 1	0.162/ 3	toluene	60	0.5	no rxn

entry	diene <b>108</b> [mmol]/ eq	dienophile <b>105</b> [mmol]/ eq	solvent [0.1 mL]	T [°C]	t [h]	observation
8	0.055/ 1	0.162/ 3	toluene	60	3	no rxn
9	0.055/ 1	0.162/ 3	toluene	180	1	decomp.
10	0.055/ 1	0.162/ 3	<i>o</i> -DCB	60	0.5	no rxn
11	0.055/ 1	0.162/ 3	<i>o</i> -DCB	60	3	no rxn
12	0.055/ 1	0.162/ 3	<i>o</i> -DCB	180	1	decomp.
13 <sup>a</sup>	0.055/ 1	1.62/ 30	neat	100	1	decomp.

<sup>a</sup> Reaction in microwave with dienophile **105** as solvent

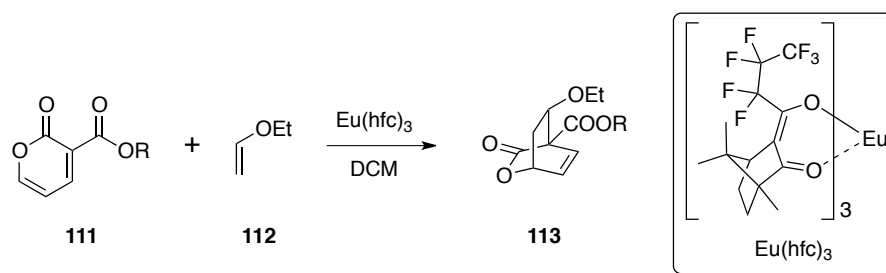
In this screening no reaction conditions were found in which desired DIELS-ALDER reaction was realised, increased stability of the pyrone due to protection was clearly observed, though. While reactions at 60 °C and 120 °C in different solvents did not indicate any reactivity (entries 1–8, 10 and 11), harsher conditions, such as heating to 180 °C (entries 9 and 12) or neat reaction in a microwave reactor (entry 13), lead to full decomposition of starting materials and polymerisation of DHP (**105**) respectively. As DHP (**105**) readily polymerises, a more stable dienophile was found in furan (**109**). Whilst another equivalent of dienophile was used (4 equivalents with respect to pyrone acetate **108**) the solutions were made more dilute to prevent undesired side reactions, most prominently polymerisation.

**Table 4.** Second solvent screening for envisaged pyrone DIELS-ALDER with furan (**109**) as dienophile

entry	diene <b>108</b> [mmol]/ eq.	dienophile <b>109</b> [mmol]/ eq.	solvent [0.5 mL]	T [°C]	t [h]	observation
1	0.055/ 1	0.22/ 4	DMSO	120	3	no rxn
2	0.055/ 1	0.22/ 4	benzene	120	3	no rxn
3	0.055/ 1	0.22/ 4	toluene	120	3	no rxn
4	0.055/ 1	0.22/ 4	<i>o</i> -DCB	120	3	no rxn
5	0.055/ 1	0.22/ 4	toluene	180	1	decomp.
6	0.055/ 1	0.22/ 4	<i>o</i> -DCB	180	1	decomp.

To summarise the second solvent screening (see Table 4) again temperatures up to 120°C (entries 1 to 4) did not promote any reaction, regardless of the solvent in use, upon further heating again only decomposition of both diene (**109**) and dienophile (**108**) was observed (entries 5 and 6). No trace of desired cycloadduct **110** was found by <sup>1</sup>H NMR and GC-MS analyses. Based on these observations, no further conclusions regarding a suitable solvent could be made. To investigate potential catalysts to the envisaged DA-reaction, toluene and *o*-dichlorobenzene were chosen for solvents as they are non-coordinating and tolerate LEWIS-acids, toward which the focus was turned at that point in the project.

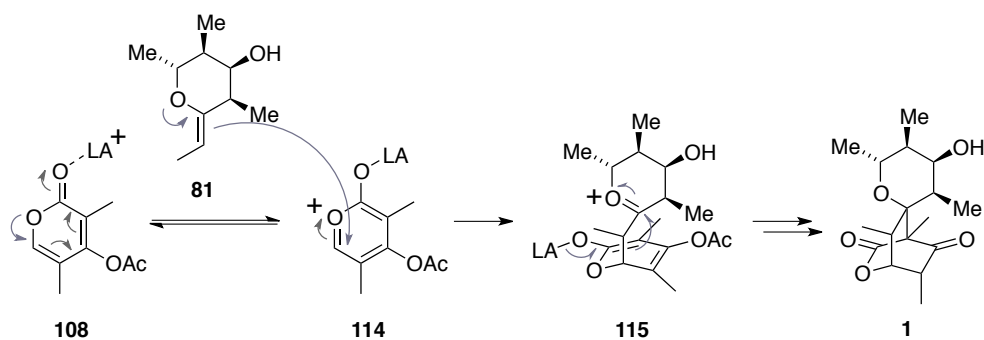
In 1960 YATES and EATON reported the enhancement of type I DIELS-ALDER reactions upon equimolar treatment using aluminium chloride.<sup>[72]</sup> Since then LEWIS acid catalysis has become a key concept in modern DIELS-ALDER chemistry. In 1992, MARKÓ *et al.*<sup>[73]</sup> and POSNER *et al.*<sup>[74]</sup> independently reported successful catalysis of type III DIELS-ALDER reactions with electron deficient pyrones and electron rich dienophiles such as ethyl vinyl ether (**112**) using lanthanide catalysts, an exemplary reaction of which is shown in Scheme 30.



**Scheme 30.** Europium catalysed pyrone-Diels-Alder reaction

Following up on this and similar model systems, asymmetric catalysis was developed for pyrones with carbonyl substituents in 3-position. In context of the envisaged portentol DA-reaction following facts are notable, however: LEWIS acid coordination in pyrones similar to **111** may be emphasised upon the 1,3-dicarbonyl moiety. Also, the ester in 3-position of the pyrone leads to more electron deficient diene-systems. Thirdly, the ether moiety in **113** ends up at the “wrong” side for portentol (**1**). Considering steric demand of the methyl groups in pyrone **108** as well as already discussed steric demand of envisaged dienophile **81**, presented research by MARKÓ and co-workers was a valid landmark for our envisaged DIELS-ALDER reaction.

Regarding LEWIS acid catalysts, MARKÓ and co-workers suggested in particular, that stronger LEWIS-acids would trigger formation of pyryllium species, which would prevent a concerted DA-reaction upon aromatisation. Acknowledging this statement we decided to still try some slightly stronger LEWIS acids too, as we envisaged, that formation of the very pyryllium species **114** may lead to a step wise reaction of envisaged northern building block **81** thus resemble our biosynthetic hypothesis (*vide infra*). A possible mechanism for the stepwise reaction upon LEWIS-acid catalysis is outlined in Scheme 31.

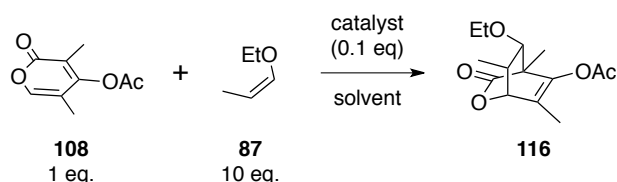


**Scheme 31.** Step wise reaction of LEWIS-acid adduct **108** and northern building block **81**

In described case, pyryllium ion **114** would be attacked by the double-bond of **81** forming carboxonium ion **115**, which may be attacked in analogue fashion to our biosynthetic hypothesis by the LEWIS-acid induced enol double bond. Subsequent functional group modification may then give rise to portentol (**1**).

To survey these plausible reaction mechanisms (step wise or *via* a concerted DA-reaction), a thorough screening of different LEWIS-acids and reaction conditions was performed and is summarised in Table 5.

**Table 5.** Catalysis screening for pyrone DIELS-ALDER reaction



entry	LEWIS acid	solvent [1 mL]	T [°C]	t [h]	observation
1	AlCl <sub>3</sub>	toluene	-78	2	no rxn
2	AlCl <sub>3</sub>	toluene	25	2	no rxn
3	AlCl <sub>3</sub>	toluene	60	2	decomp.
4	AlCl <sub>3</sub>	<i>o</i> -DCB	0	2	no rxn
5	AlCl <sub>3</sub>	<i>o</i> -DCB	25	24	1
6	Zn	benzene	25	24	1
7	Sc(OTf) <sub>3</sub>	toluene	-78	2	no rxn
8	Sc(OTf) <sub>3</sub>	toluene	25	2	1
9	BF <sub>3</sub> •OEt <sub>2</sub>	toluene	-78	2	no rxn
10	BF <sub>3</sub> •OEt <sub>2</sub>	toluene	25	2	no rxn
11	BF <sub>3</sub> •OEt <sub>2</sub>	toluene	100	1	decomp.
12	Yb(OTf) <sub>3</sub>	toluene	-78	2	no rxn
13	Yb(OTf) <sub>3</sub>	toluene	25	2	1
14	Yb(OTf) <sub>3</sub>	toluene	100	1	decomp.
15	Yb(OTf) <sub>3</sub>	<i>o</i> -DCB	25	2	1

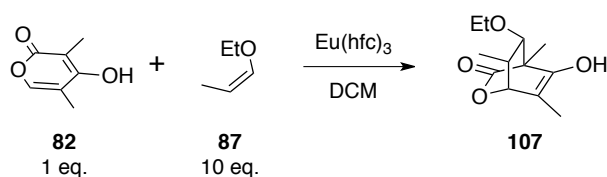
entry	LEWIS acid	solvent [1 mL]	T [°C]	t [h]	observation
16	Yb(OTf) <sub>3</sub>	<i>o</i> -DCB	100	1	decomp.
17	Eu(OTf) <sub>3</sub>	toluene	-78	2	no rxn
18	Eu(OTf) <sub>3</sub>	toluene	25	96	<sup>1</sup>
19	Eu(OTf) <sub>3</sub>	toluene	100	2	decomp.
20	Eu(OTf) <sub>3</sub>	<i>o</i> -DCB	25	96	<sup>1</sup>
21	Eu(OTf) <sub>3</sub>	<i>o</i> -DCB	100	2	decomp.
22	CSA <sup>2</sup>	<i>o</i> -DCB	25	24	<sup>1</sup>
23	CSA <sup>2</sup>	<i>o</i> -DCB	60	3	<sup>1</sup>

<sup>1</sup> partial or complete decomposition of dienophile (**87**), full recovery of pyrone **108**

<sup>2</sup> considering the envisaged biomimetic key step, a BRØNSTED acid was tested in this screening too

This screening focused on different LEWIS, or in case of CSA, BRØNSTED-acids and their reactivity with pyrone **108** and a suitable dienophile (**87**) at different temperatures. In the course of this investigation, a first series of test reactions was performed at -78 °C. At these temperatures, no LEWIS acid tested could promote any reaction (entries 1, 7, 9, 12 and 17). As a consequence, higher temperatures were investigated next. At ambient temperature (here 25 °C, entries 2, 5, 5, 8, 10, 13, 15, 18, 20 and 22) only consumption of the starting materials was observed in all cases except entries 2 (AlCl<sub>3</sub> in toluene) and 10 (BF<sub>3</sub>•OEt<sub>2</sub> in toluene). However, no indication of a desired product could be observed by means of <sup>1</sup>H NMR or mass spectroscopy analyses. Finally, a third series of test reactions was performed at 100 °C (entries 11, 14, 16 19 and 21 /60 °C for entries 3 and 23). Starting materials were then fully consumed, however, no desired reaction could be observed.

It was thus decided to move closer to published findings by MARKÓ and co-workers.<sup>[71,73]</sup> Considering their observation, that a coordinating group attacked to the pyrone would pre coordinate or “guide” coordination of a suitable LEWIS acid, that our acetate protecting group was however in 4-position, thus probably competing with coordination on the pyrone carbonyl moiety, we decided to return to protecting group free pyrone **82**. Also, free enol in an envisaged [2.2.2] cycle could tautomerise, reducing ring strain in the obtained system.

**Table 6.** Eu(hfc)<sub>3</sub> screened as catalyst for the portentol DA-reaction

entry	(LEWIS)-acid	temperature [°C]	time [h]	observation
1	Eu(hfc) <sub>3</sub>	23	3	no rxn
2	Eu(hfc) <sub>3</sub>	23	96	decomposition

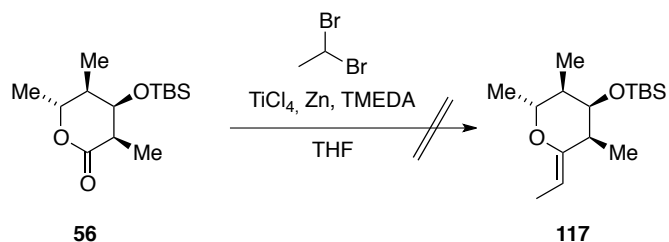
Also under these mild conditions, which according to literature do not promote the formation of a pyryllium species,<sup>[71]</sup> the intended DIELS-ALDER reaction could not be observed. After three hours, at room temperature, the starting materials were dissolved in the solvent without any consumption (entry 1). Upon longer subjection to these reaction conditions (entry 2), decomposition of both diene **82** and dienophile **87** was evident. While electronically, the use of differently strong LEWIS acids should be more than capable of compensating the inducing effect of the methyl groups in pyrone **82**, the steric hindrance of these two substituents may prevent desired reactivity to a tricyclic system such as **107**.

### 3.2.4 Synthetic Progress on the Northern Fragment

To accomplish the northern building block **81**, a direct conversion of lactone **56** by means of a modified TAKEI-LOMBARDO-type reaction,<sup>[75-77]</sup> was intended. In contrast to a standard TAKEI-LOMBARDO methenylation<sup>[75-77]</sup> this method is based on the reaction of a 1,1-dihalogenide (mostly bromide) with TiCl<sub>4</sub> and elemental zinc. Utilizing these reaction conditions, esters were successfully reacted to alkenylethers in high *Z*-stereoselectivity. Whilst standard LOMBARDO conditions lead to methenylation of even less reactive carbonyl groups such as esters, this modified version may even be used on lactones. In addition, installation of an ethenyl moiety is feasible.<sup>[77]</sup>

The active species was prepared according to literature procedures<sup>[76]</sup> by treating a THF solution of  $\text{TiCl}_4$  with tetramethylethyl diamine (TMEDA) at room temperature. After 10 minutes, activated zinc dust was added. Then the gem-dibromide and lactone were added and the reaction stirred at conditions summarised in Table 7.

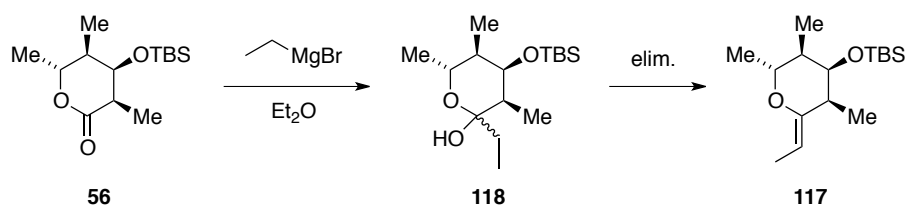
**Table 7.** Conditions screening for a TAKAI-LOMBARDO conversion of lactone **81**



entry	$\text{TiCl}_4$ [eq.]	TMEDA [eq.]	Zn [eq.]	$\text{C}_2\text{H}_4\text{Br}_2$ [eq.]	T [°C]	t [h]	observation
1	4	8	9	2.2	23	2	no reaction
2	4	8	9	2.2	23	12	no reaction
3	4	8	9	2.2	60	2	no reaction
4	4	8	9	2.2	60	12	no reaction
5	4	8	9	2.2	60	12	no reaction
6	4	8	9	2.2	150	72	no reaction
7	8	16	18	4.4	150	72	no reaction

Equivalents of reagents refer to 1 equivalent of applied lactone **56**. All test reactions were performed at 0.01 to 0.07 mmol scales.

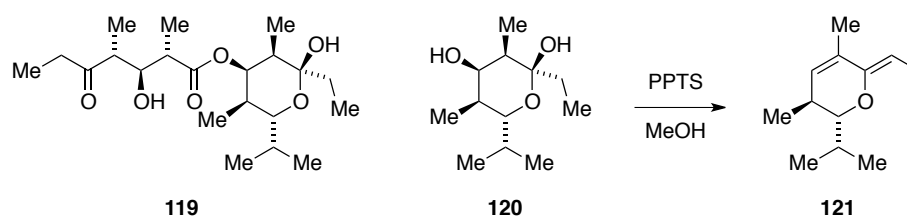
As this ambitious attempt to directly convert lactone **56** to alkenylether **117** was unsuccessful, a two-step sequence was envisaged. Thereby, reaction of lactone **56** with  $\text{EtMgBr}$  should form a hemiacetal, which could collapse upon elimination to desired exocyclic double bond in **117** as outlined in Scheme 32.



**Scheme 32.** Envisaged 2 step sequence to building block **117**

Along these lines, lactone **56** was treated with 1.5 equivalent of EtMgBr, following procedures by LIN and co-workers, a following elimination should yield enol ether **117**.<sup>[78]</sup> In this work a two-step transformation of various gluconates to corresponding *exo*-glucals, utilising trifluoroacetic anhydride/pyridine to eliminate intermediate hemiacetals was demonstrated. Preliminary tests, however, only lead to inconclusive results and fast decomposition of intermediates. Though lactone **56** was fully consumed in the course of reactions, no further intermediate could be cleanly isolated. It may be reasoned, that following a similar reaction pathway, elimination reactions upon a highly basic reaction medium in perused GRIGNARD-reaction may have lead to decomposition of lactone **56**.

Similar observations were reported in a synthetic study directed towards a total synthesis of dolabriferol **119**.<sup>[79]</sup> DIAS *et al.* prepared hemiacetal **120**, a building block which features the exactly same stereochemical pattern as corresponding pyrane ring in portentol (**1**). Upon treatment of **120** with PPTS in MeOH the only isolable material was diene **121**. Also they described hemiacetal **120** as “extremely acid labile and prone to decomposition”.<sup>[79]</sup>



**Scheme 33.** Dolabriferol **119** and double-elimination of building block **120** to diene **121**

### 3.2.5 Conclusion and Strategic Considerations

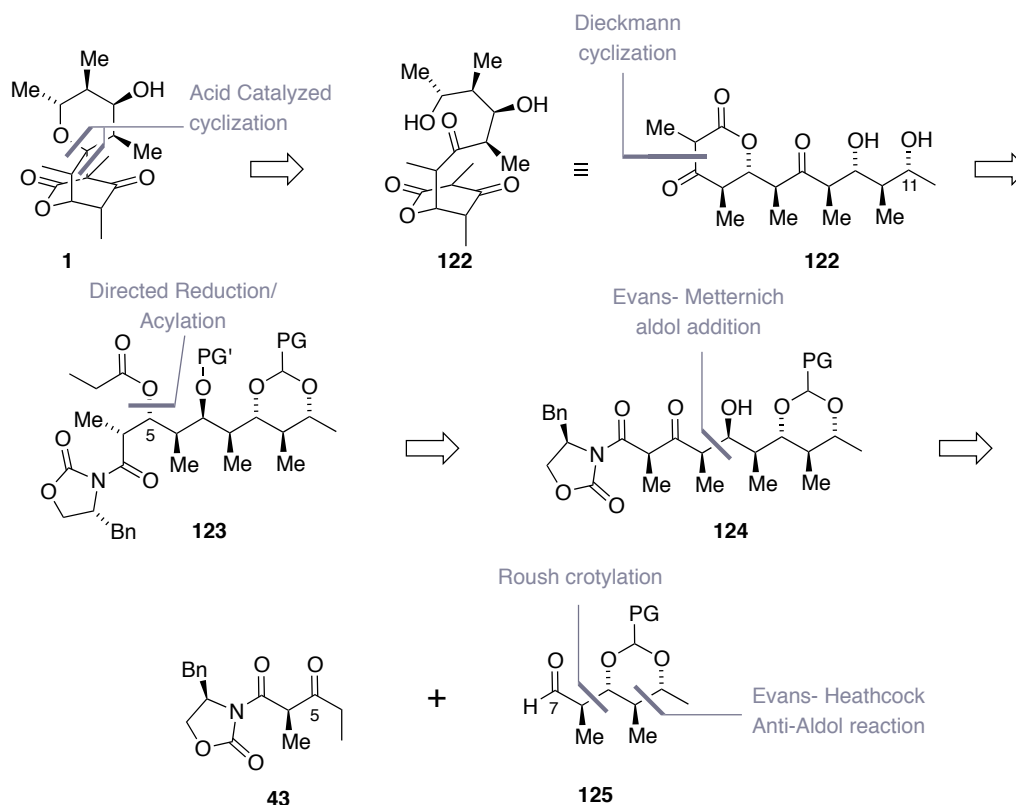
In the course of synthetic studies directed toward a total synthesis of portentol (**1**) by means of a DIELS-ALDER reaction, literature known southern building block **82** was successfully synthesised. In addition its X-ray crystal structure was obtained. This pyrone (**82**) in due course was converted to its corresponding acetate **108**. In attempt to establish a novel pyrone DIELS-ALDER reaction, both pyrones and suitable dienophiles were extensively screened. Unfortunately, this challenge was not met with success. In addition, preliminary synthetic studies towards required northern building block **81** and a generally observed sluggish reactivity of previously synthesised lactone **56** prompted consideration of different synthetic routes, which would feature required cyclisation of the northern pyrane fragment of portentol (**1**) at a later stage. Accordingly, modifications in the retrosynthetic analysis and strategic outline for the envisaged total synthesis are presented and discussed in the following section.

## 3.3 The Chain Approach

This section summarises all synthetic studies towards linear chain fragments of potential portentol-precursors and all strategies pursued, aiming for late stage cyclisations in combination with a final, acid catalysed key step. Detailed retrosynthetic analyses of respective synthetic strategies are discussed in the corresponding subsections.

### 3.3.1 Retrosynthetic Analysis

Following our biosynthetic hypothesis, which has been outlined in detail in section 2.2.2 (*vide infra*) and having encountered challenges in the synthetic progress at this point in the project, another retrosynthetic analysis of portentol **1** was considered. This should both introduce alternate synthetic routes and methodology as well as more efficient solutions to overcome the counteracting stereochemical bias discussed above.



**Scheme 34.** Retrosynthetic analysis of portentol **1** according to the "chain"-strategy

The first retrosynthetic disconnection (Scheme 34) leads to intermediate **122** wherein the “southern”  $\beta$ -ketolactone moiety would already be installed and a nucleophilic attack of the secondary hydroxy group at C11 into the ketone found in the linear chain would trigger the formation of portentol (**1**). The  $\beta$ -ketolactone moiety again was envisaged to be formed upon DIECKMANN cyclisation.<sup>[2]</sup> As previous work in our group had shown, a large substituent adjacent to the ring-oxygen of similar  $\beta$ -ketolactones greatly improved stability.<sup>[29]</sup> The desired propionate **123** may be derived from linear fragment **124**. This key intermediate may be retrosynthetically bifurcated by means of an all-*syn* variant of the EVANS-METTERNICH reaction.<sup>[7]</sup> As the alcohol thus formed at C7 would be oxidised later on in the sequence, its stereochemistry at this stage is inconsequential in this synthetic route. However, it may elegantly be used for an *anti*-selective reduction to achieve desired stereochemistry for propionate **123** at C5 by directed reduction with  $\text{NaHB}(\text{OAc})_3$ .<sup>[80]</sup> After this reduction, however, two secondary hydroxyl groups at C5 and C7 would have to be differentiated, which poses an interesting synthetic challenge. Notably, the all-*syn* reactivity is not contradicting the strong intrinsic diastereofacial bias of aldehyde **125**. The two hydroxyl groups in precursor **125** do not require differentiable protecting groups and thus could be protected as an acid

labile acetal. This way, necessary late stage deprotection could trigger a desired, biomimetic cyclisation at the same time and elegantly conclude the synthetic sequence.

### 3.3.2 Synthetic Progress

The first key- C–C bond formation to build up the main chain fragment of portentol (**1**) was envisaged to be achieved by means of an EVANS-METTERNICH aldol reaction.<sup>[7]</sup> In this reaction, the kinetic enolate of  $\beta$ -ketoimide **43** is formed rather than a thermodynamic enolate, which would be more stabilised by hyperconjugation. Depending on the LEWIS acid used, different stereochemical outcome may be obtained in this reaction as may be deduced from transition states **126** and **127**, depicted in Figure 14.<sup>[7]</sup>

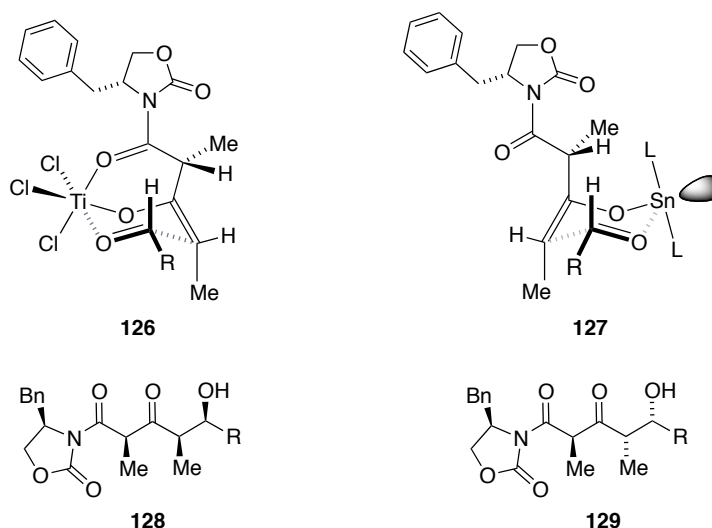
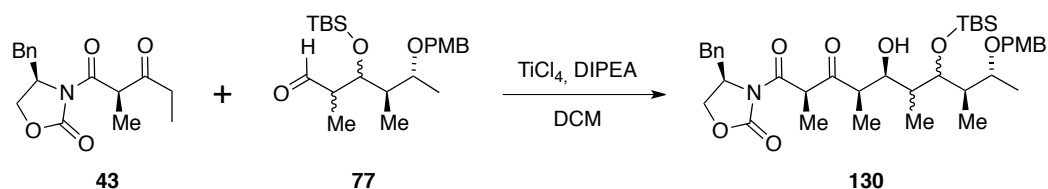


**Figure 14.** Transition states in Ti- and Sn- mediated EVANS-METTERNICH aldol reactions and corresponding stereochemical outcome

In both the titanium and the tin mediated case of EVANS-METTERNICH aldol chemistry, the kinetic *Z*-enolate is formed and is supposed to arrange with an appropriate aldehyde, forming a 6 membered ZIMMERMAN-TRAXLER transition state.<sup>[43]</sup> In both cases, the larger substituent of the aldehyde would prefer a pseudoequatorial position. Also, the logic of repulsive dipole–dipole interactions between carbonyl groups (as discussed above) applies, if not overridden by coordination to a transition metal (titanium in the case of **126**). Relative stereochemistry of different products **128** and **129** is thus determined by the facial coordination of the aldehyde in the transition state, which again is determined by the position of the auxiliary and the corresponding side chain. Whilst in transition state **127** tin does not

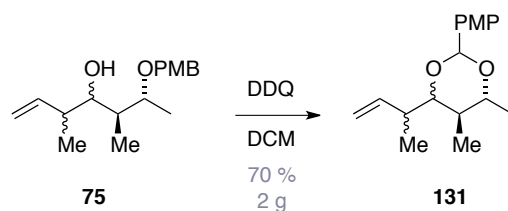
offer another coordination site, titanium tethers the auxiliary upon coordination. Therefore, the opposite site of the enolate is shielded. In case of the herein discussed (*R*)-auxiliary, the titanium mediated reaction triggers an attack on an aldehyde from the *re*-face, whereas tin as LEWIS acid leads to an attack from the *si*-face. Product **128** therefore is an “all-*syn*” adduct, whereas product **129** represents an *anti-syn*- relationship with respect to the two methyl substituents and the obtained hydroxyl group of the polyketide fragment.

To familiarise with this particular EVANS-chemistry, initial investigations towards key intermediates of portentol (**1**) were made, using corresponding aldehydes from our previous strategies bearing a PMB and a TBS protecting group (**77**).



**Scheme 35.** Initial EVANS  $\beta$ -ketoimid chemistry

Following standard literature procedures<sup>[81-83]</sup> a titanium enolate of **43** was generated at  $-40^\circ\text{C}$  to  $-10^\circ\text{C}$  upon treatment with DIPEA over the course of 1 hour. Subsequent cooling to  $-78^\circ\text{C}$  and addition of a solution of freshly prepared aldehyde **77**, prepared as discussed above (*vide infra*), it was expected to furnish a diastereomeric mixture of **130** with respect to the two diastereoisomers obtained in the ROUSH crotylation (*vide infra*). Gradual warming of the reaction mixture to  $-10^\circ\text{C}$  and quenching of the mixture with pH= 7 phosphate buffer exclusively yielded recovered  $\beta$ -ketoimide **43**, as well as small amounts of aldehyde **77** along with decomposition products. Neither crude  $^1\text{H}$  NMR analysis nor mass spectrometry suggested the formation of desired polypropionate **130**. Focus was therefore laid on a sterically less demanding aldehyde, which would also reflect the current protecting group strategies as outlined in retrosynthetic analysis in Scheme 34. As depicted in Scheme 36 synthetic investigations proceeded by converting homoallyl alcohols **75** to the corresponding PMP acetals **131** upon treatment with DDQ in the absence of water.



**Scheme 36.** Protection of homoallylic alcohol **75** as PMP acetal (**131**)

With this transformation, homoallylic alcohol **75** could not only be successfully protected as the corresponding acetal in good yields (ca. 70%) but also elegantly utilised the already installed PMB- protecting group. In contrast to lactones **75**, the obtained diastereoisomers from this sequence were obtained cleanly and allowed for unambiguous stereochemical assignment. Namely, two stereoisomers **132** and **133** were isolated from this oxidative ring closure. Careful analysis of 2D NMR spectra identified two isomers, stemming from the ROUSH crotylation as discussed above (*vide infra*). Due to its steric demand, the *para*-methoxybenzyl- substituent avoids *axial* positioning in the newly formed 6 membered acetal ring. Therefore, no further stereoisomers were observed.

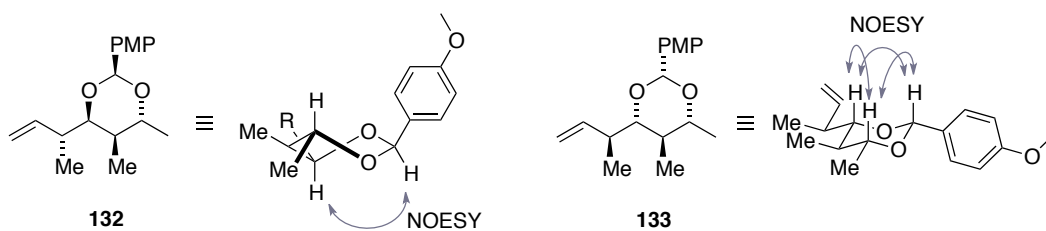


**Figure 15.** Obtained PMP acetals and NMR identification

Upon analysis of 1D and 2D  $^1\text{H}$  and  $^{13}\text{C}$  NMR spectroscopy data, protons could be assigned and their vicinity investigated upon NUCLEAR-OVERHAUSER-EFFECT spectroscopy (NOESY).<sup>[84]</sup> Indicated NOESY correlations in **133**, thus, clearly identify a chair conformation of the 6-membered ring, with the highlighted hydrogen atoms all in axial position. Desired PMP acetal **133** was unfortunately found to be the minor diastereoisomer at a ratio of **132/133** = 20/1.

In addition to discussed spectroscopic data, it was possible to grow single crystals of **133**, confirming above discussed stereochemistry.

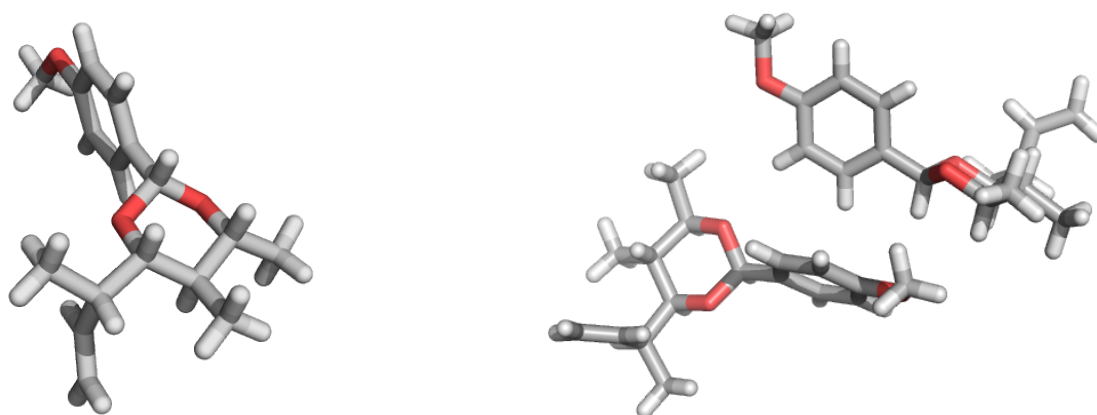
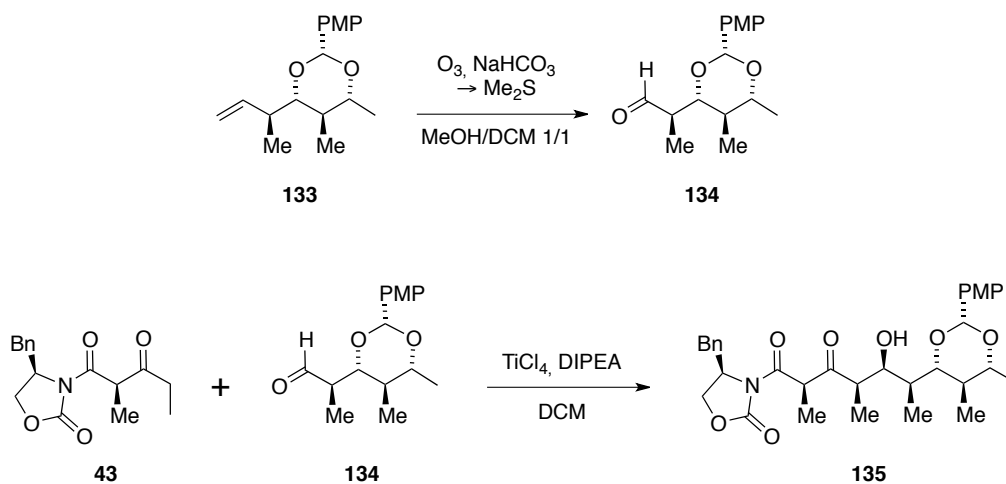


**Figure 16.** X-ray crystal structure of PMP acetal **133** (colour code: grey: carbon, red: oxygen, white: hydrogen)

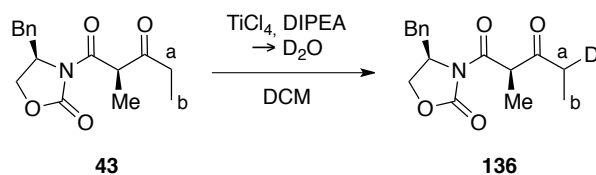
As can be seen in Figure 16, the all-*anti* relationship between the methyl and hydroxyl groups is evident in **133**, the equatorial *p*-methoxyphenyl group is oriented in an almost perfectly perpendicular fashion with respect to the two C–O bonds of the polyketide backbone. Avoiding pentane *gauche* interactions the preferred orientation of the carbon skeleton illustrates the full magnitude of the synthetic challenge of a *re*-attack on an aldehyde, which can be prepared readily from the terminal double-bond.

With the desired intermediate in hand, further investigations on the envisaged EVANS-METTERNICH reaction after conversion of **133** to corresponding aldehyde **134** by means of ozonolysis followed by reductive work up with DMS as outlined in Scheme 37 were made. This conversion proceeded in good to excellent yields, which due to its sensitivity, was assessed by crude NMR. That is, column chromatography on deactivated silica again leads to epimerisation of the  $\alpha$ -stereocentre, and consequently, crude aldehyde **134** was used in subsequent conversions.

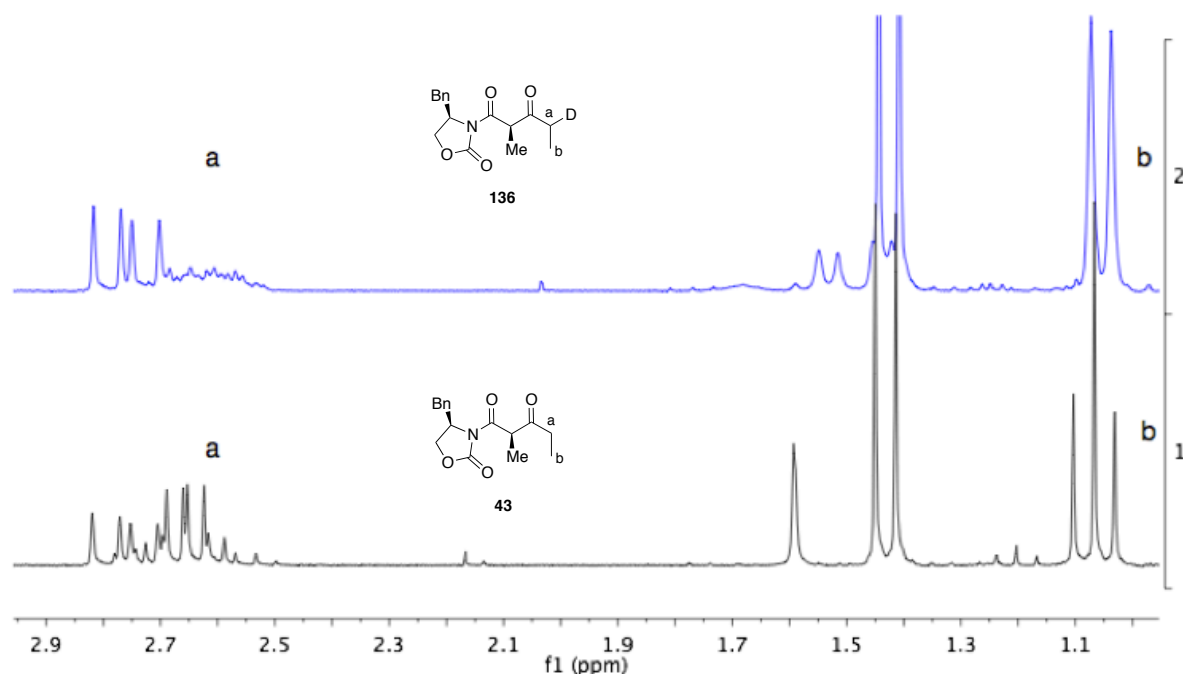


**Scheme 37.** Formation of PMP-aldehyde **134** and attempted EVANS chemistry

Several conditions were screened to synthesise the desired advanced intermediate **135**. Firstly, a titanium enolate was formed by adding  $\text{TiCl}_4$  (neat) to a solution of  $\beta$ -ketoimide **43** in DCM at  $-40^\circ\text{C}$ , followed by addition of HÜNIG's base. Upon stirring for one hour the mixture was allowed to warm to  $-10^\circ\text{C}$  and then cooled to  $-78^\circ\text{C}$  for addition of an aldehyde solution. To ensure, that the desired titanium enolate was formed, described protocol was carried out and the mixture was quenched at  $-10^\circ\text{C}$  after one hour upon addition of  $\text{D}_2\text{O}$  as depicted in Scheme 38.



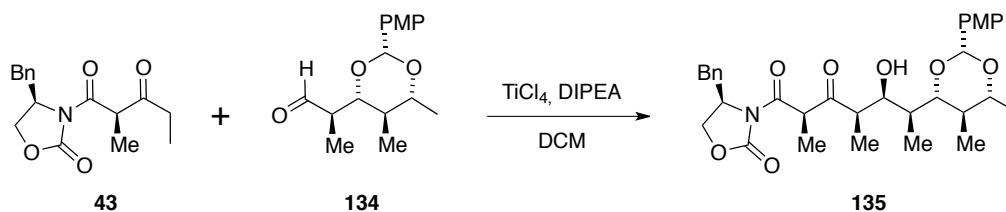
**Scheme 38.**  $\text{D}_2\text{O}$  quench of titanium enolate of **43**



**Figure 17.**  $^1\text{H}$  NMR spectra of **43** and its deuterated analogue **136**

Figure 17 compares the  $^1\text{H}$  NMR spectra of **43** (black trace 1) and the spectrum of isolated, deuterated analogue **136** (blue trace 2). Indicated  $\alpha$ -protons “a” of imide **43** appear as multiplet between 2.5 and 2.8 ppm with an integration of 2, whilst protons “b” from the terminal  $\text{CH}_3$  group can be seen as triplet around 1.1 ppm. After enolisation and subsequent trapping by  $\text{D}_2\text{O}$ , the blue spectrum indicates an altered multiplet structure in the region of 2.6 ppm, the area of which now only integrating to 1. This confirms, that a titanium enolate was successfully formed, and deuterated quantitatively. Altered multiplicity of b (doublet in blue trace) confirms the formation of the kinetic enolate and consequently formation of product **136**. Accordingly, this enolisation protocol was used in all screenings.

The reaction therefore was investigated regarding reaction time, temperature and quenching methods. Enquired conditions and observations are summarised in Table 8.

**Table 8.** EVANS-METTERNICH screening with **134**

entry	equivalents			t [h]	T [°C]	work up	observation
	$\text{TiCl}_4$	DIPEA	aldehyde				
1	1.1	1.1	1	3.5h	-78°C (0.5h) to -10°C	phosphate buffer aq.	no product formation
2	1.1	1.1	1	3.5h	-78°C	phosphate buffer aq.	no product formation
3	1.1	1.1	1	15h	-78°C	phosphate buffer aq.	no product formation
4	1.1	1.1	1	40.5h	-78°C (40h) to -40°C	phosphate buffer aq.	no product formation
5	2.2	2.2	1	4.5h	-78°C (4h) to -40°C	phosphate buffer aq.	no product formation
6	1.4	1.4	1	40h	-78°C	phosphate buffer aq.	no product formation
7	1.4	1.4	1	4h	-78°C to -40°C	phosphate buffer aq.	no product formation
8	1.4	1.4	1	4h	-78°C to -40°C	phosphate/ MeOH	no product formation
9	1.4	1.4	1	4h	-78°C to -40°C	citric acid buffer	no product formation

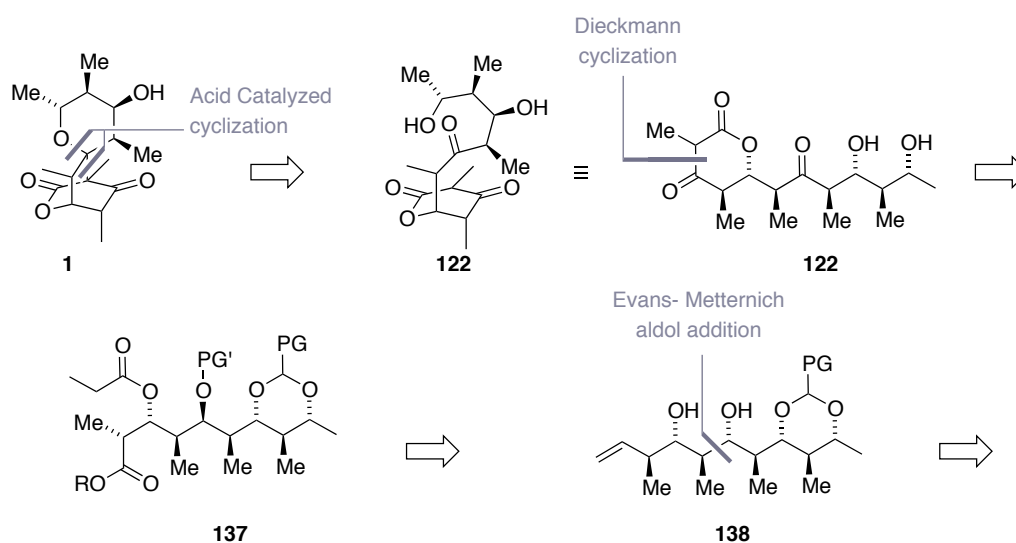
Equivalents refer to 1 equivalent of ketoimide **43**

Unfortunately none of the screened condition produced desired intermediate **135**. As the successful formation of the titanium enolate had been shown, low reactivity of aldehyde **134**, presumably due to peculiar steric demand of the all-*anti* configuration was considered. Another plausible explanation of initial unsuccessful results was the possibility of a retro aldol reaction occurring upon work up. A special focus thus was laid on the quenching method (entries 6 to 9), unfortunately also leaving no indication of desired product **135**. Only starting materials were recovered from all reactions. While imide **43** could be recovered

almost quantitatively, aldehyde **134** epimerised upon column chromatography (as observed for similar systems previously). Also, NMR analysis of by-products indicated, that the PMP acetal had been opened upon reaction conditions. Though several examples of titanium mediated all-*syn* modification of this very reaction are found in literature, some of which also with sterically demanding aldehydes,<sup>[85,86]</sup> the titanium-mediated reaction appears to be delicate towards reaction with sterically highly demanding aldehydes such as **134**.

### 3.3.3 Revised Retrosynthetic Analysis

At this point, we turned our focus on a novel methodology of particular efficiency in challenging mismatched double asymmetric crotylboration, developed by ROUSH and co-workers.<sup>[8,87]</sup> Considering this methodology as an alternative to the EVANS-METTERNICH-aldol chemistry, the retrosynthetic analysis was adapted accordingly (Scheme 39).

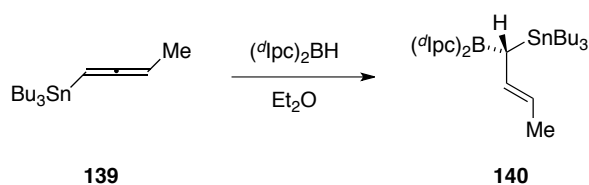


**Scheme 39.** Adopted retrosynthetic analysis for chain approach

In this retrosynthetic analysis, the previously discussed precursor **122** could be derived from **123** by means of a DIECKMANN cyclisation again, which may be prepared from homoallylic alcohol **138**. In contrast to the previous retrosynthetic analysis, this revised strategy does not require a directed reduction and subsequent differentiation of two alcohols but allows to directly set the C5 and C7 stereogenic centres of **138**. Therefore a directed reduction remains unnecessary.

### 3.3.4 Synthetic Progress

The novel methodology features a chiral reagent, derived from a racemic mixture of allenylstannane ( $\pm$ **139**) that undergoes hydroboration with ( $d^4$ Ipc) $_2$ BH, as depicted in Scheme 40.



**Scheme 40.** Hydroboration of racemic allenylstannane **139**

The striking fact, that both enantiomers of the allenylstannane may be used to derive the same reagent (**140**) is based on suprafacial 1,3-borotropic shifts, which occur fast and fully stereospecific.<sup>[87]</sup> This way, the stereoselectivity of the initial hydroborations occurring on both stannanes is “transported” to the resulting stereogenic centre, leading to reagent **140**. Though geminal positioning ( $d^4$ Ipc)-borane and *tri*-butylstannyl- residues appears sterically unfavourable, DFT-calculations provide convincing evidence that positive interactions of the C–Sn bond to the empty p orbital on boron greatly support the formation of **140**.<sup>[88]</sup>

ROUSH and co-workers showed, that formed reagent **140** was highly successful in the crostannylation of aldehydes with  $\beta$ -branches so we judiciously chose this reagent to solve the problem of previously discussed ROUSH crotylation with aldehyde **62** (Figure 18).

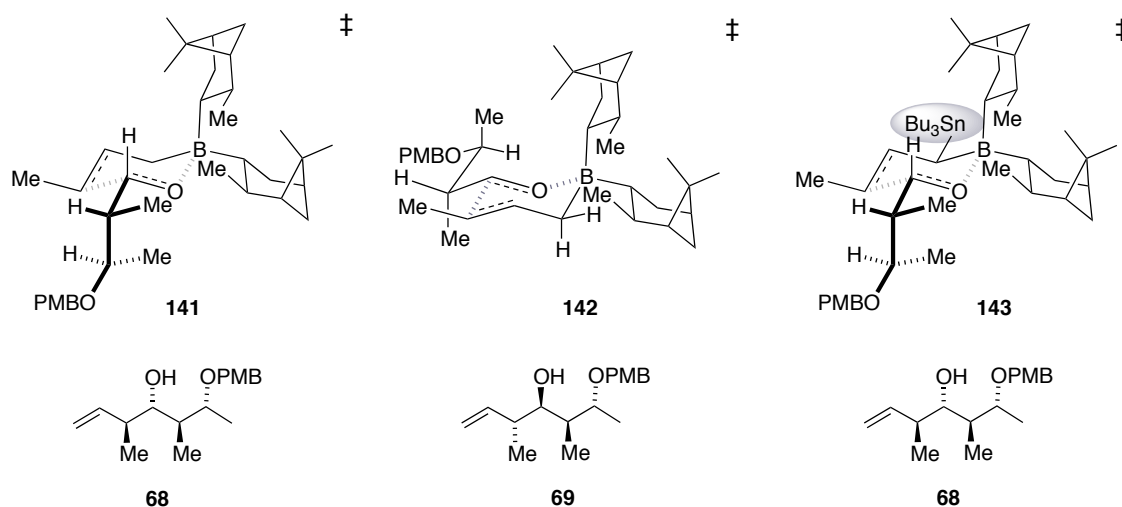
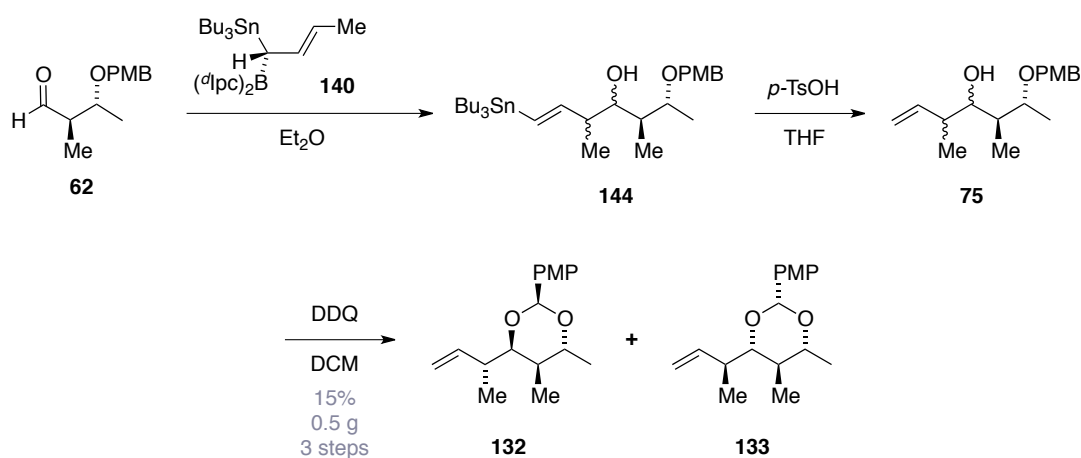


**Figure 18.** Transition states of  $d^4$ Ipc-borane derived crotylation reagents and stereochemical outcome

The increased diastereoselectivity of ROUSH's novel methodology may be explained considering resulting transition states with aldehyde **62**. Comparing transition states of the standard <sup>d</sup>Ipc-borane derived crotylation agent with discussed aldehyde **62** (mismatched case), transition state **141** again may cause adverse pentane *gauche* interactions and disfavour the *anti*-selective crotylation. Alternatively, undesired product **69** may be obtained as major product by a reaction, proceeding *via* transition state **142**, wherein *gauche*-interactions would be avoided, upon coordination of the aldehyde from the opposite site. This way a *si*-attack of the double bond would occur. Novel, tributylstannyl containing reagent **140** on the other face fully shields the rear coordination site, thus forcing the aldehyde towards coordination on the front site, as depicted in transition state **143**.



**Scheme 41.** Sequence to obtain PMP acetal **133** using ROUSH's novel methodology

As displayed in Scheme 41, it was envisaged to also use this novel methodology to obtain **133** in larger quantities. Thus, aldehyde **62** was reacted with reagent **140** to obtain stannane **144**, at which stage isopinocampheol by-products could not be separated from the product by means of flash column chromatography. The sequence was thus carried on upon treatment of the obtained mixture with *p*-TsOH. After protodestannylation,<sup>[89]</sup> the mixture of homoallylic alcohols **75** was converted into corresponding PMP-acetals. Unfortunately, the overall yield for this sequence did not exceed 15% for both diastereomers **132** and **133**. Disappointingly, the desired PMP-acetal **133** was the minor product, at a ratio of about 20/1. Apparently, aldehyde **62** represents an unsuitable substrate for this novel, double asymmetric crotylation methodology. Indeed, the traditionally used isopropyltartrate based boronate **64** delivers better results for aldehyde **62**.

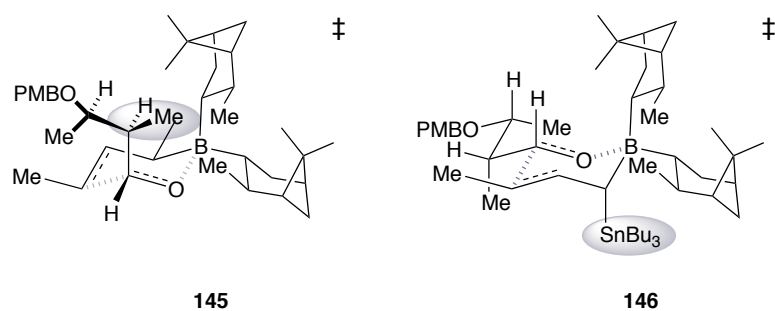
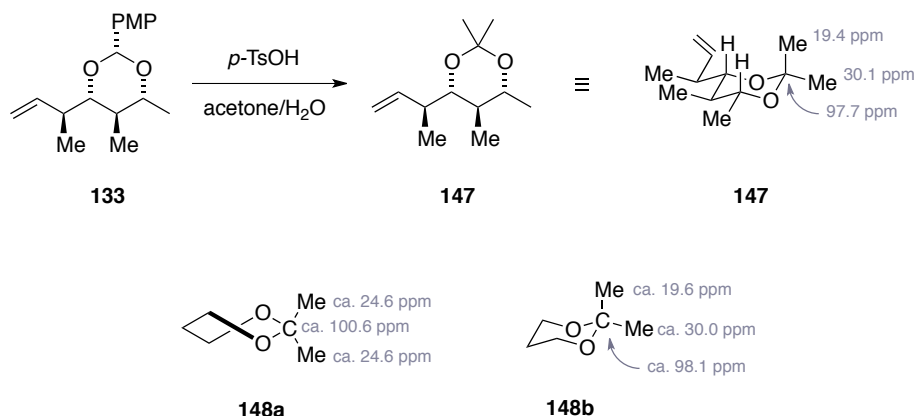


**Figure 19.** Possible transition states yielding undesired *syn*-crotylation

The fact that aldehyde **62** can “override” the diastereoselectivity of novel reagent **140** cannot be directly deduced from the transition states discussed by ROUSH and co-workers.<sup>[8,89]</sup> The six membered ZIMMERMAN–TRAXLER transition state<sup>[43]</sup> does not provide a reasonable explanation for the observed diastereoselectivity, but infers a three dimensional orientation of the aldehyde side chain. The distinct stereochemistry of the  $\beta$ -branch conflicts with the orientation of the aldehyde (**62**) in the transition state. As suggested in transition states **145** and **146** (Figure 19), undesired *syn*-crotylation could be conveyed from a pseudoaxial positioning of the large aldehyde residue, pointing towards the viewer in this projection (**146**), or upon coordination of aldehyde **62** from the other site of the boron atom. The latter case would, however, lead to a pseudoaxial position of the sterically demanding  $\text{Bu}_3\text{Sn}$  group. Then the reaction would yield the all-*syn* product, which was not observed. Thus, this transition state does not occur. Though both cases do not appear to be optimal, the double asymmetric, mismatched crotylation leading to desired homoallyl alcohol **68** could only be observed as a minor product. It seems, that substrate **62** represents a borderline case, wherein the steric demand of a methyl group as the  $\beta$ -branch is just enough to override selectivity of known crotylation reagents, yet be small enough to adopt an alternative transition state (either **145** or **146**), by comparison all show cases published by ROUSH and co-workers indeed featured substantially larger  $\beta$ -branches.<sup>[8]</sup>

Although the desired homoallylic alcohol **68** represented the minor product, 1.5 g of PMP-acetal **133** could be obtained using ROUSH’s old protocol. The use of the novel methodology was envisaged for this more advanced intermediate. We also decided to exchange PMP protecting group at this stage with an acetonide, thus decreasing steric bulk and increasing reactivity. This swap still allowed the overall strategy to trigger an acid catalysed cyclisation after diol deprotection. Accordingly, PMP acetal **133** was stirred in

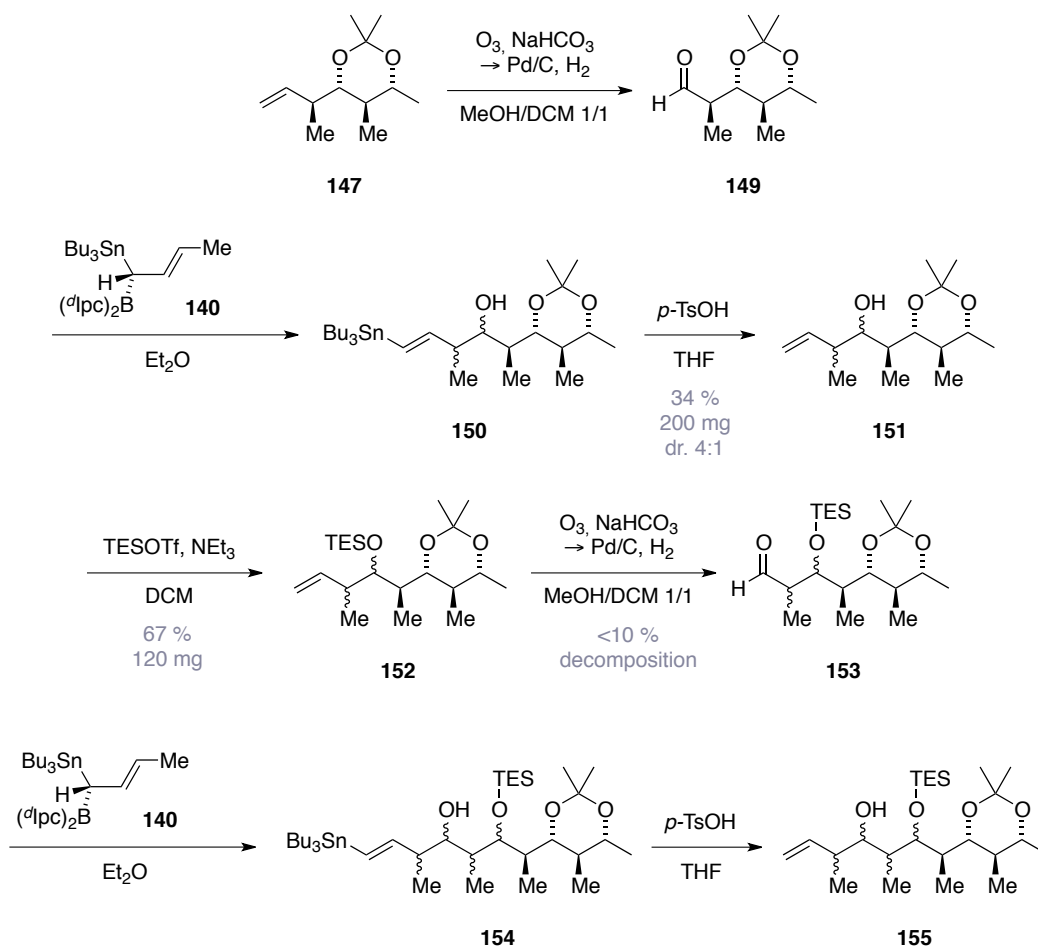
acetone in the presence of stoichiometric amounts of water and catalytic amounts of *p*-TsOH (Scheme 43).



**Scheme 42.** Swapping the 1,3-diol protecting group and conformational analysis

Although at best only 50% conversion to acetonide **147** was achieved (96% b.o.r.s.m.) repeatedly resubjecting the recovered starting material lead to full conversion. At this stage, relative stereochemistry of **147** was confirmed based on RYCHNOVSKY'S  $^{13}\text{C}$  NMR studies on the influence of chair and twist boat conformations on the chemical shifts of acetonide carbon atoms.<sup>[90]</sup> As outlined in Scheme 42, a twist boat conformation (**148a**) results in a chemical shift of the tetrasubstituted carbon of ca. 100.6 ppm, whereas both methyl carbon atoms are found at ca. 24.6 ppm. In contrast, a chair conformation (**148b**) shifts the tetrasubstituted carbon atom of the protecting group to ca. 98.1 ppm. Also, the two methyl groups feature distinct chemical shifts due to an axial (ca. 19.6 ppm) and an equatorial (ca. 30.0 ppm) orientation. The  $^{13}\text{C}$  signals of compound **147** could be assigned unambiguously using 2D NMR experiments and revealed chemical shifts of the corresponding carbon atoms of 19.4, 30.1 and 97.7 ppm chemical shifts, clearly confirming the chair conformation of the six membered ring in **147**. Additionally, NOESY correlations between the axial protons and the axial methyl group of the acetonide were observed.

With intermediate **147** in hand, advanced C-C bond formations could be studied, as depicted in Scheme 43.



Scheme 43. Synthesis of advanced portentol-intermediates

Hydrophobic acetonide **147** appeared to be volatile upon evaporation at ambient temperature and extremely volatile upon removal of residual solvent on high vacuum. To minimise loss of material in the subsequent ozonolysis, a reductive work up by means of hydrogenolysis with palladium on activated charcoal in a solvent mixture of DCM/MeOH was chosen. Simple filtration over a celite plug, followed by standard aqueous work up thus cleanly furnished aldehyde **149** without the need of column chromatography. With aldehyde **149** in hand, crotylation was applied to obtain stannane **150** which was directly subjected to the protodestannylation protocol mentioned above (*vide infra*).<sup>[89]</sup> At this stage, it was possible to remove isopinocampheol derivatives and isolate homoallylic alcohol **151** as a 4/1 mixture of diastereoisomers. At this point, it was decided to proceed this synthetic route and see, if the final asymmetric crotylation could be achieved (as the final C3 fragment would be installed upon acylation). Therefore, homoallylic alcohols **151** were TES protected as preliminary test reactions on previous systems revealed issues in attempts to remove a more stable TBS group. This sterically demanding protection was successfully achieved using TESOTf which afforded the desired protected alcohol in 67% yield on a 120 mg scale. With

TES protected intermediate **152** in hand, another ozonolysis, followed by reductive work up was attempted. Though conversion of **152** to its corresponding ozonide proceeded in a spot to spot reaction (according to TLC-analysis), decomposition occurred upon reductive work up. Aldehyde **153** was thus obtained in low yield (ca. 10 % according to  $^1\text{H}$  NMR analysis of the crude mixture) along with unidentified by-products. For reasons discussed above, the crude mixture was directly subjected to double asymmetric crostannylation, to give envisaged product **154**, followed by protodestannylation to obtain advanced intermediate **32**. Unfortunately, no indication of stannane **154** after neither asymmetric C-C bond formation, nor homoallylic alcohol **32** could be observed after this sequence.

### 3.3.5 Conclusion and Strategic Considerations

The third conceptual approach towards a total synthesis of portentol (**1**) envisaged a late stage cyclisation approach, wherein the carbon backbone of portentol (**1**) was to be achieved by means of asymmetric EVANS-METTERNICH aldol chemistry or a novel crostannylation, introduced by ROUSH and co-workers. The latter method was also used to address the previously observed material loss in formation of the C8–C9 bond in portentol (**1**). The immense intrinsic diastereoselectivity of corresponding aldehyde **62** could, however, not be overridden successfully. Thorough investigations on EVANS-METTERNICH chemistry did not lead to desired intermediates. As a consequence, a final attempt focused on ROUSH's novel methodology with sterically demanding, late stage aldehydes, such as **149**.

In the course of these final synthetic studies, novel intermediates were prepared. The relative stereochemistry could not be assigned based on 2D NMR experiments. For lack of material, no cyclic derivatives, allowing for an unambiguous assignment of newly formed stereogenic centres, could be prepared. The final sequence used an extremely sterically demanding aldehyde **153** and was unfortunately met without success. Due to the extensive efforts we employed in attempt to overcome steric biases in this system, we do not expect the intrinsic crowding in our strategies to be easily overcome through modern organic techniques. Rather, an alternative synthetic strategy could be preferred. Our findings shed light into the fact that portentol (**1**) has not been synthesised despite the fact that it was isolated more than four decades ago.

## 4 SUMMARY AND OUTLOOK

Portentol (**1**) remains an intriguing and highly challenging substrate for modern organic chemistry and addresses the most difficult tasks in asymmetric aldol and crotylation chemistry. As all synthetic studies on this molecule show, the increasing steric demand of advanced intermediates calls for a synthetic strategy, wherein key C–C bond formations should be performed as early in the sequence as possible. Final complexity of the unique portentol skeleton should be achieved in a biomimetic, acid catalysed cascade reaction.

Three different synthetic approaches towards a total synthesis of portentol **1** were investigated thoroughly in the course of this work. The first strategy, which was referred to as the “double DIECKMANN” approach, featured  $\beta$ -ketolactone **44** as a first key intermediate. As this compound displayed a highly unstable nature and could not be converted into isolable intermediates, a first synthetic rerouting envisaged an asymmetric crotylation and late stage lactonisation to derive TBS protected  $\beta$ -hydroxylactone **56**.

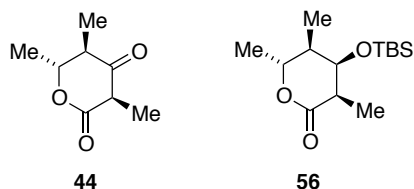


**Figure 20.** Envisaged key intermediate **44** and synthetically elaborate TBS protected compound **56**

The synthetic sequence to obtain lactone **56** firstly revealed the extremely high intrinsic diastereofacial selectivity of the  $\beta$ -branched aldehydes, necessary for the correct stereochemistry in the carbon backbone of portentol (**1**). As the desired all-*anti* isomer was shown to be the minor product in a double asymmetric crotylation and a large-scale synthesis of lactone **56** was not feasible, the search for a more convergent approach inspired the second synthetic route towards a total synthesis of portentol (**1**), the “DIELS-ALDER” approach.



**Figure 21.** EFFENBERGER's pyrone **82** and its first X-ray crystal structure

Investigating this second synthetic route, literature known pyrone (**82**/ Figure 21) was synthesised and thoroughly tested as a highly challenging diene in inverse electron demand DA-reactions. Unfortunately, this ambitious DA- reaction could not be accomplished. As synthetic approaches towards the synthesis of the corresponding dienophile proved difficult too, a new strategy was developed, wherein state of the art, asymmetric methodologies were tested to elaborate the highly challenging all-*anti* backbone of portentol (**1**).

Systematically investigating different synthetic options, acetals **133** and **147** were successfully prepared and fully characterised (Figure 22).

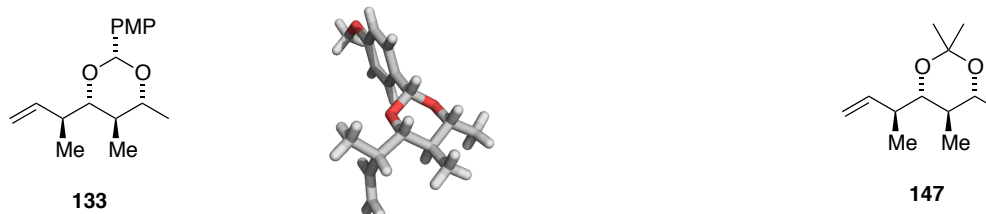


**Figure 22.** PMP acetal **133** with X-ray crystal structure and acetonide **147**

These advanced intermediates were the basis upon which further C-C bond formations were tested. Utilising a novel methodology introduced by ROUSH and co-workers, as a key step, highly complex intermediate **152** was synthesised.

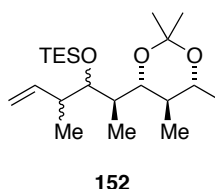
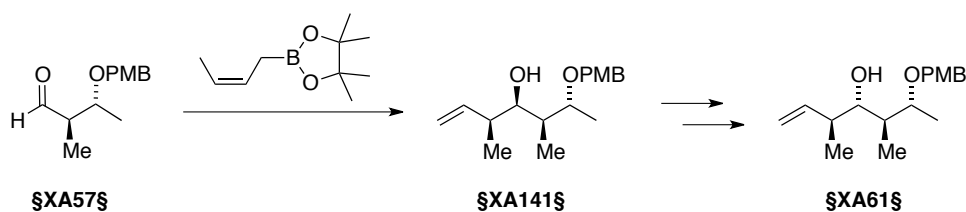


**Figure 23.** Advanced intermediate **152**

The TES protected homoallylic alcohol **152** (Figure 23) has six stereogenic centres and represents a synthetic equivalent of a C<sub>10</sub> fragment of portentol (**1**) framework.

Although a total synthesis of the highly complex polyketide natural product portentol (**1**) was not achieved in the course of this project, the work presented in this thesis represents a profound basis for future synthetic investigations and systematically covers reactivity and characteristics of highly functionalised, complex intermediates. Limits, perspectives and future challenges in the field of highly asymmetric carbon-carbon bond formation reactions were investigated and discussed in the context of mechanistic considerations and three dimensional transition states. In addition to detailed insights into the diastereoselectivity of mismatched, double asymmetric reagents, four new X-ray crystal structures were obtained in this work.

As the intrinsic diastereoselectivity of corresponding aldehyde intermediates pose a seemingly insurmountable problem, alternative strategies should be considered to build up the intermediates, such as **147**. Though less step economic, all-*syn* crotylation approaches, followed by stereochemical inversion of hydroxyl bearing stereogenic centres, may be considered. As depicted in Scheme 44, such a future approach may potentially deliver larger quantities of key intermediate species.



**Scheme 44.** Matched asymmetric crotylation to all-*syn* intermediate **88** as a potential precursor for building block **65**

The novel crotylation methodology, discussed in the last section of this chapter, still appears to be the most promising tool on the way to establish a total synthesis of portentol (**1**). Establishing a reliable route to deliver large quantities of suitable precursors, the issue of diastereoselectivity of this method may be addressed and ultimately lead to suitable precursors to attempt a final cyclisation cascade.



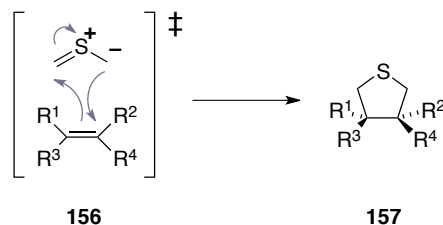


**CHAPTER II:**  
**THIOCARBONYL YLID BASED 1,3-DIPOLES**



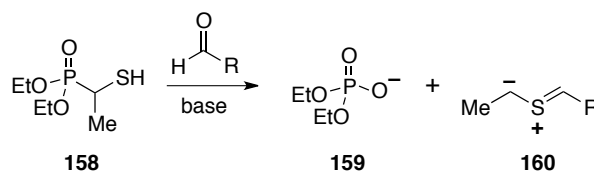
# 1 PROJECT AIMS

Cycloadditions are an elegant and powerful tool in modern organic synthesis, creating complex and highly functional molecules in a stereoselective and convergent way. In this context, [3+2] cycloadditions have proven effective reactions, proceeding cleanly and often upon benign reaction conditions. Pioneering work of HUISGEN and co-workers established many 1,3-dipoles as suitable reaction partners in [3+2] cycloadditions, among which also thiocarbonyl ylides were found. As there is an on going interest in the development of novel reagents for organic chemistry, and thio centred 1,3-dipoles belong to the lesser well described and investigated systems, this project focused on thiocarbonyl ylides as reactants for 1,3-dipolar cycloadditions.



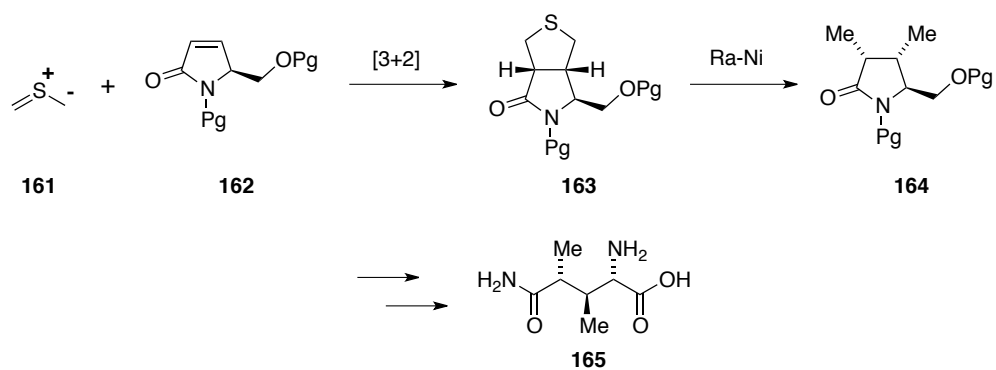
**Scheme 45.** Simplest thiocarbonyl ylid reacting with a tetrasubstituted double bond to yield tetrahydrothiophene derivative **156**

In a first stage of this project, thiophosphonates were to be investigated as novel precursors for the generation of thiocarbonyl ylides **160**. The formation of 1,3-dipoles and further reactivity in cycloadditions should be tested and was envisaged to follow HORNER-WADSWORTH-EMMONS type reaction pathways starting from thiophosphonate **158**.



**Scheme 46.** Thiocarbonyl ylid from thiophosphonate **158**

Another aspect of this project focused on an intriguing, yet comparatively rarely used reagent, which should be revisited for catalysis and also be used in a show case formal synthesis of L-dimethylglutamine.



**Scheme 47.** Envisaged key-sequence in the formal synthesis of dimethylglutamine

As depicted in Scheme 47, two methyl groups in **164** would be introduced in a two-step sequence. Herein [3+2]-cycloaddition of thiocarbonyl ylid **161** over the electron poor double bond in **162** followed by hydrogenolysis of intermediate **163**, should give a key intermediate in a formal synthesis of dimethylglutamine. The sulphur atom in **163** could be “erased” by RANEY nickel. This two-step sequence would thus represent an elegant synthetic equivalent to the addition of ethane over a double bond, an intriguing challenge in modern organic chemistry.

## 2 INTRODUCTION

### 2.1 [3+2] Cycloadditions: Background and Significance

In 1938, SMITH reviewed the concept of then called 1,3-additions, presenting numerous 1,3-dipoles (Figure 24) and their addition over double bonds.<sup>[91]</sup> The great potential of these compounds to furnish novel 5-membered heterocycles by means of one transformation, a 1,3-dipolar cycloaddition, is reflected by the fact that many of the most prominent organic chemists of this generation had contributed to this field.

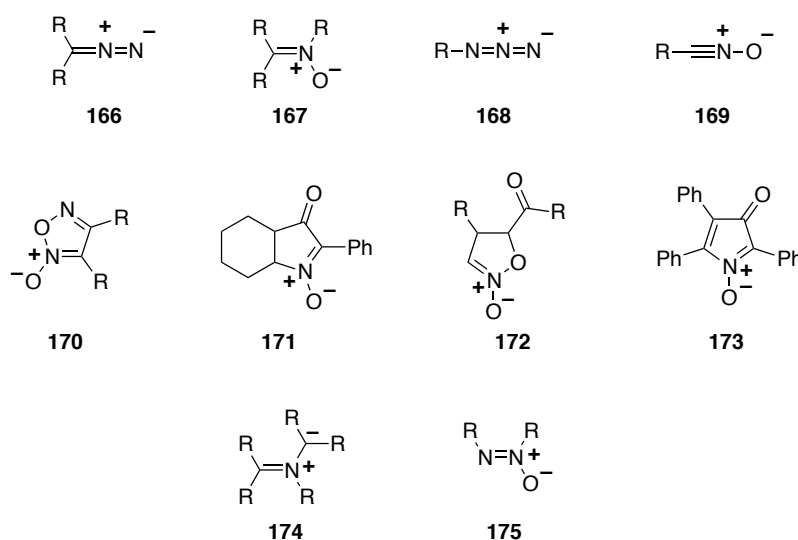


**Figure 24.** First generation 1,3-dipoles used in cycloadditions

At this point, aliphatic diaza compounds, which had first been described by CURTIUS **166**,<sup>[92]</sup> nitrones **167**, azides **168** and nitrile oxides **169** had been successfully used in 1,3-dipolar cycloadditions. Non-aliphatic systems, such as WIELAND's and SEMPER's furoxans **170** and isatogens **171**,<sup>[93]</sup> isoxazoline oxides **172** as well as cyclic nitrones **173** by KOHLER or STAUDINGER's nitrenes **174** and azoxy compounds **175**,<sup>[94]</sup> had also been used as 1,3-dipoles in cycloaddition reactions. Since then, an overwhelming number of different 1,3-dipoles have been introduced and found their way into modern organic chemistry. Equally, the range of reaction partners, so-called dipolarophiles is vast. In essence, two atoms connected *via* an unsaturated bond, may be adequate reaction partners. Systematic work by HUISGEN and co-

workers later mapped out the rich field of 1,3-dipolar cycloadditions and unclosed detailed mechanistic understanding of this reaction type to the chemical community.<sup>[95]</sup>

In general, 1,3-dipolar cycloadditions are [3+2] cycloadditions, which form uncharged 5-membered rings. The 1,3-dipole may be a molecule or molecule fragment.<sup>[95]</sup> One atom is required to bear an electron sextet. Hence, this atom possesses an incomplete valence shell and a positive charge. Another atom needs to carry a negative charge, thus forming a dipole. Typically, such systems may be achieved upon octet stabilisation (see resonance structures in Scheme 48). In such cases, central atom b may serve as a  $\pi$ -donor. Consequently, a resonance structure is obtained, wherein the central atom b now carries the positive charge. In most cases, nitrogen or oxygen atoms are found in central position of 1,3-dipoles. Sulphur, in contrast, is found less often, but serves equally well as an octet stabilising atom for such dipoles.

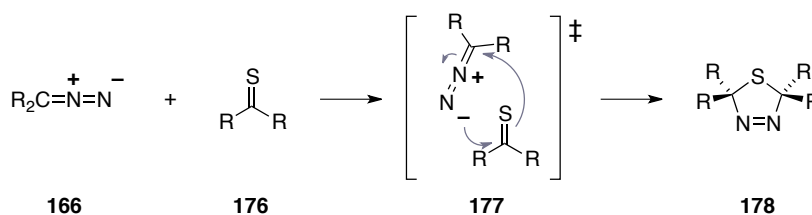


**Scheme 48.** Generic description of 1,3-dipolar cycloadditions

In the course of a reaction with a suitable dipolarophile, a cyclic electron shift of two  $\pi$ -electrons of the dipolarophile and four  $\pi$ -electrons of the dipole occurs in a concerted fashion similar to a DIELS-ALDER cycloaddition. Analogously, also two new  $\sigma$ -bonds are also formed at the expense of two  $\pi$ -bonds, building up a 5-membered ring (Scheme 48).<sup>[95]</sup>

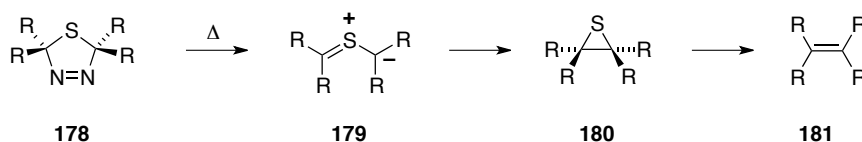
## 2.2 Thiocarbonyl Ylides: Formation and Reactivity

Due to their reactivity, thiocarbonyl ylides are normally formed *in situ* and classified according to their type of formation. For example, formation of thiocarbonyl ylides by extrusion of nitrogen from 1,3,4-thiadiazoles **178** is a popular method (Scheme 49).<sup>[95]</sup> These dihydrothiadiazoles are readily available, for instance, from 1,3-dipolar cycloadditions of diazomethane derivatives **166** and thiones **176** (Scheme 49).



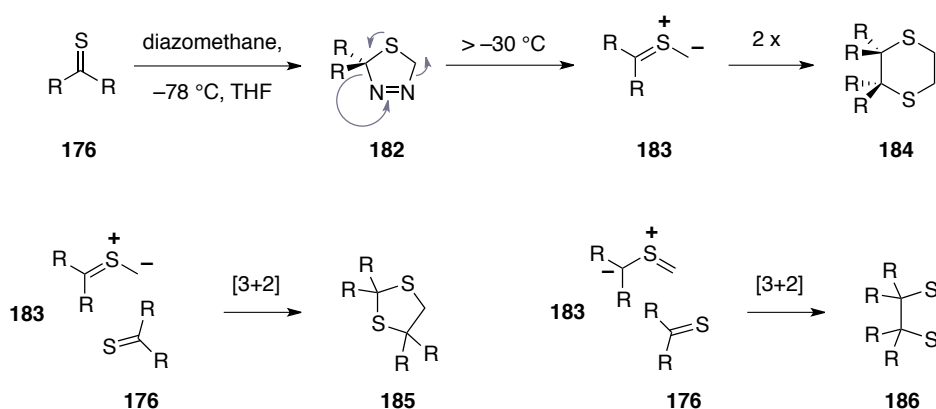
**Scheme 49.** 1,3-dipolar cycloaddition of diazomethane derivative **166** over thione **176**

Dihydrothiadiazoles were investigated thoroughly by several groups starting in the 1970s. Some fundamental work regarding their reactivity as 1,3-dipoles was achieved in the groups of MIDDLETON<sup>[96]</sup>, KRAPCHO<sup>[97]</sup> and KELLOGG.<sup>[98]</sup> In a typical reaction pathway of thiocarbonyl ylides **179**, the conrotatory electrocycloisatation to thiiranes **180** upon pyrolysis of thiadiazoles was described. Further extrusion of sulphur ultimately yields alkenes (**181**), as outlined in Scheme 50.



**Scheme 50.** Reactivity of thiocarbonyl ylides derived from generic thiadiazole **178** upon pyrolysis

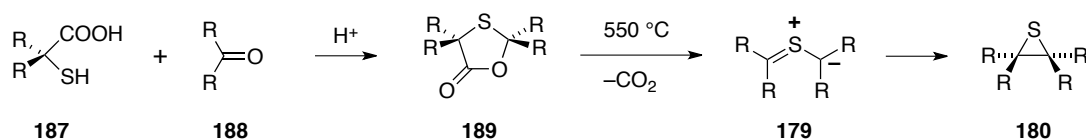
Using milder reaction conditions, HUISGEN and co-workers used diazomethane-derived thiadiazoles to generate thiocarbonyl ylides (Scheme 51). Those were successfully reacted pair wise, giving 1,4-dithianes,<sup>[99]</sup> but also could undergo [3+2] cycloadditions with thiones as dipolarophiles.<sup>[100]</sup>



**Scheme 51.** Further reactivity of thiocarbonyl ylides derived from diazomethane and generic thiones

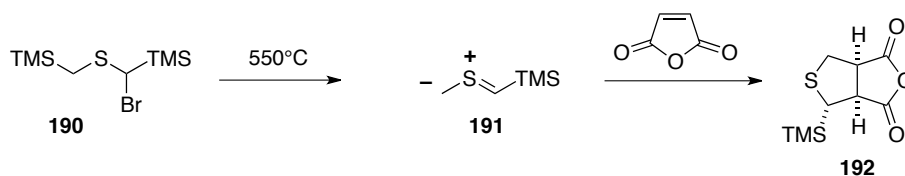
As depicted in Scheme 51, thiadiazanes **182**, derived from diazomethane, form their corresponding dipoles **183** already at much lower temperatures and may, consequently, dimerise to form **184**. Notably, in the case of cycloadditions with thiones **176**, regioselectivity is largely governed by the sterical and electronic nature of substituents R.<sup>[100]</sup> Reacting dipole **183** with thione **176** thus yields 1,3-dithiolanes **185** or **186**.

A conceptually related option for the generation of thiocarbonyl ylides was presented by PINNICK and co-workers.<sup>[101]</sup> Reacting  $\alpha$ -mercapto carboxylic acid **187** with ketones **188** under acidic conditions furnishes 1,3-oxathiolan-5-ones **189**. Upon thermal extrusion of CO<sub>2</sub>, thiocarbonyl ylides **179** are obtained. As previously discussed, again these reaction conditions lead to fast transformation of the ylides to thiirane derivatives **180** (Scheme 50).



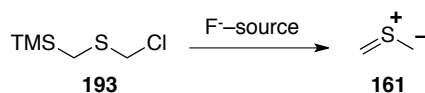
**Scheme 52.** Formation of thiocarbonyl ylides *via* extrusion of CO<sub>2</sub>

In 1985, ACHIWA and co-workers introduced a milder way to furnish thiocarbonyl ylides by thermal extrusion of TMSBr, starting from precursor **190**.<sup>[102]</sup> The formed ylid **191** was successfully reacted with different cyclic and acyclic MICHAEL-systems such as maleic anhydride to give the corresponding cycloadducts **192** (Scheme 53).



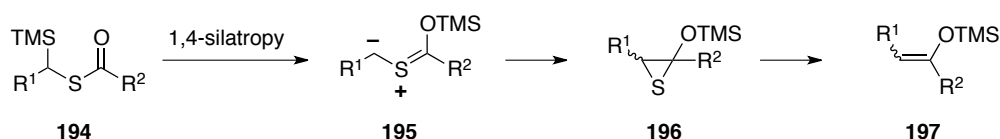
**Scheme 53.** ACHIWA's methodology to create thiocarbonyl ylides by TMSBr extrusion/ subsequent cycloaddition

One year later, SAKURAI and co-workers introduced a structurally related reagent, namely **193**.<sup>[103]</sup> The conceptual difference rests upon the mode of TMS-halide extrusion. Herein an external fluoride source initiates the dipole formation upon generation of TMSF, while chloride acts as a leaving group. **161** can be generated at ambient temperatures and also is the simplest representative of this group of highly reactive dipoles.



**Scheme 54.** The simplest thiocarbonyl ylid (**161**) derived from SAKURAI's reagent

More recently, 1,4-silatropy of  $\alpha$ -silyl thioesters was introduced to generate thiocarbonyl ylides.<sup>[104]</sup> Due to the strength of silyl–oxygen bonds, the TMS migration of intermediates **194** leads to thiocarbonyl ylides **195**. As high reaction temperatures are required, formation of thiirane derivatives **196** and subsequent sulphur extrusion is observed. This strategy represents a novel way to synthesize TMS enol ethers such as **197**.



**Scheme 55.** 1,4-silatropy generating thiocarbonyl ylides

## 2.3 Dimethylglutamine: Background and Synthetic Approaches

The nonproteinogenic  $\alpha$ -amino acid (3*S*, 4*R*)-Dimethyl-L-glutamine (**165**/ Figure 25) was first encountered by MINABLE and co-workers during their characterisation of callipeltin A (**198**), a natural product, which was isolated from the shallow water Lithistida sponge *Callipelta sp.* in the waters off New Caledonia.<sup>[105]</sup> Callipeltin A (**198**) has been found to protect cells infected by the HI- virus<sup>[106]</sup> and shows antifungal<sup>[106]</sup> as well as antitumor activity against several different tumour cell lines.<sup>[107]</sup> Also, compound **165** is incorporated in papuamides A–D, isolated from sponges *Theonella mirabilis* and *Theonella swinhoei* found in Papua New Guinea.<sup>[108]</sup> Papuamide A and B both inhibit the infection of human T-lymphoblastoid cells by HIV-1<sub>RF</sub> in vitro, while papuamide A is also cytotoxic against a panel of human cancer cell lines.<sup>[108]</sup>

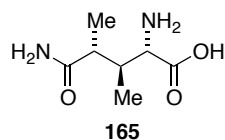


**Figure 25.** (3*S*, 4*R*)-Dimethyl-L-glutamine

Upon heating (3*S*, 4*R*)-Dimethyl-L-glutamine (**165**), water is eliminated, forming the nonproteinogenic cyclic  $\alpha$ -amino acid (3*S*, 4*R*)-Dimethyl-L-pyrroglutamic acid, which is found in the cyclic depsipeptide callipeltin B (**199**). This compound was also isolated from the shallow water Lithistida sponge *Callipelta sp.* and has been found to be cytotoxic against various human carcinoma cells.

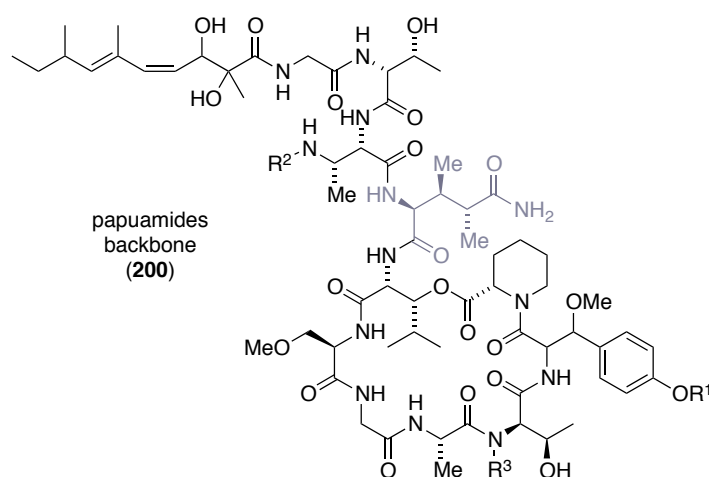
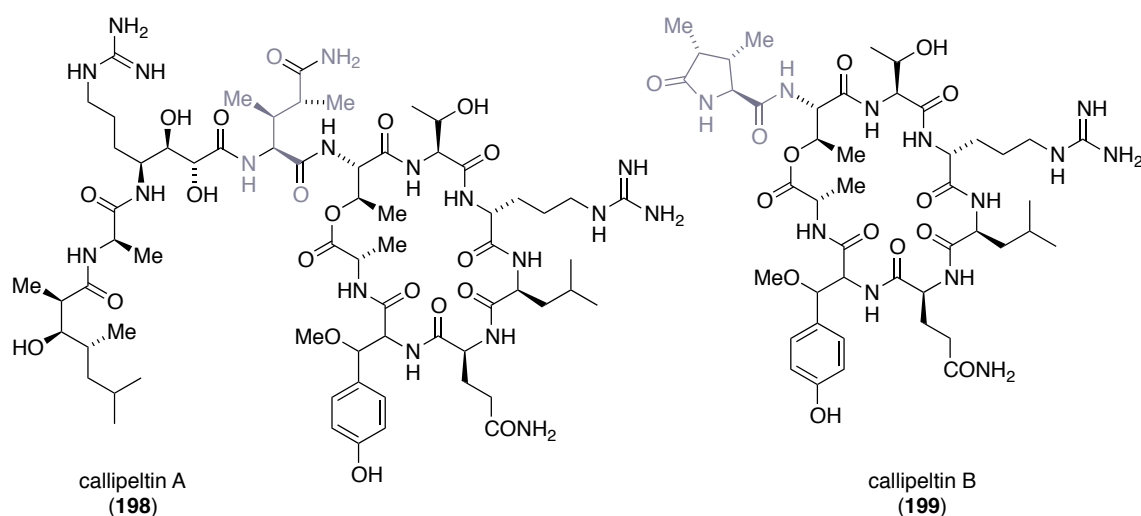
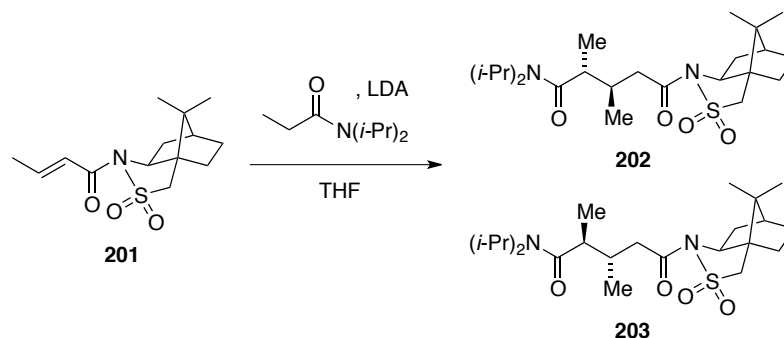


**Figure 26.** Callipeltines A (**198**) and B (**199**) and common skeleton of the papuamides **200**

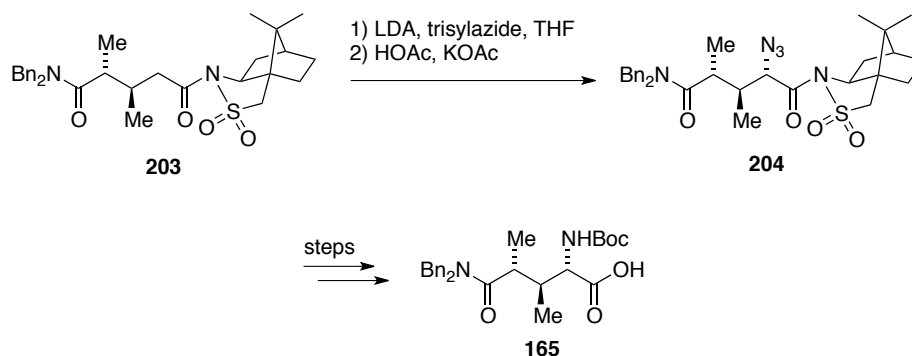
As a synthetic target, dimethylglutamine (**165**) was first discussed by JOULLIÉ and co-workers.<sup>[109]</sup> Their approach featured a camphorsulphonic acid-based auxiliary **201**, which was used to furnish an asymmetric MICHAEL addition. As depicted in Scheme 56, two

diastereoisomers **202** and **203** were obtained from this reaction. Initial stereoselectivity was not beyond 3:1 in favour of the desired stereochemical outcome, but could be improved to 25:1 swapping the amide protecting group from dibenzyl to diisopropyl, achieving an overall yield of 80 % yield.<sup>[109]</sup>



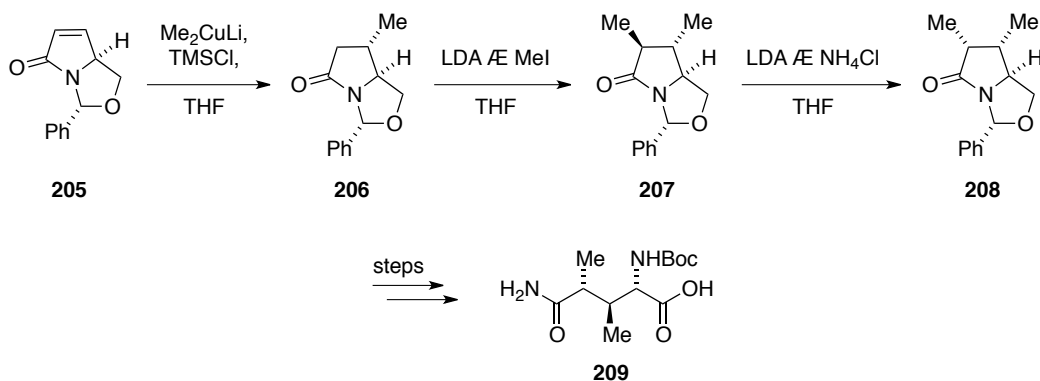
**Scheme 56.** Asymmetric MICHAEL addition to establish the C3-C4 bond with the two methyl groups in *anti* configuration

The synthetic sequence continued with the desired diastereoisomer (with a benzyl protection groups) with the stereoselective introduction of an azide at the  $\alpha$ -carbon. Reduction of the azide, Boc-protection and further functional group modifications then furnished intermediate **204**. Further functional group modification let to fully *N*-protected dimethylglutamine derivative **205** (Scheme 57).



**Scheme 57.** Introduction of the  $\alpha$ -amino group as an azide and final dimethylglutamine derivative **205**

Another synthetic approach towards dimethylglutamine **165** was presented by HAMADA and co-workers.<sup>[9]</sup> Conceptually, the pyroglutamine scaffold was used to derive compound **165** upon adding the two methyl groups subsequently to MICHAEL system **250**. This approach is similar to previous work, presented by AVECEDO *et al.*<sup>[107]</sup>



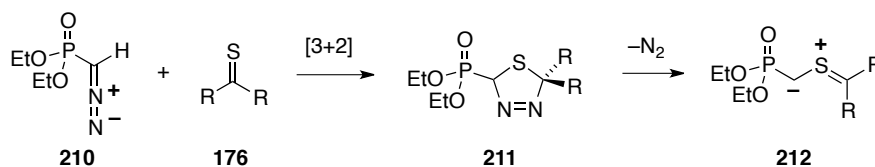
**Scheme 58.** HAMADA's approach to dimethylglutamine **165**

As depicted in Scheme 58, stereoselective cuprate 1,4-addition on intermediate **205** using GILMAN's cuprate installed the C3 methyl in intermediate **206** in a 95:5 ratio favouring the desired stereochemistry in an 86 % with respect to both stereoisomers. Upon  $\alpha$ -methylation the second methyl group was installed in 77 % yield, however, with the undesired stereochemistry in compound **207**. Upon inversion, desired intermediate **208** was achieved. After necessary protection group modifications, aminolysis delivered Boc-protected dimethylglutamine **209**.

### 3 RESULTS AND DISCUSSION

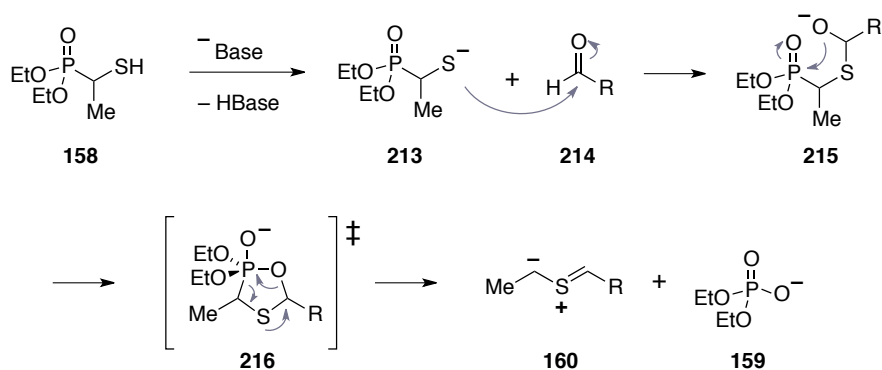
#### 3.1 Thiocarbonyl Ylids from Horner-Wadsworth-Emmons-Type Reactions

Recently, phosphonate derivatives have successfully been introduced as novel precursors for thiocarbonyl ylides.<sup>[110]</sup> The SEYFERTH–GILBERT reagent (**210**)<sup>[111,112]</sup> was used in a 1,3-dipolar cycloaddition to thiones **176**, yielding thiadiazane phosphonates **211**. As nitrogen extrusion of these systems occurs at ambient temperature, resulting dipole **212** was observed to dimerise or to undergo [3+2] cycloadditions with another equivalent of thiones **176**.



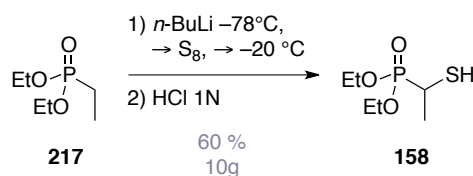
**Scheme 59.** Phosphonate-based thiocarbonyl ylides generated upon extrusion of nitrogen

The phosphonate portion does not account in the formation of the dipole, however. The inspiration for this project was the idea to create thiocarbonyl ylides from literature-known mercaptoethane phosphonate **158** precursor, by applying typical phosphonate reactivity as observed in HORNER-WADSWORTH-EMMONS (HWE) reactions.<sup>[113]</sup> Herein, as depicted in Scheme 60, reaction of deprotonated mercaptoethane phosphonate **213** could be reacted with generic aldehyde **214** to yield intermediate **215**. Similar to the key intermediate of the HWE reaction, nucleophilic attack of oxygen on the centre phosphor-atom would then give cyclic intermediate oxathiaphosphetane **216**, a 5-membered “thio analogue” of four membered oxaphosphetanes. Upon electrocyclicisation and release of a phosphate ester **159**, thiocarbonyl ylid **160** may be formed.



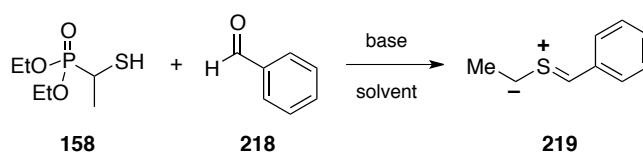
**Scheme 60.** Envisaged HORNER-WADSWORTH-EMMONS type formation of thiocarbonyl ylid **160**

To investigate this envisaged reactivity, mercaptophosphonate **158** was derived from ethyl phosphonate **217** upon deprotonation of the  $\alpha$ -carbon with *n*-BuLi and subsequent addition of sulphur, followed by treatment with aqueous hydrochloric acid.<sup>[114]</sup>



**Scheme 61.** Synthesis of mercaptoethane phosphonate **158**

To investigate this concept, several different reaction conditions were tested, screening different bases, solvents and aldehydes. To start with a simple system, benzaldehyde (**218**) was chosen as a substrate. NaH and  $\text{K}_2\text{CO}_3$  were picked as suitable bases, as both would easily deprotonate the thiol, but not deprotonate the  $\alpha$ -proton of phosphonate **158**. The organic solvents  $\text{Et}_2\text{O}$ , THF and DMSO were tested, in which both substrates were readily soluble. All screening reactions were carried out under inert conditions, at concentrations of 100 mg/mL. Test reactions were carried out at 0.25 mmol scales and substrates and base were applied in equimolar ratios. Findings from the first set of screenings are summarised in Table 9.

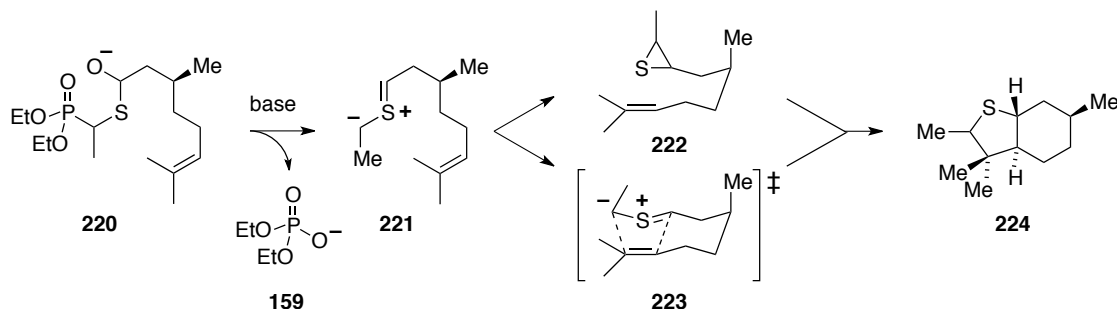
**Table 9.** First screening for HWE type thiocarbonyl ylid formation

entry	solvent	base	T [°C]	t [h]	observation
1	Et <sub>2</sub> O	NaH	25	2	no reaction
2	Et <sub>2</sub> O	K <sub>2</sub> CO <sub>3</sub>	25	2	no reaction
3	THF	NaH	25	2	no reaction
4	THF	NaH	80/ sealed tube	2	decomposition
5	DMSO	K <sub>2</sub> CO <sub>3</sub>	25	2	no reaction
6	DMSO	K <sub>2</sub> CO <sub>3</sub>	80	2	decomposition
7	DMSO	K <sub>2</sub> CO <sub>3</sub>	190/ seal tube	2	decomposition

Upon mixing mercapto phosphonate **158** and benzaldehyde (**218**) in Et<sub>2</sub>O at ambient temperature, (entries 1 and 2), no reaction was observed within two hours with either base. Consequently, THF was chosen as a solvent, so that higher reaction temperatures could be tested. Whilst a reference reaction with NaH as base at ambient temperature (entry 3) again did not yield any reaction, heating of the substrates in a sealed tube at 80°C for two hours (entry 4) lead to decomposition of the phosphonate **158**. Similarly, different temperatures were screened, using DMSO for a solvent (entries 5–7). In this set of reactions, K<sub>2</sub>CO<sub>3</sub> was used as a base. Again, a reference reaction at ambient temperature did not indicate any reactivity (entry 5). Moving to higher temperatures (entries 6 and 7) only lead to quantitative decomposition of the phosphonate **158**. No indication of anticipated products, stemming from an initial thiocarbonyl ylid formation, was evident.

As the thiophosphonate **158** obviously required milder reaction conditions to avoid decomposition, a different aldehyde was chosen to conduct further experiments. (*R*)-citronellal (**219**) was selected for two reasons. Firstly, the sp<sup>3</sup> hybridized α-CH<sub>2</sub> group of the aldehyde represents a sterically less demanding moiety and thus could ease the nucleophilic attack of the deprotonated thiol. Secondly, the isopropenyl moiety of citronellal (**219**) features

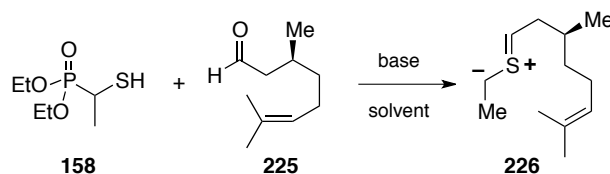
an intramolecular double–bond that may intercept a formed 1,3-dipole by means of a [3+2] cycloaddition (see Scheme 62).



**Scheme 62.** Envisaged reactivity of a citronnellal-based thiocarbonyl ylid **221**

Deprotonated hemithioacetal **220** may undergo the envisaged formation of thiocarbonyl ylid **221** upon elimination of phosphate ester **158**. Depending on reaction conditions, subsequent conrotatory electrocycloaddition to thiirane **222** or [3+2] cycloaddition *via* transition state **223** may occur. In both cases, addition over the prenyl double–bond may finally give bicycle **224**.

As the first screening revealed that mercaptophosphonate **158** would not withstand higher reaction temperatures, the initial equilibrium between the substrates and their corresponding thio hemiacetal was of great interest. If the equilibrium rested on the product side, later addition of base and subsequent increase of reaction temperature would potentially support the desired reactivity. Careful literature research led to a side note, in which  $^1\text{H}$  NMR experiments with thiols reacting with aldehydes were reported in the course of studies to enzymatic resolution of  $\alpha$ -acetoxysulphides.<sup>[115]</sup> Pleasingly, it was reported, that generally slow equilibration could be catalysed upon addition of  $\text{SiO}_2$  in less than an hour in all cases (Scheme 63).

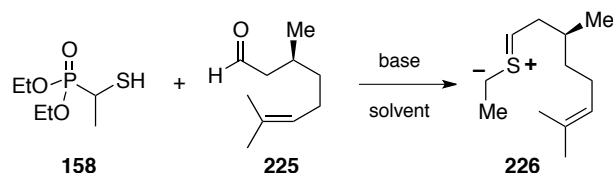


**Scheme 63.** Equilibrium between substrates **158** and **219** and hemithioacetal **226**

To ensure equilibration between substrates **158** and **225** and their hemithioacetal **226**, in all test reactions of the second screening, substrates were stirred for one hour in the respective solvent with catalytic amounts of  $\text{SiO}_2$ . A test reaction in  $\text{CDCl}_3$  confirmed, that an

equilibrium, which lay on the side of hemithioacetal **219**, had been established. After filtration base was added in the respective entries and the mixture heated according to entries in Table 10.

**Table 10.** Second screening towards thiocarbonyl ylides from HWE type reactions



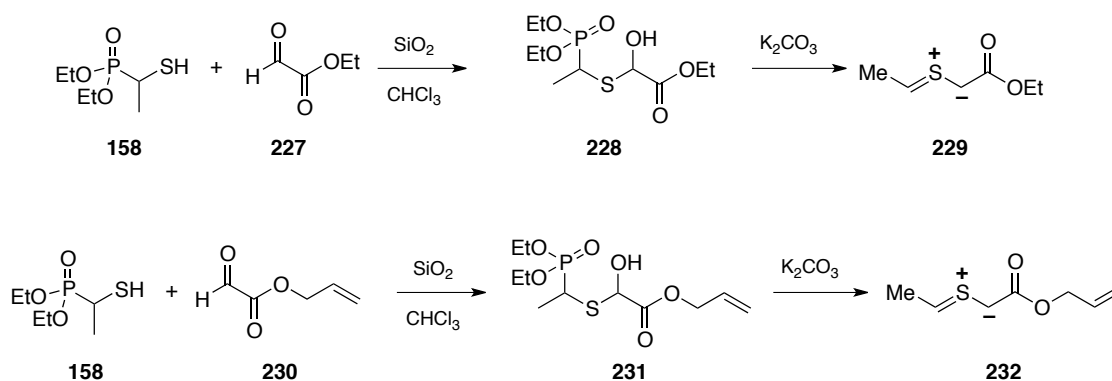
entry	solvent	base	T [°C]	t [h]	observation
1	MeCN	NaH	80	2	no reaction
2	MeCN	K <sub>2</sub> CO <sub>3</sub>	80	2	no reaction
3	MeCN	K <sub>2</sub> CO <sub>3</sub>	180	2	decomposition
4	DMSO	NaH	80	2	no reaction
5	DMSO	K <sub>2</sub> CO <sub>3</sub>	80	2	no reaction
6	DMSO	NaH	180	2	decomposition
7	DMSO	K <sub>2</sub> CO <sub>3</sub>	180	2	decomposition
8	CHCl <sub>3</sub>	K <sub>2</sub> CO <sub>3</sub>	60	2	no reaction
9	acetone	K <sub>2</sub> CO <sub>3</sub>	80	2	no reaction
10	THF	K <sub>2</sub> CO <sub>3</sub>	80	2	no reaction
11	DMF	K <sub>2</sub> CO <sub>3</sub>	80	2	no reaction
12	toluene	K <sub>2</sub> CO <sub>3</sub>	180	2	decomposition

With acetonitrile, another solvent was tested in this screening. Reference reactions with both NaH (entry 1) and K<sub>2</sub>CO<sub>3</sub> (entry 2) at 80 °C did not reveal any reactivity. In this system, all substrates could at least withstand higher temperatures. Upon further heating (entry3), decomposition was observed again.

As DMSO had been tested in the first screening as well, a series of test reactions with aldehyde **219** were conducted in this series too (entries 4–7). Whilst a temperature of 80 °C was tolerated by all substrates in this solvent system as well (entries 4 and 5) higher

temperatures again lead to decomposition (entries 6 and 7). The use of different bases (NaH and  $K_2CO_3$ ) did not result in any different reactivity, and hence, further efforts in this screening extended to the use of other solvents, such as  $CHCl_3$  (entry 8), acetone (entry 9), THF (entry 10) and DMF (entry 11). In all these set ups,  $K_2CO_3$  was used as a base. Heating each set up under reflux did however not promote any reaction. Finally, toluene was tested as a solvent (entry 12). Upon heating at  $180^\circ C$  only decomposition was observed. As no suitable reaction conditions were found in this second screening, two more aldehydes were considered as suitable reaction partners for the desired thiocarbonyl ylid formation.

As literature reported a quantitative formation of the hemithioacetal in solutions of thiols and ethyl glyoxylate, another approach was envisaged, using aldehydes **227** and **230**.<sup>[115]</sup>



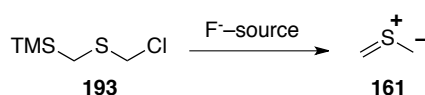
**Scheme 64.** Envisaged thiocarbonyl ylides derived from glyoxalates

As depicted in Scheme 64, test reactions were performed similar to the second screening. Freshly prepared aldehydes **227** and **230** were pre-mixed in chloroform and stirred in the presence of catalytic  $SiO_2$  for 1 hour, at which point corresponding hemithioacetals **228** and **231** were formed, as could be seen in  $^1H$  NMR analysis. Thereafter, the mixtures were filtered,  $K_2CO_3$  was added and the mixtures stirred for an additional hour at ambient temperatures. Aliquots were taken, worked up and analysed, however, no reaction was observed. The mixtures were subsequently heated at reflux ( $60^\circ C$ ) for another two hours. Unfortunately, conversion to thiocarbonyl ylides **229** and **232** were not indicated upon any product formation. It would appear that thio hemiacetals formed from **158** are not undergoing the envisaged formation of ylides. As the initial hemithioacetal can be formed, and the oxophilicity of phosphorous should also support the desired reaction pathway, it would appear, that the C–P bond is too strong in this system. Thus, future investigations may focus

on further developed thiophosphonates, which may stabilise the resulting dipole and ease the envisaged electrocyclisation, leading to 1,3-dipoles.

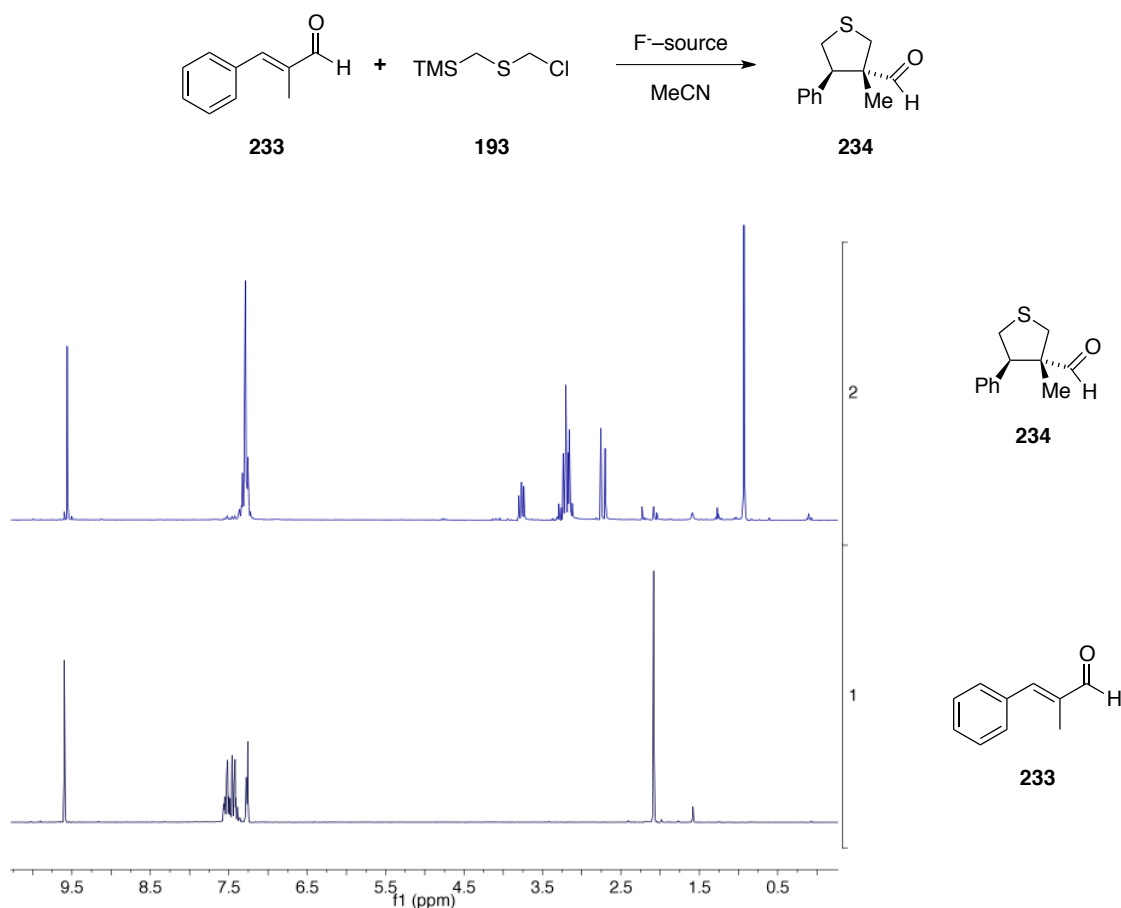
### 3.2 Revisiting Sakurai's Reagent

Another aspect of this project was a systematic investigation of SAKURAI's reagent **193**, which represents a handy precursor to generate the simplest thiocarbonyl ylid **161**. Though representing a highly efficient way of deriving the simplest thiocarbonyl ylid, SAKURAI's reagent **193**<sup>[103]</sup> has only found sporadic use in organic synthesis. Additionally, it has not been used in combination with RANEY-nickel, to formally establish a *syn* addition of ethane over a double bond. Also, the issue of catalysis has not been addressed. Reported yields in cycloadditions were only moderate. Thus, a series of reactions were performed to better understand reactivity and scope of this intriguing reagent.



**Scheme 65.** Reagent **193** as readily available precursor to the simplest thiocarbonyl ylid **161**

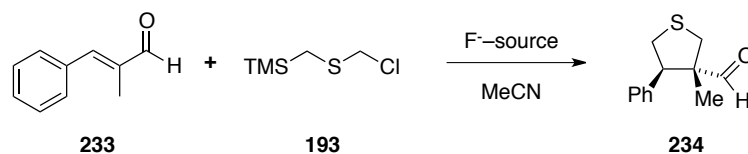
As a suitable test substrate,  $\alpha$ -methylcinnamic aldehyde (**233**) was chosen, as it not only provides an electron poor double bond, but also leads to clean reaction progress in the addition of **161**. Furthermore, no by-products are observed and clearly distinguishable <sup>1</sup>H NMR signals, allowing for direct comparison of crude reaction mixtures, are obtained (Figure 27).



**Figure 27.** <sup>1</sup>H NMR comparison of  $\alpha$ -methylcinnamic aldehyde (**233**, track 1 dark blue) and tetrahydrothiophene **234** (track 2, blue)

While  $\alpha$ -methylcinnamic aldehyde (**233**) only displays an aldehyde peak beyond 9.5 ppm, a multiplet around 7.5 ppm and a singlet around 2.0 ppm, the spectrum of the tetrahydrothiophene **234**, generated from 1,3-dipolar cycloaddition of thiocarbonyl ylid **161**, moves the aromatic signals to 7.3 ppm, but more obviously the methyl group singlet is largely shifted high field to around 1.0 ppm. In addition, all protons of the newly formed, five membered ring are found between 2.5 and 4.0 ppm.

All test reactions were carried out under inert conditions, using 1 equivalent of aldehyde (**233**), 1.3 equivalents of SAKURAI's reagent **193**, and 3 equivalents of a fluoride source in acetonitrile (0.12 M with respect to aldehyde **233**). Findings of initial investigations are summarised in Table 11.

**Table 11.** Test system for 1,3 cycloadditions on  $\alpha$ -methylcinnamic aldehyde (**233**) using SAKURAI's reagent (**193**)

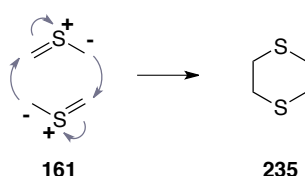
entry	F <sup>-</sup> source	T [°C]	t [h]	observations*
1	CsF	23	1	5% conversion
2	CsF	23	3	17% conversion
3	CsF	23	48	80% conversion
4	CsF	80	8	40% conversion
5	CsF	90	48	10% + by-products
6	CsF + Sc(OTf) <sub>3</sub>	23	3	no rxn
7	AgF	23	3	no rxn
8	AgBF <sub>4</sub>	23	3	no rxn
9	HF*py, py	23	3	no rxn
10	TBAF	23	3	23% conversion

\* conversion determined by crude <sup>1</sup>H NMR analysis of worked up reactions

At first, three reference reactions were performed according to standard literature procedures (entries 1–3).<sup>[103]</sup> After 1 and 3 hours reaction times (entries 1 and 2 respectively), only minimal reaction progress was observed. After stirring for 48 hours, however, a satisfying yield of 80% is obtained (entry 3). As 1,3-dipolar cycloadditions are known to proceed very rapidly, slow reaction progress observed in entries 1 to 3 suggests, that the formation of thiocarbonyl ylid **161** is the rate determining step in this test system. As CsF does not dissolve in MeCN, a very low steady state concentration of F<sup>-</sup> ions in solution may be assumed. Consequently, reactive intermediate **161** is formed in very low concentration too. While increase of reaction temperature to reflux conditions for 8 hours (entry 4) slightly increased the conversion **233** to **234**, harsher conditions as in entry 5 lead to decomposition of most of the materials. Entry 6 represents the attempt to use a LEWIS acid to increase the reaction rate. As most LEWIS acids do not tolerate fluoride ions, scandium triflate was chosen

in this case. The test system however, appears to be incompatible with these reaction conditions. A plausible explanation for the complete shut down of reactivity in this reaction may stem from coordination of scandium to the dipole, thus preventing further reactivity.

Evaluating different fluoride sources (entries 7–10), only revealed TBAF (entry 10) as suitable alternative to CsF. A slightly improved conversion was observed along with a new  $^1\text{H}$  NMR signal, a singlet at 2.8 ppm. The corresponding by-product was identified as 1,4-dithiane (**235**), which can be interpreted as the “dimer”, formed upon reaction of two equivalents of **161**, as shown in Scheme 66.



**Scheme 66.** “dimerization” of **161** to yield 1,4-dithiane (**235**)

Apparently, using TBAF the 1,3-dipole was derived much faster than it could react with cinnamic aldehyde **233**. Decreasing the amount of TBAF to only 1.3 equivalents with respect to 1 equivalent of aldehyde, gave a similar yield of 25%. Therefore, a novel reaction set up was designed, wherein a solution of precursor **193** was added to a solution, containing dipolarophile **233** and TBAF. Only 1 equivalent of each reagent was used.

**Table 12.** Further optimisation of test system with TBAF as fluoride source

entry	T [°C]	t addition [h]	t reaction [h]*	observations*
1	rt.	30 min	1	52 % conversion
2	rt.	90 min	2	94 % conversion

\* t reaction refers to the time between start of addition and aqueous work up

Short optimisation (Table 12) led to a reaction setup, wherein desired 1,3-dipolar cycloaddition were performed in almost quantitative yields within 2 hours instead of two days. After this successful optimisation, the potential of asymmetric catalysis was addressed

next. Accordingly, JØRGENSEN's<sup>[116]</sup> (**236**) and 1<sup>st</sup> generation MACMILLAN catalyst<sup>[117]</sup> (**237**) were introduced to the test system.

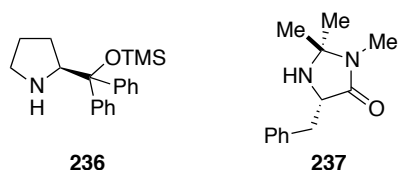
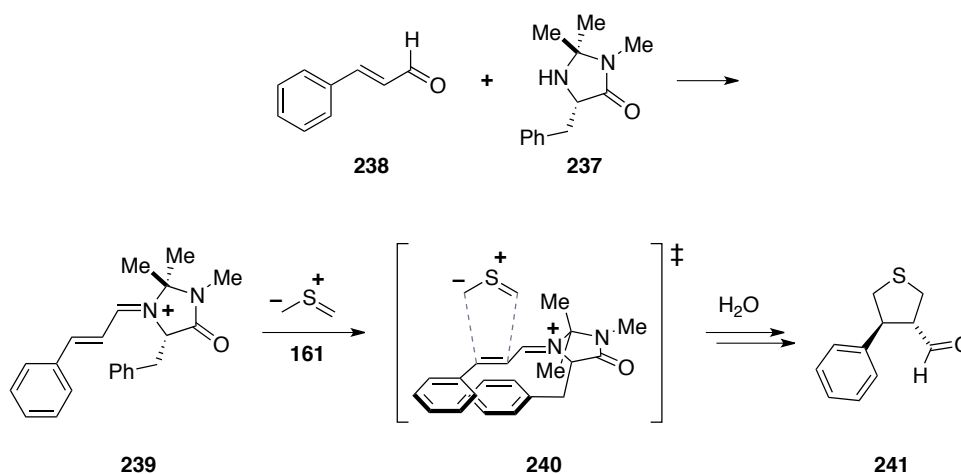


**Figure 28.** JØRGENSEN (**236**) and 1<sup>st</sup> generation MACMILLAN (**237**) catalysts

For test reactions, both suitable fluoride sources (CsF and TBAF) were considered again. Though it had been shown previously, that the cycloaddition was proceeding quickly, introduction of asymmetric information upon use of either catalysts was an interesting exploration for systems without stereochemical bias, such as the tested cinnamic aldehydes. In contrast to previous test reactions, water was used as co-solvent to enable recycling of the catalysts. In all cases, dihydrothiophenes were isolated and optical rotation was measured. No indication for enantiomeric excess was observed, however. Conversion decreased upon use of JØRGENSEN's catalyst, presumably due to use of fluoride ions to deprotect the tertiary OTMS-group. To rule out a repulsive steric interaction of the  $\alpha$ -methyl group in **233**, another series of test reactions was performed with the 1<sup>st</sup> generation MACMILLAN catalyst and cinnamic aldehyde.



**Scheme 67.** Envisaged organocatalysis using MACMILLAN's catalyst **237**

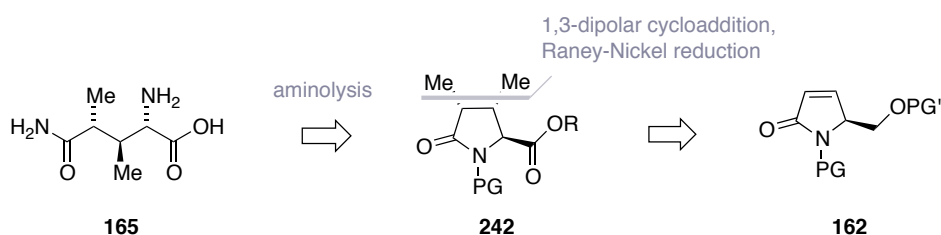
As depicted in Scheme 67, organocatalysis of cinnamic aldehyde **238** and 1<sup>st</sup> generation MACMILLAN catalyst should form iminium species **239**. Upon steric information of **237** the bottom face of the reactive species in transition state **240** is shielded, thus

thiocarbonyl ylid **161** would approach the double bond from the top face. Upon hydrolysis, enantiomer **241** would be formed as main product. The isolated tetrahydrothiophene carbaldehyde mixture, however, did not indicate any enantiomeric excess either. Apparently, the reaction rate of the dipolar cycloaddition exceeds the rate of formation of the organocatalytic iminium species **239** at a 10 mol % catalyst load.

Concluding this part of the project, a successful optimisation of [3+2] cycloadditions of thiocarbonyl ylid **161** was accomplished upon use of TBAF and an altered reaction protocol, in which SAKURAI's reagent **193** was added slowly to a solution of the dipolarophile and TBAF. Attempts to further catalyse this reaction and introduce asymmetric information upon use of organocatalysis remained unsuccessful.

### 3.3 Formal Synthesis of Dimethyl-L-glutamin

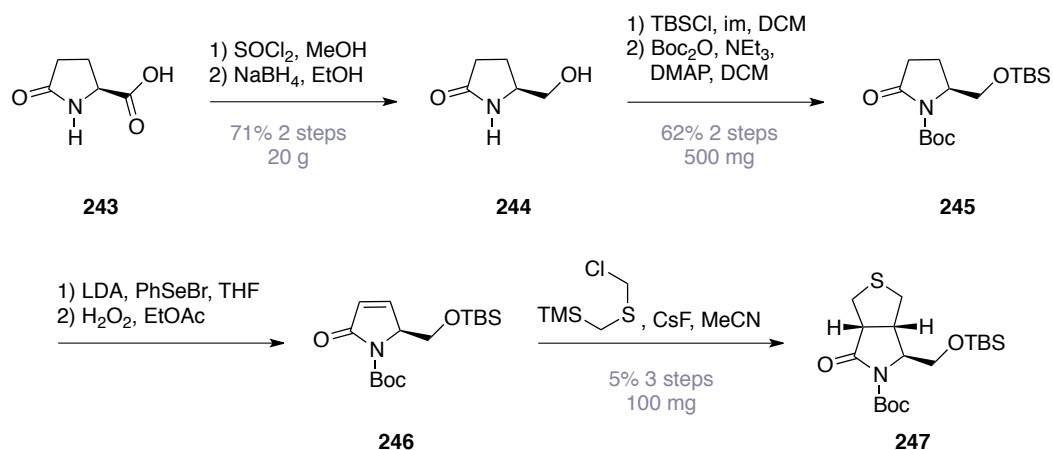
To showcase the potential of 1,3-dipolar cycloadditions with thiocarbonyl ylides in combination with sulphur removal by means of RANEY nickel, which is equal to the formal addition of ethane over a double bond, nonproteinogenic amino acid dimethyl-L-glutamine (**165**) was chosen. Retrosynthetically, **165** can be traced back to dimethyl pyroglutamine derivative **242**. This derivative again can be derived from protected intermediate **162** by the envisaged 1,3-dipolar cycloaddition/ RANEY nickel sequence (Scheme 68).



**Scheme 68.** Retrosynthetic analysis of dimethyl-L-glutamine (**165**)

In a forward sense, an elegant protecting group strategy is key to a successful synthesis of **165**. It was envisaged to Boc- protect the amide and use TBS as a protecting group for the alcohol. The latter is necessary, as previous synthetic studies on similar systems revealed fast epimerisation of the  $\chi$ -stereocentre. It was envisaged, that upon use of excess amounts of a fluoride source, not only the thiocarbonyl ylid may be derived, but the alcohol could be deprotected as well.

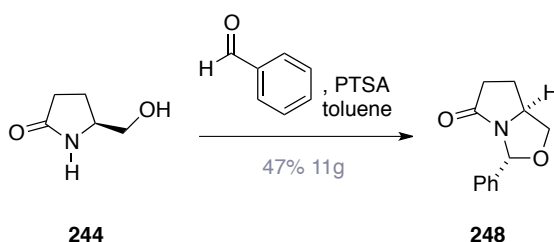
To test this hypothesis, L-pyroglutamic acid (**243**) was converted to glutaminol (**244**) and subsequently fully protected to give intermediate **245**. Phenylselenenyl bromide and subsequent treatment with hydrogen peroxide furnished **246**, which was subjected to the cycloaddition conditions (Scheme 69).



**Scheme 69.** First synthetic approach towards dimethyl-L-glutamine (**165**)

Unfortunately, the sequence starting from fully protected intermediate **245** only yielded 5% of thiophene **247** over three steps, along with decomposition products. A tetrahydrothiophene derivative with an unprotected hydroxyl group was not observed, however. Further synthetic studies, which will be discussed in detail (*vide supra*) suggest, that upon used reaction conditions deprotected **246** apparently lead to decomposition of the starting material.

As a one pot deprotection of the alcohol competing with the cycloaddition appeared non advisable, an alternate protecting group strategy which had been reported previously by HAMADA and co-workers was chosen.<sup>[9]</sup> As depicted in Scheme 70, the amide and alcohol were simultaneously protected as the corresponding aminal upon treatment of glutaminol **244** with benzaldehyde in a DEAN-STARK set up under acidic conditions.



**Scheme 70.** Aminal protection of glutaminol (**244**)

In a small scale test reaction, the desired aminol bicycle **248** was obtained. In addition also a minor stereoisomer that could not be separated by column chromatography delivered a second set of the same peaks with slightly different chemical shifts in the  $^1\text{H}$  NMR. The minor product could be isolated upon crystallisation. Suitable crystals for X-ray crystallography were obtained and revealed dimer **249**.

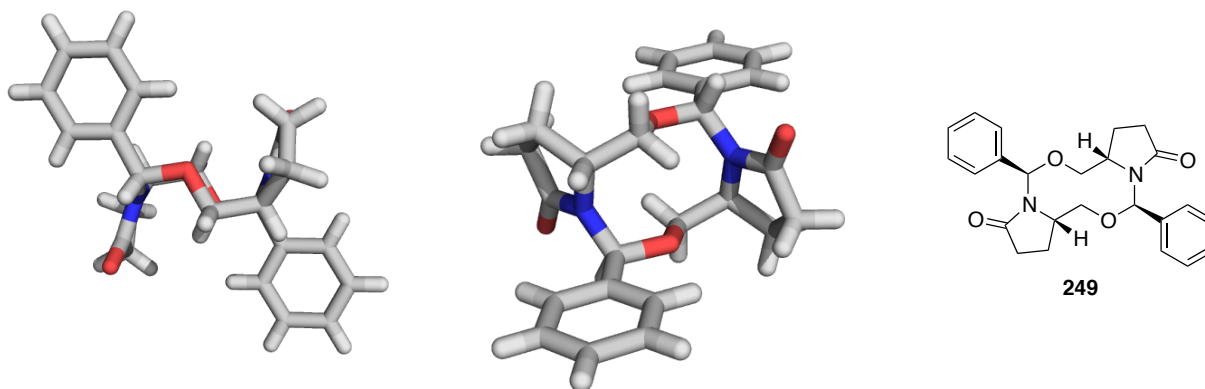
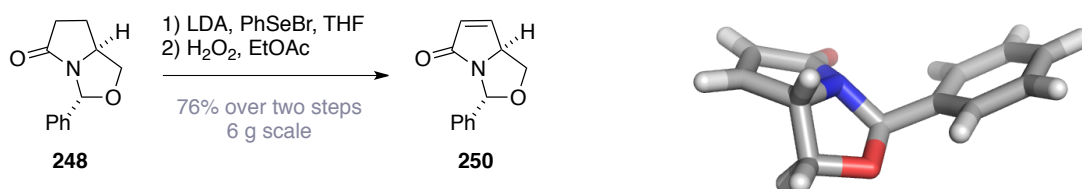


**Figure 29.** X-ray crystal structure of **249** (Colour code: grey: carbon, red: oxygen, blue: nitrogen, white: hydrogen)

As can be seen in the left plotting of **249** in Figure 29, the dioxadiazadecene backbone displays the typical “boat–chair–boat” conformation to avoid repulsive eclipsed interactions. Notably, due to the partial double bond character of C-N amide bond, the five membered pyroglutamin moieties appear in an almost flat conformation.

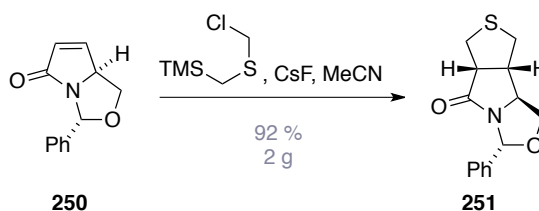
With protected intermediate **248** in hand, again the double bond was introduced by converting the lithium enolate of **248** to the  $\alpha$ -seleno species, which upon oxidation and release of selenoic acid gave **250** in good yield over two steps as a colourless crystalline solid. This intermediate was successfully recrystallized to obtain suitable crystals for X-ray diffraction analysis.



**Scheme 71.** Establishing the double bond in **250** with X-ray crystal structure (colour code: grey: carbon, red: oxygen, blue: nitrogen, white: hydrogen)

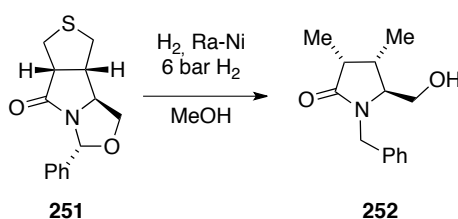
A remarkable feature of this double bond is the  $sp^3$ -nitrogen in the amide bond, promoted by the ring strain of the aminol–five membered ring. Furthermore, a prominent, ample “open-book-effect” is evident, which should promote a 1,3–cycloaddition to occur from the desired convex face.

With intermediate **250** in hand, the stage was set again for the 1,3-dipolar cycloaddition, which had already proofed to conceptually work for a similar system. After optimising reaction conditions, this key step was successfully accomplished in an excellent yield (92%) on a 2 g scale (Scheme 72) using mild reaction conditions. Though test systems had shown, that a TBAF promoted formation of thiocarbonyl ylid **161** was advantageous (*vide infra*), employment of these reaction conditions in combination with **250** exclusively leads to decomposition. Upon vigorous stirring and 48 hours reaction time, CsF was successfully applied as fluoride source and promoted clean formation of the thiocarbonyl ylid, thus furnishing desired cycloadduct **251**. As suggested upon examination of the X-ray crystal structure of **244**, the cycloaddition proceeded from the convex face exclusively. The other diastereoisomer, which would stem from an attack of the thiocarbonyl ylid from the concave side of the dipolarophile, was not observed.



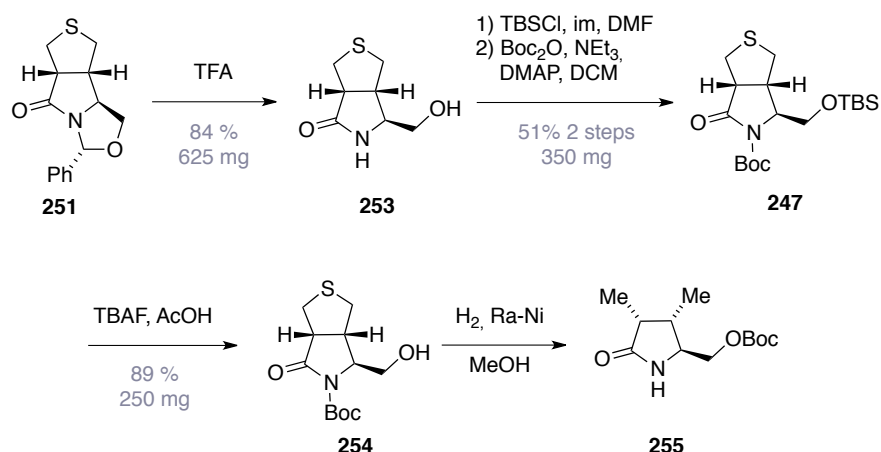
**Scheme 72.** Key [3+2] cycloaddition of thiocarbonyl ylid **161**

With advanced intermediate **251** in hand, the removal of sulphur was envisaged as concluding step to the formal synthesis of dimethylglutamine **165**. RANEY nickel reduction of compound **251** at 6 bar  $H_2$  pressure, not only removed the sulphur bridge, but also cleaved the benzylic C-O bond (**252**/ Scheme 73).



**Scheme 73.** Initial reduction protocol yielding compound **252**

As all attempts to remove the benzyl “protecting” group failed, and all efforts to proceed a synthetic sequence by means of aminolysis rendered fruitless as well, a dual strategy was proceeded to obtain a literature known intermediate and complete a formal synthesis of dimethylglutamine **165**. The first route followed up on the initial plan to remove sulphur right after the cycloaddition, carefully optimising reaction conditions. Findings of this attempt will be reported in due course (*vide supra*). A second alternative proceeded with the synthetic sequence as accomplished by HAMADA and co-workers<sup>[9]</sup> with the sulphur still in place.

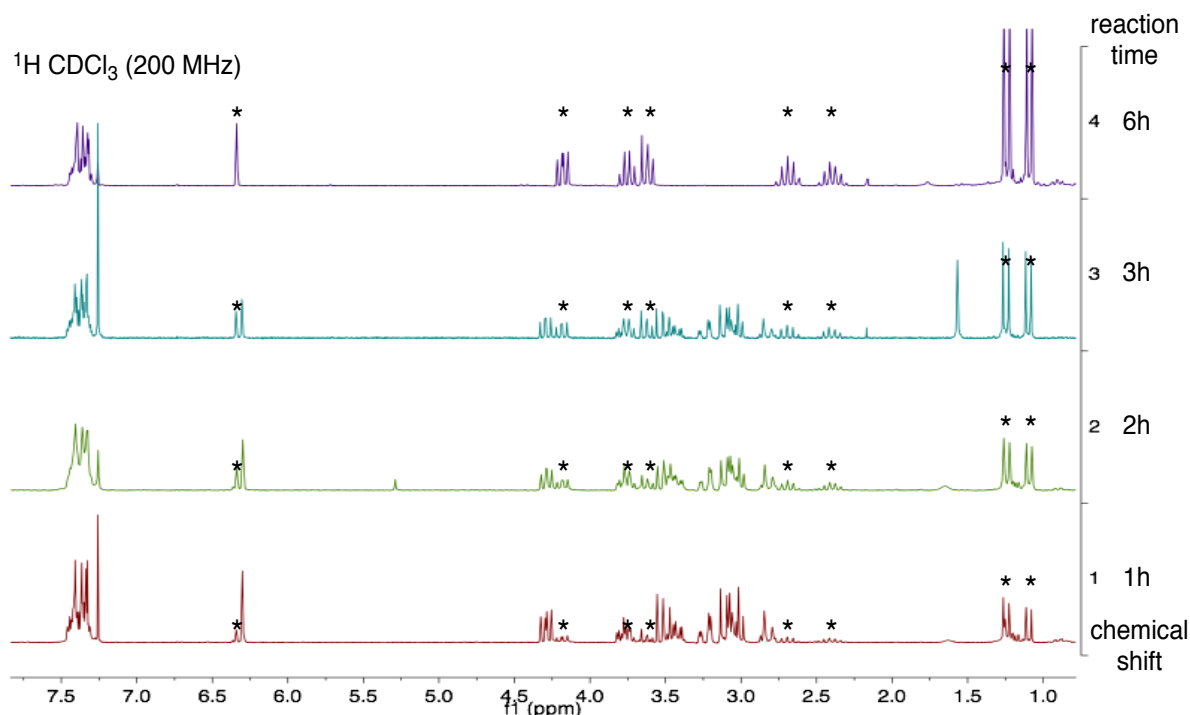
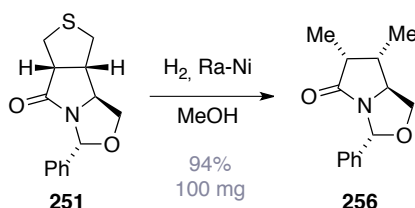


**Scheme 74.** Synthetic sequence with the dihydrothiophene moiety in place

As depicted in Scheme 74, tricycle **251** was successfully deprotected with trifluoroacetic acid. As nitrogen protection would be necessary for HAMADA’s sequence, the hydroxyl group was protected first by means of TBS silylation. The two step sequence to fully protected intermediate **247** proceeded in moderate yields. Subsequent removal of the TBS- group gave compound **254** in good yields and the stage was set for the removal of the sulphur bridge again. Treatment with RANEY nickel at this stage did however not only promote the desired removal of sulphur, but also lead to a nucleophilic attack of the hydroxyl group at the Boc carbonyl, thus yielding carbonate **255**. While this unexpected synthetic obstacle prevented the conclusion of a formal synthesis of dimethylglutamine **165**, careful optimisation of the previously discussed reduction of **251** lead to the desired synthetic break through.

Applying only 1 atm of H<sub>2</sub> <sup>1</sup>H NMR analyses revealed, that the reduction of sulphur proceeded before the aminol ring was opened. As both compounds **251** and **208** co-eluate on

TLC, crude reaction mixtures were filtered over celite, concentrated *in vacuo* and re-dissolved in  $\text{CDCl}_3$ .



**Scheme 75.** Progress of selective Ra-Ni reduction of **251** (track 1, red: reaction after 1h, track 2, light green: reaction after 2 hours, track 3, dark green: reaction after 3 h, track 4, purple: reaction after 6 h/ clean conversion to **208**

As depicted in Scheme 75, mild reduction conditions over the course of 6 hours cleanly furnished literature known compound **208**, representing the successful formal synthesis of dimethylglutamine **165** according to the synthetic sequence published by HAMADA and co-workers.<sup>[9]</sup> In contrast to their sequence, the two methyl groups were introduced stereoselectively by means of a [3+2] cycloaddition of 1,3-dipole **161**. Subsequent reduction with RANEY nickel furnished intermediate **208** in 86% isolated yield after two steps from compound **250**. In contrast to HAMADA's sequence (51% over three steps from compound **250**) the yield could be significantly improved, inversion of undesired stereochemistry was not necessary and the cycloaddition of thiocarbonyl ylid **161** gave only one diastereoisomer. Formally, an addition of ethane over a double bond in this the presented

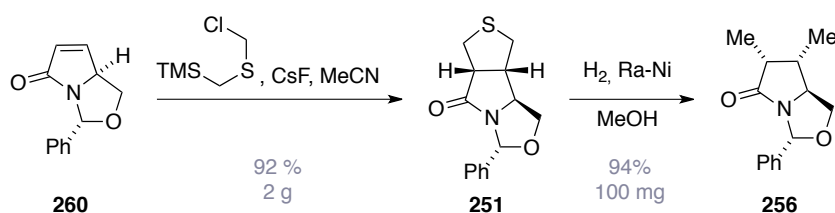
two step sequence was accomplished and displays the synthetic potential of the described methods.

## 4 SUMMARY AND OUTLOOK

This project dealt with different aspects of thiocarbonyl ylid chemistry. In a first stage of this research, reaction pathways to generate novel thiocarbonyl ylides from thiophosphonates such as **158** were thoroughly investigated. Unfortunately, the expected reactivity of generated intermediates could not be observed. Still, this work represents a solid basis for future investigations. Future work in this field may focus on further tuning of mercaptophosphonates.

A second stage of this project revisited SAKURAI's reagent **193**, a potent but relatively little known precursor for the simplest thiocarbonyl ylid **161**. In the course of systematic investigations, TBAF was established as suitable fluoride source for the generation of named ylid, optimising yields and reaction times. Organocatalysis of the investigated model system could not be achieved.

Finally, the showcase synthesis of advanced intermediates for a synthesis of dimethylglutamine **165** was accomplished, combining a highly stereoselective [3+2] cycloaddition of thiocarbonyl ylid **161** with a RANEY nickel reduction. This way, the two methyl groups of dimethylglutamine **165** were introduced stereoselectively and in significantly higher yields compared to previously reported synthetic sequences.



**Scheme 76.** Highly efficient synthetic equivalent for the "addition of ethane over a double bond"

Investigating different synthetic routes to this formal total synthesis, all intermediates were fully characterised, and two novel X-ray crystal structures of key intermediates **249** and **250** were obtained as well.

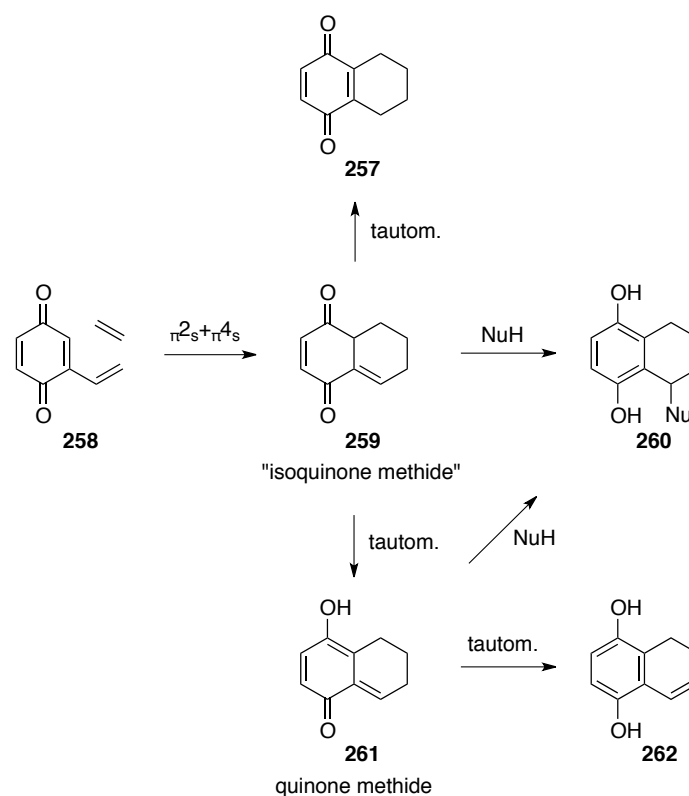


**CHAPTER III:**  
**VINYL-QUINONE-DIELS-ALDER REACTIONS**

This part of the work was conducted together with FLORIAN LÖBERMANN. Both authors contributed equally to this project. Results of this project will also be discussed in the PhD thesis of FLORIAN LÖBERMANN.

# 1 PROJECT AIMS

The DIELS-ALDER (DA) reaction of vinyl quinones **258** provides a rapid entry to highly functionalized bi- and polycyclic ring systems. They involve the inverse electron-demand cycloaddition of an electron rich dienophile to a vinyl quinone, which presumably generates an “isoquinone methide” **259**. This reactive intermediate could then tautomerise in several ways to yield quinone methides **261**, bicyclic quinones **257** or hydroquinones **262**. If the isoquinone methide or quinone methide is intercepted by a nucleophile inter- or intramolecularly, a functionalized tetraline hydroquinone may result (Scheme 77).<sup>[118]</sup>



**Scheme 77.** DIELS-ALDER reactions of vinyl quinones and possible subsequent transformations

In comparison to classical DA reactions involving quinones and electron rich dienes, which have been extensively used in synthesis, vinyl quinone Diels-Alder (VQDA) reactions still remain largely unexplored and underutilized. In this context, an asymmetric intermolecular version would further enhance the usability and largely extend the scope of this mode of DA reactions. Hence, exploiting the synthetic potential of the VQDA reaction could give access to many potentially bioactive natural and non-natural products enantioselectively in a swift and elegant fashion. In this context, a thorough research of

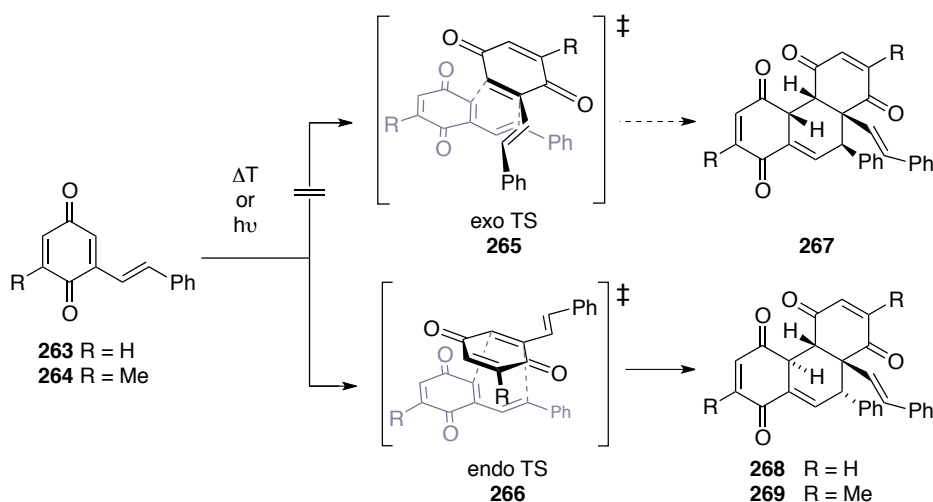
reactivity of obtained intermediates, such as isoquinone methides **259** or quinone methides **260** was envisaged.

Another aim of this project was to further extend the substrate scope of VQDA reactions and possibly to accomplish an enantioselective variant of the VQDA reaction utilising chiral LEWIS acid catalysts.

## 2 INTRODUCTION

The DA reaction was discovered almost eight decades ago,<sup>[3-6]</sup> and to this day continues to attract synthetic organic chemists. This is largely due to the great synthetic potential of this atom-economic reaction. With a broad substrate scope it allows the creation of up to four contiguous stereocentres with usually remarkably high regio- and diastereoselectivity.

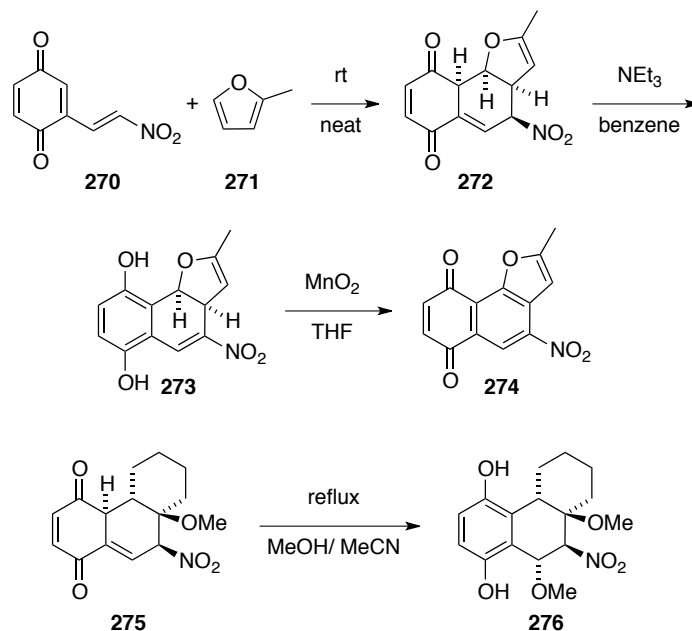
The first example for the DA reaction involving vinyl quinones as dienes was reported by IRNGARTINGER *et al.*<sup>[119]</sup> When examining the chemistry of electron-rich alkenyl substituted quinones **263**, a self-dimerization reaction, yielding hydrophenanthrenes **268** in excellent regio- and diastereoselectivity (Scheme 1.2) was observed. The products were unambiguously assigned by NMR and X-ray crystallography. The stereochemical outcome suggests, that this inverse electron demand DA reaction proceeds *via* an *endo* transition state **266**, where the most electron rich double bond in the quinone system reacts with the vinyl quinone diene (Scheme 78). Later, IWAMOTO *et al.* reported a similar reaction, when irradiation of vinyl quinone **264** with UV light gave DA type product **269**, with the same remarkable regio- and diastereoselectivity.<sup>[120]</sup> Products of the type **267**, which could be derived from an *exo* transition state **265** were not observed.



Scheme 78. Self-dimerisation of vinyl-*para*-quinones.

The scope of this reaction was then further extended by NOLAND and KEDROWSKI, when they showed, that the electron-poor nitrovinylquinone **270** smoothly undergoes [4+2]

cycloaddition reactions with electron rich dienophiles, such as furans, indoles or acyclic enol-ethers, to give dihydro naphthoquinones like **272**, in again perfect regio- and diastereoselectivity (**Scheme 79**).<sup>[121]</sup> However, the initial resulting isoquinone methide DA products were not isolated in all cases, as they easily tautomerised to the aromatic phenol form. Only when they employed a thoroughly dried, non-polar solvent for the reaction, precipitation of the quinoid cycloadduct **272** could be observed. Contact with polar solvents or base almost immediately caused tautomerization to the phenolic form **273**.

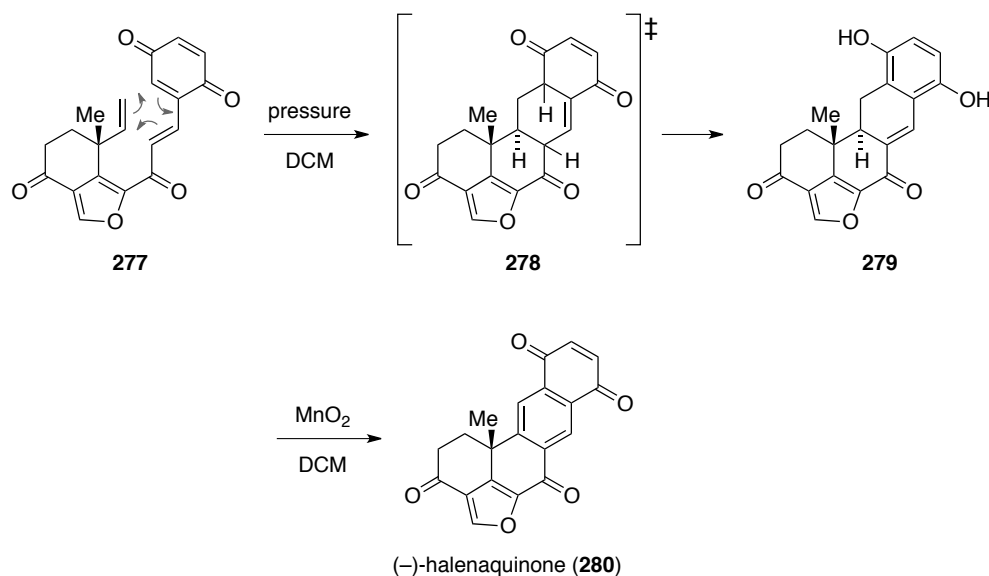


**Scheme 79.** Reaction of nitrovinylquinone **270** with 2-methylfuran (**271**) and reactivity of initially formed isoquinone methides.

It was shown, that the thus resulting hydroquinones and isoquinone methides can be further functionalized into more complex molecules or alternatively be fully aromatized. Heating of hydroquinone **273** with  $\text{MnO}_2$  as the dehydrogenating agent resulted in an aromatic, highly substituted quinone **274**. Instead of wasting the synthetic potential of the isoquinone methide through tautomerisation, it can be intercepted by nucleophiles such as MeOH, as shown in the conversion of **275** to **276**. In that example only one diastereoisomer was observed for the addition of methanol into the isoquinone methide.<sup>[122]</sup>

The first example for an intramolecular version of the VQDA reaction was reported by TRAUNER and co-workers in the total synthesis of (-)-halenaquinone (**280**).<sup>[123]</sup> This fast and elegant synthesis was at the same time the first example for the application of a DA reaction involving a vinyl-*para* quinone in total synthesis. Halenaquinone (**280**) attracted considerable

interest of the synthetic community due to its multifaceted biological profile.<sup>[7,8]</sup> Precursor **277** for the VQDA reaction underwent the desired [4+2] cycloaddition reaction under LEWIS-acid catalysis or upon heating in toluene. However, the highest yield was obtained, when very high pressure of almost 1 GPa was applied, affording vinyl hydroquinone **279** *via* transition state **278** in 78% yield. The initial DA adduct could never be isolated. The natural product **280** was obtained after oxidation with MnO<sub>2</sub>. However, this synthesis did not utilize the synthetic value of the *ortho*-quinone methide.



**Scheme 80.** Synthesis of (-)-halenaquinone (**280**) *via* an intramolecular VQDA reaction

Given the abundance of quinones in nature, it is entirely possible that VQDA reactions bear some biosynthetic relevance. Indeed, many natural products can be identified that contain the corresponding retrons. These include the pycnanthuquinones (**281** – **283**),<sup>[124,125]</sup> glaziovianol (**284**),<sup>[126]</sup> pleurotin (**285**),<sup>[127]</sup> and, in a modified form, rossinone B (**286**).<sup>[128]</sup> In most of these natural products, the retrosynthetic application of the VQDA reaction would lead to simple meroterpenoid quinones, which are common natural products themselves.

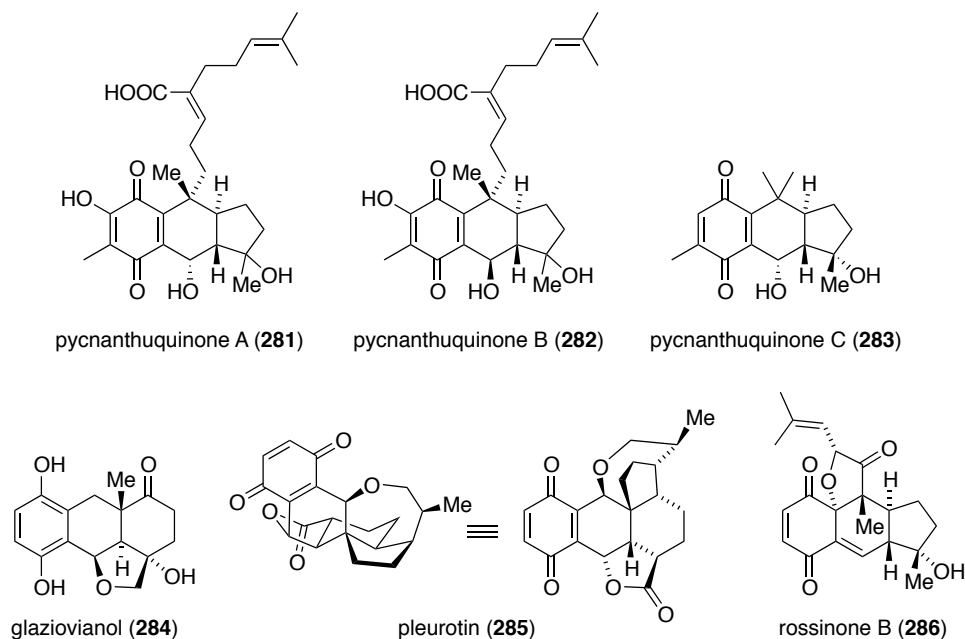
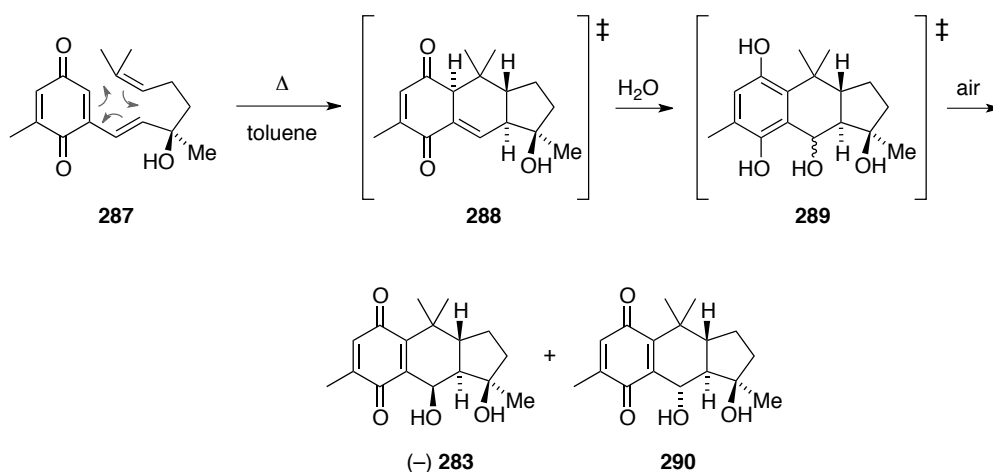


**Figure 30.** Natural products bearing VQDA retron

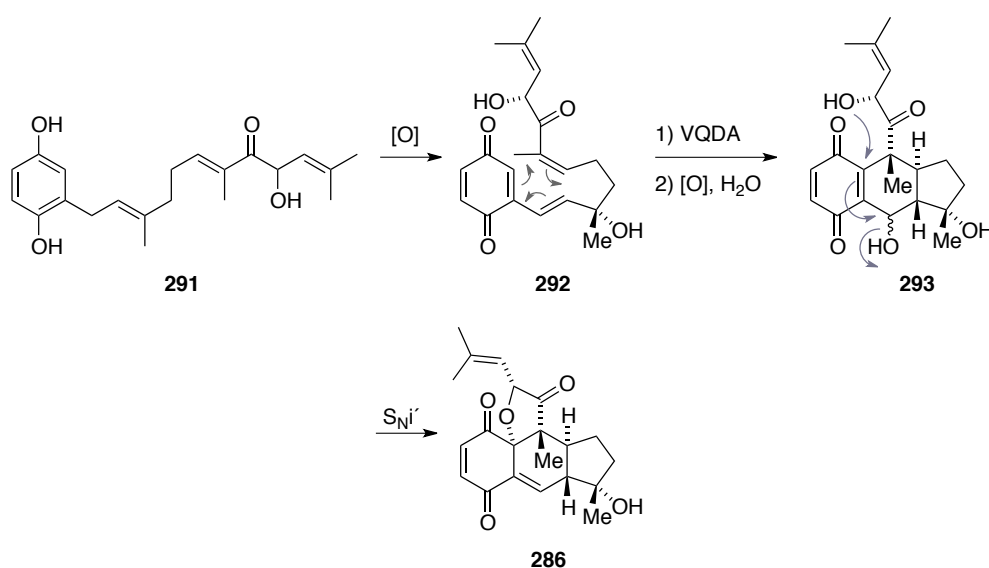
Recently, two biomimetic syntheses, both showing the synthetic value of the initially formed isoquinone methides, have been reported. TRAUNER and co-workers suggested biosynthetic pathways for the formation of pycnanthuquinone C (**283**) and rossinone B (**286**), involving a VQDA reaction as the key transformation.<sup>[118]</sup> They supported their biosynthetic hypothesis by employing this strategy in a very concise and elegant synthesis of the natural product pycnanthuquinone C (**283**).

The quinone precursor **285** for the DA reaction was readily available in two steps. The key reaction of this synthesis presumably involved a highly diastereoselective VQDA reaction to afford the putative isoquinone methide **288**. The reactive intermediate **288** was then attacked by water in a non-stereoselective fashion to yield hydroquinone **289**, which was subsequently oxidized by air to (–)-**283** and its diastereoisomer **290**, under the reaction conditions (Scheme 1.5). This synthesis is remarkably short for a molecule of that complexity. Additionally the absolute configuration of the natural product has been elucidated through this total synthesis.



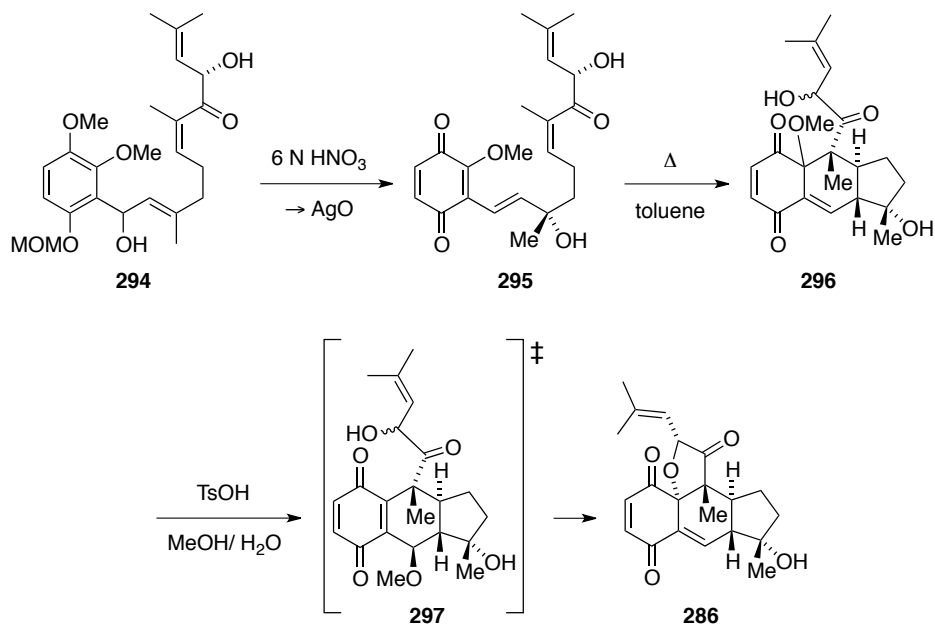
**Scheme 81.** Synthesis of (-)-pycnanthuquinone C (**283**) via a biomimetic VQDA reaction

The biosynthetic relevance of the VQDA reaction was further underlined by yet another biomimetic total synthesis. ZHANG *et al.* completed the synthesis of rossinone B (**286**) by following the biosynthetic proposal of TRAUNER and co-workers.<sup>[118,129]</sup> Not only the unusual structure, but also the diverse biological profile renders rossinone B an intriguing target for total synthesis. The unique quinoid core-structure can be seen as a stabilized isoquinone methide. It was proposed,<sup>[118]</sup> that this natural product stems directly from rossinone A (**291**), which was isolated from the same natural source. Oxidation of compound **291** to intermediate **292**, followed by VQDA reaction, addition of water, and further oxidation would initially afford quinone **293**, which closely resembles the pycnanthuquinones. In this case, however, the VQDA sequence is followed by an intramolecular S<sub>Ni</sub>' reaction that yields the tetracyclic framework of rossinone B **286**.



**Scheme 82.** Proposed biosynthesis of rossinone B (**286**) from known congener rossinone A (**291**)

The total synthesis closely follows the proposed biosynthetic pathway. Advanced intermediate **294** was transformed into DA precursor **295** under acidic, oxidative conditions. After VQDA reaction a diastereomeric mixture of **295** was obtained, which reacted in the presence of TsOH *via* intermediate **297** to give rossinone B (**286**).<sup>[129]</sup>



**Scheme 83.** Bio inspired synthesis of rossinone B (**286**)

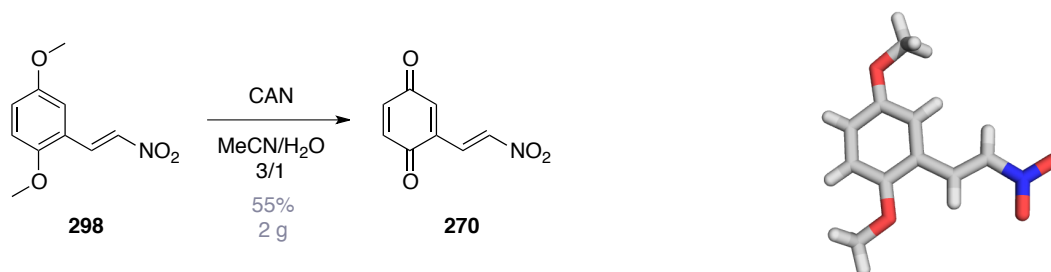
## 3 RESULTS AND DISCUSSION

### 3.1 Strategical Considerations

Considering reactivity of the vinyl quinone substrates, different functional groups adjacent to the vinyl double bond would allow for the fine-tuning of reactivity in envisaged VQDA reactions. To familiarise with this chemistry, we first focused on a nitro (NO<sub>2</sub>) substituent, according to NOLAND's successful investigations,<sup>[121]</sup> in parallel, we envisaged to establish ketones, esters or less electron withdrawing groups such as aryls as neighbouring groups. Also, at a later stage of the project, hetero-DIELS-ALDER reactions were envisaged whereby an imine double bond could be introduced to the quinone-ring. Also, the possibility of highly stereoselective catalysis should be addressed. Therefore, a methoxy group in 2-position of the quinone should serve as suitable coordination site for potential LEWIS- or BRØNSTED acid catalysts.

### 3.2 Scope of VQDA Reactions: Synthetic Progress

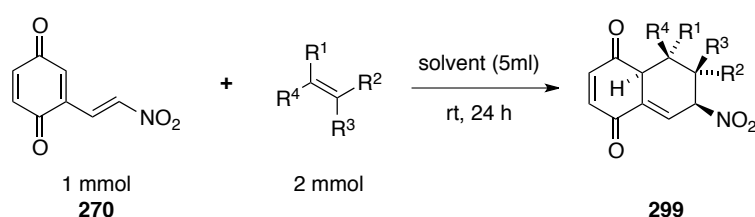
To familiarise ourselves with the intriguing chemistry of established VQDA systems, first synthetic studies focused on revisiting NOLAND's nitrovinyl quinone **270**,<sup>[121]</sup> which was established upon CAN-oxidation from the methoxyhydroquinone **298**. In the course of this work, single crystals of **298** suitable for X-ray crystallographic analysis were obtained.

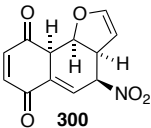
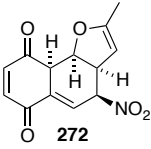
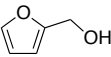
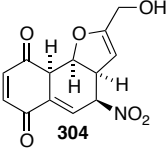
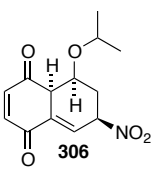


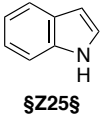
**Scheme 84.** X-ray crystal structure of methoxy quinone **298** and its oxidation to quinone **270**. Colour code: grey: carbon, red: oxygen, blue: nitrogen, white: hydrogen

With quinone **270** in hand, the stage was set for screening different dienophiles in VQDA reactions. Findings of these screenings are summarised in Table 13 and Table 14. In all screenings, 1 mmol of quinone **270** was reacted with 2 mmol of a corresponding, electron-rich dienophile in 5 mL of reported solvent. Envisaged outcomes refer to the isoquinonmethides and do not take further tautomerisation in account. Also, introduced structures illustrate the relative stereochemistry of one enantiomer in the racemic mixture with respect to the observed *endo*-selectivity, which will be discussed in more detail in the corresponding subsection (*vide supra*).

**Table 13.** VQDA screening with **270** as diene part I

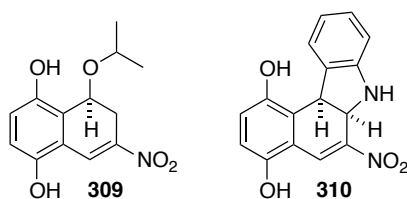


entry	solvent	dienophile	envisaged outcome	observation
1	PhH	 <b>109</b>	 <b>300</b>	decomposition upon work up
2	PhH			isolated yield 45%
3	toluene	 <b>271</b>	 <b>272</b>	isolated yield 63%
4	DCM			isolated yield 66%
5	toluene	 <b>301</b>	 <b>302</b>	decomposition upon work up
6	PhH	 <b>303</b>	 <b>304</b>	isoquinonemethide and hydroquinone mixture/ decomposition upon work up
7	PhH	 <b>305</b>	 <b>306</b>	isolated yield hydroquinone 57%

entry	solvent	dienophile	envisaged outcome	observation
8	PhH			mixture hydroquinone and by-products/ decomposition upon work up
9	toluene			mixture hydroquinone and by-products/ decomposition upon work up

For all entries in Table 13, consumption of vinylquinone precursor **270** was observed according to TLC analyses. It was found, that a fine balance between steric and electronic properties of envisaged quinonemethides determines stability of these intriguing intermediates. While the VQDA product of **270** and furan (**109**/ entry 1) appeared to start decomposing already during the reaction (or on silica), introduction of only one additional methyl group to dienophile **271**, (entries 2 – 4) yielded an isoquinonemethide **272**, which was stable in the reaction mixture, regardless of the solvent in use. Furthermore, the isolated, beige powder of **272** could be stored in the freezer and was even bench stable for several hours.

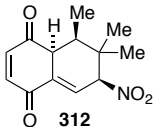
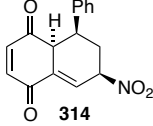
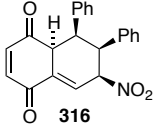
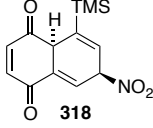
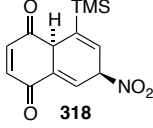
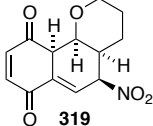
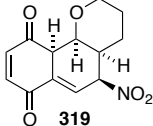
Adding more steric bulk to the system, using dimethylfuran **301** (entry 5) or changing electronics slightly upon addition of one hydroxyl group to the dienophile (furfuryl alcohol **303**), both had a negative effect on the stability of products. While obtained products from the VQDA reaction in entry 5 immediately decomposed upon work up, crude <sup>1</sup>H NMR analysis of the reaction described in entry 6 revealed spontaneous tautomerisation of isoquinonemethide **304** and subsequent decomposition. A novel product, which had non been previously described in literature, was obtained, using vinyl ether **305** (entry 7). The isolated product was not isoquinonemethide **306**, but its tautomer hydroquinone **309** (Figure 31). Similarly, a high rate of tautomerisation of isoquinonemethide **308**, obtained from VQDA reaction with indol (**307**/ entries 8 and 9) was evident, using either benzene (entry 8) or toluene (entry 9) for solvent. Corresponding hydroquinone **310** (Figure 31) proofed less stable in comparison than **307**. The nature of the solvents used (polarity or coordinating abilities), appears to have a subordinated role for the tautomerisation rate, as described isoquinonemethides **306** and **308** spontaneously tautomerised in non polar, non coordinating solvents, whereas isoquinonemethide **272** does not tautomerise until water or acetone are added.



**Figure 31.** Stable tautomers from VQDA reactions with novel isopropylvinyl-ether derived hydroquinone **309** and indol (as described by NOLAND **310**)

To gain further insight into the reactivity of quinone **270** and to enrich the scope of VQDA reactions of this precursor, a second screening focused on less electron-rich dienophiles. This second screening is summarised in Table 14.

**Table 14.** VQDA screening with **270** as diene part II

entry	solvent	dienophile	envisaged outcome	observation
1	toluene	 <b>311</b>	 <b>312</b>	decomposition
2	toluene	 <b>313</b>	 <b>314</b>	decomposition
3	toluene	 <b>315</b>	 <b>316</b>	decomposition
4	toluene	 <b>317</b>	 <b>318</b>	decomposition
5	CDCl <sub>3</sub>	 <b>317</b>	 <b>318</b>	decomposition
6	benzene	 <b>105</b>	 <b>319</b>	decomposition
7	toluene	 <b>105</b>	 <b>319</b>	decomposition

This second screening aimed for the use of electron-rich alkenes, mainly without adjacent heteroatoms (entries 1 – 3), testing 2-methyl-2-butene (**311**/ entry 1), styrene (**313**/ entry 2) or *cis* stilbene (**315**/ entry 3). In the presence of named dienophiles, only

decomposition of starting quinone **270** was observed. Further investigations were conducted with alkyne **317** (entries 4 and 5), as well as DHP (**105**/ entries 6 and 7). Again, only decomposition of the quinone **270** was observed. The decomposition of the quinone **270** was evident after one to two hours according to  $^1\text{H}$  NMR analysis, conducted with crude samples, taken from the reaction batch as described in entry 5.

To summarise Table 14, no VQDA reactions yielding envisaged products **312**, **314**, **316**, **318** or **319** were observed. All reaction setups finally lead to decomposition of the starting nitrovinylquinone **270**. It would appear, that in contrast to successfully reacted dienophiles described by NOLAND and co-workers,<sup>[121]</sup> vinyl oxygen or vinyl nitrogen motives are required to meet the electronic needs to promote envisaged VQDA reaction. This however does not explain, why reactions with dihydropyrene (DHP/ **105**/ entries 6 and 7) did not result in VQDA products.

As the VQDA reaction between silvan (**271**) and quinone **270** delivered stable isoquinonemethide **272**, this system was chosen for detailed investigations, starting with thorough  $^1\text{H}$  NMR analysis. For this purpose, 60 mg (1 equivalent, 0.34 mmol) of nitrovinylquinone **270** was dissolved in  $\text{CDCl}_3$  (1.2 mL). The reaction was started upon addition of silvan (**271**, 2 equivalents, 0.67 mmol). Temporal progress of this reaction followed by means of  $^1\text{H}$  NMR is shown in Figure 32.

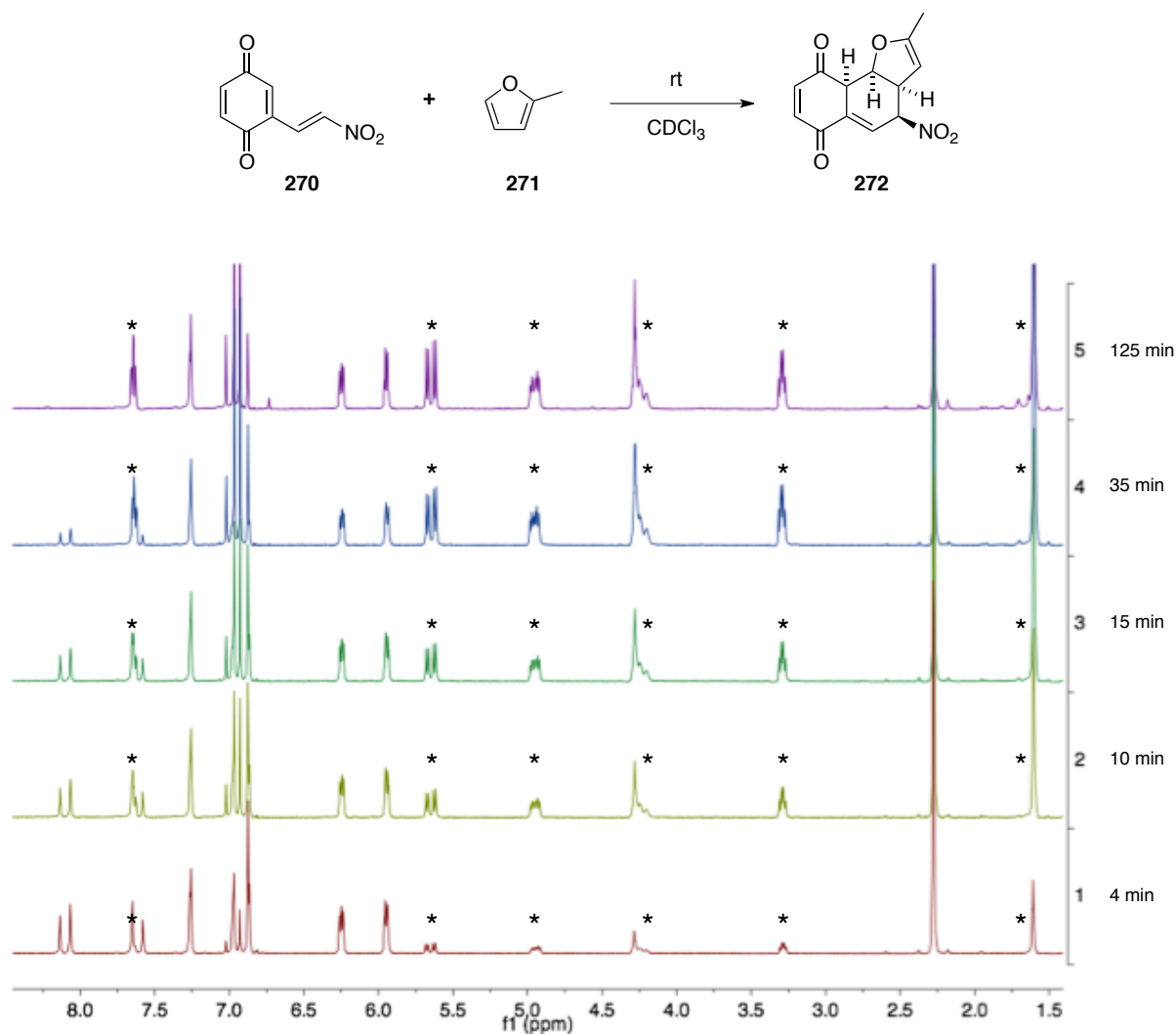


**Figure 32.** Progress of VQDA in  $\text{CDCl}_3$ , trace 1: 4 minutes, trace 2: 10 minutes, trace 3: 15 minutes, trace 4: 35 minutes, trace 6: 125 minutes/ signals of isoquinonemethide **272** highlighted with \*

Proton spectra in Figure 32 indicate the clean conversion of the starting vinylquinone **270** to corresponding isoquinonemethide **272** (NMR peaks highlighted with an asterisk) upon [4+2] cycloaddition. After 125 minutes, no more starting material **270** can be observed. Silvan (**271**) and isoquinonemethide **272** are found in a 1/1 mixture, as two equivalents of starting dienophile **271** were used to furnish appropriate time scales. The temporal progress of this reaction is also shown in Figure 33. Relative conversion was determined by peak integral ratios. At a 1 to 2 ratio of starting quinone **270** and dienophile **271**, the reaction proceeds smoothly on an hour time scale whereby a 50% conversion is achieved after ca. 10 minutes.

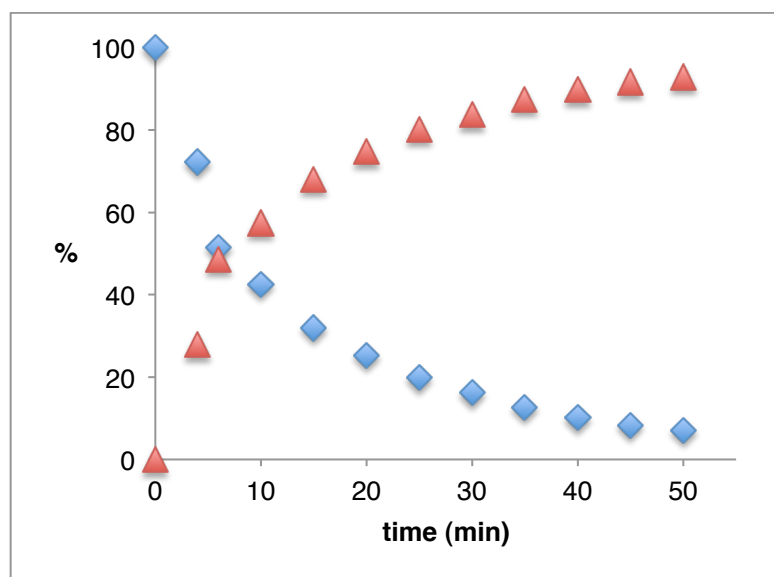
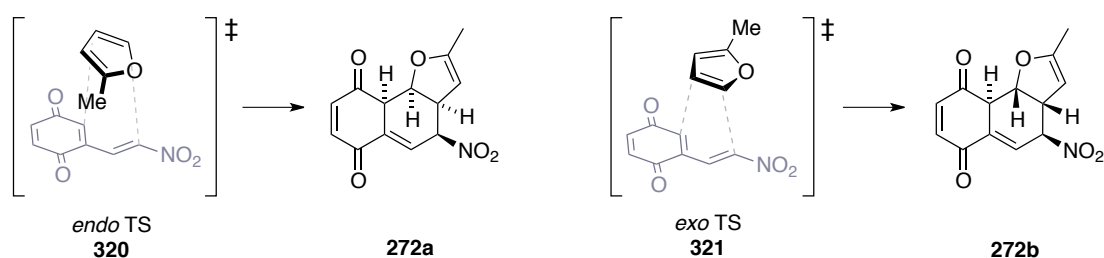


**Figure 33.** Conversion in VQDA reaction of nitrovinylquinone (**270**, blue rhombi) to the corresponding isoquinonemethide (**272**, red triangles)

Careful analysis of the only product obtained (isoquinonemethide **272**) indicates a relative stereochemistry as depicted in Scheme 85/ **272a**. Therefore, an *endo* transition state (**320**) may be considered for this VQDA reaction, as opposed to alternate *exo* transition state **321**. Apparently, the sterically less accessible, trisubstituted double bond in silvan (**271**) does not react as dienophile in this reaction. Though this double bond would be more electron rich, the steric bulk completely governs regioselectivity of this reaction.



**Scheme 85.** *endo* and *exo* transition **320** and **321** states for the VQDA reaction between **270** and **271**

As depicted in Scheme 85, the *endo* transition state would lead to an all-*syn* alignment of the protons on the newly generated stereogenic centres, resulting in comparably small coupling constants, following the KARPLUS curve.<sup>[66]</sup> In contrast, an *exo* transition state would lead to an *anti-syn-anti* configuration, hence larger coupling constants for the *anti*-standing protons on the newly created stereocentres would be expected. <sup>1</sup>H NMR analysis indeed shows, that corresponding coupling constants of respective protons are found in a range between 2.2 – 3 Hz, which translates to dihedral angles of 60 to 70°, thus strongly supporting an *endo* transition state and the resulting all-*syn* correlation. To support this proposal for

compound **272**, an NOESY experiment was carried out, which confirmed the configuration of **272a** (Figure 34). All proton substituents on the formed stereocentres in the DA reaction display coupling to one another. In an *anti-syn-anti* relationship, this would not be observed.

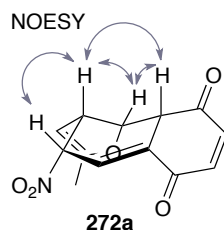
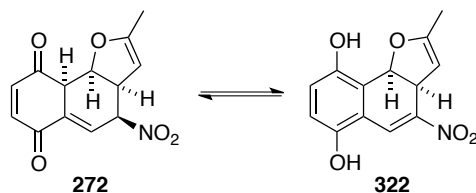


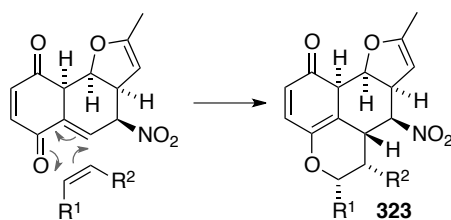
**Figure 34.** NOESY coupling of isoquinonemethide **272**

In addition to studies on VQDA reactions, we focused on the tautomerisation behaviour of isoquinonemethide **272**. When dissolved in acetone, a colour change from pale yellow to red-brown occurred immediately. Upon  $^1\text{H}$  NMR analysis in acetone ( $d_6$ ) a complete tautomerisation to the corresponding hydroquinone (**322**) was evident in less than 10 minutes. In this medium however, the hydroquinone appeared to be far less stable. Possibly, upon intermolecular reaction between nucleophiles and the dihydrofuran moiety, formation of less stable by-products is triggered. This suggested type of reactivity was observed during further studies on **272** and will be discussed in more detail (*vide supra*).



**Scheme 86.** Tautomerisation of isoquinonemethide **272** to hydroquinone **322**

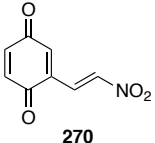
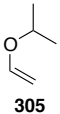
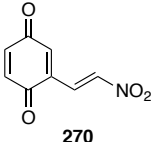
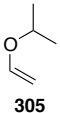
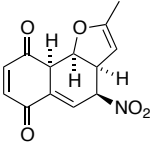
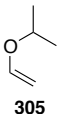
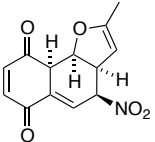
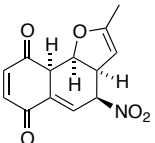
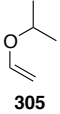
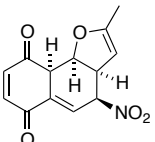
Going on to investigate VQDA systems and their potential as suitable building blocks in modern organic synthesis, further investigations of the reactivity of above discussed isoquinonemethide **272** were carried out. Firstly, focus was laid on the possibility to use the obtained MICHAEL system of the isoquinonemethide as potential diene in a hetero-DIELS-ALDER reaction (Scheme 87).



**Scheme 87.** Investigating further reactivity of isoquinonemethide **272** in hetero-DIELS-ALDER reactions

Two reaction pathways were investigated. Firstly, Isopropyl vinyl ether **305** was reacted with nitrovinyl quinone **270** to establish a “tandem-DA” reaction. Secondly, isoquinonemethide **272** was subjected to excess amounts of dienophiles **305** and **271**, respectively. Findings of these investigations are summarised in Table 15.

**Table 15.** Studies on tandem- and hetero

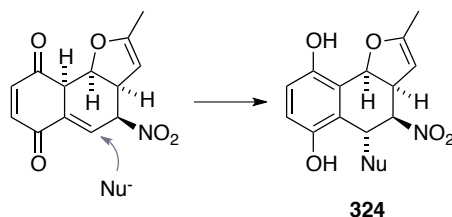
entry	reactant 1	reactant 2	solvent	conditions		observation	
				T [°C]	t [h]		
1	 <b>270</b>	1 eq  <b>305</b>	100 eq	DCM	23	0.5	decomposition
2	 <b>270</b>	1 eq  <b>305</b>	50 eq	neat	55	0.5	decomposition
3	 <b>272</b>	1 eq  <b>305</b>	2 eq	DCM	23	0.5	no rxn
4	 <b>272</b>	1 eq  <b>271</b>	2 eq	DCM	23	0.5	no rxn
5	 <b>272</b>	1 eq  <b>305</b>	100 eq	neat	60	12	decomposition
6	 <b>272</b>	1 eq  <b>271</b>	100 eq	neat	60	12	decomposition

In the first attempt to achieve a tandem-DA reaction with vinylquinone **270** (entry 1) a 100-fold excess of vinyl ether **305** was added to the starting material at ambient temperature. As this setup only lead to decomposition, the reaction was carried out at 55 °C, using ether

**305** as solvent to establish faster reaction of intermediately formed isoquinonemethide **272** (entry 2). Again, only decomposition of the starting materials was observed. Presumably, intermediate **272** decomposed after tautomerisation, leading to several decomposition pathways.

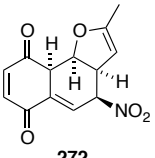
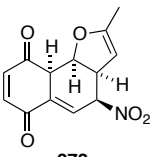
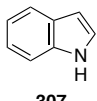
Isoquinonemethide **272** was also used as a substrate for envisaged DA reactions with isopropyl vinyl ether (entries 3 and 5) as well as silvan (**271**/ entries 4 and 6). While two equivalents of dienophile in DCM at ambient temperatures did not yield any reactivity (entries 4 and 5), neat conversions with 50-fold excess of dienophiles exclusively lead to decomposition of the isoquinonemethide **272** again (entries 5 and 6).

After all attempts to achieve further DA reactions failed, nucleophilic attacks on isoquinonemethide **272** were investigated next. Nucleophilic attack of suitable reaction partners was envisaged to proceed *via* 1,4- addition as outlined in Scheme 88.

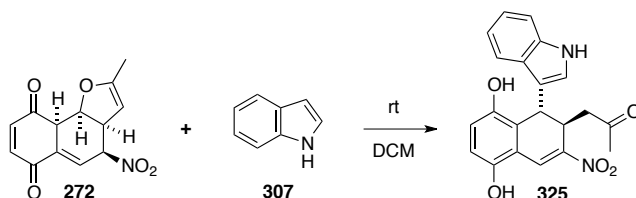


**Scheme 88.** Reactivity of isoquinonemethide **272** with nucleophiles

As nucleophilic reaction partners, iodide and cyanate were tested. Also, we were interested in the reactivity of indol (**307**), which could potentially react in both ways, as nucleophile or dienophile.

entry	reactant 1	reactant 2	solvent	conditions		observation	
				T [°C]	t [h]		
1	 272	1 eq NaI	30 eq	THF	23	12	decomposition
2	 272	1 eq KCN	2.5 eq	THF	23	12	decomposition
3	 272	1 eq KCN 18-crown-6	2.5 eq 2.5 eq	THF	23	12	decomposition
4	 272	1 eq  307	2 eq	DCM	23	0.5	conversion

Whilst attempts to use iodide or cyanate as nucleophiles only lead to decomposition of the starting material **272** (entries 1 –3), conversion with indol (**307**/ entry 4) gave a novel product, which precipitated upon applied reaction conditions. After 30 minutes, the starting material was fully converted to this novel product. To our surprise, neither envisaged nucleophilic attack on the methide-carbon, nor hetero-DIELS-ALDER reaction occurred. Careful NMR analysis suggested a different product, wherein the furan moiety had been opened upon nucleophilic attack of the indol (**307**) as depicted in Scheme 89.



**Scheme 89.** Nucleophilic attack of indol (**307**) on isoquinonemethide **272**

Crystallisation attempts lead to single crystals, suitable for X-ray diffraction analysis. Findings confirmed product **325**.

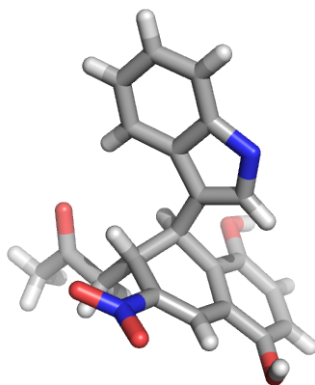


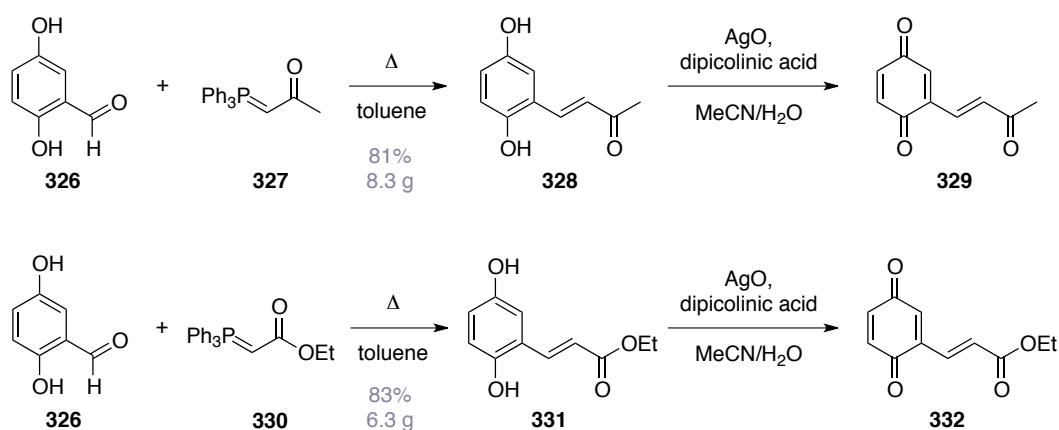
**Figure 35.** X-ray crystal structure of **325**, colour code: grey: carbon, red: oxygen, blue: nitrogen, white: hydrogen

Due to disorder of cocrystallised DCM, this X-ray crystal structure does not fit publication standards but supports NMR analyses indicating the opening of the furan moiety upon attack of indol **307** from the opposite face. To the best of our knowledge, this is the first example of a furan opening by means of a nucleophilic attack of indol. As no similar reaction could be observed using other nucleophiles, mechanistic proposals would be highly speculative at this point. Similar reactions may however deliver a plausible reason for observed decomposition, as the formed ketone may be attacked. Also, if water could open the furan in a similar fashion, elimination of a hydroxy group could lead to highly reactive intermediates.

### 3.3 Alternative Precursors and Oxidation Methods

After having further explored the reactivity of nitrovinyl quinones as DA dienes, the attention was focussed on extending the substrate scope of suitable dienes for VQDA reactions. Because nitro-substituted vinyl quinones, such as the parent system studied by NOLAND and KEDROWSKI,<sup>[122]</sup> are very electron-poor and thus very reactive towards electron-rich dienophiles, observed VQDA reactions proceeded within minutes (see Figure 4). Enabling a DA reaction with different vinyl quinones would allow to study the influence of electronics on the reaction performance and at the same time introduce a broader variety of synthetic handles into the products. Both of which would further increase the usability of VQDA reactions.

Replacing the nitro moiety with carbonyl functionalities in the vinyl system would render the resultant diene less electron-poor than the nitro-substituted counterpart, but still set the stage for a DA reaction with inverse electron-demand. To explore, whether such a significantly less electron-poor system would indeed still be suited for a DA reaction, quinones **329** and **332** were targeted for synthesis. Both vinylquinone precursors **328** and **331** were obtained in good yield through a WITTIG-reaction with the corresponding phosphor ylid.<sup>[130]</sup> Both vinylhydroquinones were oxidised with activated silver oxide to give the desired vinyl-quinones **329** and **332**. In this case it was chosen to synthesise the free phenol derivatives, since clean oxidation of the corresponding methoxyhydroquinones had proven very difficult. The quinones presumably decomposed more rapidly upon the harsher reaction conditions necessary.



**Scheme 90.** Synthesis of vinyl quinones **329** and **332**

As quinones **329** and **332** displayed only limited stability in solution, these intermediates were taken on in further reactions immediately after isolation. Both vinyl-quinones were reacted with excess silvan (**271**) as the electron-rich dienophile. However, no precipitation of a [4+2] cycloadduct could be observed and TLC analyses of the crude reaction mixtures always revealed a complex product mixture, presumably due to the high instability of any formed intermediate. Only when heating a sample of **332** and methyl-furan in  $\text{CDCl}_3$  the formation of isoquinone methide **333** could be observed (Figure 6). Attempts to force the reaction to completion through prolonged reaction times and higher temperatures as well as attempted isolation of the product by precipitation with non-polar solvents or chromatography all lead to decomposition. For this reason, the observed product could not unambiguously be assigned, but based on previous observations, the signals marked with an asterisk suggest the formation of DA adduct **333**.

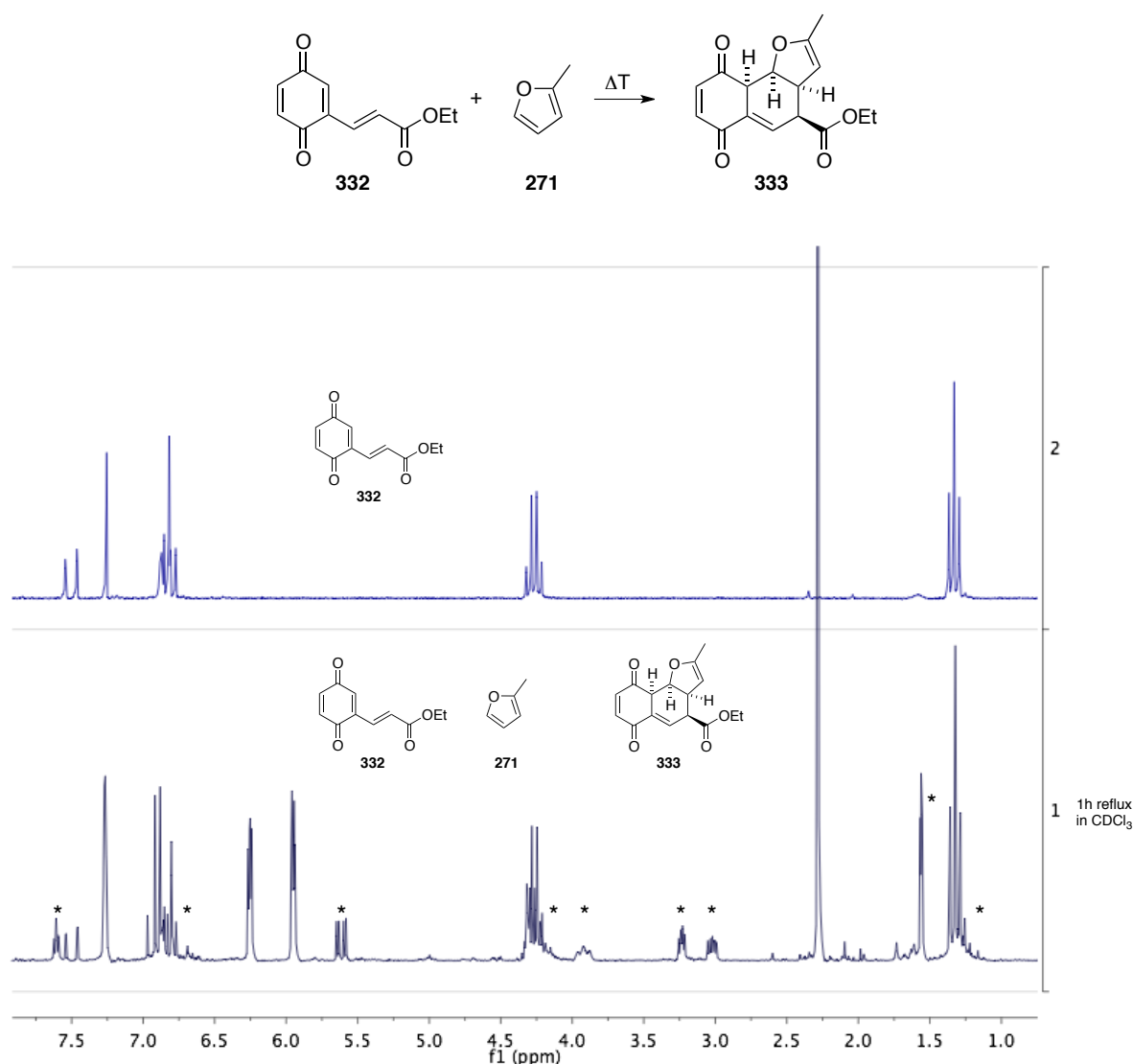
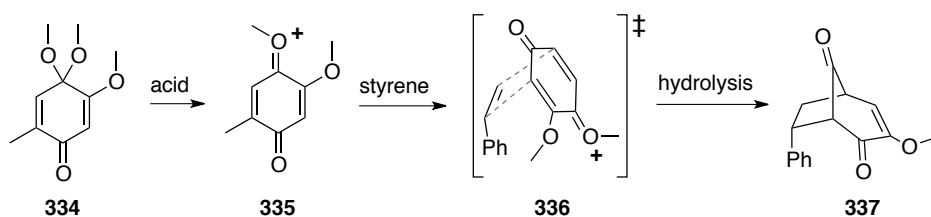


**Figure 36.** Crude NMR analysis of VQDA reaction between sylvan (**271**) and quinone **332**

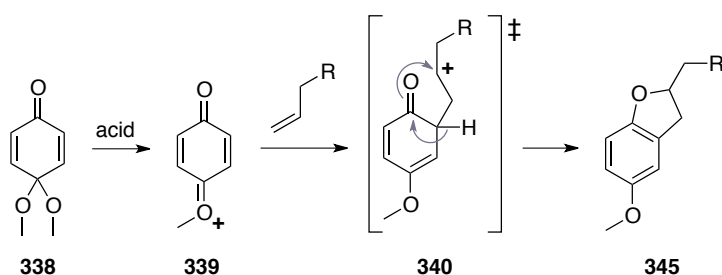
Attempts to drive this reaction to completion upon further heating did not only lead to full consumption of the starting quinone, but also triggered decomposition of the resulting product. These results suggested, that the system was not activated enough anymore to effectively enable a [4+2] cycloaddition before decomposition occurred.

It was first shown by GRIECO and co-workers,<sup>[131,132]</sup> that quinone monoketals in highly polar media readily undergo [5+2] cycloaddition reactions. The reaction presumably commences with the formation of an oxonium-ion **335**, which is generated from the quinone monoketal **334** in an acidic environment. This sets the stage for an intermolecular [5+2] cycloaddition (transition state **336**) with styrene (**313**), giving di-ketones of the type **337** in good to excellent yields.



**Scheme 91.** An acid promoted intermolecular [5+2] cycloaddition reaction between quinone monoketal **334** and styrene

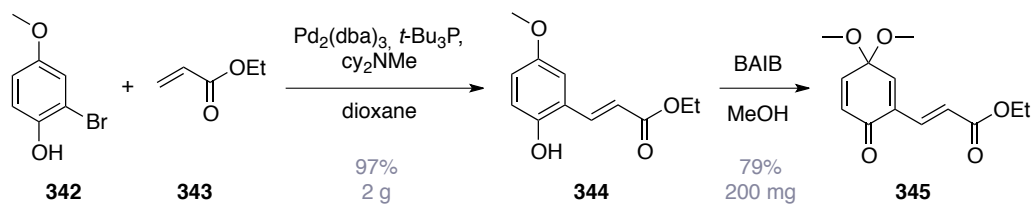
Another example for a formal cycloaddition reaction involving quinone monoketals was recently described by KITA and co-workers.<sup>[133,134]</sup> They reported a BRØNSTED-acid promoted, formal [3+2] cycloaddition of alkenes to quinone monoketals. Again, by treatment of quinone monoketal **338** with acid a reactive intermediate **339** was generated to which various alkenes were coupled. The formal [3+2] reaction presumably proceeds step-wise via a charged intermediate **340** to finally result in a hydrobenzofuran **341**.



**Scheme 92.** A BRØNSTED-acid promoted formal [3+2] cycloaddition reaction involving quinone monoketal **338** resulting in hydrobenzofurans

If a vinylquinone monoketal such as **345** is treated with acid, a positively charged vinylquinone type intermediate may be generated. This positive charge may now further activate the diene-system. Hence, it might well be possible, that a cationic [4+2] type cycloaddition proceeds faster than the corresponding [5+2] or [3+2] competing reactions. This envisaged enhancement could also provide reaction rates fast enough, to isolate resulting VQDA adducts before decomposition.

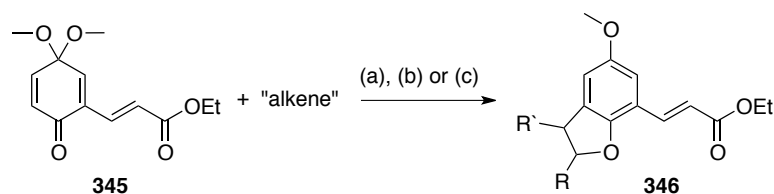
To explore the reactivity of vinylquinone monoketals towards electron rich alkenes, compound **345** was chosen as a test-system. Vinyl methoxyphenol **344** was obtained after HECK cross-coupling<sup>[135-138]</sup> between arylbromide **342** and methyl acrylate (**343**), which was transformed into desired vinylquinone monoketal **345** by treatment with bis(acetoxy)iodobenzene (BAIB) in anhydrous methanol.



**Scheme 93.** Synthesis of vinylquinone monoketal **345**

Vinylquinone monoketal **345** was submitted to acidic conditions, as reported by GRIECO and KITA, in the presence of alkenes. In all cases (entries 1–5) the reaction proceeded very sluggishly and the resulting products were very instable and could not be isolated. However, crude NMR and HRMS data suggest, that a formal [3+2] instead of the anticipated [4+2] cycloaddition occurred under all conditions tested.

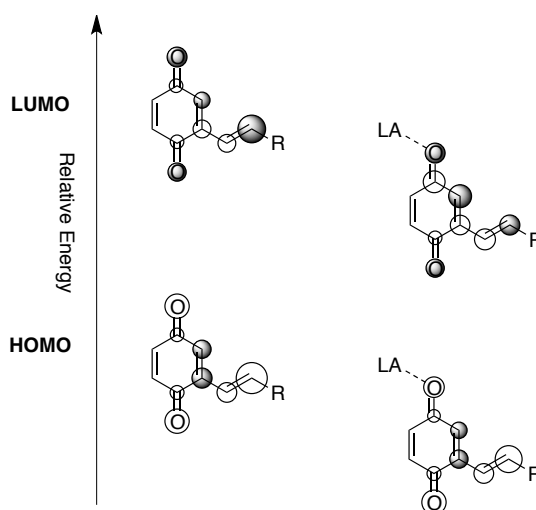
**Table 16.** Reactivity of vinylquinone monoketal **345** towards various alkenes under acidic conditions



entry	alkene	reaction conditions	observation
1	 271	3 M LiClO <sub>4</sub> , TMSOTf, –15 °C	decomposition
2	 313	3 M LiClO <sub>4</sub> , TMSOTf, –15 °C	 347
3		3 M LiClO <sub>4</sub> , TMSOTf, –15 °C	
4	 305	BF <sub>3</sub> •OEt <sub>2</sub> , DCM, –78 °C	
5		Montmorillonite K-10, DCM, –78 °C	 348

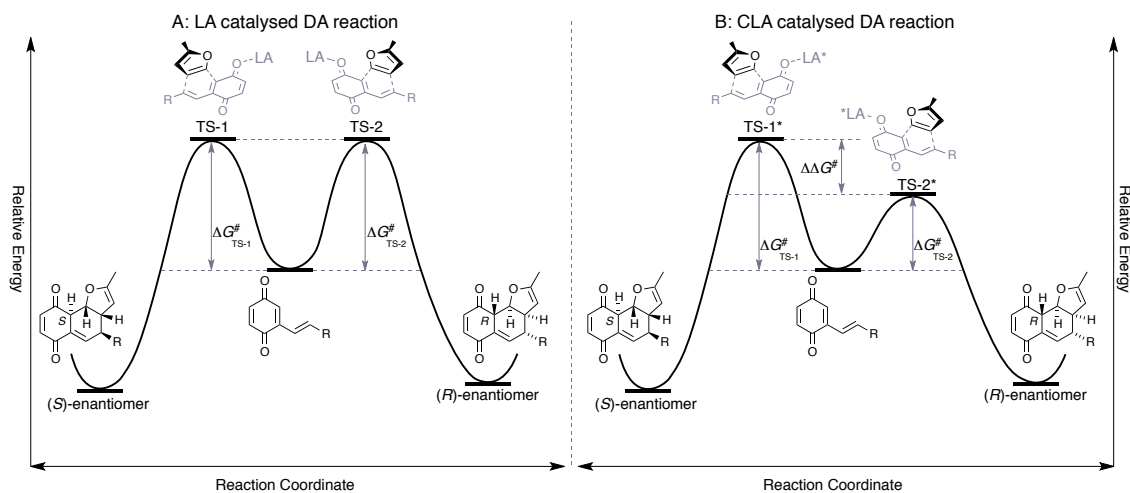
### 3.4 Catalysis attempts

It is well known, that the reaction rate and diastereoselectivity of DA reactions can be enhanced through the addition of catalytic or stoichiometric amounts of LEWIS acid (LA). In literature many examples for LA catalysed DA reactions with normal electron demand can be found. In those cases the LA can selectively coordinate to heteroatoms of one of the reaction components. This interaction strongly influences the electronic environment of the molecule. Not only the HOMO and LUMO orbital energies are lowered, but also the size of orbital coefficients is changed. In the case of the VQDA reaction the LA could coordinate to the carbonyl moiety of the quinone as shown in Figure 6. Lowering the orbital energies of the diene in consequence also lowers the energy gap between the HOMO<sub>dienophile</sub> and LUMO<sub>diene</sub> which then results in a higher reactivity and often an improved regio- and diastereoselectivity.



**Figure 37.** Coordination of a LEWIS-acid to a vinylquinone and the influence on the energy levels of its HOMO and LUMO

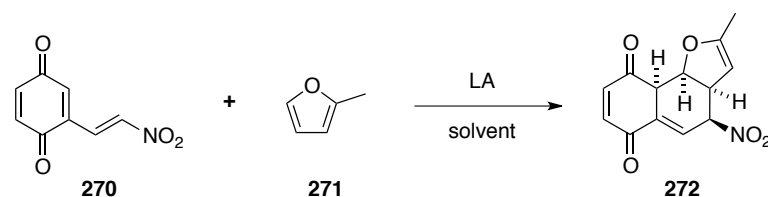
When utilizing chiral LEWIS acids (CLA) for the catalysis of DA reactions, additionally high enantioselectivities can be achieved. Upon coordination to one of the substrates, the CLA and the two reactants can form diastereomeric transition states (TS-1\* and TS-2\*) (Figure 38). As both enantiomeric products have the same relative energy, the reaction needs to proceed under kinetic control to achieve high enantioselectivities.



**Figure 38.** Exemplary transition states of a DA reaction catalysed with LA and CLA

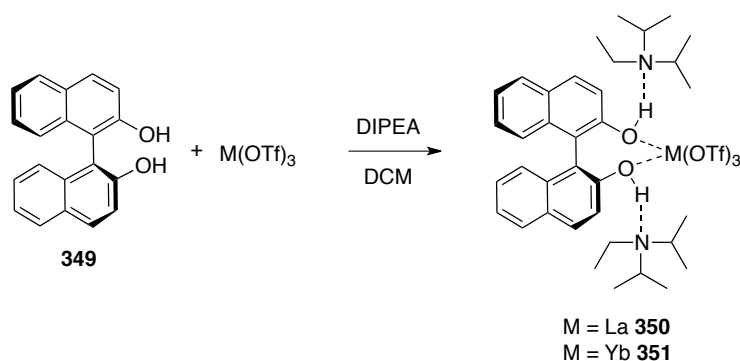
This means, that the activation barrier for one of the diastereomeric transition states needs to be substantially lower in energy relative to the competing diastereomeric transition states. The example in Figure 38B shows a CLA catalysed DA reaction, which would proceed through  $TS-2^*$  due to kinetic control and hence give predominantly the corresponding (*R*)-enantiomer. Hence, in order to favour one diastereomeric transition state over another, the CLA should activate one component selectively and at the same time provide a well defined stereochemical environment that results in a significantly lower activation barrier of one of the diastereomeric transition states.

The nitrovinyl quinone **270** has proven as a reliable diene in VQDA reactions. As the VQDA reactions proceed smoothly with a variety of dienophiles in usually good to excellent yield. Also, the products were isolable in most cases. Therefore it was chosen as the test-system to investigate if this system can be activated through LA catalysis and ultimately whether an enantioselective version can be achieved. To explore whether the VQDA reaction can be catalysed, several LA have been applied as additives in the reaction between **270** and methyl furan **271** (Table 5).

**Table 17.** Influence of achiral LA on the DA reaction between **270** and **271**

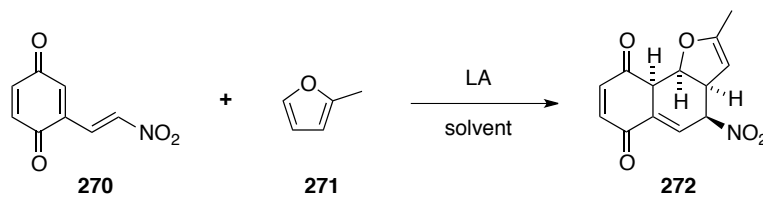
entry	LA	reaction conditions	observation
1	None	DCM, $-78^{\circ}\text{C}$	no reaction
2	$\text{BF}_3\text{OEt}_2$ (5%)	DCM, $-78^{\circ}\text{C}$	decomposition
3	$\text{Et}_2\text{AlCl}$ (10%)	toluene, $-20^{\circ}\text{C}$	decomposition
4	$\text{Ti}(i\text{-PrO})_4$ (5%)	DCM, $-78^{\circ}\text{C}$	precipitation
5	$\text{Yb}(\text{OTf})_3$ (5%)	DCM, $-78^{\circ}\text{C}$	decomposition
6	$\text{Eu}(\text{OTf})_3$ (5%)	DCM, $-78^{\circ}\text{C}$	decomposition
7	$\text{Sc}(\text{OTf})_3$ (5%)	DCM, $-78^{\circ}\text{C}$	decomposition
8	$\text{La}(\text{OTf})_3$ (5%)	DCM, $-78^{\circ}\text{C}$	decomposition
9	$\text{SnCl}_4$ (5%)	toluene, $0^{\circ}\text{C}$	decomposition

All triflate LAs only lead to decomposition, which might be due to the acid sensitivity of the vinyl quinone and the cycloaddition adducts. The binol LA complexes reported by KOBAYASHI *et al.* are chiral and significantly less acidic.<sup>[139]</sup> Hence it was anticipated that directly an asymmetric version of the VQDA reaction could be achieved. The chiral lanthanide binol complexes were obtained by reacting (*S*)-binol with the corresponding lanthanide triflates in the presence of a base.

**Scheme 94.** Preparation of binol based CLAs **350** and **351**

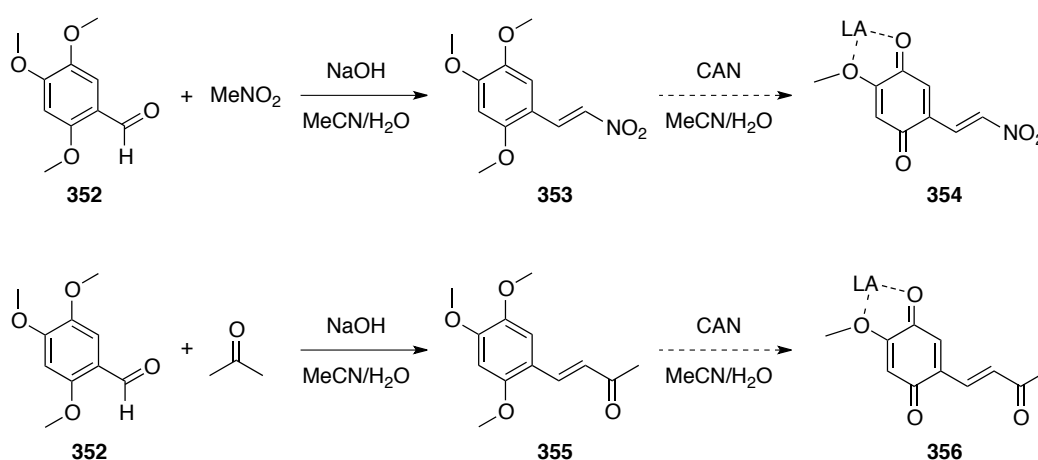
Those CLAs freshly prepared for each reaction and then tested to catalyse a VQDA reaction (Table 18).

**Table 18.** Influence of CLAs on the DA reaction between **270** and **271**



entry	LA	reaction conditions	observation
1	<b>350</b> (30%)	DCM, 0°C	decomposition
2	<b>351</b> (30%)	DCM, 0°C	decomposition

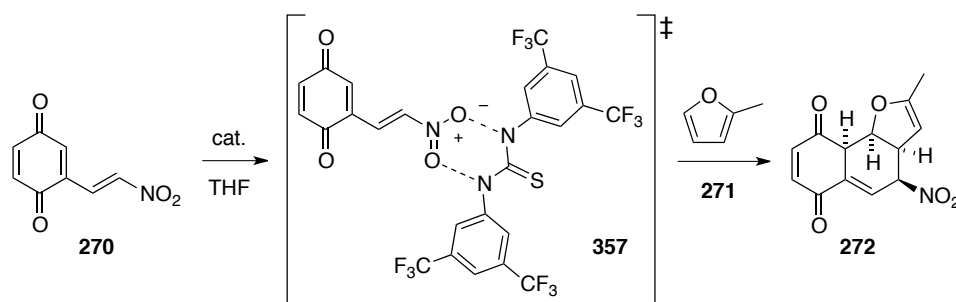
All tested conditions and LA did not result in a rate accelerated VQDA reaction. One potential issue could be that the LAs do not coordinate in a well-defined fashion to the vinyl quinone. To test this hypothesis, vinyl quinones with an additional methoxy moiety to aid coordination of transition metals were designed.



**Scheme 95.** Attempted synthesis of vinyl quinones with an extra coordination site for LEWIS acids

Aldol condensation of aldehyde **352** gave the corresponding vinyl methoxyhydroquinone derivatives **353** and **355** in good to excellent yields. However, it was not possible to obtain the corresponding quinones **354** and **356** upon oxidation with CAN, as the products quickly decomposed upon aqueous workup.

Since it was not possible to activate the vinyl quinone systems with traditional LAs, presumably due to the high instability of both, the products and starting materials, the possibility of organocatalysis was investigated. It is well known that electron poor thiourea derivatives can coordinate to nitro functionalities (Scheme 96). However, no rate accelerating effect could be detected, when adding 1,3-bis(3,5-bis(trifluoromethyl)phenyl)thiourea to the reaction mixture.



**Scheme 96.** Influence of an electron poor thiourea on the VQDA reaction



## 4 CONCLUSION

Thorough investigations of intermolecular VQDA reactions have been conducted, researching reaction pathways, scope, catalysis and further reactivity of obtained intermediates. The notorious instability of most precursors and products puts limitations to this methodology, however.

In terms of reaction scope, readily available nitrovinylquinone **270** may be reacted with novel electron rich dienophiles, such as isopropyl vinyl ether **307**. Less electron-rich double bonds could not be reacted with quinone **270**, however.

Vinyl quinones bearing carbonyl groups represented a further focus in the systematic investigation towards a larger scope of intermolecular VQDA reactions. Though NMR experiments indicated, that the desired VQDA proceeded smoothly upon appropriate conditions, subsequent isolation could not be achieved.

The limited stability of substrates and products may be the reason, why all LEWIS acids screened only lead to decomposition of materials. Further attempts to apply thiourea derivatives to promote faster reactions remained fruitless too.

Closer investigating reactivity of stable isoquinonemethide **272** revealed an intriguing reaction pathway, when indol (**307**) did not react with the  $\alpha,\beta$ -unsaturated carbonyl moiety, but rather opened the furan moiety.

In the course of synthetic studies in the TRAUNER group, intramolecular VQDA reactions are continuously used and appear to have greater potential for modern organic synthesis.



**CHAPTER IV:**  
**THE CRYSTAL STRUCTURE OF THE DESS-MARTIN**  
**PERIODINANE**

Results and text passages in “Part Four: The Crystal Structure of the DESS-MARTIN Periodinane” are taken from the manuscript “The Crystal Structure of the DESS-MARTIN Periodinane by SCHRÖCKENEDER, STICHNOTH, MAYER and TRAUNER.”<sup>[12]</sup>



# 1 PROJECT AIMS

The so-called DESS-MARTIN periodinane<sup>[10,11]</sup> (DMP, **358**, Figure 39) is a highly efficient oxidant, which is widely used in organic synthesis.

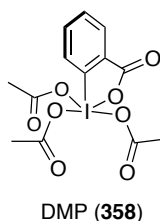


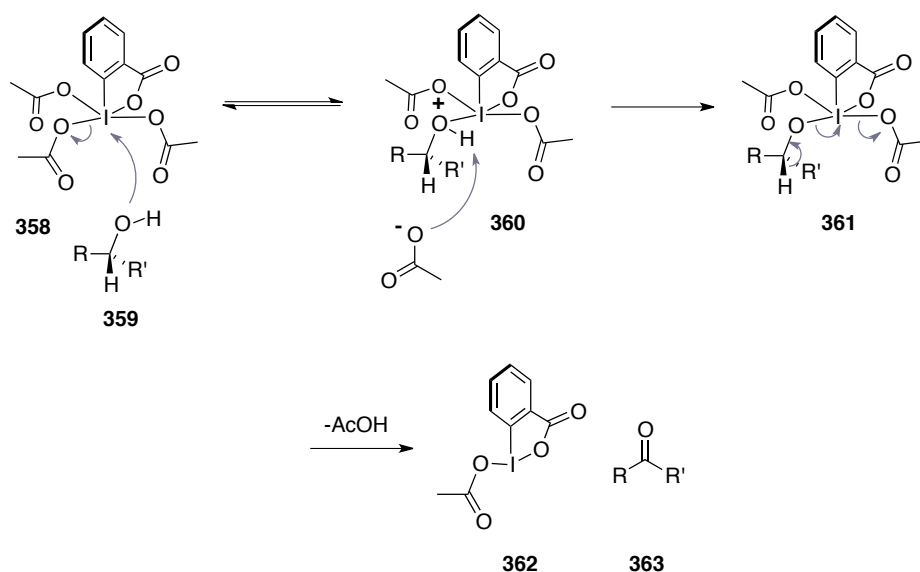
**Figure 39.** Molecular structure of DESS-MARTIN periodinane (DMP/ **358**)

Even though this popular reagent was introduced in 1983 and DESS and MARTIN themselves characterised numerous hypervalent iodine species by means of X-ray crystallography, no X-ray crystal structure of DMP (**358**) was reported to date. This astonishing fact was discovered in the course of a large-scale synthesis of DMP (**358**) in our laboratory, which, however, only yielded a highly crystalline iodine(III)- species (see detailed discussion in section 3). Although the initially obtained crystals were quickly identified to be not DMP (**358**), and thus, the goal of this project was to obtain the first X-ray crystal structure of this important oxidation agent and, if possible of related species.

## 2 BACKGROUND AND SIGNIFICANCE

Triacetoxybenziodoxolone has found wide use as oxidising agent in modern organic synthesis. It is, however, more commonly known as DESS-MARTIN periodinane (DMP, **358**), named after their inventors DESS and MARTIN, who introduced this novel iodine(V) species in 1983 as a potent alternative to the well-established 2-iodoxobezoic acid (IBX, **365**) oxidant. While activity and scope of these two hypervalent iodine species are largely the same, **365** is only sparingly soluble in most organic solvents, but is readily soluble in DMSO. DMP (**358**), on the other hand, exhibits much higher solubility in less polar solvents, most prominently in chloroform or DCM. In addition, this reagent is very stable, tolerates temperatures up to 130 °C, yet is typically capable of oxidising even sterically demanding secondary alcohols at ambient temperatures. DESS-MARTIN periodinane (**358**) thus represents a highly efficient oxidation agent, allowing for shorter reaction times and high selectivity under comparably benign reaction conditions. In comparison to other prominent oxidation methods, such as pyridinium chlorochromate (PCC)<sup>[140]</sup> and SWERN<sup>[141-146]</sup> oxidation, DMP also forms less toxic by-products and furthermore, work up procedures are uncomplicated.

The generally accepted mechanism for the DESS-MARTIN oxidation is mostly based on studies by DESS and MARTIN themselves,<sup>[10,11]</sup> as well as work by SCHREIBER and co-workers.<sup>[147]</sup>



**Scheme 97.** Generally accepted mechanism of oxidation using the DMP

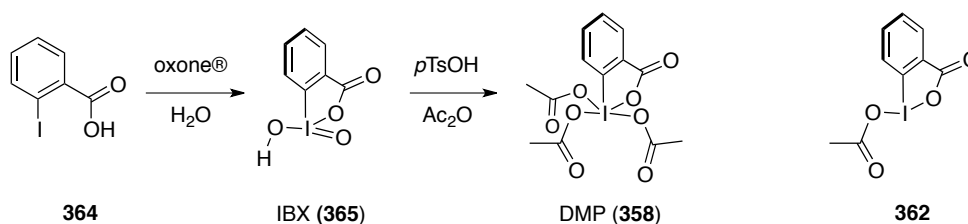
As depicted in **Scheme 97**, oxidation of generic alcohol **359** commences upon ligand exchange of one acetate group of DMP (**358**) which, as has been studied extensively using  $^1\text{H}$  NMR techniques, is a fast or instantaneous process specifically occurring on the axial position of the central, hypervalent iodine.<sup>[11,147,148]</sup> Proton transfer then occurs from the coordinated alcohol in **360** to the substituted acetate, forming intermediate **361**. Next, the rate-determining step, which is the conversion of intermediate **361** to the desired product, ketone **363**, and iodine(III)-species **362**.<sup>[11,147,148]</sup> If a more electron-donating “ligand”, such as water or another equivalent of a non-oxidisable alcohol is present, product formation occurs instantly. Even though this effect has been studied in detail, the question of whether this final step in the mechanism of the DESS-MARTIN oxidation proceeds *via* an intramolecular deprotonation of the  $\alpha$ -proton by the leaving acetate, or *via* intermolecular deprotonation remains unanswered.

The significance of DESS-MARTIN periodinane (**358**) is not only reflected by the fact that it is constantly used even nearly thirty years after its introduction to the chemical community, but also that despite its “classic” use as oxidant for primary and secondary alcohols to the corresponding aldehydes and ketones, other reactions have also been introduced. For instance, HANTZSCH esters<sup>[149]</sup> can be aromatised using DMP (**358**), if no oxidisable alcohol moiety is evident in the molecule.<sup>[150]</sup> Furthermore, decarboxylative bromination of  $\alpha,\beta$ -unsaturated carboxylic acids may be achieved in combination with tetraethylammonium bromide.<sup>[151]</sup> Another use of DMP is the formation of imides from corresponding amides,<sup>[152]</sup> or the generation of iminoquinones from corresponding amines.<sup>[153]</sup> Recently,  $\alpha$ -bromination of 1,3-dicarbonyl compounds using tetrabutylammonium bromide, was reported.<sup>[154]</sup> Given this vast distribution of DESS-MARTIN periodinane (**358**), it appears even more astonishing that the X-ray crystal structure of this intriguing reagent had never been reported in the literature.

### 3 THE CRYSTAL STRUCTURE OF THE DESS-MARTIN PERIODINANE (MANUSCRIPT)

#### 3.1 Introduction

As depicted in **Scheme 98** DMP (**358**) is usually prepared from 2-iodobenzoic acid (**364**) in a two-step procedure that involves oxidation with Oxone®, a formulation of peroxomonosulfate,<sup>[155]</sup> followed by heating of the intermediary iodine(V)-species IBX (**365**) in acetic anhydride and catalytic amounts of *p*-toluenesulfonic acid.<sup>[156]</sup>



**Scheme 98.** The chemical structures of DMP (**358**), 2-iodobenzoic acid (**364**), IBX (**365**) and **362**

Upon repeating this procedure with an older and less active batch of Oxone®, well-defined single crystals of acetoxy-1,2-benziodoxolin-3-one (**362**) were obtained as a by-product. We quickly established that the crystal structure of this partially oxidized compound had already been described by GOUGOUTAS and CLARDY four decades ago,<sup>[157]</sup> and the X-ray structure of IBX (**365**) was also known.<sup>[158]</sup>

Surprisingly, when browsing the Cambridge Crystallographic Data Centre, however, it was found that no X-ray crystal structure of **358** itself has been published to date. Thus, a range of crystallization conditions was investigated, to obtain the first X-ray crystal structure of DMP (**358**). This could serve as a basis for computational investigations concerning the mechanism of the DESS-MARTIN oxidation.

## 3.2 Results and Discussion

The difficulty in obtaining suitable single crystals for X-ray diffraction analysis of DMP (**358**) might lie in the high crystallinity of the compound. Indeed, microcrystalline **358** precipitates from the acetic anhydride solution upon cooling at the end of the procedure used for its preparation. Various recrystallization methods also yielded **358** as a microcrystalline powder that was unsuitable for single crystal X-ray analysis. However, the standard protocol for the preparation of **358** requires filtration and washing of the filter cake with ether. The combined filtrates thus consist of a solution of residual **358** and various by-products, including iodine(III)-intermediates, in a mixed solution of ether and acetic anhydride. We reasoned that the presence of these impurities might slow down nucleation and allow for the growth of larger crystals. Indeed, slow evaporation of the filtrate under a constant stream of nitrogen at ambient temperature over the course of four days did yield single crystals suitable for X-ray analysis.

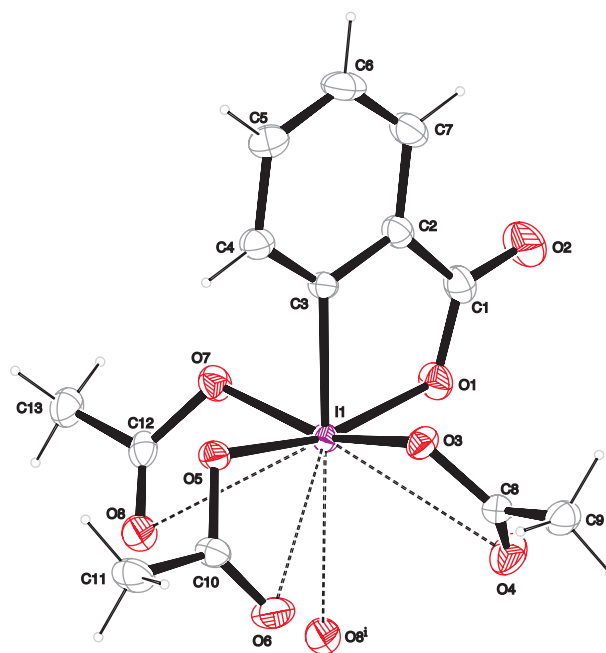


**Figure 40.** ORTEP drawing (50% probability level) of **358** with numbering scheme

DMP (**358**) crystallizes in a triclinic unit cell that is occupied by two molecules. An ORTEP plot and numbering scheme for monomeric DMP (**358**) with 50% probability ellipsoids is shown in **Figure 40**. Important bond lengths and angles are provided in **Table 19**.

**Table 19.** Selected bond lengths and angles in **358**

Iodine bond lengths (Å)		Iodine angles (°)			
I1-C3	2.1025(16)	O1-I1-O3	92.84(5)	O3-I1-O7	159.77(5)
I1-O1	2.0888(14)	O1-I1-O5	165.06(5)	O3-I1-C3	80.50(6)
I1-O3	2.0656(13)	O1-I1-O7	88.66(5)	O5-I1-O7	89.05(5)
I1-O5	2.0670(13)	O1-I1-C3	79.66(6)	O5-I1-C3	85.40(6)
I1-O7	2.1141(13)	O3-I1-O5	84.32(5)	O7-I1-C3	79.93(6)

Several structural features of monomeric **358** are noteworthy. The central iodine atom resides in a distorted octahedral environment that is in accordance with a simple VSEPR model. Acetoxy groups occupy the equatorial positions, whereas the phenyl ring and the lone electron pair occupy the apical positions, respectively. Due to the steric demands of the electron pair, which is engaged in supramolecular interactions (see below), the acetoxy substituents are pushed toward the phenyl ring. As a consequence, the iodine atom lies 0.315(1) Å below a plane formed by oxygens O1, O3, O5 and O7 and all iodine-oxygen bonds form an acute angle with the iodine-carbon bond in the apical position. (see **Table 19**: iodine angles). All three acetoxy groups are bound in a covalent  $\eta$ -1 fashion, showing typical iodine-oxygen bond lengths (I1-O3 = 2.0656(13) Å, I1-O5 = 2.0670(13) Å, I1-O7 = 2.1141(13) Å).<sup>[159]</sup> The length of the iodine-oxygen bond of the iodoxolone ring lies also well within the range of a covalent iodine-oxygen bond (I1-O1 = 2.0888(14) Å)). The iodine-carbon bond has a length of I1-C3 = 2.1025(16) Å and forms an angle of 79.66(6)° with the I1-O1 bond. Interestingly, the I1-O1 bond (2.0888(14) Å) in **358** is shorter than the I1-C3 bond (2.1025(16) Å). By contrast, the corresponding bond lengths in iodoxolone **362** are 2.3236 Å and 2.1061 Å, respectively,<sup>[157]</sup> and in iodoxolone **365** they are 2.1289 Å and 2.0121 Å, respectively.<sup>[158]</sup>

Notably, the two lateral acetoxy groups in **358** are bound to the central iodine atom with significantly different bond lengths (I1-O5 = 2.0670(13) Å, I1-O7 = 2.1141(13) Å), which desymmetrizes the molecule overall. This desymmetrization cannot be attributed to crystal packing effects since it is also apparent in a structural model of **358** calculated by

MOCCI and co-workers using DFT theory at the PBE0/LANL2DZdp level in the gas phase and at room temperature.<sup>[13]</sup> Overall, the calculated structure is in good agreement with the experimentally determined X-ray crystal structure, determined at  $T = 173$  K, as the geometry around the central iodine atom is very similar. A closer look at the iodoxolane ring in the X-ray structure of **358**, however, reveals that the substituents O1 and O5 are not located in the least-square plane of the phenyl ring. The O1- and O5-iodine bonds deviate from the least-square plane by  $5.34(8)^\circ$  and  $5.26(8)^\circ$  respectively. This distortion is not evident in the structure calculated by MOCCI and co-workers.<sup>[13]</sup>

The supramolecular structure of **358**, which has not been calculated before, is depicted in Figure 41, Figure 42Figure 43. The unit cell is occupied by a centrosymmetric dimer that is held together, in part, by two intermolecular halogen-oxygen bonds between the iodine and a carbonyl group of the adjacent molecule. The intermolecular iodine-oxygen distance of  $3.3 \text{ \AA}$  lies well below the sum of the van der Waals radii,  $3.46 \text{ \AA}$ .<sup>[160]</sup> Angles of  $159.1^\circ$  (C3a-I1a-O8b) and  $120.2^\circ$  (I1a-O8b-C12b) are also in accordance with the presence of halogen bonds.<sup>[161]</sup> Similar bonds between iodine atoms and  $sp^2$ -hybridized oxygen atoms have been observed in a range of other hypervalent iodine species,<sup>[157,158,162-166]</sup> as well as iodine(I)-compounds.<sup>[167,168]</sup>

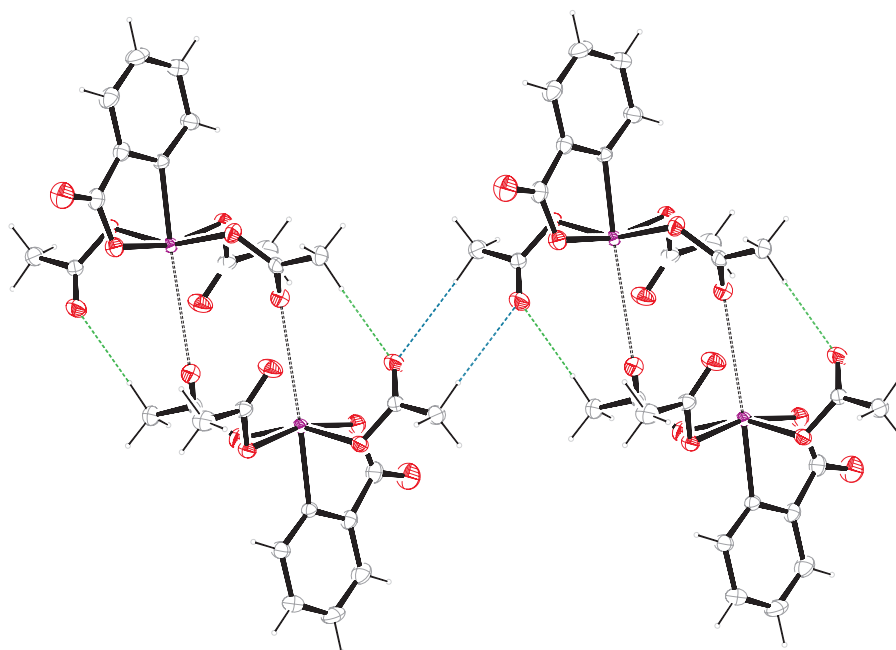


**Figure 41.** Supramolecular structure of **358** with halogen bonds and selected hydrogen bonds

In addition to halogen bonds, the dimer is stabilized by two weak hydrogen bonds of the type C13-H13A...O4 (green dashed bonds in Figure 41). In terms of graph-set analysis<sup>[169]</sup>, the resulting 16-membered ring may be assigned a  $R_2^2(16)$  descriptor. The dimers themselves are linked by two weak hydrogen bonds of the type C9-H9A...O4 (blue dashed bonds in Figure 41, Table 20). The descriptor for this linking cyclic hydrogen-bond is  $R_2^2(8)$ . As a consequence of the two different types of hydrogen bonds, the dimers form infinite chains along the *c*-axis. The chains appear on the binary level with a  $C_2^1(10)$  descriptor, as the shortest repeating unit of the chain consists of ten atoms including two donor atoms and only one acceptor atom. There are two additional weak hydrogen bonds, which link adjacent molecules by cyclic centrosymmetric hydrogen-bond systems (Figure 42).

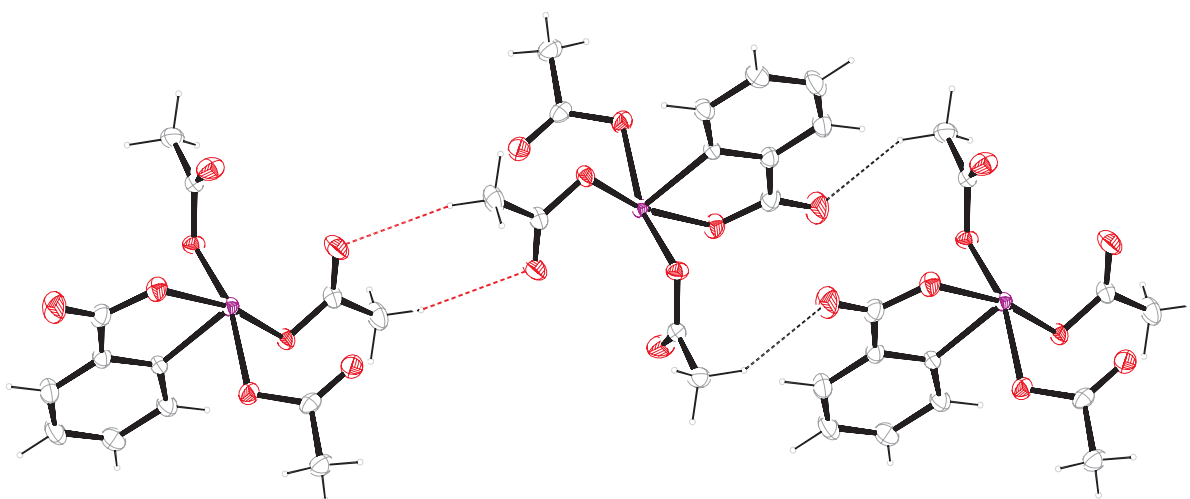


**Figure 42.** Further hydrogen-bonding interactions in the supramolecular structure of **358**

A 16-membered ring with a  $R_{22}(16)$  descriptor is established by involvement of the iodoxolane carbonyl in a weak hydrogen bond C9-H9C...O2= 3.3 Å (black dashed lines in Figure 42). An 8-membered ring comparable to the one discussed above is formed by two hydrogen bonds of the type C11-H11A...O6= 3.5 Å (red dashed lines in Figure 41) resulting in a  $R_{22}(8)$  descriptor. The combination of the two different hydrogen bonds depicted in Figure 41Figure 42 leads to the formation of infinite chains along [111], which appear on the binary level with a  $C_{22}(16)$  descriptor. In the packing, the phenyl planes are arranged approximately parallel to the *b*-axis with a deviation angle of only 1.58(7)° (Figure 43). There are, however, no  $\pi$ -stacking interactions. Least-square planes of the four oxygen atoms bound covalently to iodine are nearly parallel to the *c*-axis (deviation angle 0.79(4)°).

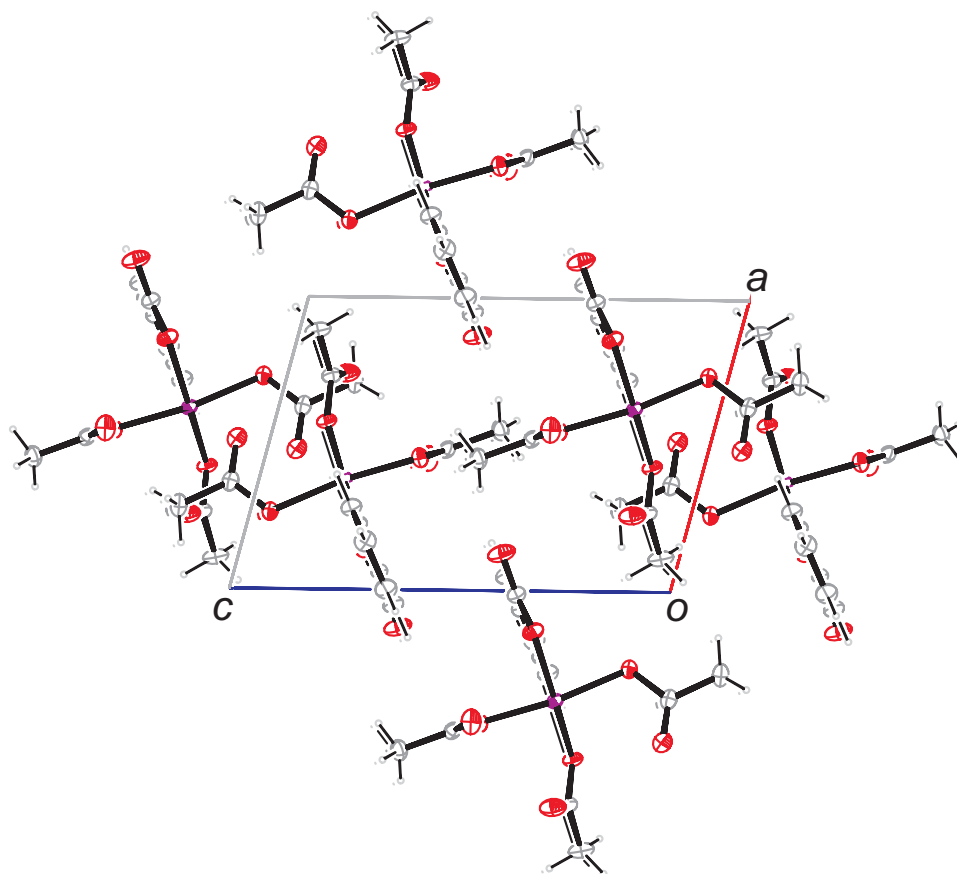


**Figure 43.** Supramolecular structure of **358** viewed along b-axis

**Table 20.** Halogen and hydrogen bond lengths in **358**

Bond lengths in the crystal lattice of <b>1</b> (Å)	
I1...O8	3.2635(15)
C9-H9A...O5	2.877(2)
C9-H9C...O2	3.312(3)
C11-H11A...O6	3.470(3)
C13-H13A...O4	3.265(3)

### 3.3 Unpublished Results and Discussion

After establishing the first X-ray crystal structure of DMP (**358**), several co-crystallisation attempts were investigated also in order to obtain a crystal structure of DMP-derived species coordinating non-oxidisable alcohols such as *tert*-butanol (**366**), pentafluorophenol (**367**) and pinacol (**368**) (Figure 44).

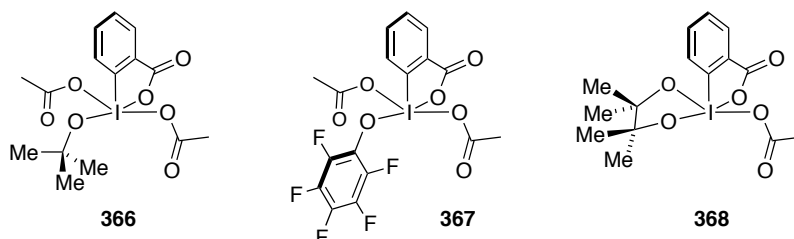


**Figure 44.** *In situ* generated, DMP-derived intermediate crystallisation targets (**366**, **367**, **368**)

As described previously, again different crystallisation methods were investigated. Crystalline DMP (**358**), which was dissolved in DCM, benzene or cyclohexane together was combined with 1 equivalent of the corresponding, non oxidisable alcohols at 0 °C. As rapid precipitation occurred, filtration was performed and the mother liquor in each attempt left in the freezer. However, no single crystals suitable for X-ray crystallography were obtained. In analogy to the successful crystallisation of DMP (**358**), more crystallisation attempts were performed with combined phases of acetic anhydride and ether, taken from the preparation of DMP (**358**). Herein, a careful estimate of DMP-molarity in solution was made based on isolated yield. Accordingly, non-oxidisable alcohols were introduced and left at 4 °C in the fridge to crystallise. In the course of these attempts the crystal structure of iodine(III) species **362** was obtained, which had already been described by CLARDY and co-workers.<sup>[170]</sup>

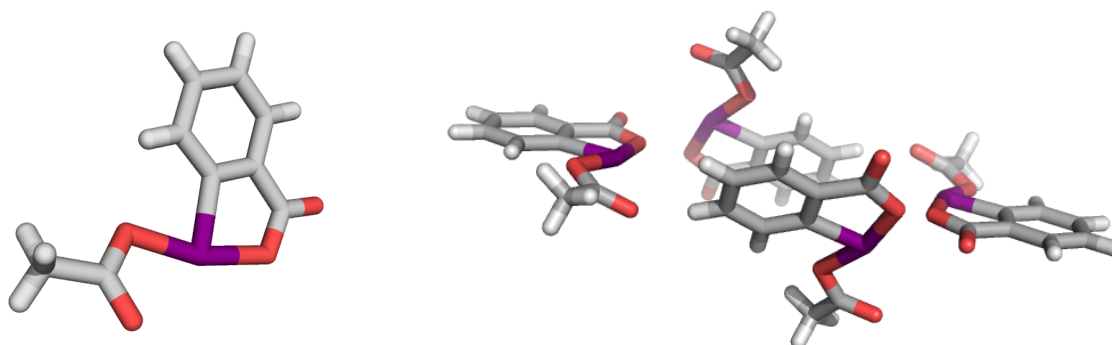


**Figure 45.** X-ray crystal structure of **362** as single molecule and in the asymmetric unit (colour code: grey: carbon, red: oxygen, purple: iodine)

Though undesired at this point, the high crystallinity of the almost perfectly flat molecule **362**, which drew our attention towards the Cambridge Crystallographic Data Centre (CCDC) in the first place. As discussed above (*vide infra*), this iodine(III)-species is the result of decomposition of the iodine(V)-species, particularly with electron-donating groups. Apparently, crystallisation even at low temperatures (4 °C) did not occur before the reduction of the iodoxolone.

## 4 CONCLUSION

In conclusion, the first solid-state structure of the DESS-MARTIN periodinane (**358**), a popular reagent in organic synthesis was achieved. The similarity of the experimentally determined structure with a calculated gas-phase structure of monomeric **358** underscores the power of Density Functional Theory. A network of halogen and hydrogen bonds in the supramolecular structure explains the high crystallinity of **358** and has implications with respect to the mechanism of DESS-MARTIN oxidation. This X-ray structure will serve as a starting point for detailed quantum mechanical calculations to address this topic. Additional work has been done in the field of crystallisation of non-oxidisable alcohols to DMP (**358**). As thorough screenings of different crystallisation methods were screened did not yield suitable single crystals of the target molecules, powder diffraction analysis may be considered as potent alternative tool in the course of this project.



## **EXPERIMENTAL PROCEDURES AND ANALYTICAL DATA**

## GENERAL EXPERIMENTAL SECTION

### General Experimental Details

Unless stated otherwise, all reactions were performed in oven-dried or flame-dried glassware under a positive pressure of nitrogen or argon. Commercial reagents and solvents were used as received with the following exceptions. Tetrahydrofuran (THF) was distilled from benzophenone and sodium prior to use. *N,N*-diisopropylethylamine (DIPEA), Triethylamine (TEA) and diisopropylamine (DIPA) were distilled over calcium hydride before use. Reactions were magnetically stirred and monitored by crude NMR or analytical thin-layer chromatography (TLC) using E. Merck 0.25 mm silica gel 60 F<sub>254</sub> precoated glass plates. TLC plates were visualised by exposure to ultraviolet light (UV, 254 nm) and/or exposure to an aqueous solution of ceric ammoniummolybdate (CAM) or an aqueous solution of potassium permanganate (KMnO<sub>4</sub>) followed by heating with a heat gun. Flash column chromatography was performed as described by *STILL et al.* employing silica gel (60 Å, 40-63 µm, Merck) and a forced flow of eluent at 1.3–1.5 bar pressure.<sup>[171]</sup> Yields refer to spectroscopically (<sup>1</sup>H NMR and <sup>13</sup>C NMR) pure material. Diastereomeric ratios were determined by comparison of the integrals of base line separated peaks.

### Instrumentation

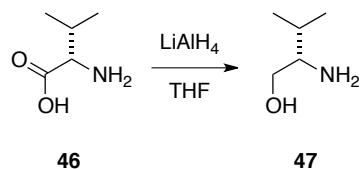
Proton nuclear magnetic resonance (<sup>1</sup>H NMR) spectra were recorded on Varian VNMRS 300, VNMRS 400, INOVA 400 or VNMRS 600 spectrometers. Proton chemical shifts are expressed in parts per million (ppm/ δ scale) and are calibrated using residual undeuterated solvent as an internal reference (CHCl<sub>3</sub>: δ 7.26, MeOH: δ 3.31, H<sub>2</sub>O: δ 4.79). Data for <sup>1</sup>H NMR spectra are reported as follows: chemical shift (δ ppm) (multiplicity, coupling constant (Hz), integration, assignment). Multiplicities are reported as follows: s = singlet, d = doublet, t = triplet, q = quartet, m = multiplet, *br* = broad, or combinations thereof. Carbon nuclear magnetic resonance (<sup>13</sup>C NMR) spectra were recorded on Varian VNMRS 300, VNMRS 400, INOVA 400 or VNMRS 600 spectrometers. Carbon chemical shifts are

expressed in parts per million (ppm/  $\delta$  scale) and are referenced from the carbon resonances of the solvent (CDCl<sub>3</sub>:  $\delta$  77.0, MeOH:  $\delta$  49.0). Peaks in <sup>1</sup>H and <sup>13</sup>C spectra were assigned to the depicted compounds based on COSY, HSQC, HMBC and NOESY spectra.

Infrared (FTIR) spectra were recorded on a Perkin Elmer Spectrum BX II (FTIR System). FTIR Data is reported in frequency of absorption (cm<sup>-1</sup>). Mass spectroscopy (MS) experiments were performed on a Thermo Finnigan MAT 95 (EI) or on a Thermo Finnigan LTQ FT (ESI) instrument. Optical rotation  $[\alpha]_D^T$  was measured on a Perkin-Elmer 241 Polarimeter. Optical rotation data is given in degrees °, concentration *c* in g mol<sup>-1</sup> of sample and used solvent. Microwave reactions were performed on a CEM machine (Model: Discovery System, No. 908010)

## EXPERIMENTAL DATA

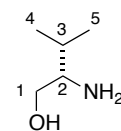
### Portentol



**(S)-2-amino-3-methylbutan-1-ol (47)** was synthesized as described in literature.<sup>[172]</sup> To a suspension of lithium aluminiumhydride (70.0 g, 1.75 mol) in THF (2.0 L), (L)-valine (**46**) (104.0 g, 0.88 mol) was added in portions at 0 °C. After addition was complete, the reaction was allowed to warm to room temperature and then heated at reflux for 16 hours. The reaction was quenched by addition of aqueous NaOH (2M, 250 mL) at 0 °C. The resulting white slurry was filtered off. The filter cake was extracted with THF (250 mL) under reflux and subsequently filtered. Combined organic phases were dried over MgSO<sub>4</sub> and concentrated *in vacuo* (30 °C bath temperature, 20 mbar) to give **47** as yellow oil, which crystallised upon cooling as white crystals.

$[\alpha]_D^{20} = +12.84^\circ$  ( $c = 1.0$ , CHCl<sub>3</sub>).

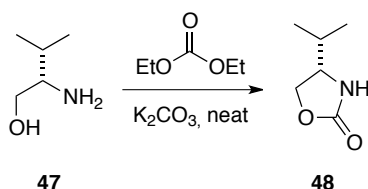
<sup>1</sup>H-NMR (400 MHz, CDCl<sub>3</sub>):  $\delta = 3.65$  (m, 1H, H-1), 3.32–3.26 (m, 1H, H-1), 2.58–2.52 (m, 1H, H-2), 2.12 (s, 3H, OH and 2x NH), 1.61–1.54 (m, 1H, H-3), 0.93–0.89 (m, 6H, 3x H4 and 3x H-5).



<sup>13</sup>C-NMR (150 MHz, CDCl<sub>3</sub>):  $\delta = 64.67$  (C-1), 38.45 (C-2), 31.40 (C-3), 19.30 (C-4 or C-5), 18.37 (C-4 or C-5).

IR (ATR):  $\tilde{\nu} = 3256.4$  (v), 2958.0 (s), 1737.4 (m), 1685.7 (m), 1436.7 (m), 1212.0 (s), 1180.3 (s) cm<sup>-1</sup>.

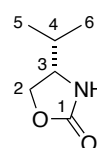
HRMS (EI): calcd. for C<sub>5</sub>H<sub>13</sub>NO<sup>+</sup>: 103.0997 [M]<sup>+</sup>  
 found [M]<sup>+</sup>.: 103.0991



**(S)-4-isopropylloxazolidin-2-one (48)** was synthesized as described in literature.<sup>[172]</sup> In a 250 mL round bottom flask mounted with a VIGREUX column (10 cm) and a distillation bridge (L)-valinol (**47**) (70.0 g, 679 mmol), anhydrous potassium carbonate (9.47 g, 679 mmol) and diethylcarbonate (91.3 mL, 746 mmol) were mixed and stirred at 135 °C until no further ethanol was distilled (12 h). The resulting slurry was diluted with EtOAc and filtered. The organic phase was dried over MgSO<sub>4</sub> and concentrated *in vacuo* (30°C bath temperature, 20 mbar) to 250 mL. The solution was cooled to 0 °C effecting crystallization of substance **24**. The mother liquor was concentrated and another fraction of crystals was obtained from EtOAc/hexanes 1/1.

$$[\alpha]_D^{20} = +6.32^\circ (c\ 0.95, \text{CHCl}_3)$$

<sup>1</sup>H-NMR (400 MHz, CDCl<sub>3</sub>): δ = 6.71 (s, 1H, NH), 4.44–4.40 (t, *J* = 8.66 Hz, 1H, H-2), 4.09–4.06 (dd, *J* = 6.34 Hz, 8.71 Hz, 1H, H-2), 3.62–3.56 (ddd, *J* = 6.32 Hz, 7.13 Hz, 8.65 Hz, 1H, H-3), 1.78 – 1.61 (m, 1H, H-4), 1.0–0.91 (d, *J* = 6.66 Hz, 3H, 3x H-5 or 3x H-6), 0.9 – 0.84 (d, *J* = 6.79 Hz, 3H, 3x H-5 or 3x H-6).

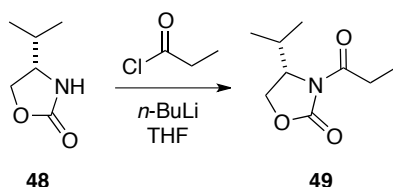


<sup>13</sup>C-NMR (100 MHz, CDCl<sub>3</sub>): δ = 160.6 (C-1), 68.6 (C-2), 58.4 (C-3), 32.7 (C-4), 18.0 (C-5 or C-6), 17.6. (C-5 or C-6).

IR (ATR):  $\tilde{\nu}$  = 3256.4 (v), 2958.0 (s), 1737.4 (m), 1685.7 (m), 1436.7 (m), 1212.0 (s), 1180.3 (s) cm<sup>-1</sup>.

HRMS (EI): calcd. for C<sub>6</sub>H<sub>11</sub>NO<sub>2</sub><sup>+</sup>:129.0790 [M]<sup>+</sup>

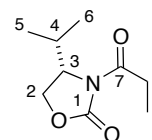
found: 129.0780 [M]<sup>+</sup>.



**(S)-4-isopropyl-3-propionyloxazolidin-2-one (49)** was synthesized as described in literature.<sup>[39]</sup> To a solution of the oxazolidinone **48** (30.0 g, 232 mmol) in THF (450 mL) *n*-BuLi (2.2 M in *n*-hexanes, 91.1 mL) was added dropwise at  $-78\text{ }^\circ\text{C}$ . Thereafter, freshly distilled propionyl chloride (22.3 mL, 23.6 g, 255 mmol) was added dropwise. After the addition was complete, the mixture was kept at  $-78\text{ }^\circ\text{C}$  for 10 minutes and then allowed to warm to room temperature in a water bath. After 20 minutes at ambient temperature, the reaction was quenched upon addition of  $\text{NH}_4\text{Cl}$  solution (sat. aq., 350 mL). The phases were separated and the resulting white slurry was diluted with water (50 mL) and re-extracted with EtOAc (3 x 200 mL). Combined organic phases were washed with brine (100 mL), dried over  $\text{MgSO}_4$  and concentrated *in vacuo* (30  $^\circ\text{C}$  bath temperature, 20 mbar). Purification by column chromatography (EtOAc/hexanes 1:10) yielded product **49** as a colourless oil (41.3 g, 223 mmol, 96%).

$$[\alpha]_D^{20} = +15.70^\circ \text{ (} c \text{ 1.35, CHCl}_3 \text{)}$$

$^1\text{H-NMR}$  (400 MHz,  $\text{CDCl}_3$ ):  $\delta = 4.51 - 4.34$  (dt,  $J = 8.0, 3.6$  Hz, 1H, H-3), 4.31 – 4.13 (m, 2H, 2x H-2), 3.11 – 2.76 (m, 2H, 2x H-8), 2.44 – 2.31 (m,  $J = 7.0, 3.9$  Hz, 1H, H-4), 1.23 – 1.10 (t,  $J = 7.4$  Hz, 3H, 3x H-9), 1.01 – 0.81 (2x d,  $J = 7.0$  Hz, 6H, 3x H-5 and 3x H-6).

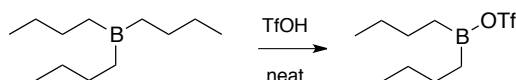


$^{13}\text{C-NMR}$  (300 MHz,  $\text{CDCl}_3$ ):  $\delta = 174.2$  (C-7), 154.3 (C-1), 63.4 (C-2), 58.4 (C-3), 29.2 (C-8), 28.3 (C-4), 18.0 (C-5 or C-6), 14.6 (C-5 or C-6), 8.4 (C-9).

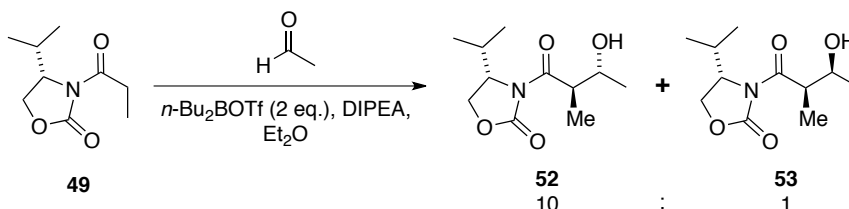
IR (ATR):  $\tilde{\nu} = 2963.1$  (w), 2877.0 (v), 1771.9 (s) 1698.2 (s)  $\text{cm}^{-1}$

HRMS (EI): calcd. for  $\text{C}_9\text{H}_{15}\text{NO}_3^+$ : 185.1052  $[\text{M}]^+$

found: 185.1049  $[\text{M}]^+$ .



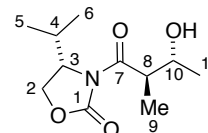
**Dibutyl(((trifluoromethyl)sulfonyl)oxy)borane** was prepared modifying literature procedures.<sup>[173]</sup> Trifluoromethanesulfonic acid (24.4 mL, 274 mmol) was added dropwise to tributylborane (66.9 mL, 274 mmol) under vigorous stirring at 30 °C at a rate that gas evolution was moderate. After completed addition (ca. 1 h) the mixture was further heated to 50 °C for two hours until gas evolution ceased. Vacuum distillation over a VIGREUX-column (10 cm) yielded di-*n*-butyl borontriflate as a colourless liquid (47 °C, 0.27 mbar, 37.6 g, 137 mmol, 50%).



**(S)-3-((2R,3R)-3-hydroxy-2-methylbutanoyl)-4-isopropylloxazolidin-2-one (52)** was synthesized as described in literature.<sup>[40]</sup> A solution of **49** (2.22 g, 12 mmol) in anhydrous ether (36 mL) was cooled to 0 °C. Freshly distilled Bu<sub>2</sub>BOTf (5.98 mL, 6.58 g, 24 mmol) was added dropwise over a period of 10 minutes to give a bright yellow solution. After addition of diisopropylethylenamide (2.28 mL, 17.10 g, 13 mmol) the resulting white slurry was cooled to –78 °C and a solution of freshly distilled acetaldehyde (0.53 g, 0.68 mL, 12 mmol) in Et<sub>2</sub>O (12 mL) was added over 15 minutes. The mixture was kept at –78 °C for 4 hours and then quenched with tartaric acid (9.0 g). The resulting mixture was allowed to warm to room temperature and then stirred for 2 hours. The dark green mixture was then partitioned between water and ether and tartaric acid was filtered off (Thorough washing with Et<sub>2</sub>O). The organic phase was washed with NaHCO<sub>3</sub> (sat. aq. 2 x 25 mL) and the combined aqueous phases were re-extracted with Et<sub>2</sub>O (2 x 25 mL). The combined organic phases were then cooled to 0 °C and a solution of MeOH/H<sub>2</sub>O<sub>2</sub> (30 %) (3/1, 30 mL) was added. After stirring for 30 minutes at room temperature, the yellow solution was dried over MgSO<sub>4</sub> and concentrated *in vacuo*. Purification by column chromatography (EtOAc/Hex 1/3) and recrystallization from EtOAc/hexanes mixtures gave desired product **52** (1.93 g, 8.4 mmol, 70 %, dr. >20/1).

$[\alpha]_D^{20} = +39.53$  (*c* 0.85, CH<sub>2</sub>Cl<sub>2</sub>)

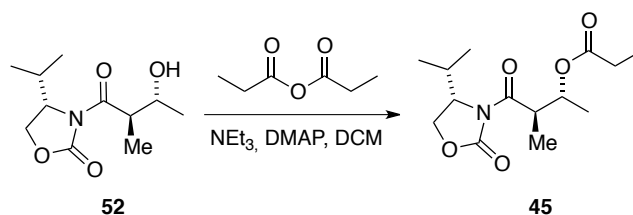
$^1\text{H}$  NMR (600 MHz,  $\text{CDCl}_3$ )  $\delta$  [ppm] = 4.50 – 4.37 (ddd,  $J$  = 8.2, 3.9, 2.9 Hz, 1H, H-3), 4.31 – 4.12 (m, 2H, 2x H-2), 3.91 – 3.79 (m, 2H, H-8 and H-10), 2.55 – 2.50 (s, 1H, OH), 2.45 – 2.34 (dq,  $J$  = 7.0, 3.9 Hz, 1H, H-4), 1.29 – 1.23 (d,  $J$  = 6.2 Hz, 3H, 3x H-11), 1.18 – 1.13 (d,  $J$  = 6.8 Hz, 3H, 3x H-9), 0.94 – 0.85 (2x d,  $J$  = 7.0 Hz, 6H, 3x H-5 and 3x H-6).



$^{13}\text{C}$  NMR (600 MHz,  $\text{CDCl}_3$ )  $\delta$  [ppm] = 176.7 (C-7), 154.4 (C-1), 70.8 (C-10), 63.3 (C-3), 58.8 (C-2), 44.8 (C-8), 28.4 (C-4), 21.3 (C-11), 17.9 (C-5 or C-6), 14.6 (C-5 or C-6), 14.4 (C-9).

IR (ATR):  $\tilde{\nu}$  = 3504.0 (v), 2967.0 (w), 2877.0 (v), 1769.7 (s), 1692.9 (s), 1486.6 (v), 1454.1 (w), 1372.3 (s), 1300.2 (m), 1210.0 (s), 1142.3 (m), 1109.1 (m), 1056.3 (m), 1015.5 (m), 988.1 (m), 970.2 (w), 951.6 (m), 911.2 (w), 829.8 (v), 751.1 (s), 707.8 (m), 666.8 (w)

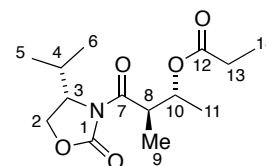
HRMS (EI),  $m/z$  calc. for  $\text{C}_{11}\text{H}_{19}\text{NO}_4$   $[\text{M}]^{++}$ : 229.1314;  
found  $[\text{M}]^{++}$ : 229.1308



**(2R,3R)-4-((S)-4-isopropyl-2-oxooxazolidin-3-yl)-3-methyl-4-oxobutan-2-yl propionate (45)** was prepared similar to literature procedures.<sup>[29]</sup> To a solution of **52** (1.87 g, 8.15 mmol) in DCM (70 mL), propionic anhydride (1.38 g, 10.6 mmol),  $\text{NEt}_3$  (1.5 mL, 1.09 g, 10.8 mmol) and DMAP (278 mg, 2.28 mmol) were added and the mixture heated at reflux for 4 h. After cooling to ambient temperature, the yellowish solution was washed with 1 M HCl (50 mL),  $\text{NaHCO}_3$  (sat. aq. 50 mL) and brine (50 mL), dried over  $\text{Na}_2\text{SO}_4$ , concentrated *in vacuo* and purified by column chromatography (EtOAc/ hexanes: 1/4), yielding **45** as colourless crystals (2.33 g, 8.16 mmol, 94%).

$[\alpha]_{\text{D}}^{22} = +30.0$  ( $c$  0.5,  $\text{CH}_2\text{Cl}_2$ )

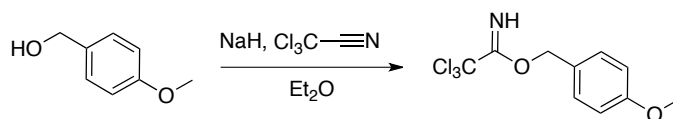
$^1\text{H}$  NMR (300 MHz,  $\text{CDCl}_3$ )  $\delta$  [ppm] = 5.17 (dq,  $J = 9.0, 6.3$ , 1H, H-10), 4.47 – 4.39 (m, 1H, H-3), 4.29 – 4.13 (m, 2H, 2x H-2), 4.04 (dq,  $J = 9.0, 7.0$ , 1H, H-8), 2.30 (tdd,  $J = 12.1, 7.5, 4.6$ , 1H, H-4), 2.24 – 2.08 (m, 2H, 2x H-13), 1.25 (d,  $J = 6.3$ , 3H, 3x H-11), 1.14 (d,  $J = 7.0$ , 3H, 3x H-9), 1.07 (t,  $J = 7.6$ , 3H, 3x H-14), 0.87 (t,  $J = 7.2$ , 6H 3x H-5 and 3x H-6).



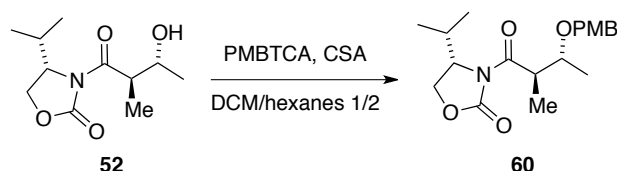
$^{13}\text{C}$  NMR (600 MHz,  $\text{CDCl}_3$ )  $\delta$  [ppm] = 174.70 (C-7), 173.51 (C-12), 153.82 (C-1), 72.11 (C-10), 63.28 (C-3), 58.65 (C-2), 42.95 (C-8), 28.45 (C-4), 27.85 (C-13), 18.12 (C-11), 17.36 (C-5 or C-6), 14.75 (C-5 or C-6), 14.02 (C-9), 9.27 (C-14).

IR (ATR):  $\tilde{\nu} = 2961.6$  (v), 17.849 (s), 1731.9 (s), 1697.1 (s), 1485.6 (w) $\text{cm}^{-1}$

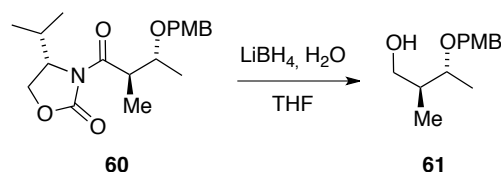
HRMS (EI), $m/z$	calc. for $[\text{M}]^{++}$ $\text{C}_{14}\text{H}_{23}\text{NO}_5$ :	285.1576
	found $[\text{M}]^{++}$ :	285.1570



**4-methoxybenzyl 2,2,2-trichloroacetimidate (PMBTCA)** was prepared as described in literature.<sup>[50]</sup> To a suspension of NaH (0.58 g, 14.5 mmol) in anhydrous ether (45 mL) 4-methoxybenzylalcohol (20.4 g, 145 mmol) was added over a period of 60 minutes. After stirring for one hour at ambient temperature, the mixture was cooled to 0 °C and trichloroacetonitrile (22.8 g, 158 mmol) was added over a 80 minutes period. Thereafter, the reaction mixture was allowed to warm to room temperature and stirred for 2 hours. Subsequently, the mixture was concentrated *in vacuo* (30 °C bath temperature, 20 mbar) and the residue was taken up in a mixture of *n*-pentane (94 mL) and MeOH (0.35 mL). Filtration over celite and concentration *in vacuo* (30 °C bath temperature, 20 mbar) yielded PMBTCA as crude, yellow oil, which was used in the next step without further purification (28.7 g, 101 mmol, 70%).



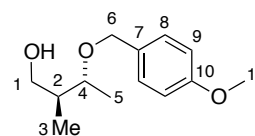
**(S)-4-isopropyl-3-((2R,3R)-3-((4-methoxybenzyl)oxy)-2-methylbutanoyl)oxazolidin-2-one (60)** was prepared following literature procedures.<sup>[50]</sup> Crude PMBTCA (13.6 g, 48.3 mmol) was added to a solution of **52** (8.56 g, 37.3 mmol) in DCM/ hexanes (1/2, 51 mL) at 0 °C. After addition of CSA (434 mg, 1.87 mmol) the mix was allowed to warm to ambient temperatures and stirred for 40 hours. The resulting mixture was filtered over a celite plug, washed with hexanes and concentrated *in vacuo*. Product containing fractions after column chromatography (EtOAc/ hexanes 1/5) were concentrated and re-dissolved in CHCl<sub>3</sub> at 4°C. Further trichloroacetamide was removed upon cold filtration. As the product could not be fully purified, the crude was carried on to the next step.



**(2S,3R)-3-((4-Methoxybenzyl)oxy)-2-methylbutan-1-ol (61)**: LiBH<sub>4</sub> (4 M solution in hexanes, 19.1 mL, 76.2 mmol) was added dropwise to a solution of crude **60** (22.2 g, 63.5 mmol) in THF at 0 °C over ten minutes, followed by addition of water (1.72 mL, 95.3 mmol). The mixture was stirred at 0 °C for 20 minutes and then at ambient temperature for 1 hour. NH<sub>4</sub>Cl solution (aq., half saturated) was added, until no further gas development was evident. The resulting mixture was partitioned between a minimum amount of water and EtOAc (75 mL). The aqueous phase was washed with EtOAc (3x 75 mL), combined organic phases were washed with brine (20 mL), dried over MgSO<sub>4</sub> and concentrated *in vacuo* (30 °C bath temperature). Column chromatography (EtOAc/ hexanes 1/5) gave **61** as colourless oil (12.8 g, 57.2 mmol, 90 %).

$$[\alpha]_{\text{D}}^{20} = -56.31 \text{ (} c \text{ 0.65, CH}_2\text{Cl}_2 \text{)}$$

<sup>1</sup>H NMR (600 MHz, CDCl<sub>3</sub>)  $\delta$  [ppm] = 7.27 – 7.24 (m, 2H, 2x H-8), 6.92 – 6.84 (m, 2H, 2x H-9), 4.62 – 4.57 (d,  $J$  = 11.2 Hz, 1H, H-6), 4.36 – 4.32 (d,  $J$  = 11.1 Hz, 1H, H-6), 3.83 – 3.78 (s, 3H, H-11), 3.66



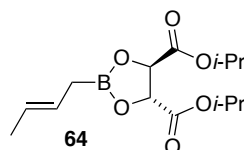
– 3.59 (ddd,  $J = 10.8, 7.2, 3.5$  Hz, 1H, H-1), 3.58 – 3.52 (ddd,  $J =$

10.8, 7.2, 3.5 Hz, 1H, H-1), 3.51 – 3.40 (dq,  $J = 7.4, 6.1$  Hz, 1H, H-4), 3.02 – 2.88 (dd,  $J = 7.2, 3.5$  Hz, 1H, OH), 1.82 – 1.69 (m, 1H, H-2), 1.27 – 1.21 (d,  $J = 6.1$  Hz, 3H, 3x H-5), 0.94 – 0.82 (d,  $J = 6.1$  Hz, 3H, 3x H-3).

$^{13}\text{C}$  NMR (150 MHz,  $\text{CDCl}_3$ )  $\delta$  [ppm] = 159.4 (C-10), 130.2 (C-7), 129.4 (2x C-8), 113.8 (2x C-9), 80.4 (C-4), 77.2 (C-6), 70.6 (C-1), 55.4 (C-11), 41.4 (C-2), 17.6 (C-5), 14.2 (C-3).

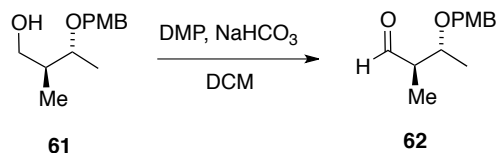
IR: [ $\text{cm}^{-1}$ ] = 3415.9 (v), 2964.2 (w), 2932.9 (w), 2876.2 (w), 2835.0 (w), 1611.4 (m), 1585.5 (v), 1511.2 (s), 1463.4 (w), 1373.5 (w), 1337.2 (v), 1301.1 (w), 1244.1 (s), 1172.3 (m), 1104.0 (m), 1063.2 (m), 1080.0 (s), 932.2 (w), 908.9 (w), 881.9 (w), 818.9 (m), 753.5 (w), 707.0 (v)

HRMS (EI), $m/z$	calc. for $\text{C}_{13}\text{H}_{20}\text{O}_3$ [ $\text{M}]^{++}$ :	224.1412
	found [ $\text{M}]^{++}$ :	224.1393

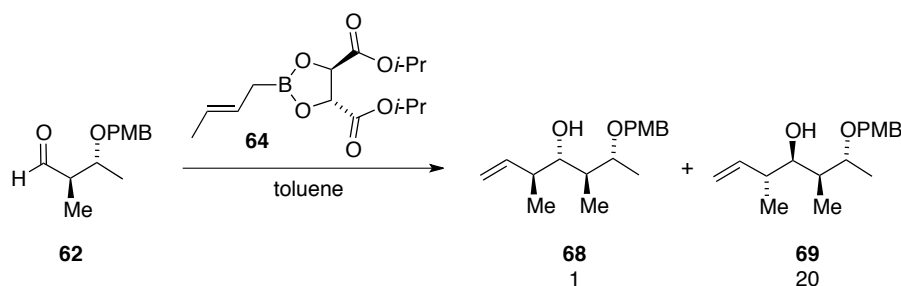


**(4*R*,5*R*)-diisopropyl 2-((*E*)-but-2-en-1-yl)-1,3,2-dioxaborolane-4,5-dicarboxylate (64)** was prepared according to literature procedures.<sup>[53,174]</sup> A solution of  $\text{KO}t\text{-Bu}$  (9.80 g, 85.0 mmol) in THF (42 mL) was cooled to  $-78$  °C and (*E*)-2-butene (5.72 g, 102 mmol) was slowly added. *n*-BuLi (2.5 M solution in hexanes 35.4 mL, 85.0 mmol) was added dropwise over a 50 minutes period, keeping the internal reaction temperature below  $-65$  °C. After the addition was complete, the mixture was allowed to warm to  $-50$  °C for exactly 25 minutes. After immediate re-cooling to  $-78$  °C, triisopropylborate (20 mL, 16.3 g, 85.0 mmol) was added over a period of 50 minutes, maintaining an internal reaction temperature below  $-65$  °C. After 10 minutes, the solution was rapidly treated with HCl (1 M, 160 mL) saturated with NaCl by mixing thoroughly. The aqueous layer was adjusted to pH= 1 upon addition of HCl (1 M, 55 mL). A solution of (+)-diisopropyl-tartrate (20.3 g, 85.0 mmol) in  $\text{Et}_2\text{O}$  (30 mL) was added and the mixture shaken vigorously. Phases were separated, the aqueous layer was extracted with  $\text{Et}_2\text{O}$  (3x 40 mL) and the combined organic phases were dried over  $\text{MgSO}_4$  for 2.5 hours. Filtration under a nitrogen blanket and concentration *in vacuo* gave a colourless, viscous

liquid, which was dissolved in toluene (60 mL) to form a clear, ca. 0.64 M solution of (+)-diisopropyl tartrate (*E*)-crotylboronate (**64**).



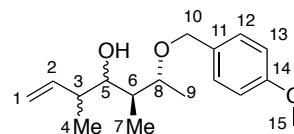
**(2*R*,3*R*)-3-((4-methoxybenzyl)oxy)-2-methylbutanal (62)**: To a suspension of protected alcohol **61** (5.0 g, 22.3 mmol) and sodium bicarbonate (11.2 g, 134 mmol) in DCM (30 mL), DMP (**358**/ 17.2 g, 40.6 mmol) was added at 0 °C. The mixture was allowed to warm to ambient temperature stirred for 60 minutes. A solution of saturated NaHCO<sub>3</sub>, saturated Na<sub>2</sub>S<sub>2</sub>O<sub>3</sub> and H<sub>2</sub>O (1/1/1, 30 mL) was added and the mixture stirred vigorously for 90 minutes. Then, phases were separated and the aqueous layer was washed with DCM (2x 20 mL) and combined organic phases were washed with NaHCO<sub>3</sub> (sat. aq., 3x 50 mL) and brine (2x 20 mL). Drying over MgSO<sub>4</sub> and concentration *in vacuo* yielded **62** as a yellow oil, which was used in the next step without further purification.



**(3*S*,4*S*,5*S*,6*R*)-6-((4-methoxybenzyl)oxy)-3,5-dimethylhept-1-en-4-ol (68)** was prepared following literature procedures.<sup>[64]</sup> A solution of aldehyde **62** (6.0 g, 27.0 mmol) in toluene (18 mL) was added dropwise to reagent **64** (0.64 M solution in toluene, 63.3 mL, 40.5 mmol) at -78 °C. At this temperature, the solution was stirred for 12 hours and then quenched upon addition of aqueous NaOH solution (1.5 M, 30 mL). The mix was allowed to warm up to ambient temperature and stirred vigorously for 1 hour. Phases were separated, the aqueous layer washed with Et<sub>2</sub>O (6x 30 mL), combined organic layers were washed with aqueous NaHCO<sub>3</sub> solution (sat. 30 mL) and brine (30 mL). Drying over MgSO<sub>4</sub> and concentration *in vacuo* gave a yellow oil, which was subjected to column chromatography (EtOAc/ hexanes 1/5). Product containing fractions gave a mixture of **68/69** = 1/20 (6,0 g, 21.6 mmol, 80 %

conversion). (Characterisation of the product mixture **75**. Assignment of protons and carbons based on peaks of the major diastereoisomer).

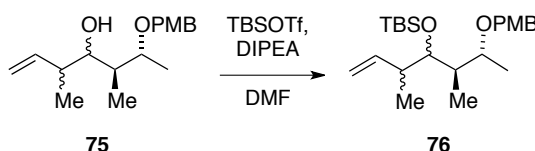
$^1\text{H}$  NMR (300 MHz,  $\text{CDCl}_3$ )  $\delta$  [ppm] = 7.32 – 7.19 (m, 2H, 2x H-12), 6.91 – 6.80 (m, 2H, 2x H-13), 6.01 – 5.71 (m, 1H, H-2), 5.17 – 4.98 (m, 2H, 2x H-1), 4.62 – 4.26 (m, 2H, 2x H-10), 3.91 – 3.53 (m, 5H, 3x H-15, H-5 and H-8), 3.00 – 2.77 (s, 1H, OH), 2.52 – 2.09 (m, 1H), 2.03 – 1.33 (m, 2H, H-3 and H-6), 1.33 – 1.03 (m, 3H, 3x H-9), 1.03 – 0.75 (m, 6H, 3x H-4 and H-7).



$^{13}\text{C}$  NMR (75 MHz,  $\text{CDCl}_3$ )  $\delta$  [ppm] = 159.2 (C-14), 142.4 (C-2), 130.6 (C-11), 129.4 (2x C-12), 114.7 (C-1), 113.8 (2x C-13), 78.6 (C-5 or C-8), 73.5 (C-5 or C-8), 71.0 (C-10), 55.2 (C-15), 41.6 (C-3), 39.9 (C-6), 17.5 (C-9), 16.7 (C-4), 10.3 (C-7)

IR (ATR):  $\tilde{\nu}$  = 3473.9 (v), 3071.0 (v), 2968.9 (w), 2930.0 (w), 2834.4 (w), 1637.3 (v), 1611.8 (m), 1585.9 (v), 1512.0 (s), 1455.0 (m), 1418.6 (w), 1374.2 (m), 1323.4 (w), 1301.3 (m), 1245.0 (s), 1172.2 (m), 1106.2 (m), 1060.4 (m), 1034.0 (s), 998.0 (m), 908.5 (m), 820.2 (m), 752.9 (w), 719.7 (v), 690.0 (v)  $\text{cm}^{-1}$

HRMS (EI), $m/z$	calc. for $[\text{M}]^+$ $\text{C}_{17}\text{H}_{26}\text{O}_3$ :	278.1882
	found $[\text{M}]^{++}$ :	278.1883



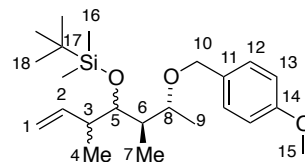
***tert*-butyl(((3*S*,4*S*,5*R*,6*R*)-6-((4-methoxybenzyl)oxy)-3,5-dimethylhept-1-en-4-yl)oxy)**

**dimethyl silane (76):** (mixture of diastereoisomers carried on through this sequence)

Homoallylic alcohol mixture **75** (2.12 g, 7.62 mmol) was dissolved in DMF (3 mL) and cooled to  $-40$  °C. DIPEA (1.97 g, 15.2 mmol) was added, the mixture stirred for 15 minutes, then TBSOTf (3.42 g, 12.9 mmol) was added dropwise at ca.  $-30$  °C. The mixture was allowed to warm to ambient temperature and stirred for 12 hours. The resulting mixture was partitioned between  $\text{Et}_2\text{O}$  (20 mL) and  $\text{NaHCO}_3$  (aq. sat. 10 mL) and phases were separated. The aqueous phase was washed with  $\text{Et}_2\text{O}$  (2x 20 mL), combined organic phases were washed with  $\text{NaHCO}_3$  (sat. aq., 2x 10 mL) and brine (10 mL), dried over  $\text{MgSO}_4$  and concentrated *in*

*vacuo*. Column chromatography (EtOAc/ hexanes: 1/10) yielded product mixture **76** (2.82 g, 7.18 mmol, 94 %) as yellow oil.

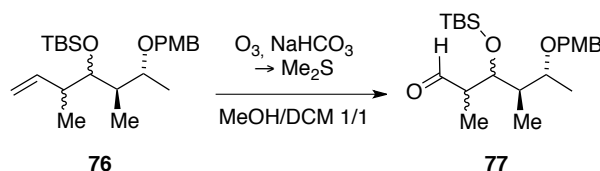
$^1\text{H}$  NMR (300 MHz,  $\text{CDCl}_3$ )  $\delta$  [ppm] = 7.34 – 7.19 (m, 2H, 2x H-12), 6.88 (d,  $J = 8.7$ , 2H, 2x H-13), 6.05 – 5.74 (m, 1H, H-2), 5.02 – 4.91 (m, 2H, 2x H-1), 4.57 – 4.25 (m, 2H, 2x H-10), 3.81 (s, 3H, 3x H-15), 3.79 – 3.39 (m, H-8 and H-5), 2.31 (m, 1H, H-6), 1.83 – 1.77 (m, 1H, H-3), 1.06 (d,  $J = 6.18$ , 3H, 3x H-9), 1.02 (d,  $J = 6.82$ , 3H, 3x H-7), 0.91 (s, 9H, 9x H-18), 0.85 (d,  $J = 6.99$ , 3H, 3x H-4), -0.04 (s, 3H, 3x C-16), -0.01 (s, 3H, 3x H-16).



$^{13}\text{C}$  NMR (75 MHz,  $\text{CDCl}_3$ )  $\delta$  [ppm] = 158.95 (C-14), 141.30 (C-2), 131.30 (C-11), 129.23 (C-12), 114.19 (C-1), 113.70 (C-13), 76.29 (C-8), 75.34 (C-5), 69.58 (C-10), 55.25 (C-15), 44.10 (C-6), 41.35 (C-17), 41.06 (C-3), 26.16 (3x C-18), 18.45 (C-7), 16.08 (C-9), 10.90 (C-4), -3.78 (C-16), -3.83 (C-16).

IR (ATR):  $\tilde{\nu} = 3070.9$  (w), 2957.2 (m), 2929.5 (m), 2885.4 (m), 2856.6 (m), 1639.0 (w), 1613.2 (m), 1587.1 (w), 1513.4 (s), 1462.6 (m), 1246.9 (s)  $\text{cm}^{-1}$

HRMS (EI),  $m/z$       calc. for  $[\text{M}]^+\text{C}_{23}\text{H}_{40}\text{O}_3\text{Si}$ :    392.2747  
                               found  $[\text{M}]^+$ :                                392.2732



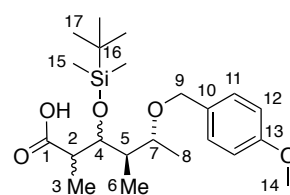
***tert*-butyl(((3*S*,4*S*,5*R*,6*R*)-6-((4-methoxybenzyl)oxy)-3,5-dimethylhept-1-en-4-yl)oxy)**

**dimethylsilane (77)**: (mixture of diastereoisomers carried on through this sequence) **76** (0.55 g, 1.4 mmol) was dissolved in DCM/MeOH (1/1, 1 mL), solid  $\text{NaHCO}_3$  was added (0.12 g, 1.4 mmol) and the mixture cooled to  $-78$  °C. Ozone was bubbled through the solution until TLC analysis indicated complete consumption of the starting material. Nitrogen was bubbled through, then dimethylsulfide (0.17 g, 2.8 mmol) was added and the mix stirred at ambient temperature overnight. The mix was diluted with DCM, filtered over celite and concentrated *in vacuo*. The crude material (yellow oil) was used in the next step without further purification.



**(2*R*,3*R*,4*R*,5*R*)-3-((*tert*-butyldimethylsilyl)oxy)-5-((4-methoxybenzyl)oxy)-2,4-dimethyl hexanoic acid (78)**: (mixture of diastereoisomers carried on through this sequence) Aldehyde **77** (0.552 g, 1.4 mmol) was dissolved in *t*-BuOH (5.5 mL) and 2-methyl-2-butene (4 mL). A solution of sodium phosphate buffer (monobasic, 0.339 g, 2.80 mmol) and sodium hypochlorite (0.228 g, 2.52 mmol) in H<sub>2</sub>O (3.5 mL) was added and the mixture stirred vigorously for 45 minutes. Na<sub>2</sub>S<sub>2</sub>O<sub>3</sub> (sat. aq., 5 mL) was added and the mix further stirred for 15 minutes. After concentration *in vacuo* the slurry was re-dissolved in a minimum amount of H<sub>2</sub>O and extracted with DCM (3x 30 mL). Combined organics were washed with brine (20 mL), dried over Na<sub>2</sub>SO<sub>4</sub> and subjected to column chromatography (acetone/ DCM: 1/50 to 1/10) to give diastereomeric mixture of acid **78** as a white solid (0.466 g, 1.13 mmol, 81 %).

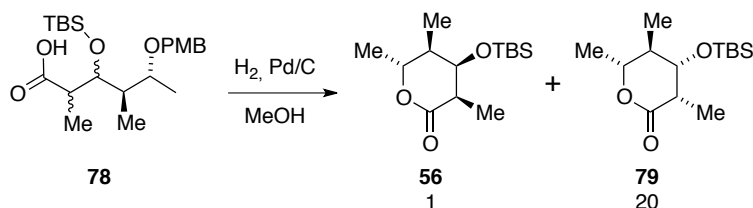
<sup>1</sup>H NMR (599 MHz, CDCl<sub>3</sub>) δ [ppm] = 7.31 – 7.14 (m, 2H, 2x H-11), 6.97 – 6.80 (m, 2H, 2x H-12), 4.65 – 4.42 (m, 1H, H-9), 4.42 – 4.29 (m, 1H, H-9), 4.14 – 4.11 (m, 1H, H-4), 3.73 (s, 3H, 3x H-14), 3.49 – 3.31 (m, 1H, H-7), 2.75 – 2.58 (m, 1H, H-2), 1.99 – 1.62 (m, 1H, H-5), 1.18 – 1.13 (m, 6H, 3x H-8 and 3x H-3), 0.88 (s, 9H, 9x H-17), 0.86 – 0.85 (m, 3H, 3x H-6), 0.22 – -0.11 (m, 6H, 6x H-15).



<sup>13</sup>C NMR (151 MHz, CDCl<sub>3</sub>) δ [ppm] = 177.87 (C-1), 158.99 (C-13), 130.89 (C-10), 129.02 (C-11), 113.74 (C-12), 75.92 (C-7), 74.05 (C-4) 69.58 (C-9), 55.24 (C-14), 45.54 (C-2), 42.18 (C-5), 26.00 (3x C-17), 25.95 (C-16) 18.34 (C-8), 16.58 (C-3), 9.84 (C-6), -4.36 (2x C-15).

IR (ATR):  $\tilde{\nu}$  = 2953.6 (m), 2929.7 (m), 2886.1 (m), 2656.1 (m), 1706.9 (s), 1612.9 (m), 1587.1 (w), 1513.6 (s), 1462.6 (m) cm<sup>-1</sup>

HRMS (EI), *m/z*      calc. for [M]<sup>++</sup> C<sub>22</sub>H<sub>38</sub>O<sub>5</sub>Si:    410.2489  
                              found [M]<sup>++</sup>:                                not found

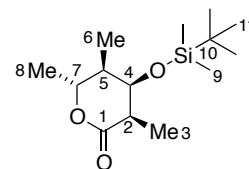


**(3*R*,4*R*,5*R*,6*R*)-4-((*tert*-butyldimethylsilyloxy)-3,5,6-trimethyltetrahydro-2*H*-pyran-2-**

**one (79).** Acid **78** (0.236 g, 0.575 mmol) was dissolved in MeOH (1 mL). Pd/C (0.060 g) was added and the system purged with hydrogen 5 times. After 40 minutes, the system was purged with nitrogen, filtered over a celite plug, concentrated *in vacuo* and subjected to column chromatography (EtOAc/ hexanes: 1/10), yielding a mixture of **56** and **79** (138 mg, 0.51 mmol, 88 % dr. 1/20)

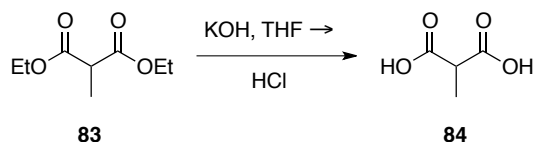
$$[\alpha]_D^{20} = +39.53 \text{ (} c \text{ 0.85, CH}_2\text{Cl}_2\text{)}$$

$^1\text{H NMR}$  (600 MHz,  $\text{CDCl}_3$ )  $\delta$  [ppm] = 4.93 (qd,  $J = 6.7, 3.1$ , 1H, H-7), 3.84 (t,  $J = 3.6$ , 1H, H-4), 2.57 (qd,  $J = 7.1, 3.5$ , 1H, H-5 or H-2), 1.91 – 1.69 (m, 1H, H-5 or H-2), 1.29 (d,  $J = 6.8$ , 3H, 3x H-8), 1.24 (d,  $J = 7.1$ , 3H, 3x H-6 or H-3), 0.97 (d,  $J = 7.2$ , 3H, 3x H-6 or H-3), 0.89 (s, 9H, 9x H-11), -0.08 (s, 3H, 3x H-9), -0.06 (s, 3H, 3x H-9).



$^{13}\text{C NMR}$  (151 MHz,  $\text{CDCl}_3$ )  $\delta$  [ppm] = 174.06 (C-1), 74.31 (C-7), 74.01 (C-4), 38.72 (C-2 or C-5), 36.64 (C-2 or C-5), 26.00 (C-10), 25.69 (3x C-11), 17.85 (C-8), 12.93 (C-3), 10.22 (C-6 or C-3), -4.61 (C-9), -4.93 (C-9).

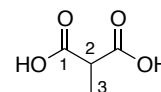
HRMS (EI), $m/z$	calc. for $[\text{M}-t\text{Bu}]^{++}$	$\text{C}_{14}\text{H}_{28}\text{O}_3\text{Si}$ :	215.1098
	found $[\text{M}-t\text{Bu}]^{++}$	$\text{C}_{10}\text{H}_{19}\text{O}_3\text{Si}$ :	215.1103



**2-methylmalonic acid (84)** was prepared according to literature procedures.<sup>[69]</sup> A solution of KOH (35.2 g, 627 mmol) in EtOH (abs. 200 mL) was added to a solution of diethyl 2-methylmalonate (**83**) (29.3 g, 168 mmol) in EtOH (abs. 200 mL) at 0 °C. The mixture was stirred at ambient temperature over night. The salt was filtered off, washed with  $\text{Et}_2\text{O}$  (4x 50 mL) and dried *in vacuo*. The cooled solution of the salt in  $\text{H}_2\text{O}$  (50 mL) was treated with

concentrated HCl (40 mL). After addition was complete, the mixture was allowed to warm to ambient temperature and stirred for two hours. The resulting suspension was extracted with Et<sub>2</sub>O (3x 75 mL). The combined organic extracts were dried with brine and Na<sub>2</sub>SO<sub>4</sub> and concentrated *in vacuo* to give **84** (18.3 g, 155 mmol, 92%). (The extraction needs to be repeated in four to five cycles to achieve reported yields).

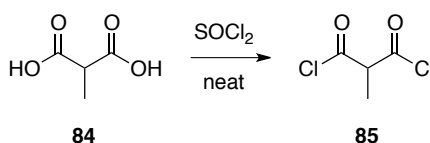
<sup>1</sup>H NMR (200 MHz, CD<sub>3</sub>OD) δ [ppm] = 3.40 (q, *J* = 7.2, 1H, H-2), 1.35 (d, *J* = 7.2, 3H, 3x H-3).



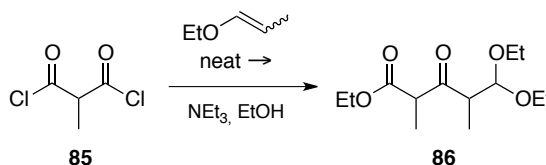
<sup>13</sup>C NMR (600 MHz, CD<sub>3</sub>OD) δ [ppm] = 176.54 (2x C-1), 49.59 (C-2), 16.68 (C-3).

IR (ATR):  $\tilde{\nu}$  = 2891.0 (v), 1687.3 (s), 1467 (m), 1410.8 (s), 1289.5 (s) cm<sup>-1</sup>

HRMS (EI), <i>m/z</i>	calc. for [M] <sup>+</sup> C <sub>4</sub> H <sub>6</sub> O <sub>4</sub> :	118.0266
	found [M] <sup>+</sup> :	118.0262

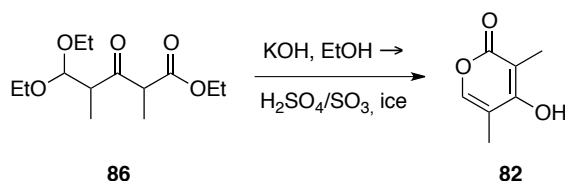


**2-methylmalonyl dichloride (85)** was prepared according to literature.<sup>[69]</sup> 2-methylmalonic acid (**84**) (16.4 g, 139 mmol) and thionyl chloride (49.6 g, 30.2 mL, 417 mmol) were heated to 50 °C for 36 hours. Excess thionyl chloride was removed *via* a VIGREUX column (10 cm). The product was distilled (32 °C, 15 mbar) as a clear, colourless liquid (15.8 g, 102 mmol, 74 %). The product **85** was stored under an Argon atmosphere and used as obtained in the next reaction.



**Ethyl 5,5-diethoxy-2,4-dimethyl-3-oxopentanoate (86)** was prepared according to literature.<sup>[68]</sup> Methylmalonyl chloride (**85** 0.649 g, 4.19 mmol) was added dropwise to ethylpropenyl ether at ambient temperature over 10 minutes. After three hours, the resulting solution was cooled to 0 °C and EtOH (abs. 2.1 mL) was added dropwise. The solution was

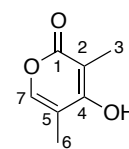
stirred at 0 °C for 15 minutes and then quenched upon addition of NEt<sub>3</sub> (0.85 g, 8.5 mmol) in Et<sub>2</sub>O (2.5 mL). The mixture was diluted with Et<sub>2</sub>O and NH<sub>4</sub>Cl was filtered off. The organic phase was washed with a minimum amount of H<sub>2</sub>O two times and then dried over Na<sub>2</sub>SO<sub>4</sub>. Concentration *in vacuo* gave a diastereomeric mixture that is **86** (6.97 g, 3.73 mmol 89 %).



**4-hydroxy-3,5-dimethyl-2H-pyran-2-one (82)** was prepared according to literature.<sup>[68]</sup> A solution of **86** (0.919 g, 3.53 mmol) in EtOH (abs. 3.5 mL) was treated with KOH (0.466 g, 7.06 mmol) in EtOH (abs. 3.5 mL). The mixture was stirred at ambient temperature for two days. The solvent was removed *in vacuo*. The obtained solid was treated with oleum (30 % SO<sub>3</sub>, 7.5 mL) at 0 °C and the resulting solution refluxed at 100 °C for one hour. The hot solution was then poured onto ice (25 g). The obtained mixture was extracted with EtOAc (6x 50 mL), combined organics were washed with NaHCO<sub>3</sub> (sat. 5x 50 mL), dried over MgSO<sub>4</sub> and concentrated *in vacuo*. Column chromatography (EtOAc/ hexanes: 3/1) yielded a yellow solid, which could be recrystallized, from EtOAc, giving colourless crystals of **82** (0.217 g, 1.55 mmol, 44 %)

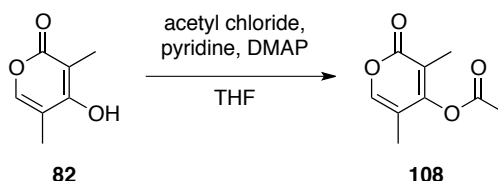
<sup>1</sup>H NMR (600 MHz, DMSO d<sub>6</sub>) δ [ppm] = 7.40 (s, 1H, H-7), 3.31 (s, 1H, OH), 1.81 (s, 6H, 3x H-3 and 3x H-6).

<sup>13</sup>C NMR (101 MHz, CDCl<sub>3</sub>) δ [ppm] = 165.33 (C-4), 164.45 (C-1), 146.16 (C-7), 111.57 (C-5), 99.81 (C-2), 11.34 (C-6), 9.63 (C-3).



IR (ATR):  $\tilde{\nu}$  = 2929 (s), 1656 (v), 1541 (v), 1462 (s), 1379 (m), 1303 (s), 1225 (v) cm<sup>-1</sup>

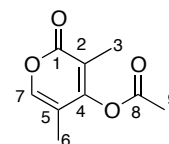
HRMS (EI), <i>m/z</i>	calc. for [M] <sup>++</sup> C <sub>7</sub> H <sub>8</sub> O <sub>3</sub> :	140.0473
	found [M] <sup>++</sup> :	140.0478



**3,5-dimethyl-2-oxo-2H-pyran-4-yl acetate (108):** Acetylchloride (77.6 mg, 0.979 mmol) was dissolved in THF (0.2 mL) and cooled to 0 °C. Pyridine (235 mg, 0.24 mL, 2.94 mmol), pyrone **82** (140 mg, 0.979 mmol) and DMAP (cat.) was added in one portion. The mixture was warmed to ambient temperature and stirred for 2 days. The obtained mixture was partitioned between Et<sub>2</sub>O (10 mL) and H<sub>2</sub>O (10 mL), the aqueous layer washed with Et<sub>2</sub>O (2x 10 mL), combined organics were washed with NaHCO<sub>3</sub> (sat. aq., 10 mL) and brine (10 mL), dried over Na<sub>2</sub>SO<sub>4</sub> and concentrated *in vacuo*. Column chromatography (EtOAc/ hexanes: 1/3) gave **108** as yellow oil, which crystallised in high vacuum (143 mg, 0.783 mmol, 70 %).

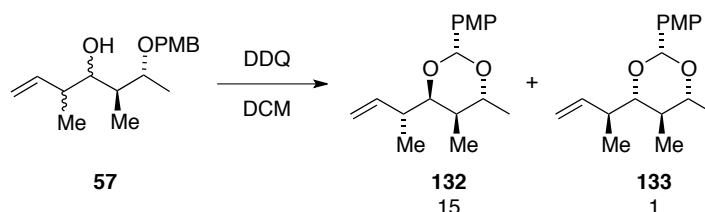
<sup>1</sup>H NMR (300 MHz, CDCl<sub>3</sub>) δ [ppm] = 7.25 (s, 1H, C-7), 2.37 (s, 3H, 3x H-3), 1.95 (s, 3H, 3x H-6), 1.87 (s, 3H, 3x H-9.)

<sup>13</sup>C NMR (75 MHz, CDCl<sub>3</sub>) δ [ppm] = 166.66 (C-8), 164.35 (C-1), 158.40 (C-4), 145.27 (C-7), 115.86 (C-5), 112.61 (C-2), 20.27 (C-9), 11.11 (C-6), 10.23 (C-3).



IR (ATR):  $\tilde{\nu}$  = 3456 (w), 2990 (w), 2937 (w), 1772 (s), 1733 (vs), 1714 (s), 1671 (m), 1580 (m), 1467 (m), 1446 (m), 1372.3 (s), 1343 (m), 1309 (m), 1274 (m) cm<sup>-1</sup>

HRMS (EI), <i>m/z</i>	calc. for [M] <sup>+</sup> C <sub>9</sub> H <sub>10</sub> O <sub>4</sub> :	182.0579
	found [M] <sup>+</sup> :	182.0582



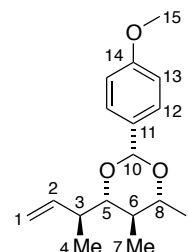
**(2R,4S,5R,6R)-4-((S)-but-3-en-2-yl)-2-(4-methoxyphenyl)-5,6-dimethyl-1,3-dioxane (133)**

A solution of diastereomeric mixture **75** (0.67 g, 2.4 mmol) in DCM (15 mL) was stirred over 4 Å MS for 30 minutes. Then, DDQ (0.72 g, 3.2 mmol) was added and the resulting mixture stirred for 1 hour. The suspension was filtered through a silica plug and washed (50 mL) DCM. The organic phase was washed with H<sub>2</sub>O (5x 20 mL), dried over MgSO<sub>4</sub>, and

concentrated *in vacuo*. Column chromatography (EtOAc/hexanes: 1/4) yielded the product **132** and **133** as white solid (combined yield 73 %, dr. 15/1, **132** 454 mg, 1.54 mmol, **133**, 30 mg, 0.11 mmol).

**133:**  $[\alpha]_D^{20} = +24.24^\circ$  (*c* 0.85, DCM)

$^1\text{H}$  NMR (600 MHz,  $\text{CDCl}_3$ )  $\delta$  [ppm] = 7.47 – 7.40 (m, 2H, 2x H-12), 6.92 – 6.85 (m, 2H, 2x H-13), 6.08 – 5.78 (m, 1H, H-2), 5.46 (s, 1H, H-10), 5.07 – 5.03 (m, 1H, H-1), 5.02 – 4.99 (m, 1H, H-1), 3.80 (s, 3H, 3x H-15), 3.59 – 3.49 (dq,  $J = 9.7, 6.1$ , 1H, H-8), 3.37 – 3.30 (dd,  $J = 10.0, 2.2$ , 1H, H-5), 2.58 – 2.47 (m, 1H, H-3), 1.58 – 1.54 (m, 1H, H-6), 1.31 – 1.26 (d,  $J = 6.1$ , 3H, 3x H-9), 1.21 – 1.12 (d,  $J = 7.0$  Hz, 3H, 3x H-4), 0.83 – 0.78 (d,  $J = 6.6$  Hz, 3H, 3x H-7).



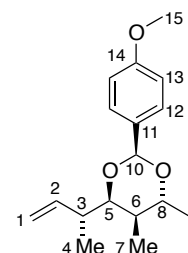
$^{13}\text{C}$  NMR (75 MHz,  $\text{CDCl}_3$ )  $\delta$  [ppm] = 159.9 (C-14), 139.9 (C-2), 139.9 (C-11), 132.0 (C-12), 127.5 (C-1), 115.2 (C-13), 113.6 (C-13), 100.5 (C-14), 85.3 (C-5), 78.4 (C-8), 55.4 (C-15), 39.9 (C-3), 38.2 (C-6), 19.5 (C-4), 18.4 (C-4), 11.9 (C-7).

IR (ATR):  $\tilde{\nu} = 3072.3$  (v), 3011.3 (v), 2963.7 (w), 2931.2 (v), 2896.6 (v), 2834.8 (v), 1713.0 (w), 1610.9 (m), 1585.1 (v), 1517.7 (m)  $\text{cm}^{-1}$

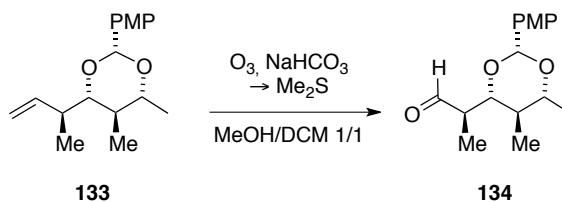
HRMS (EI), $m/z$	calc. for $[\text{M}]^{++}$ $\text{C}_{17}\text{H}_{24}\text{O}_3$ :	276.1825
	found $[\text{M}]^{++}$ :	276.1730

**132:**

$^1\text{H}$  NMR (400 MHz,  $\text{CDCl}_3$ )  $\delta$  [ppm] = 7.45 – 7.39 (m, 2H, H-12), 6.92 – 6.85 (m, 2H, H-13), 6.07 – 5.96 (m, 1H, H-2), 5.75 (s, 1H, H-11), 5.13 – 5.01 (m, 2H, 2x H-1), 4.14 (q,  $J = 7.0$ , 1H, H-6), 3.79 (s, 3H, 3x H-15), 3.79 – 3.73 (m, 1H, H-5), 2.47 – 2.34 (m, 1H, H-3), 1.56 – 1.51 (m, 1H, H-6), 1.50 (d,  $J = 7.0$ , 3H, 3x H-9), 1.24 (d,  $J = 6.9$ , 3H, 3x H-7), 0.96 (d,  $J = 6.9$ , 3H, 3x H-4).

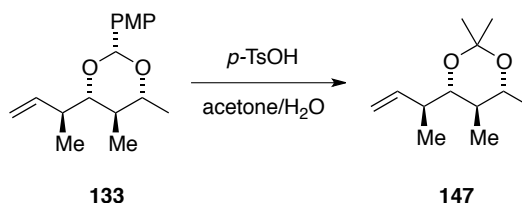


$^{13}\text{C}$  NMR (101 MHz,  $\text{CDCl}_3$ )  $\delta$  [ppm] = 159.67 (C-14), 141.81 (C-2), 131.92 (C-11), 127.33 (C-12), 113.70 (C-1), 113.50 (C-13), 94.19 (C-10), 78.21 (C-5), 75.88 (C-8), 55.28 (C-15), 38.13 (C-3), 33.50 (C-6), 17.04 (C-9), 14.22 (C-4), 12.96 (C-7).



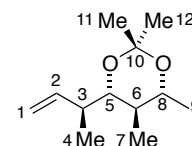
**(R)-2-((2R,4R,5R,6R)-2-(4-methoxyphenyl)-5,6-dimethyl-1,3-dioxan-4-yl)propanal (134):**

A solution of PMP acetal **133** (30.0 mg, 0.151 mmol) in DCM/MeOH (2 mL, 1/1) was cooled to  $-78$  °C. Ozone was bubbled through the mixture for 25 seconds. Nitrogen was bubbled through the mixture, DMS (0.186 g, 3.0 mmol) was added. The solution was stirred at ambient temperature over night and concentrated *in vacuo* to yield substance **134** as a crude oil, which was used without further purification.



**(4S,5R,6R)-4-((S)-but-3-en-2-yl)-2,2,5,6-tetramethyl-1,3-dioxane (147):** To a solution of **133** (100 mg, 0.362 mmol) in dry acetone (2 mL) DL-10 Camphorsulfonic acid (84.1 mg, 0.362 mg) was added and the reaction was stirred at room temperature over night. The reaction was subsequently diluted with Et<sub>2</sub>O (10 mL), washed with NaHCO<sub>3</sub> (aq. sat. 10 mL) dried over MgSO<sub>4</sub>, and concentrated *in vacuo* (4 °C bath temperature, 20 mbar). Purification by column chromatography (Et<sub>2</sub>O/pentane: 1/6) yielded **147** (Due to volatility of the product, residual solvents could not be removed from product (40 mg, 0.200 mmol, 55 %, 94 % b.o.r.s.m.).

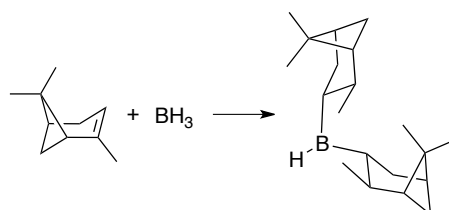
<sup>1</sup>H NMR (599 MHz, CDCl<sub>3</sub>) δ [ppm] = 5.90 – 5.82 (m, 1H, H-2), 5.03 – 4.95 (m, 2H, 2x H-1), 3.58 (dq, *J* = 10.1, 6.0, 1H, H-8), 3.36 (dd, *J* = 10.3, 2.2, 1H, H-5), 2.44 – 2.37 (m, 1H, H-3), 1.41 (s, 3H, 3x H-11), 1.36 (s, 3H, H-12), 1.31 – 1.27 (m, 1H, H-6), 1.15 (d, *J* = 6.0, 3H, 3x H-9), 1.05 (d, *J* = 7.0, 3H, 3x H-4), 0.75 – 0.73 (d, *J* = 7.0, 3H, 3x H-7).



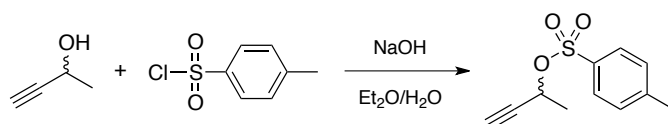
<sup>13</sup>C NMR (151 MHz, CDCl<sub>3</sub>) δ [ppm] = 139.82 (C-2), 114.74 (C-1), 97.68 (C-10), 77.33 (C-5), 70.52 (C-8), 39.51 (C-3), 38.14 (C-6), 30.11 (C-12), 19.77 (C-9), 19.43 (C-11), 18.05 (C-4), 11.78 (C-7).

IR (ATR):  $\tilde{\nu} = 3073.7$  (w), 2977,8 (m), 2932.9 (m), 2853.0 (m), 1644.3 (w), 1455.8 (m), 1379.2 (s), 1256.1 (s), 1200.6 (s)  $\text{cm}^{-1}$

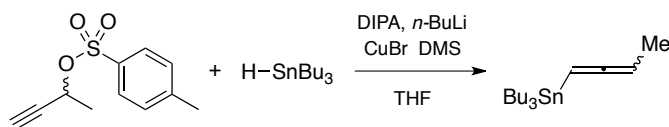
HRMS (EI), $m/z$	calc. for $[\text{M}-\text{Me}]^{++}$ $\text{C}_{11}\text{H}_{19}\text{O}_2$ :	183.1380
	found $[\text{M}]^{++}$ :	183.1387



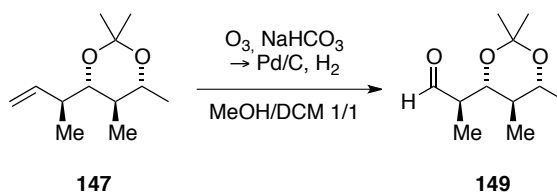
**bis((1*R*,2*S*,3*R*,5*R*)-2,6,6-trimethylbicyclo[3.1.1]heptan-3-yl)borane** was prepared, following literature procedures.<sup>[175]</sup> Freshly distilled (–)  $\alpha$ -pinene (20 mbar, 45 °C, 20.9 mL, 132 mmol) was dissolved in THF (25 mL). The solution was cooled to 0 °C and borane complex ( $\text{BH}_3 \cdot \text{THF}$  1M solution in THF, 55 mL, 55 mmol) was added over 2 minutes. Upon complete addition, the solution was stirred at ambient temperatures for 5 minutes, then stirring was seized and THF was partially removed upon a gentle stream of nitrogen. Crystallisation started after 1 hour and proceeded over night. Then, the crystals were filtered off, washed thoroughly with  $\text{Et}_2\text{O}$  (2x 15 mL), the crystals were crushed and stored in a glove box (7.6 g, 26.5 mmol, 48 %).



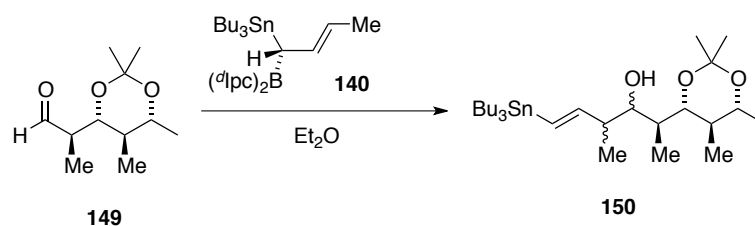
**but-3-yn-2-yl 4-methylbenzenesulfonate** was prepared analogous to literature procedures.<sup>[176]</sup> 3-Butyn-2-ol (19.0 g, 271 mmol) was dissolved in  $\text{H}_2\text{O}$  to obtain a ca. 50% aqueous solution.  $\text{Et}_2\text{O}$  (240 mL) and toluol-4-sulfonylchlorid (64.6 g, 339 mmol) were added and the biphasic mixture was cooled to 0 °C. NaOH (67.8 g, 1694 mmol) was added and the mixture stirred at 0 °C for 2 hours. The mix was allowed to warm to ambient temperature, diluted with  $\text{H}_2\text{O}$  (50 mL) and  $\text{Et}_2\text{O}$  (200 mL), phases were separated and the organic layer dried over  $\text{MgSO}_4$ . Concentration *in vacuo* yielded a yellow oil, which solidified at ambient temperature. Recrystallization from  $\text{Et}_2\text{O}$  gave colourless crystals (55.2 g, 271 mmol, 91 %).



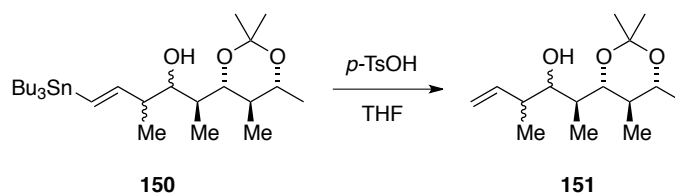
(±)Buta-1,2-dien-1-yltributylstannane (**139**) was prepared as described in literature.<sup>[87,89]</sup> DIPA (2.83 g, 28.0 mmol) was dissolved in THF (100 mL). *n*-BuLi (2.5 M solution in hexanes, 11.2 mL, 28 mmol) was added at 0 °C and the solution stirred for 30 minutes. HSnBu<sub>3</sub> (8.15 g, 28 mmol) was added and the yellow solution stirred another 30 minutes. After cooling to -78 °C CuBr•DMS complex (5.76 g, 28.0 mmol) was added in portions over 5 minutes. The dark brown solution was stirred for 30 minutes then the tosylate (6.28 g, 28 mmol) was added in one portion. After another 15 minutes, the black mixture was poured into a rapidly stirred mixture of NH<sub>4</sub>Cl (aq. sat.)/NH<sub>3</sub>-H<sub>2</sub>O = 9/1 (400 mL) and Et<sub>2</sub>O (300 mL). After phases cleared out the organic layer was separated, dried over MgSO<sub>4</sub> and concentrated *in vacuo* to give **139** as yellow oil (7.3 g, 21.3 mmol, 76 %). Stannane **139** was stored under Argon and passed through a short column of silica, containing 10 w% K<sub>2</sub>CO<sub>3</sub> with hexanes.



(*R*)-2-((4*R*,5*R*,6*R*)-2,2,5,6-tetramethyl-1,3-dioxan-4-yl)propanal (**149**): A solution of acetone **147** (30.0 mg, 0.151 mmol) in DCM/MeOH (2 mL, 1/1) was cooled to -78 °C. Ozone was bubbled through for 25 seconds. Nitrogen was bubbled through the reaction mixture, MeOH (2 mL) and Pd/C (catalytic amount) were added. The reaction mixture was purged with hydrogen and stirred at ambient temperature for five minutes. After purging with nitrogen, filtration over celite (DCM, 25 mL), washing with brine (10 mL) and drying with MgSO<sub>4</sub>, the aldehyde **149** was concentrated *in vacuo* (4 °C, 20 mbar) and used in the next step without further purification.

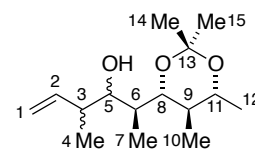


**(2S,3S,4S,E)-4-methyl-2-((4S,5R,6R)-2,2,5,6-tetramethyl-1,3-dioxan-4-yl)-6-(tributylstannyl)hex-5-en-3-ol (150)**: ( $^d\text{Ipc}$ )<sub>2</sub>BH (1.22 g, 4.25 mmol) was dispensed in Et<sub>2</sub>O (1 mL) and stannane **139** (1.46 g, 4.25 mmol) was added at 0 °C. The mixture was stirred at this temperature for 5 hours and turned into a clear solution over this period. The solution was cooled to -78 °C and a solution of aldehyde **149** (320 mg, 1.6 mmol) in Et<sub>2</sub>O (2 mL) was added dropwise. The mixture was warmed to ambient temperature and stirred for 35 hours. NaHCO<sub>3</sub> (aq. sat., 4.25 mL) and H<sub>2</sub>O<sub>2</sub> (30 % aq., 8.5 mL) was added and the mixture stirred vigorously for 5 hours. The mix was diluted with Et<sub>2</sub>O (10 mL), phases were separated and the aqueous layer washed with Et<sub>2</sub>O (4x 10 mL). Combined organic layers were washed with brine (10 mL), dried over MgSO<sub>4</sub> and concentrated *in vacuo*. Column chromatography (EtOAc/ hexanes 1/10) was performed, **150** could not be obtained cleanly. Product containing fractions were thus subjected to following reaction procedures.



**(2S,3S,4S)-4-methyl-2-((4S,5R,6R)-2,2,5,6-tetramethyl-1,3-dioxan-4-yl)hex-5-en-3-ol (151)**: Crotylstannane **150** (436 mg, 0.80 mmol) was dissolved in THF (16 mL), *p*-TsOH monohydrate (152 mg, 0.80 mmol) was added and the mixture stirred for 1 hour at ambient temperature. NaHCO<sub>3</sub> (aq. sat. 16 mL) was added, phases were separated and the aqueous layer washed with EtOAc (4x 20 mL). Combined organic layers were washed with brine (10 mL), dried over Na<sub>2</sub>SO<sub>4</sub> and concentrated *in vacuo*. Homoallylic alcohol **151** was obtained upon column chromatography (EtOAc/ hexanes 1/20 to 1/10) as colourless oil (140 mg, 0.55 mmol, 34 %, calculated from aldehyde **149**, d.r. 5/1 based on <sup>1</sup>H NMR). Peaks reported for major diastereoisomer.

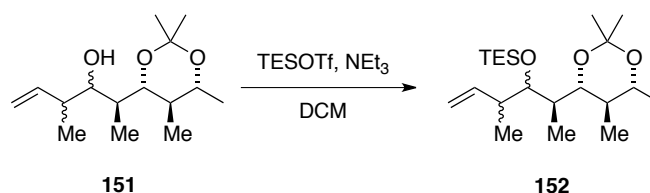
$^1\text{H}$  NMR (599 MHz,  $\text{CDCl}_3$ )  $\delta$  [ppm] = 5.91 (ddd,  $J = 17.3, 10.3, 7.8$ , 1H, H-2), 5.11 – 5.03 (m, 2H, 2x H-1), 3.68 (dd,  $J = 9.4, 1.3$ , 1H, H-5), 3.66 – 3.57 (m, 2H, H-11 and H-8), 2.32 – 2.24 (m, 1H, H-3), 1.97 – 1.92 (m, 1H, H-6), 1.65 – 1.58 (m, 1H, H-9), 1.40 (s, 3H, 3x H-15), 1.37 (s, 3H, 3x H-14), 1.21 – 1.18 (m, 3H, 3x H-12), 1.04 – 1.01 (m, 3H, 3x H-7), 0.92 (m, 3H, 3x H-4), 0.77 (d,  $J = 5.9$ , 3H, 3x H-10).



$^{13}\text{C}$  NMR (151 MHz,  $\text{CDCl}_3$ )  $\delta$  [ppm] = 142.54 (C-2), 113.84 (C-1), 98.45 (C-13), 80.67 (C-8), 73.78 (C-5), 70.73 (C-11), 41.13 (C-3), 40.82 (C-9), 33.03 (C-6), 30.11 (C-14), 19.74 (C-12), 19.02 (C-15), 17.46 (C-4), 14.62 (C-10), 11.97 (C-7).

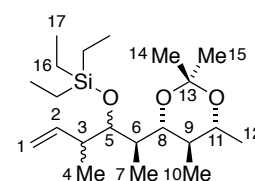
IR (ATR):  $\tilde{\nu} = 3396.1$  (v), 2970.9 (m), 2936.1 (m), 2875.5 (m), 1640.9 (w), 1457.9 (m), 1416.2 (m), 1381.1 (s)  $\text{cm}^{-1}$

HRMS (EI), $m/z$	calc. for $[\text{M}-\text{Me}]^{++}\text{C}_{14}\text{H}_{25}\text{O}_3$ :	241.1798
	found $[\text{M}-\text{Me}]^{++}$ :	241.1789



**triethyl(((2*R*,3*S*,4*S*)-4-methyl-2-((4*R*,5*R*,6*R*)-2,2,5,6-tetramethyl-1,3-dioxan-4-yl)hex-5-en-3-yl)oxy)silane (152)**: Homoallylic alcohol **151** (125 mg, 0.488 mmol) was dissolved in DCM (1 mL) and cooled to 0 °C. 2,6-lutidine (115 mg, 1.07 mmol) and TESOTf (155 mg, 0.585 mmol) were added and the mixture stirred at ambient temperature for 14 hours. The mixture was then diluted with DCM (10 mL) and  $\text{NaHCO}_3$  (aq. sat. 5 mL). The aqueous layer was washed with DCM (3x 10 mL), combined organic layers were washed with brine (5 mL), dried over  $\text{Na}_2\text{SO}_4$  and concentrated *in vacuo*. Column chromatography (EtOAc/ hexanes 1/20 to 1/10) gave **152** as colourless liquid (122 mg, 0.329 mmol, 67 %). Peaks reported for the major diastereoisomer.

$^1\text{H}$  NMR (599 MHz,  $\text{CDCl}_3$ )  $\delta$  [ppm] = 5.89 – 5.81 (m, 1H, H-2), 5.04 – 4.97 (m, 2H, 2x H-1), 3.91 (t,  $J = 3.7$ , 1H, H-8), 3.54 (dq,  $J = 9.8$ , 6.0, 1H, H-11), 3.35 (dd,  $J = 10.5, 2.4$ , 1H, H-5), 2.20 (qt,  $J = 9.0, 4.5$ , 1H, H-3), 1.85 – 1.78 (m, 1H, H-6), 1.40 (s, 3H, 3x H-15), 1.38 (s, 3H,

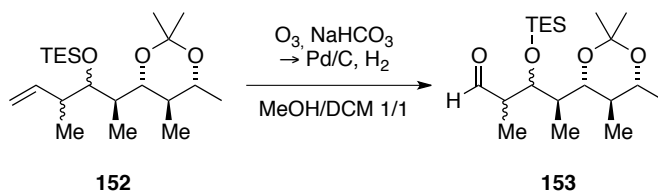


3x H-14), 1.29 – 1.24 (m, 1H, H-9), 1.18 (d,  $J = 6.0$ , 3H, 3x H-12), 1.03 (d,  $J = 6.9$ , 3H, 3x H-4), 0.98 – 0.95 (m, 12H, 9x H-17), 0.92 – 0.90 (m, 3H, 3x H-7), 0.75 (d,  $J = 6.5$ , 3H, 3x H-10), 0.70 – 0.64 (m, 6H, 6x H-16).

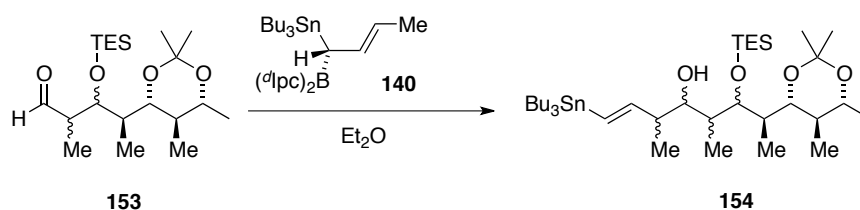
$^{13}\text{C}$  NMR (151 MHz,  $\text{CDCl}_3$ )  $\delta$  [ppm] = 140.90 (C-2), 114.39 (C-1), 97.83 (C-13), 78.14 (C-5), 73.52 (C-8), 70.87 (C-11), 45.65 (C-3), 37.71 (C-9), 37.48 (C-6), 30.26 (C-14), 20.01 (C-12), 19.57 (C-15), 16.66 (C-4), 14.47 (C-7), 12.85 (C-10), 7.13 (2x C-17), 6.79 (C-17), 5.41 (2x C-16), 3.89 (C-16).

IR (ATR):  $\tilde{\nu} = 2958.9$  (m), 2935.9 (m), 2911.9 (m), 2876.4 (m), 1639.7 (w), 1457.9 (m), 1416.2 (w), 1378.6 (s)  $\text{cm}^{-1}$

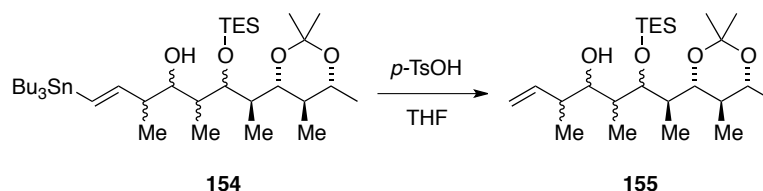
HRMS (EI), $m/z$	calc. for $[\text{M}-\text{Me}]^{+\cdot} \text{C}_{20}\text{H}_{39}\text{O}_3\text{Si}$ :	355.2663
	found $[\text{M}]^{+\cdot}$ :	355.3009



**(2R,3R,4R)-2-methyl-4-((4R,5R,6R)-2,2,5,6-tetramethyl-1,3-dioxan-4-yl)-3-((triethylsilyloxy)pentanal (153)**: A solution of intermediate **152** (112 mg, 0.302 mmol) in DCM/MeOH (3 mL, 1/1) was cooled to  $-78$  °C. Ozone was bubbled through for 25 seconds. Nitrogen was bubbled through the reaction mixture, MeOH (2 mL) and Pd/C (catalytic amount) were added. The reaction mixture was purged with hydrogen and stirred at ambient temperature for five minutes. After purging with nitrogen, filtration over celite (DCM, 25 mL), washing with brine (10 mL) and drying with  $\text{MgSO}_4$ , a complex mixture of products was obtained. Crude  $^1\text{H}$  NMR analysis indicated no formation of aldehyde. The mixture was dissolved in DCM (3 mL) DMS (1 mL) was added and the solution stirred over night. Concentration *in vacuo* gave a mixture of products. An aldehyde peak indicated a minor content of **153**. The mixture was carried on through the next synthetic sequence.

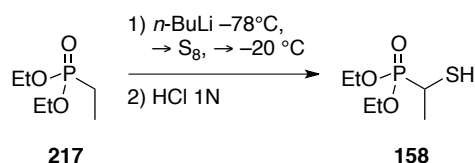


**(3*S*,4*S*,5*S*,6*S*,7*R*,*E*)-3,5-dimethyl-7-((4*R*,5*R*,6*R*)-2,2,5,6-tetramethyl-1,3-dioxan-4-yl)-1-(tributylstannyl)-6-((triethylsilyl)oxy)oct-1-en-4-ol (154)**:  $(^d\text{Ipc})_2\text{BH}$  (1.22 g, 4.25 mmol) was dispensed in  $\text{Et}_2\text{O}$  (1 mL) and stannane **139** (1.46 g, 4.25 mmol) was added at 0 °C. The mixture was stirred at this temperature for 5 hours and turned into a clear solution over this period. The solution was cooled to -78 °C and a solution of aldehyde **153** (product mixture, 0.302 mmol theoretical amount) in  $\text{Et}_2\text{O}$  (2 mL) was added dropwise. The mixture was warmed to ambient temperature and stirred for 35 hours.  $\text{NaHCO}_3$  (aq. sat. 4.25 mL) and  $\text{H}_2\text{O}_2$  (30 % aq., 8.5 mL) was added and the mixture stirred vigorously for 5 hours. The mix was diluted with  $\text{Et}_2\text{O}$  (10 mL), phases were separated and the aqueous layer washed with  $\text{Et}_2\text{O}$  (4x 10 mL). Combined organic layers were washed with brine (10 mL), dried over  $\text{MgSO}_4$  and concentrated *in vacuo*. The crude mixture was directly subjected to the next reaction protocol.



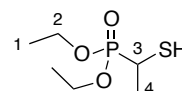
**(3*S*,4*S*,5*S*,6*S*,7*R*)-3,5-dimethyl-7-((4*R*,5*R*,6*R*)-2,2,5,6-tetramethyl-1,3-dioxan-4-yl)-6-((triethylsilyl)oxy)oct-1-en-4-ol (155)**: Crotylstannane **154** (0.302 mmol theoretical amount) was dissolved in THF (8 mL), *p*-TsOH monohydrate (57 mg, 0.30 mmol) was added and the mixture stirred for 1 hour at ambient temperature.  $\text{NaHCO}_3$  (aq. sat. 10 mL) was added, phases were separated and the aqueous layer washed with  $\text{EtOAc}$  (4x 10 mL). Combined organic layers were washed with brine (10 mL), dried over  $\text{Na}_2\text{SO}_4$  and concentrated *in vacuo*. Column chromatography ( $\text{EtOAc}$ / hexanes 1/20 to 1/10) was performed. Only decomposed material was obtained. No indication of the successful formation of **155** were found by means of  $^1\text{H}$  NMR or mass spectroscopy.

## Thiocarbonyl Ylid Based 1,3-Dipoles



**Diethyl (1-mercaptoethyl)phosphonate (158)** was prepared following literature procedures.<sup>[114]</sup> Diethyl ethylphosphonate **217** (1.66 g, 9.79 mmol) was dissolved in THF (10 mL) and cooled to  $-78^\circ\text{C}$ . *n*-butyllithium (2.5 solution in hexanes, 3.9 mL, 9.79 mmol) was added dropwise over five minutes. After further stirring for 5 minutes powdered sulphur (0.317 g, 1.22 mmol) was added in one portion. Over the course of 2 hours, the mixture was gradually warmed to  $-20^\circ\text{C}$ .  $\text{H}_2\text{O}$  (10 mL) was added and the resulting mixture was concentrated *in vacuo* to remove the organic solvents. The obtained aqueous solution was acidified with 1 N HCl at  $0^\circ\text{C}$  and the resulting mixture was extracted with  $\text{CHCl}_3$  (3x 20 mL). The combined organic layers were washed with brine (10 mL) and dried over  $\text{MgSO}_4$ . Removal of the solvent *in vacuo* and purification by column chromatography (EtOAc/Hex = 5/1 to 7/1) gave **158** as colourless oil.

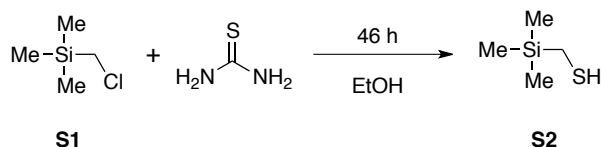
$^1\text{H}$  NMR (400 MHz,  $\text{CDCl}_3$ )  $\delta$  [ppm] = 4.27 – 4.08 (m, 4H, 4x H-2), 3.00 – 2.83 (m, 1H, H-3), 2.08 – 1.96 (t,  $J = 8.0$ , 1H, SH), 1.51 (dd,  $J = 17.1, 7.3$ , 3H, 3x H-4), 1.38 – 1.28 (m, 6H, 6x H-1).



$^{13}\text{C}$  NMR (600 MHz,  $\text{CDCl}_3$ )  $\delta$  [ppm] = 63.24 – 63.17 (d, C-2), 63.02 – 62.93 (d, C-2), 29.18 – 27.67 (d, C-3), 19.12, 19.08 (d, C-4), 16.49 – 16.43 (d, C-1).

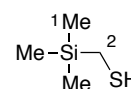
IR (ATR):  $\tilde{\nu} = 3481.1$  (m), 2980.3 (m), 2932.4 (w), 2909.2 (w), 2872.4 (w), 2508.9 (w), 2036.2 (w), 1645.8 (w), 1478.4 (w), 1449.8 (w), 1391.8 (w), 1391.8 (w), 1368.7 (w), 1236.2 (m)  $\text{cm}^{-1}$

HRMS (EI), $m/z$	calc. for $[\text{M}]^{++}$ $\text{C}_6\text{H}_{15}\text{O}_3\text{PS}$ :	198.0480
	found $[\text{M}]^{++}$ :	198.0479



**((Trimethylsilyl)methanethiol (S2)).**<sup>[103]</sup> A solution of trimethylsilyl methyl chloride **S1** (20.2 g, 162 mmol) and thiourea (24.8 g, 323 mmol) in ethanol (250 mL) was heated under reflux for 48 hours. The mixture was allowed to cool to ambient temperature and the solvent was removed to give a white solid. H<sub>2</sub>O (200 mL) and NaOH (400 mL of a 1 M aqueous solution) were added and the resulting solution was extracted with Et<sub>2</sub>O (4 × 100 mL). The combined organic phases were washed with brine (200 mL). Et<sub>2</sub>O was removed via distillation over a VIGREUX column. The product was purified by distillation (115 °C, ambient pressure) to yield mercaptane (7.38 g, 61.6 mmol, 38 %) as colourless oil.

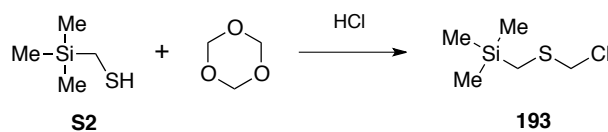
<sup>1</sup>H NMR (300 MHz, CDCl<sub>3</sub>) δ [ppm] = 1.65 (d, *J* = 7.02, 2H, 2x H-2), 1.11 (t, *J* = 7.03, 1H, SH), 0.10 (s, 9H, 9x H-9).



<sup>13</sup>C NMR (75 MHz, CDCl<sub>3</sub>) δ [ppm] = 8.21 (C-2), -2.49 (3x C-1).

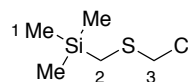
IR (ATR):  $\tilde{\nu}$  = 2955.9 (m), 2900.0 (w), 2558.8 (w), 1411.4 (w), 1389.9 (w), 1247.8 (s), 1155.6 (w) cm<sup>-1</sup>

HRMS (EI), <i>m/z</i>	calc. for [M] <sup>++</sup> C <sub>4</sub> H <sub>12</sub> SSi:	120.0429
	found [M] <sup>++</sup> :	120.0412



**((chloromethyl)thio)methyltrimethylsilane (193)** was prepared according to literature procedures.<sup>[103]</sup> A solution of mercaptane **S2** (7.38 g, 61.4 mmol) and trioxane (1.85 g, 20.1 mmol) was cooled to -10 °C. HCl gas was bubbled through the solution for 1.5 h to give a viscous oil, which was allowed to warm to 0 °C and stirred at this temperature over night. Formed H<sub>2</sub>O was removed and the residual solution was dried at 0 °C over CaCl<sub>2</sub> for 3 hours. The product was purified by bulb-to-bulb distillation (90 °C, 2-3 mbar) to give **193** (4.50 g, 27 mmol, 44 %) as colourless oil, which was stored under Argon.

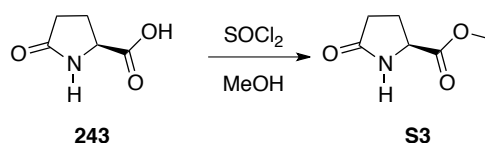
$^1\text{H}$  NMR (300 MHz,  $\text{CDCl}_3$ )  $\delta$  [ppm] = 4.73 (s, 2H, 2x H-3), 2.04 (s, 2H, 2x H-2), 0.13 (s, 9H, 9x H-1.)



$^{13}\text{C}$  NMR (75 MHz,  $\text{CDCl}_3$ )  $\delta$  [ppm] = 53.99 (C-3), 17.99 (C-2), -1.72 (3x C-1).

IR (ATR):  $\tilde{\nu}$  = 2956.3 (m), 2889.3 (w), 1390.5 (w), 1249 (s)  $\text{cm}^{-1}$

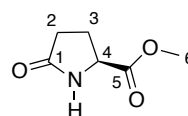
HRMS (EI), $m/z$	calc. for $[\text{M}-\text{Cl}]^{++}$ $\text{C}_5\text{H}_{13}\text{SSi}$ :	133.0502
	found $[\text{M}-\text{Cl}]^{++}$ :	133.0492



**Pyroglutamic acid methyl ester (S3):** Pyroglutamine **243** (10.0 g, 75.9 mmol) was suspended in methanol (120 mL), cooled to 0 °C and thionyl chloride was added over 30 minutes. The obtained, clear solution was stirred at 0 °C for 30 minutes, allowed to warm to ambient temperature and stirred further for one hour. The reaction was quenched upon addition of water (20 mL). Solid  $\text{NaHCO}_3$  (30.0 g) was added to buffer the mixture to pH = 8. The bulk of solvent was removed *in vacuo*, the solid was filtered off and washed with DCM. The aqueous phase was extracted with DCM (3x 50 mL) and the combined organic layers were dried over  $\text{Na}_2\text{SO}_4$ . Concentration *in vacuo* gave (9.52 g, 66.8 mmol, 88 %) of **S3** as colourless oil, which was used without further purification.

$[\alpha]_{\text{D}}^{22} = -0.60$  ( $c$  0.3,  $\text{CHCl}_3$ )

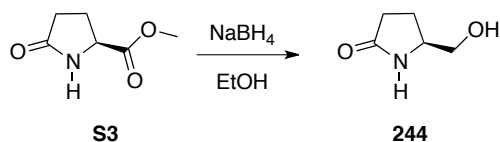
$^1\text{H}$  NMR (400 MHz,  $\text{CDCl}_3$ )  $\delta$  [ppm] = 7.43 (s, 1H, NH), 4.18 (dd,  $J$  = 8.8, 5.0, 1H, H-4), 3.67 (s, 3H, 3x H-6), 2.44 – 2.32 (m, 1H, H-3), 2.30 – 2.16 (m, 2H, 2x H-2), 2.09 (m, 1H, H-3).



$^{13}\text{C}$  NMR (101 MHz,  $\text{CDCl}_3$ )  $\delta$  [ppm] = 178.64 (C-5), 172.64 (C-1), 55.51 (C-4), 52.43 (C-6), 29.28 (C-2), 24.67 (C-3).

IR (ATR):  $\tilde{\nu}$  = 3256.4 (v), 2958.0 (w), 1737.4 (m), 1685.7 (s)  $\text{cm}^{-1}$

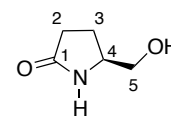
HRMS (EI), $m/z$	calc. for $[\text{M}]^{++}$ $\text{C}_6\text{H}_9\text{NO}_3$ :	143.0582
	found $[\text{M}]^{++}$ :	143.0576



**(S)-5-(hydroxymethyl)pyrrolidin-2-one (244):**<sup>[9]</sup> Methyl ester **S3** (12.7 g, 88.7 mmol) was dissolved in EtOH (120 mL) and cooled to 0 °C. NaBH<sub>4</sub> (5.0 g, 130 mmol) was added and the mixture allowed warming to room temperature. After three hours the solution was re-cooled to 0 °C and acidified to pH = 3 with 37% HCl. The mixture was run over a short silica plug (EtOAc/MeOH: 4/1). After Filtration the bulk of solvent was removed *in vacuo*, residual solvent was removed under a nitrogen stream to give **244** (8.26 g, 71.8 mmol, 81%) as colourless crystals

$[\alpha]_D^{25} = +89.9$  (*c* 13, CHCl<sub>3</sub>)

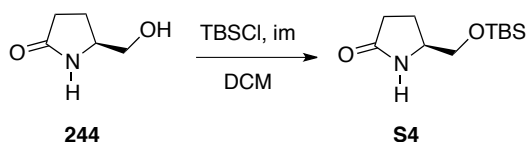
<sup>1</sup>H NMR (300 MHz, CDCl<sub>3</sub>)  $\delta$  [ppm] = 7.47 (s, 1H, NH), 4.44 (s, 1H, OH), 3.78 (s, 1H, H-4), 3.66 (d, *J* = 11.4, 1H, H-5), 3.45 (dd, *J* = 11.5, 6.7, 1H, H-5), 2.40 – 2.26 (m, 2H, 2x H-2), 2.15 (s, 1H, H-3), 1.77 (s, 1H, H-3).



<sup>13</sup>C NMR (75 MHz, CDCl<sub>3</sub>)  $\delta$  [ppm] = 179.47 (C-1), 65.75 (C-5), 56.56 (C-4), 30.32 (C-2), 22.60 (C-3).

IR (ATR):  $\tilde{\nu}$  = 3227.9 (v), 2905.8 (v), 1657.5 (s), 1462.8 (m), 1442.7 (m), 1420.7 (m), 1382.7 (m) cm<sup>-1</sup>

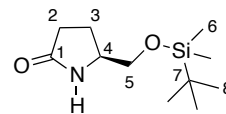
HRMS (EI), <i>m/z</i>	calc. for [M] <sup>+</sup> C <sub>5</sub> H <sub>9</sub> NO <sub>2</sub> :	115.0633
	found [M] <sup>+</sup> :	115.0638



**(S)-5-(((tert-butyldimethylsilyl)oxy)methyl)pyrrolidin-2-one (S)-5-(hydroxymethyl)pyrrolidin-2-one (S4):** Glutaminol **244** (320 mg, 2.78 mmol), imidazole (956 mg, 13.9 mmol) and TBSCl (1323 mg, 8.34 mmol) were dissolved in DCM (10 mL) and stirred at room temperature over night. NH<sub>4</sub>Cl (aq. sat. 20 mL) was added and extracted with DCM (3x 20 mL). After pH adjustment to pH = 5, extraction was repeated. The combined organic layers were washed with brine (20 mL), dried over MgSO<sub>4</sub> and concentrated *in vacuo*. Column chromatography (EtOAc/ hexanes: 1/4 to 1/2) gave **S4** (535 mg, 2.33 mmol, 84 %).

$[\alpha]_D^{22} = +31.20^\circ$  ( $c$  1.6,  $\text{CHCl}_3$ )

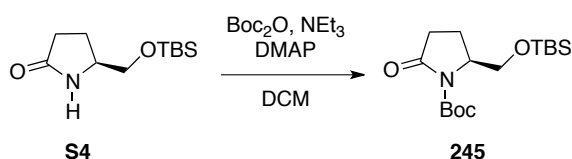
$^1\text{H}$  NMR (400 MHz,  $\text{CDCl}_3$ )  $\delta$  [ppm] = 5.98 (s, 1H, NH), 3.73 (ddd,  $J$  = 12.4, 7.8, 4.7, 1H, H-4), 3.61 (dd,  $J$  = 10.1, 4.0, 1H, H-5), 3.43 (dd,  $J$  = 10.1, 7.6, 1H, H-5), 2.42 – 2.25 (m, 2H, 2x H-2), 2.25 – 2.09 (m, 1H, H-3), 1.73 (dddd,  $J$  = 13.0, 9.3, 7.4, 5.4, 1H, H-3), 0.89 – 0.86 (m, 9H, 9x H-8), 0.06 – 0.03 (m, 6H, 6x H-6).



$^{13}\text{C}$  NMR (101 MHz,  $\text{CDCl}_3$ )  $\delta$  [ppm] = 177.95 (C-1), 66.88 (C-5), 55.76 (C-4), 29.78 (C-2), 25.79 (3x C-7), 22.72 (C-3), 18.18 (C-7), -5.46 (H-6), -5.47 (H-6).

IR (ATR):  $\tilde{\nu}$  = 3252.6 (v), 2953.6 (m), 2929.1 (m), 2886.2 (m), 2856.8 (m), 1648.4 (s)  $\text{cm}^{-1}$

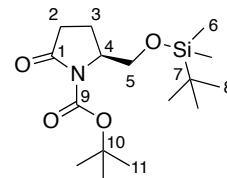
HRMS (EI), $m/z$	calc. for $[\text{M}+\text{H}]^+$ $\text{C}_{11}\text{H}_{23}\text{NO}_2\text{Si}$ :	230.1576
	found $[\text{M}+\text{H}]^+$ :	230.1567



**(S)-tert-butyl 2-(((tert-butyldimethylsilyl)oxy)methyl)-5-oxopyrrolidine-1-carboxylate (245)**: TBS protected amide **S4** (170 mg, 0.741 mmol) was dissolved in DCM (2.8 mL).  $\text{Boc}_2\text{O}$  (323 mg, 1.48 mmol),  $\text{NEt}_3$  (225 mg, 2.22 mmol) and DMAP (14.5 mg, 0.119 mmol) were added. The reaction mixture was stirred at ambient temperature for 4 hours. Citric acid (10 mL, 10 % aqueous solution) was added and the obtained mixture extracted with DCM (10 mL). Drying over  $\text{MgSO}_4$  and concentration *in vacuo* afforded **245** (173 mg, 0.526 mmol, 71 %).

$[\alpha]_D^{22} = -58.94$  ( $c$  5.6,  $\text{CHCl}_3$ )

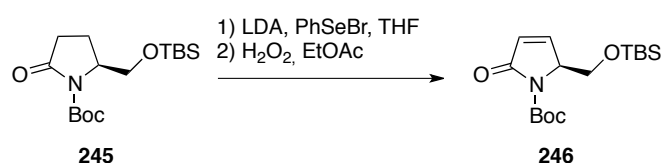
$^1\text{H}$  NMR (400 MHz,  $\text{CDCl}_3$ )  $\delta$  [ppm] = 4.17 – 4.06 (m, 1H, H-4), 3.87 (dd,  $J$  = 10.4, 3.9, 1H, H-5), 3.68 – 3.60 (m, 1H, H-5), 2.73 – 2.55 (m, 1H, H-2), 2.39 – 2.25 (m, 1H, H-2), 2.15 – 1.93 (m, 2H, 2x H-3), 1.48 (s, 9H, 9x H-11), 0.89 – 0.79 (m, 9H, 9x H-8), 0.04 – -0.06 (m, 6H, 6x H-6).



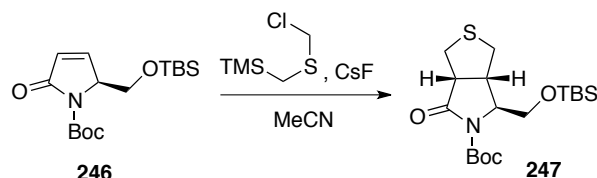
$^{13}\text{C}$  NMR (101 MHz,  $\text{CDCl}_3$ )  $\delta$  [ppm] = 174.90 (C-1), 149.99 (C-9), 82.61 (C-10), 64.26 (C-5), 58.85 (C-4), 32.31 (C-2), 28.03 (3x C-11), 25.77 (3x C-8), 21.08 (C-3), 18.13 (C-7), -5.60 (C-6), -5.64 (C-6).

IR (ATR):  $\tilde{\nu}$  = 2955.4 (m), 2930.6 (m), 2885.7 (m), 2858.0 (m), 1789.1 (s), 1751.0 (s), 1709.3 (s)  $\text{cm}^{-1}$

HRMS (EI), $m/z$	calc. for $[\text{M}]^{++}\text{C}_{16}\text{H}_{31}\text{NO}_4\text{Si}$ :	329.2022
	found $[\text{M}]^{++}$ :	not found



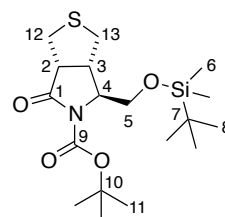
**(S)-tert-butyl 2-(((tert-butyldimethylsilyloxy)methyl)-5-oxo-2,5-dihydro-1H-pyrrole-1-carboxylate (246):** HMDS (108 mg, 0.668 mmol) was dissolved in THF (1 mL), cooled to  $-78\text{ }^\circ\text{C}$  and *n*-BuLi (1.3 M solution in hexanes 50  $\mu\text{L}$ , 0.668 mmol) was added. After 5 minutes the mixture was warmed to  $0\text{ }^\circ\text{C}$  and stirred at room temperature for 30 minutes. After re-cooling to  $-78\text{ }^\circ\text{C}$  a solution of **245** (100 mg, 0.303 mmol) in THF (1 mL) was added. A solution of phenylselenenyl bromide (128 mg, 0.546 mmol) was added after 40 minutes and the resulting mixture was stirred at  $-78\text{ }^\circ\text{C}$  for two hours.  $\text{NH}_4\text{Cl}$  (aq. sat. 3 mL) and  $\text{Et}_2\text{O}$  (5 mL) were added and the reaction mixture warmed to ambient temperature. The organic layer was washed  $\text{NH}_4\text{Cl}$  (aq. sat.  $2 \times 3\text{ mL}$ ) and brine (3 mL) then dried over  $\text{Na}_2\text{SO}_4$ . The crude product was re-dissolved in EtOAc (1 mL)  $\text{H}_2\text{O}_2$  was added (30%, 0.28 mL) and the resulting mixture was stirred at ambient temperature for 40 minutes. The mixture was then diluted with EtOAc and washed with  $\text{NaHCO}_3$  until the aqueous phase remained colourless. The organic layer was washed with brine, dried over  $\text{MgSO}_4$  and concentrated *in vacuo*. Column chromatography (EtOAc/hexanes = 1/2) gave **246**, which was directly subjected to subsequent reaction conditions.



**(3a*S*,4*S*,6a*R*)-tert-butyl 4-(((tert-butyl)dimethylsilyl)oxy)methyl)-6-oxotetrahydro-1*H*-thieno[3,4-*c*]pyrrole-5(3*H*)-carboxylate (247)**: The substrate was dissolved in acetonitrile (5 mL), 193 (100  $\mu$ L, 118 mg, 0.702 mmol) and CsF (129 mg, 0.842 mmol) were added and the resulting mixture stirred vigorously over night. Addition of NaHCO<sub>3</sub> (aq. sat. 10 mL) and extraction with EtOAc (3x 10 mL) gave a complex product mixture. Column chromatography (EtOAc/hexanes = 1/4) and preparative TLC (EtOAc/hexanes = 1/2) gave **247** (5 mg, 0.013 mmol, 4% over three steps) of the desired product.

$[\alpha]_D^{22} = -69.09$  (*c* 5.5 CHCl<sub>3</sub>)

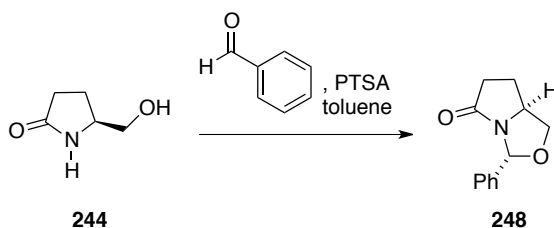
<sup>1</sup>H NMR (400 MHz, CDCl<sub>3</sub>)  $\delta$  [ppm] = 3.97 – 3.90 (m, 2H, H-4 and H-5), 3.74 (d, *J* = 8.6, 1H, H-5), 3.49 (m, 2H, H-12 and H-13), 3.29 (dd, *J* = 11.9, 2.4, 1H, H-12), 3.09 (m, 2H, H-12 and H-13), 2.90 (dd, *J* = 14.8, 7.3, 1H, H-2), 2.71 (dd, *J* = 11.8, 6.8, 1H, H-4), 1.53 (s, 9H, 9x H-11), 0.88 – 0.85 (m, 9H, 9x H-8), 0.03 (s, 3H, 3x H-6), 0.03 (s, 3H, 3x H-6).



<sup>13</sup>C NMR (101 MHz, CDCl<sub>3</sub>)  $\delta$  [ppm] = 174.78 (C-1), 149.80 (C-9), 83.25 (C-10), 66.16 (C-5), 63.46 (C-4), 52.16 (C-2), 43.51 (C-3), 38.58 (C-13), 34.69 (C-12), 28.06 (3x C-11), 25.80 (3x C-8), 18.15 (C-7), -5.53 (C-6), -5.56 (C-6).

IR (ATR):  $\tilde{\nu}$  = 3350.2 (w), 2954.0 (m), 2856.9 (m), 1929.1 (m), 1782.6 (m), 1747.3 (m), 1712.8 (s), 1471.6 (w), 1391.8 (w), 1365.9 (m), 1305.4 (s), 1252.9 (s), 1153.1 (s) cm<sup>-1</sup>

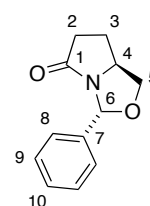
HRMS (EI), <i>m/z</i>	calc. for [M] <sup>++</sup> C <sub>18</sub> H <sub>33</sub> NO <sub>4</sub> SSi:	387.1900
	found [M] <sup>++</sup> :	387.1892



**(3R,7aS)-3-phenyltetrahydropyrrolo[1,2-c]oxazol-5(3H)-one (248):**<sup>[9]</sup> Glutaminol **244** (11.0 g, 95.5 mmol) was dissolved in toluene (90 mL). Freshly distilled benzaldehyde (13.3 g, 135 mmol) and *p*-TsOH (345 mg, 1.82 mmol) were added and the obtained mixture refluxed for 16 hours, in a DEAN–STARK apparatus. The obtained yellow solution was cooled to ambient temperature and washed with NaHCO<sub>3</sub> (aq. 5%, 10mL), Na<sub>2</sub>SO<sub>3</sub> (aq. sat. 2x 10 mL), and brine (10 mL), dried over Na<sub>2</sub>SO<sub>4</sub>, filtered and concentrated *in vacuo*. The crude oil was chromatographed (EtOAc/hexanes 1/2 to 2/1) affording **248** (9.1 g, 44.6 mmol, 47% yield) as colourless crystals.

$$[\alpha]_D^{25} = +232.4 \text{ (} c \text{ 4, CHCl}_3 \text{)}$$

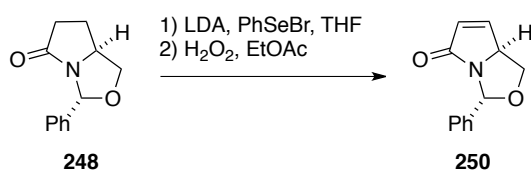
<sup>1</sup>H NMR (300 MHz, CDCl<sub>3</sub>)  $\delta$  [ppm] = 7.50 – 7.29 (m, 5H, 2x H-8, 2x H-9, H-10), 6.35 (s, 1H, H-6), 4.29 – 4.09 (m, 2H, H-4, H-5), 3.50 (t, *J* = 7.9, 1H, H-5), 2.92 – 2.75 (m, 1H, H-2), 2.57 (ddd, *J* = 17.3, 10.0, 3.8, 1H, H-2), 2.47 – 2.32 (m, 1H, H-3), 2.04 – 1.87 (m, 1H, H-3).



<sup>13</sup>C NMR (75 MHz, CDCl<sub>3</sub>)  $\delta$  [ppm] = 178.07 (C-1), 138.83 (C-7), 128.52 (C-10), 128.41 (2x C-8 or 2x C-9), 125.92 (2x C-8 or 2x C-9), 87.09 (C-5), 71.64 (C-5), 58.79 (C-4), 33.41 (C-2), 23.09 (C-1).

IR (ATR):  $\tilde{\nu}$  = 3032.8 (s), 2943.7 (s), 2879.5 (s), 1696.6 (l), 1493.9 (s), 1451.7 (s), 1375.0 (m), 1348.8 (m), 1258.8 (m), 1219.1 (m) cm<sup>-1</sup>

HRMS (EI), <i>m/z</i>	calc. for [M–H] <sup>++</sup> C <sub>12</sub> H <sub>12</sub> NO <sub>2</sub> :	202.0863
	found [M–H] <sup>++</sup> :	202.0864

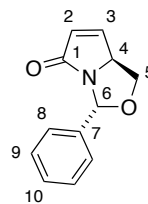


**(3R,7aS)-3-phenyl-1,7a-dihydropyrrolo[1,2-c]oxazol-5(3H)-one (250):**<sup>[9]</sup> LDA was prepared by treatment of DIPA (7.6 mL, 53.7 mmol) in THF (18 mL) with *n*-BuLi (2.8 M

solution in hexanes, 17.6 mL, 49.4 mmol) at 0 °C. A solution of protected glutaminol **248** (9.10 g, 44.8 mmol) in THF (60 mL) was added at -78 °C. After 30 minutes, a solution of phenylselenenyl bromide (10.9 g, 44.8 mmol) in THF (50 mL) was added in one portion and the resulting mixture was stirred at -78 °C for 40 minutes. Then, the cold mixture was poured into HCl (1 M, 100 mL) and extracted with Et<sub>2</sub>O (ca. 400 mL). The organic layer was washed with sat. NaHCO<sub>3</sub> (40 mL) and brine (40 mL), dried over MgSO<sub>2</sub>, filtered and concentrated *in vacuo*. The obtained yellow oil was dissolved in EtOAc (15 mL) and cooled to 0 °C. An aqueous solution of H<sub>2</sub>O<sub>2</sub> (30%, 7 mL) was added and the mixture stirred for 5 minutes. After dilution with EtOAc (ca. 100 mL) the mixture was washed with NaHCO<sub>3</sub> (aq. sat. 4x 40 mL) and brine (40 mL). The organic layer was dried over MgSO<sub>4</sub> and concentrated *in vacuo*. Column chromatography (EtOAc/ hexanes = 1/4 to 2/1) yielded **250** as a white, crystalline solid (6.85 g, 34.0 mmol, 76%).

$[\alpha]_D^{25} = +204^\circ$  (c 6, CHCl<sub>3</sub>)

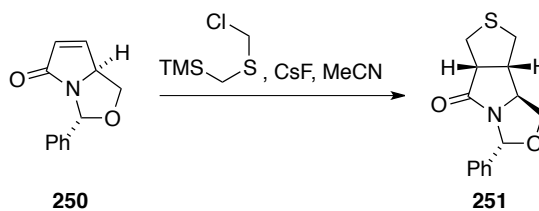
<sup>1</sup>H NMR (600 MHz, CDCl<sub>3</sub>)  $\delta$  [ppm] = 7.55 – 7.51 (m, 2H, 2x H-8 or 2x H-9), 7.42 – 7.31 (m, 3H, 2x H-8 or 2x H-9 and H-10), 7.26 (dd,  $J = 5.79, 1.95$  Hz, 1H, H-2), 6.19 (s, 1H, H-6), 6.15 (dd,  $J = 5.79, 1.56$  Hz, 1H, H-3), 4.60 (dddd,  $J = 8.61, 6.90, 1.98, 1.98, 0.45$  Hz, 1H, H-4), 4.25 (ddd,  $J = 8.13, 6.93, 0.51$  Hz, 1H, H-5), 3.42 (dd,  $J = 8.31, 8.31$  Hz, 1H, H-5).



<sup>13</sup>C NMR (75 MHz, CDCl<sub>3</sub>)  $\delta$  [ppm] = 176.93 (C-1), 147.82 (C-3), 138.65 (C-7), 129.25 (C-2), 128.66 (2x C-8 or 2x C-9 or C-10), 128.48 (2x C-8 or 2x C-9 or C-10), 126.21 (2x C-8 or 2x C-9 or C-10), 87.47 (C-6), 68.13 (C-5), 65.16 (C-4).

IR (ATR):  $\tilde{\nu} = 3032.8$  (w), 3033.0 (w), 3000.1 (w), 2947.5 (w), 2881.4 (w), 1683.3 (s), 1493.1 (w), 1471.8 (w), 1454.9 (w), 1375.8 (m), 1350.7 (m), 1330.0 (s), 1290.2 (m) cm<sup>-1</sup>

HRMS (EI), $m/z$	calc. for [M-H] <sup>+</sup> C <sub>12</sub> H <sub>10</sub> NO <sub>2</sub> :	200.0706
	found [M-H] <sup>+</sup> :	200.0698

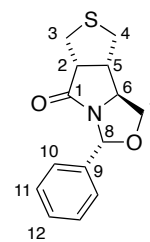


**(3*R*,5*aR*,8*aS*,8*bS*)-3-phenylhexahydrothieno[3',4':3,4]pyrrolo[1,2-*c*]oxazol-5(3*H*)-one**

**(251)**: Starting enone **250** (1.00 g, 4.97 mmol) was dissolved in degassed MeCN (40 mL), reagent **193** (1.40 g, 8.3 mmol) and CsF (2.27 g, 14.9 mmol) were added and the resulting mixture stirred vigorously under an argon atmosphere for three days. The mixture was then partitioned between H<sub>2</sub>O (30 mL) and EtOAc (60 mL), the organic layer was washed with brine (10 mL), dried over MgSO<sub>4</sub> and concentrated *in vacuo*. Column chromatography (EtOAc/ hexanes = 1/10 to 5/1) gave **251** as a white, crystalline solid (1.20 g, 4.59 mmol, 92%).

$[\alpha]_D^{22} = +96.32$  (*c* 19, CHCl<sub>3</sub>)

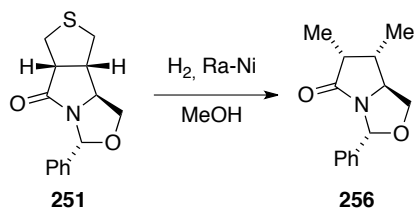
<sup>1</sup>H NMR (600 MHz, CDCl<sub>3</sub>)  $\delta$  [ppm] = 7.44 – 7.42 (m, 2H, 2x H-10 or 2x H-11), 7.38 – 7.35 (m, 2H, 2x H-10 or 2x H-11), 7.34 – 7.31 (m, 1H, H-12), 6.31 (s, 1H, H-8), 4.29 (dd, *J* = 8.4, 6.4 Hz, 1H, H-7), 3.78 (ddd, *J* = 9.2, 6.4, 3.0 Hz, 1H H-6), 3.52 (dd, *J* = 9.0, 8.1 Hz, 1H, H-7), 3.44 (dt, *J* = 8.6, 2.5 Hz, 1H, H-2), 3.24 (dd, *J* = 12.3, 2.2 Hz, 1H, H-3), 3.11 – 3.02 (m, 3H, H-3, H-5), 2.83 (d, *J* = 11.8 Hz, 1H, H-5).



<sup>13</sup>C NMR (151 MHz, CDCl<sub>3</sub>)  $\delta$  [ppm] = 178.22 (C-1), 138.37 (C-9), 128.46 (2x C-10 or 2x C-11, C-12), 125.90 (2x C-10 or 2x C-11), 87.51 (C-8), 71.04 (C-7), 65.14 (C-6), 54.28 (C-2), 44.59 (C-4), 39.85 (C-5), 36.55 (C-3).

IR (ATR):  $\tilde{\nu}$  = 2956.2 (m), 2929.3 (m), 2869.5 (w), 1723.5 (s), 1702.0 (m), 1686.1 (m), 1456.4 (w), 1378.0 (w), 1350.9 (m), 1270.4 (s) cm<sup>-1</sup>

HRMS (EI), <i>m/z</i>	calc. for [M-H] <sup>+</sup> C <sub>14</sub> H <sub>14</sub> NO <sub>2</sub> S:	260.0740
	found [M-H] <sup>+</sup> :	260.0739

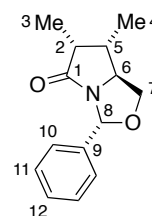


**(3*R*,6*R*,7*S*,7*aS*)-6,7-dimethyl-3-phenyltetrahydropyrrolo[1,2-*c*]oxazol-5(3*H*)-one (256):**

RANEY nickel (ca. 100 mg) was dispensed in MeOH (5 mL), tricycle **251** (100 mg, 0.38 mmol) was added and the system purged with hydrogen (1 atm). The mix was stirred at ambient temperature for 6 hours, filtered over celite and concentrated *in vacuo* giving **256** (83 mg, 0.36 mmol, 94 %)

$[\alpha]_D^{20} = +188.7$  (*c* 3, CHCl<sub>3</sub>)

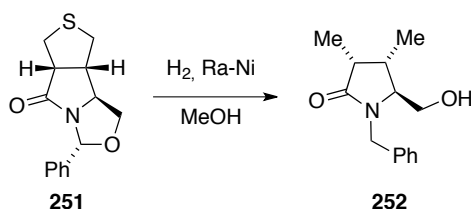
<sup>1</sup>H NMR (400 MHz, C<sub>6</sub>D<sub>6</sub>)  $\delta$  [ppm] = 7.56 – 7.50 (m, 2H, 2x H-10 or 2x H-11), 7.15 – 7.09 (m, 2H, 2x H-10 or 2x H-11), 7.07 – 7.00 (m, 1H, H-12), 6.54 (s, 1H, H-8), 3.67 – 3.53 (m, 1H, H-7), 3.08 – 2.94 (m, 2H, H-7 and H-6), 2.31 – 2.19 (m, 1H, H-2), 1.62 – 1.46 (m, 1H, H-4), 0.89 (d, *J* = 7.5, 3H, 3x H-3), 0.39 (d, *J* = 7.1, 3H, 3x H-5).



<sup>13</sup>C NMR (101 MHz, C<sub>6</sub>D<sub>6</sub>)  $\delta$  [ppm] = 180.58 (C-1), 139.55 (C-9), 128.18 (2x C-10 or 2x C-11), 128.09 (C-12), 126.08 (2x C-10 or 2x C-11), 87.22 (C-8), 69.83 (C-7), 63.65 (C-6), 44.06 (C-2), 36.83 (C-4), 13.12 (C-5), 11.28 (C-3).

IR (ATR):  $\tilde{\nu}$  = 2968.6 (m), 2934.7 (m), 2877.4 (m), 1700.0 (s), 1494.6 (w), 1450.8 (m), 1391.3 (m), 1348.9 (s) cm<sup>-1</sup>

HRMS (EI), <i>m/z</i>	calc. for [M-H] <sup>++</sup> C <sub>14</sub> H <sub>16</sub> NO <sub>2</sub> :	230.1176
	found [M-H] <sup>++</sup> :	230.1178



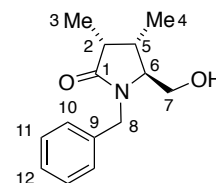
**(3*R*,4*S*,5*S*)-1-benzyl-5-(hydroxymethyl)-3,4-dimethylpyrrolidin-2-one (252):**

RANEY nickel (ca. 100 mg) was dispensed in MeOH (5 mL), tricycle **251** (100 mg, 0.38 mmol) was added and the system purged with hydrogen (5 atm). The mix was stirred at ambient

temperature for 4 hours, filtered over celite and concentrated *in vacuo* giving a product mixture. Column chromatography (EtOAc/ hexanes = 1/2) gave **252** as main product (70 mg, 0.30 mmol, 79 %)

$[\alpha]_D^{20} = +39.53$  (*c* 0.85, CH<sub>2</sub>Cl<sub>2</sub>)

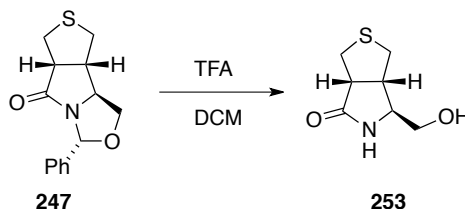
<sup>1</sup>H NMR (300 MHz, CDCl<sub>3</sub>)  $\delta$  [ppm] = 7.38 – 7.23 (m, 5H, H-12, 2x H-10 and 2x H-11), 4.92 (d, *J* = 14.9, 1H, H-8), 4.21 (d, *J* = 14.9, 1H, H-8), 3.79 (d, *J* = 12.1, 1H, H-7), 3.60 (s, 1H, H-7), 2.99 (q, *J* = 3.6, 1H, H-6), 2.85 – 2.68 (m, 1H, H-2), 2.49 – 2.36 (m, 1H, H-5), 2.30 (s, 1H, OH), 1.11 (t, *J* = 8.4, 3H, 3x H-3), 0.92 (d, *J* = 7.2, 3H, 3x H-4).



<sup>13</sup>C NMR (151 MHz, CDCl<sub>3</sub>)  $\delta$  [ppm] = 178.16 (C-1), 137.01 (C-9), 128.75 (2x C-10 or 2 C-11), 127.97 (2x C-10 or 2x C-11), 127.59 (C-12), 64.75 (C-6), 61.35 (C-7), 44.81 (C-8), 39.48 (C-2), 32.70 (C-5), 14.33 (C-4), 10.81 (C-2).

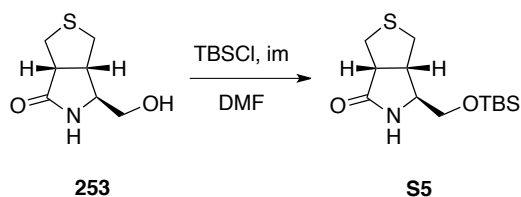
IR (ATR):  $\tilde{\nu}$  = 3375.5 (v), 2966.5 (m), 2928.8 (m), 2873.7 (m), 2360.6 (w), 1658.8 (s) cm<sup>-1</sup>

HRMS (EI), <i>m/z</i>	calc. for [M] <sup>++</sup> C <sub>14</sub> H <sub>19</sub> NO <sub>2</sub> :	233.1416
	found [M] <sup>++</sup> :	233.1407



**(3a*R*,6*S*,6a*S*)-6-(hydroxymethyl)tetrahydro-1*H*-thieno[3,4-*c*]pyrrol-4(5*H*)-one (253):**

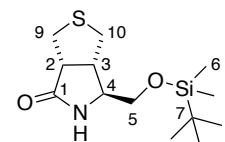
Tricycle **247** (625 mg, 2.39 mmol) was dissolved in DCM (75 mL) and TFA (3 mL, 4.61 g, 40.4 mmol) was added and the resulting solution stirred for 16 hours at ambient temperature. The resulting solution was concentrated *in vacuo*, re-dissolved in H<sub>2</sub>O (4 mL), toluene (10 mL) was added and the mixture concentrated *in vacuo*. This protocol was repeated three times, the crude product subjected to subsequent TBS- protection.



**(3a*R*,6*S*,6a*S*)-6-(((*tert*-butyldimethylsilyl)oxy)methyl)tetrahydro-1*H*-thieno[3,4-*c*]pyrrol-4(5*H*)-one (S5)**: Amidol **253** (270 mg, 1.54 mmol) was dissolved in DMF (2.2 mL). Imidazole (347 mg, 5.09 mmol) and TBSCl (279 mg, 1.85 mmol) were added and the resulting mixture stirred at ambient temperature for 24 hours. The obtained mixture was partitioned between EtOAc (20 mL) and H<sub>2</sub>O (10 mL), the aqueous phase was washed with EtOAc (3x 10 mL), combined organic layers were washed with NaHCO<sub>3</sub> (aq. sat. 10 mL), dried over MgSO<sub>4</sub> and concentrated *in vacuo*. Column chromatography (EtOAc/ hexanes = 1/1) yielded **S5** (350 mg, 1.22 mmol, 51% over two steps) as a colourless oil.

$[\alpha]_{\text{D}}^{25} = +3.69$  (*c* 6, CHCl<sub>3</sub>)

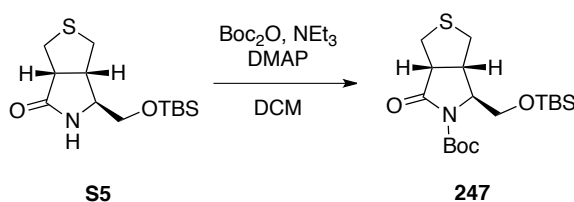
<sup>1</sup>H NMR (300 MHz, CDCl<sub>3</sub>)  $\delta$  [ppm] = 5.86 (s, 1H, NH), 3.66 (dd, *J* = 10.0, 4.4, 1H, H-5), 3.56 (dd, *J* = 10.0, 6.8, 1H, H-5), 3.47 – 3.40 (m, 1H, H-4), 3.29 – 3.18 (m, 2H, H-2 and H-10), 3.11 – 2.97 (m, 2H, H-9 and H-10), 2.90 – 2.80 (m, 1H, H-3), 2.77 (dd, *J* = 11.7, 3.3, 1H, H-9), 0.93 – 0.88 (m, 9H, 9x H-8), 0.10 – 0.06 (m, 6H, 6x H-6).



<sup>13</sup>C NMR (600 MHz, CDCl<sub>3</sub>)  $\delta$  [ppm] = 177.81 (C-1), 66.47 (C-5), 61.35 (C-4), 49.94 (C-2), 45.05 (C-3), 39.70 (C-10), 35.50 (C-9), 25.80 (3x C-8), 18.18 (C-7), –5.43 (C-6), –5.44 (C-6).

IR (ATR):  $\tilde{\nu}$  = 3260.1 (v), 2951.5 (m), 2926.3 (m), 2854.9 (m), 1696.5 (s), 1653.8 (s), 1469.7 (m), 1461.5 (m), 1448.8 (m), 1432.1 (m) cm<sup>-1</sup>

HRMS (EI), <i>m/z</i>	calc. for [M–H] <sup>+</sup> C <sub>13</sub> H <sub>25</sub> NO <sub>2</sub> SSi:	286.1292
	found [M–H] <sup>+</sup> :	286.1292

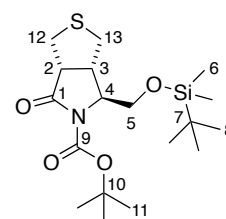


**(3a*S*,4*S*,6a*R*)-*tert*-butyl 4-(((*tert*-butyldimethylsilyl)oxy)methyl)-6-oxotetrahydro-1*H*-thieno[3,4-*c*]pyrrole-5(3*H*)-carboxylate (247)**: TBS protected intermediate **S5** (200 mg,

0.696 mmol) was dissolved in DCM (3 mL) and  $\text{NEt}_3$  (0.3 mL, 218 mg, 2.16 mmol), DMAP (15 mg, 0.123 mmol) and  $\text{Boc}_2\text{O}$  (304 mg, 1.39 mmol) were added. The mixture was stirred at ambient temperature for 4 hours. Citric acid (aq. 10 %, 10 mL) and EtOAc (20 mL) were added. The organic phase was washed with  $\text{NaHCO}_3$  (aq. sat. 10 mL), and brine (10 mL), dried over  $\text{MgSO}_4$  and concentrated *in vacuo*. Column chromatography (EtOAc/ hexanes: 1/4) afforded **247** as a colourless solid (194 mg, 0.500 mmol, 72 %).

$[\alpha]_D^{22} = -69.09$  (*c* 5,5  $\text{CHCl}_3$ )

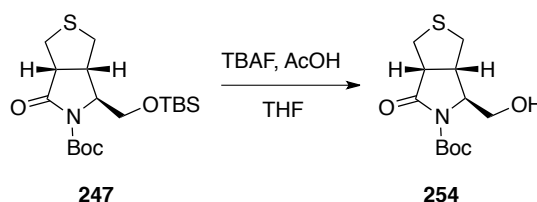
$^1\text{H}$  NMR (400 MHz,  $\text{CDCl}_3$ )  $\delta$  [ppm] = 3.97 – 3.90 (m, 2H, H-4 and H-5), 3.74 (d,  $J = 8.6$ , 1H, H-5), 3.49 (m, 2H, H-12 and H-13), 3.29 (dd,  $J = 11.9$ , 2.4, 1H, H-12), 3.09 (m, 2H, H-12 and H-13), 2.90 (dd,  $J = 14.8$ , 7.3, 1H, H-2), 2.71 (dd,  $J = 11.8$ , 6.8, 1H, H-4), 1.53 (s, 9H, 9x H-11), 0.88 – 0.85 (m, 9H, 9x H-8), 0.03 (s, 3H, 3x H-6), 0.03 (s, 3H, 3x H-6).



$^{13}\text{C}$  NMR (101 MHz,  $\text{CDCl}_3$ )  $\delta$  [ppm] = 174.78 (C-1), 149.80 (C-9), 83.25 (C-10), 66.16 (C-5), 63.46 (C-4), 52.16 (C-2), 43.51 (C-3), 38.58 (C-13), 34.69 (C-12), 28.06 (3x C-11), 25.80 (3x C-8), 18.15 (C-7), -5.53 (C-6), -5.56 (C-6).

IR (ATR):  $\tilde{\nu} = 3350.2$  (w), 2954.0 (m), 2856.9 (m), 1929.1 (m), 1782.6 (m), 1747.3 (m), 1712.8 (s), 1471.6 (w), 1391.8 (w), 1365.9 (m), 1305.4 (s), 1252.9 (s), 1153.1 (s)  $\text{cm}^{-1}$

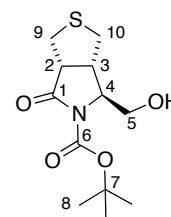
HRMS (EI), $m/z$	calc. for $[\text{M}]^+ \text{C}_{18}\text{H}_{33}\text{NO}_4\text{SSi}$ :	387.1900
	found $[\text{M}]^+$ :	387.1892



**(3a*S*,4*S*,6a*R*)-tert-butyl 4-(hydroxymethyl)-6-oxotetrahydro-1*H*-thieno[3,4-*c*]pyrrole-5(3*H*)-carboxylate (254)**: Fully protected intermediate **247** (99 mg, 0.254 mmol), was dissolved in THF (0.3 mL) and acetic acid (20  $\mu\text{L}$ ) was added. TBAF (1 M solution in THF, 0.28 mL, 0.28 mmol) was added dropwise and the resulting solution stirred at ambient temperature for 2 hours. EtOAc (20 mL) was added and the organic layer extracted with  $\text{NaHCO}_3$  (aq. sat. 10 mL). The organic layer was dried over  $\text{Na}_2\text{SO}_4$  and subjected to a short column (EtOAc/ hexanes = 1/2), affording **254** (62 mg, 0.227 mmol, 89 %) as white solid.

$[\alpha]_D^{25} = -93.60$  ( $c$  1,  $\text{CHCl}_3$ )

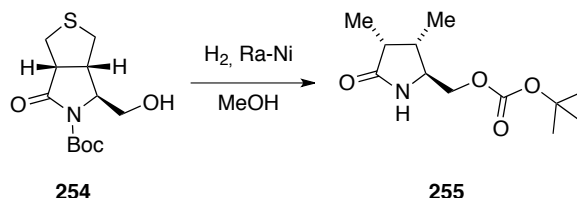
$^1\text{H NMR}$  (600 MHz,  $\text{CDCl}_3$ )  $\delta$  [ppm] = 4.01 (td,  $J = 3.7, 1.6$ , 1H, H-4), 3.92 (dd,  $J = 11.3, 3.9$ , 1H, H-5), 3.80 (dd,  $J = 11.3, 3.5$ , 1H, H-5), 3.51 (td,  $J = 8.3, 2.3$ , 1H, H-2), 3.32 (dd,  $J = 11.9, 2.2$ , 1H, H-9), 3.16 (dd,  $J = 11.8, 7.7$ , 1H, H-10), 3.07 (dd,  $J = 11.8, 8.2$ , 1H, H-3), 2.91 (td,  $J = 8.0, 1.5$ , 1H, H-10), 2.74 (dd,  $J = 11.9, 6.3$ , 1H, H-9), 2.01 (s, 1H, OH), 1.54 (d,  $J = 2.3$ , 9H, 9x H-8).



$^{13}\text{C NMR}$  (101 MHz,  $\text{CDCl}_3$ )  $\delta$  [ppm] =  $^{13}\text{C NMR}$  (101 MHz,  $\text{cdcl}_3$ )  $\delta = 174.64$  (C-1), 150.28 (C-6), 83.84 (C-7), 64.20 (C-5), 63.59 (C-4), 51.87 (C-2), 43.08 (C-3), 38.50 (C-10), 34.61 (C-9), 28.02 (3x C-8).

IR (ATR):  $\tilde{\nu} = 3439.6$  (m), 3420.2 (m), 2982.0 (w), 2952.2 (w), 2925.9 (w), 2870.3 (w), 1778.5 (vs), 1706.2 (m)  $\text{cm}^{-1}$

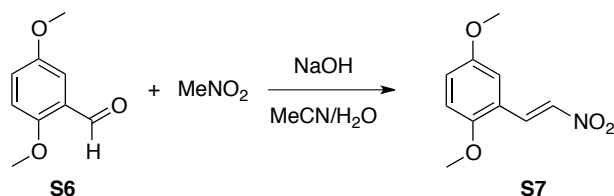
HRMS (EI), $m/z$	calc. for $[\text{M}-\text{H}]^{++}$ $\text{C}_{12}\text{H}_{18}\text{NO}_4\text{S}$ :	272.0951
	found $[\text{M}-\text{H}]^{++}$ :	272.0945



***tert*-butyl (((2*S*,3*S*,4*R*)-3,4-dimethyl-5-oxopyrrolidin-2-yl)methyl) carbonate (255):**

RANEY-nickel (aqueous suspension, ca. 200 mg) was washed with MeOH and decanted (5x 10 mL). A solution of bicycle **254** (70 mg, 0.256 mmol) in MeOH (5 mL) was added to the slurry and the system purged with hydrogen 5 times. After 10 hours the system was purged with nitrogen, filtered over celite and concentrated *in vacuo*, yielding **255** as colourless oil (58 mg, 0.238 mmol, 93 %).

## VQDA



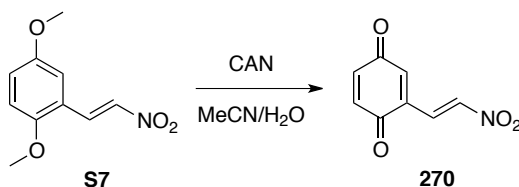
**(E)-1,4-dimethoxy-2-(2-nitrovinyl)benzene (S7)**: A solution of 2,5-dimethoxybenzaldehyde (**S6**, 33.2 g, 200 mmol) and MeNO<sub>2</sub> (12.2 g, 200 mmol) in MeCN (15 mL) was cooled to 5°C internal temperature in an ice-bath. A solution of NaOH (8.80 g, 220 mmol) in H<sub>2</sub>O (65 mL) was added dropwise at such rate, that the internal temperature did not exceed 20 °C. After stirring for 5 minutes, the reaction mixture was slowly poured into 5N HCl (500 mL). The formed precipitate was washed with H<sub>2</sub>O (100 mL), filtered off and dissolved in acetone, dried over Na<sub>2</sub>SO<sub>4</sub> and concentrated *in vacuo*. Recrystallization from *i*-PrOH/H<sub>2</sub>O yielded **S7** (26 g, 124 mmol, 62%) as intensively coloured orange needles.

<sup>1</sup>H NMR (300 MHz, CDCl<sub>3</sub>) δ [ppm] = 8.10 (d, *J* = 6.9, 1H), 7.84 (d, *J* = 6.9, 1H), 7.00 (dd, *J* = 4.7, 1.7, 1H), 6.95 (d, *J* = 1.5, 1H), 6.89 (d, *J* = 4.4, 1H), 3.89 (s, 3H), 3.79 (s, 3H).

<sup>13</sup>C NMR 75 MHz, CDCl<sub>3</sub>) δ [ppm] = 153.9, 151.5, 138.5, 135.22, 119.5, 119.1, 116.3, 112.4, 56.0, 55.8.

IR (ATR):  $\tilde{\nu}$  = 3104 (w), 2839 (vw), 1618 (m), 1489 (s), 1422 (m), 1348 (m), 1295 (m), 1250 (s), 1220 (vs), 1184 (s) cm<sup>-1</sup>

HRMS (EI), <i>m/z</i>	calc. for [M] <sup>+</sup> C <sub>10</sub> H <sub>11</sub> NO <sub>4</sub> :	209.0684
	found [M] <sup>+</sup> :	209.0683



**(E)-2-(2-nitrovinyl)cyclohexa-2,5-diene-1,4-dione (270)**: A solution of CAN (28.8 g, 52.3 mmol) in MeCN/H<sub>2</sub>O 3:1 (50 mL) was poured into a solution of compound **S7** (5 g, 23.9 mmol) in CH<sub>3</sub>CN (400 mL) under vigorous stirring. After 5 minutes brine (25 mL) was added and the mixture extracted with MeCN (2 x 25 mL). The organic phases were combined

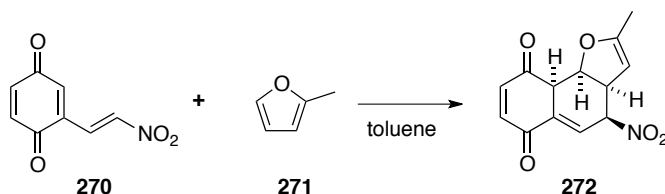
and concentrated *in vacuo* (bath temperature below 30 °C, no complete removal of solvent). The resulting slurry was partitioned between CHCl<sub>3</sub> (125 mL) and H<sub>2</sub>O (50 mL) and the aqueous layer extracted with CHCl<sub>3</sub> (50 mL). Combined CHCl<sub>3</sub> fractions were washed with H<sub>2</sub>O (25 mL), dried over Na<sub>2</sub>SO<sub>4</sub> and all volatiles removed *in vacuo*. The resulting brown solid was recrystallization from THF/cyclohexane twice to yield vinyl quinone **270** (2.35 g, 13.1 mmol, 55 %) as yellow needles.

<sup>1</sup>H NMR (300 MHz, CDCl<sub>3</sub>) δ [ppm] = 8.13 (d, *J* = 13.7, 1H), 7.65 (dd, *J* = 13.7, 0.8, 1H), 7.00 (m, 1H) 6.95-6.87 (m, 2H)

<sup>13</sup>C NMR (75 MHz, CDCl<sub>3</sub>) δ [ppm] = 186.0, 184.8, 144.5, 137.9, 137.4, 136.8, 136.4, 130.1

IR (ATR):  $\tilde{\nu}$  = 3125 (m), 3065 (w), 2857 (vw), 1752 (vw), 1651 (s), 1575 (m), 1520 (vs), 1342 (vs), 1290 (s), 1208 (m), 1092 (m) cm<sup>-1</sup>

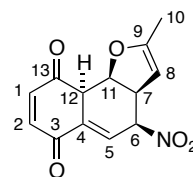
HRMS (EI), <i>m/z</i>	calc. for [M] <sup>++</sup> C <sub>6</sub> H <sub>5</sub> NO <sub>4</sub> :	179.0126
	found [M] <sup>++</sup> :	179.0221



**(3a*S*,4*S*,9a*R*,9b*S*)-2-methyl-4-nitro-3a,4-dihydronaphtho[1,2-*b*]furan-6,9(9a*H*,9b*H*)-**

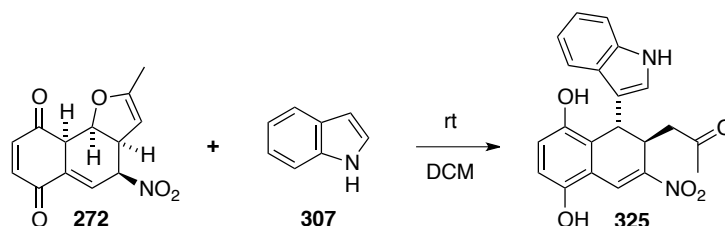
**dione (272):** Quinone **270** (0.50 g, 2.8 mmol) was suspended in toluene (5 mL) and 2-methylfuran (**271**, 0.46 g, 5.6 mmol) was added. After stirring for 16 hours at ambient temperature, a red particulate had formed. The reaction mixture was centrifuged at 4 °C and washed with dry hexane (3 mL). After another centrifugation step, the solvent was evaporated over a gentle stream of nitrogen and finally in high vacuum to yield cycloadduct **272** (0.46 g, 1.8 mmol, 63%) as a red solid.

<sup>1</sup>H NMR (300 MHz, CDCl<sub>3</sub>) δ [ppm] = 7.66 (td, *J* = 2.9, 1.0, 1H, H-5), 7.03 – 6.88 (m, 2H, H-1 and H-2), 5.66 (dd, *J* = 9.6, 3.4, 1H, H-6 or H-11), 4.98 – 4.90 (m, 1H, H-6 or H-11), 4.32 – 4.20 (m, 2H, H-8 and H-12), 3.28 (dd, *J* = 5.3, 3.1, 1H, H-7), 1.62 (t, *J* = 1.4, 3H, 3x H-10).



$^{13}\text{C}$  NMR (75 MHz,  $\text{CDCl}_3$ )  $\delta$  [ppm] = 192.62 (C-13), 181.84 (C-3), 160.19 (C-9), 142.54 (C-1 or C-2), 141.58 (C-1 or C-2), 133.60 (C-5), 131.00 (C-4), 92.93 (C-8), 82.85 (C-6 or C-11), 79.71 (C-6 or C-11), 48.14 (C-7), 47.55 (C-12), 13.11 (C-10).

HRMS (EI), $m/z$	calc. for $[\text{M}]^{++}$ $\text{C}_{13}\text{H}_{11}\text{NO}_5$ :	261.0633
	found $[\text{M}]^{++}$ :	261.0631



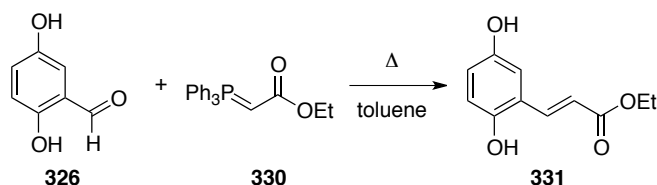
**1-((1*S*,2*R*)-5,8-dihydroxy-1-(1*H*-indol-3-yl)-3-nitro-1,2-dihydronaphthalen-2-yl)propan-2-one (325)**: Isoquinonemethide **272** (63 mg, 0.24 mmol) was suspended in DCM (1 mL) and indol (**307**, 56 mg, 0.48 mmol) was added. After stirring the reaction for 30 minutes, a red particulate formed. The reaction mixture was centrifuged at 4°C and washed with hexane (1 mL). After another centrifugation step, the solvent was evaporated over a gentle stream of nitrogen. After further drying under high vacuum product **325** (40 mg, 0.11 mmol, 44%) was obtained.

$^1\text{H}$  NMR (400 MHz, acetone  $d_6$ )  $\delta$  [ppm] = 9.82 (s, 1H), 8.82 (s, 1H), 8.35 – 8.30 (m, 2H), 7.93 (s, 1H), 7.37 – 7.26 (m, 1H), 7.14 – 7.05 (m, 2H), 6.97 – 6.79 (m, 3H), 6.34 (d,  $J$  = 1.6, 1H), 4.23 (d,  $J$  = 9.3, 1H), 2.69 (dd,  $J$  = 17.7, 2.8, 1H), 2.22 (d,  $J$  = 7.7, 3H).

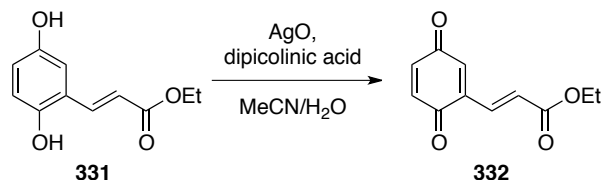
$^{13}\text{C}$  NMR (101 MHz, acetone  $d_6$ )  $\delta$  [ppm] = 206.18, 149.66, 148.17, 147.97, 137.06, 126.74, 126.48, 123.69, 122.53, 121.35, 121.12, 119.61, 118.67, 117.71, 115.68, 114.82, 111.29, 43.00, 35.05, 34.47.

IR (ATR):  $\tilde{\nu}$  = 3364 (b), 1685 (m), 1618 (m), 1482 (m), 1458 (m), 1356 (w), 1330 (m), 1309, (s), 1245 (vs), 1158 (w), 1100 (m)  $\text{cm}^{-1}$

HRMS (EI), $m/z$	calc. for $[\text{M}]^{++}$ $\text{C}_{21}\text{H}_{17}\text{N}_2\text{O}_5$ :	377.1134
	found $[\text{M}]^{++}$ :	377.1144



**Ethyl 3-(2,5-dihydroxyphenyl)acrylate (331):** 2,5-dihydroxybenzaldehyde (**326**, 6.63 g, 48.0 mmol) and phosphorane **330** (20.1 g, 57.6 mmol) were dissolved in toluene (250 mL) and heated to reflux for 3 h. After equilibration to ambient temperature, the reaction mixture was washed with brine (2x 100 mL). The organic fractions were combined and concentrated *in vacuo*. Column chromatography (EtOAc/ hexanes 1/6) furnished hydroquinone **331** (8.30 g, 40.0 mmol, 83%) as a mint green solid. As isomerization of this product on silica was observed, the product was used in subsequent conversion.



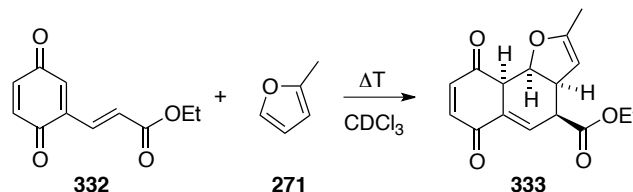
**(E)-ethyl 3-(3,6-dioxocyclohexa-1,4-dien-1-yl)acrylate (332):** To a solution of hydroquinone **331** (208 mg, 1.0 mmol) in MeCN/H<sub>2</sub>O 3/1 (24 mL), 2,6-pyridinedicarboxylic acid (418 mg, 2.5 mmol) was added. After sonication for 30 seconds silver(II) oxide (310 mg, 2.5 mmol) was added and the reaction mixture was sonicated for another 30 seconds upon which the colour changed from yellow to dark green. The reaction was complete after 5 minutes stirring at ambient temperature, subsequently diluted with EtOAc and filtered over a plug of celite. The organic layer was washed with NaHCO<sub>3</sub> (sat. aq. 4x 30mL), H<sub>2</sub>O (2x 30mL) and brine (3x 30 mL). The combined organic phases were dried over Na<sub>2</sub>SO<sub>4</sub>, filtered and concentrated under reduced pressure to receive the title compound **332** (185 mg, 0.9 mmol, 90%) as yellow solid.

<sup>1</sup>H NMR (200 MHz, CDCl<sub>3</sub>) δ [ppm] = 7.49 (dd, *J* = 16, *J* = 1, 1H), 6.86-6.85 (m, 1H), 6.80 (d, *J* = 16, 1H), 6.80-6.79 (m, 2H), 4.25 (q, *J* = 7, 2H), 1.31 (t, *J* = 7, 3H).

<sup>13</sup>C NMR (125 MHz, CDCl<sub>3</sub>) δ [ppm] = 187.4, 185.9, 165.8, 139.7, 137.2, 136.8, 135.4, 133.4, 128.1, 61.4, 14.4.

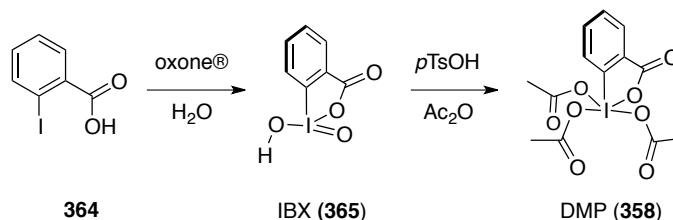
IR (ATR):  $\tilde{\nu}$  = 2360, (w), 2336 (w), 1738 (w), 1707 (m), 1654 (m), 1472 (w), 1367 (m), 1307 (w), 1265 (w), 1188 (s) cm<sup>-1</sup>

HRMS (EI), $m/z$	calc. for $[M]^{++}$ $C_{11}H_{10}O_4$ :	206.0579
	found $[M]^{++}$ :	206.0581



**(3a*S*,4*S*,9a*R*,9b*S*)-ethyl-2-methyl-6,9-dioxo-3a,4,6,9,9a,9b-hexahydronaphtho[1,2-*b*]furan-4-carboxylate (333)**: Quinone **332** (50 mg, 0.242 mmol) was dissolved in  $CDCl_3$  (3.5 mL) and 2-methylfuran (**271**, 0.131 mL, 1.45 mmol) was added. The reaction mixture was heated to reflux for 1h. Crude NMR analysis indicated partial conversion to envisaged DA adduct **333**. Longer reaction times, as well as any attempt to isolate the product lead to decomposition.

## DMP



**DMP (358)**: 2-iodobenzoic acid (100 g, 403 mmol) was added to a solution of oxone<sup>®</sup> ( $2 \cdot KHSO_5 \cdot KHSO_4 \cdot K_2SO_4$ ) (322 g, 524 mmol) in water (2 L) and stirred at 80 °C for 4 h. The suspension was cooled to 4 °C under slow stirring. The mixture was filtered and the white precipitate was washed with water (2x 100 mL) and acetone (2x 100 mL) and then dried under high vacuum to yield a colourless powder of IBX (**365**) (98 g, 87 %). IBX (**3**) (98 g, 350 mmol) was subsequently added to acetic anhydride (400 mL) and  $pTsOH \cdot H_2O$  (400 mg, 2.10 mmol) and stirred at 80 °C. After 2 h the clear solution was cooled to 4 °C and the white precipitate was filtered off, washed with ether (2x 100 mL) and dried under high vacuum to yield 126 g (85%) of DMP (**358**).

To obtain suitable crystals for X-ray analysis all filtrates were combined in a filter flask. A D3 glass frit was fitted and ether was allowed to evaporate under a gentle stream of

nitrogen at ambient temperature over the course of four days. Obtained single crystals of **1** were washed with anhydrous ether at 0°C and stored under argon.

<sup>1</sup>H NMR (300 MHz, CDCl<sub>3</sub>) δ = 8.33 – 8.24 (m, 2H), 8.11 – 8.04 (m, 1H), 7.90 (td, *J* = 0.9, 7.4 Hz, 1H), 2.32 (s, 3H), 1.99 (s, 6H).

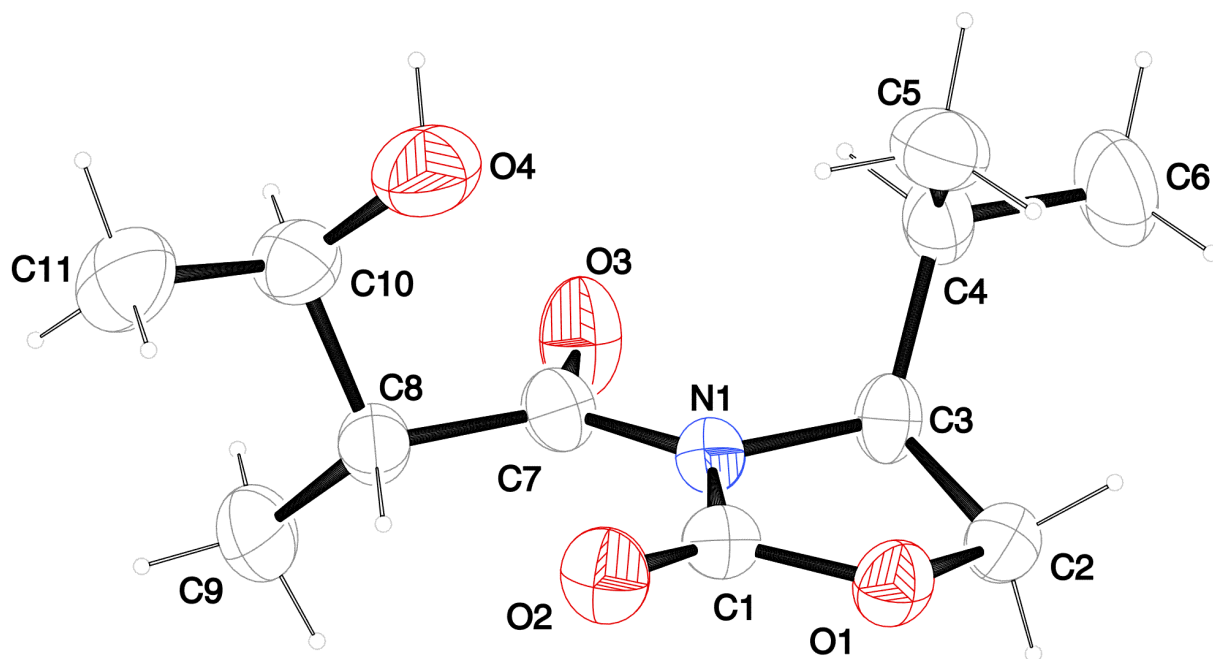
<sup>13</sup>C NMR (75 MHz, CDCl<sub>3</sub>) δ = 175.82, 174.12, 166.23, 142.32, 135.87, 133.94, 131.87, 126.59, 126.02, 20.54, 20.39.

IR (ATR):  $\tilde{\nu}$  = 1699.9 (s), 1670.6 (s).

## X-RAY CRYSTALLOGRAPHIC DATA

(*S*)-3-((2*R*,3*R*)-3-hydroxy-2-methylbutanoyl)-4-isopropylloxazolidin-2-one

(52)



**(S)-3-((2R,3R)-3-hydroxy-2-methylbutanoyl)-4-isopropylloxazolidin-2-one** **52**

netto formula	C <sub>11</sub> H <sub>19</sub> NO <sub>4</sub>		
molecular mass/ g mol <sup>-1</sup>	229.273		
Crystal size/ mm	0.40 × 0.25 × 0.25		
temperature/ K	200(2)		
radiation	MoK $\alpha$		
diffractometer	'Oxford XCalibur'		
crystal system	monoclinic		
space group	P2 <sub>1</sub>		
<i>a</i> / Å	8.8575(5)	$\alpha$ / °	90
<i>b</i> / Å	6.7825(4)	$\beta$ / °	98.944(6)
<i>c</i> / Å	10.6029(7)	$\gamma$ / °	90
volume/ Å <sup>3</sup>	629.23(7)		
<i>Z</i>	2		
calculated density/ g cm <sup>-3</sup>	1.21012(13)		
$\mu$ / mm <sup>-1</sup>	0.092		
absorption correction	'multi-scan'		
transmission factor range	0.91607–1.00000		
refls. measured	6161		
<i>R</i> <sub>int</sub>	0.0206		
mean $\sigma(I)/I$	0.0285		
$\theta$ range	3.80–25.49		
observed refls.	1926		
<i>x</i> , <i>y</i> (weighting scheme)	0.0765, 0		
hydrogen refinement	2342		
refls in refinement	150		
parameters	1		
restraints	0.0423		
<i>R</i> ( <i>F</i> <sub>obs</sub> )	0.1186		

---

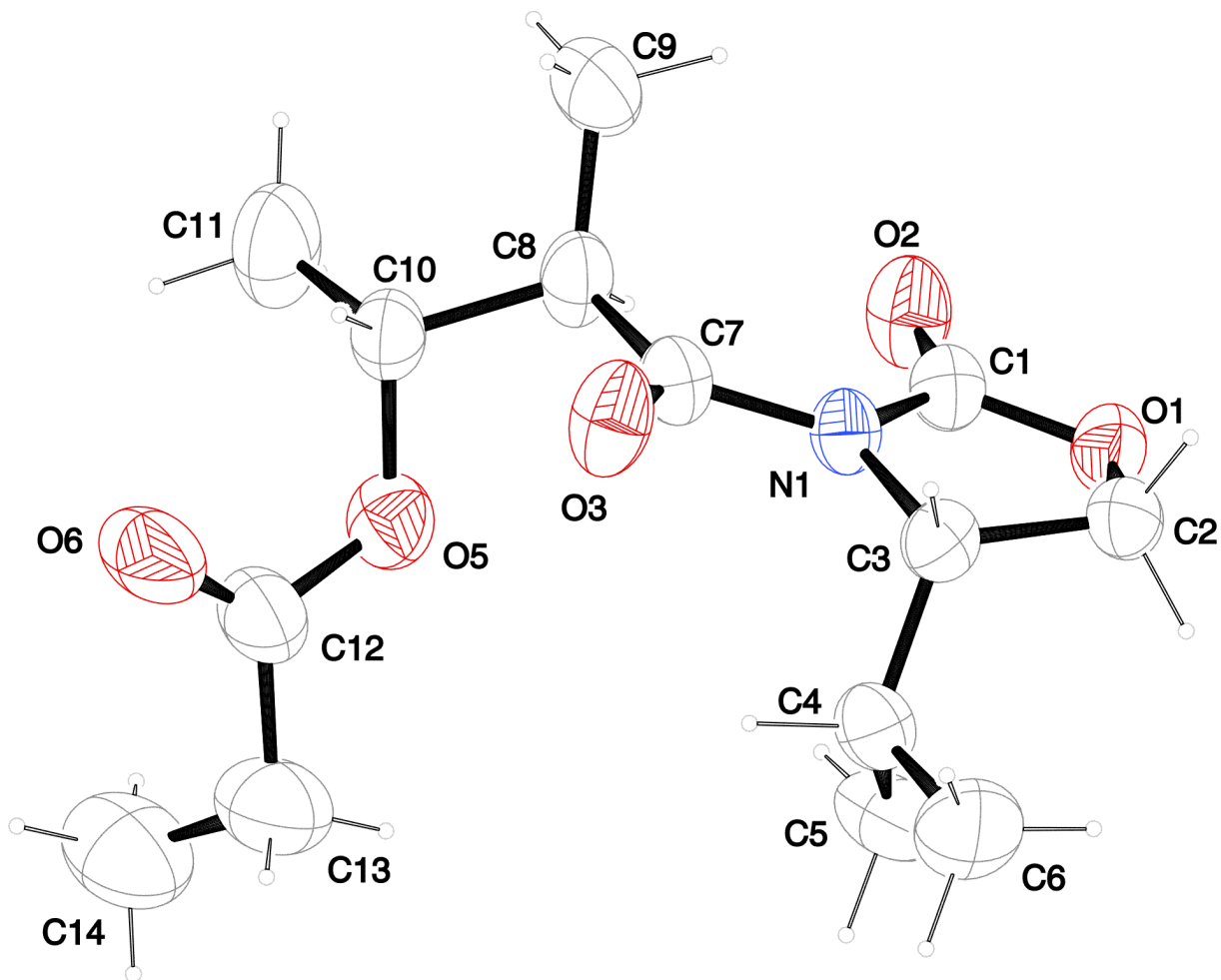
$R_w(F^2)$	1.061
$S$	0.001
shift/error <sub>max</sub>	0.549
max electron density/ e Å <sup>-3</sup>	-0.189
min electron density/ e Å <sup>-3</sup>	2342

---

(2*R*,3*R*)-4-((*S*)-4-isopropyl-2-oxooxazolidin-3-yl)-3-methyl-4-oxobutan-2-yl

propionate

(45)



(2*R*,3*R*)-4-((*S*)-4-isopropyl-2-oxooxazolidin-3-yl)-  
3-methyl-4-oxobutan-2-yl propionate **45**

netto formula	C <sub>14</sub> H <sub>23</sub> NO <sub>5</sub>		
molecular mass/ g mol <sup>-1</sup>	285.34		
Crystal size/ mm	0.15 x 0.20 x 0.35		
temperature/ K	200		
radiation	MoK $\alpha$		
diffractometer	'Oxford XCalibur'		
crystal system	orthorhombic		
space group	P2 <sub>1</sub> 2 <sub>1</sub> 2 <sub>1</sub>		
<i>a</i> / Å	6.4253(4)	$\alpha$ / °	90
<i>b</i> / Å	12.6707(8)	$\beta$ / °	90
<i>c</i> / Å	19.7785(12)	$\gamma$ / °	90
volume/ Å <sup>3</sup>	1610.23(17)		
<i>Z</i>	4		
calculated density/ g cm <sup>-3</sup>	1.177		
$\mu$ / mm <sup>-1</sup>	0.089		
absorption correction	'multi-scan'		
transmission factor range	0.91582–1.00000		
refls. measured	16294		
<i>R</i> <sub>int</sub>	0.052		
mean $\sigma(I)/I$	0.0544		
$\theta$ range	3.7,-26.0		
observed refls.	1979		
<i>x</i> , <i>y</i> (weighting scheme)	0.0460, 0		
hydrogen refinement	constr		
refls in refinement	3151		
parameters	181		
restraints	0		

EXPERIMENTAL

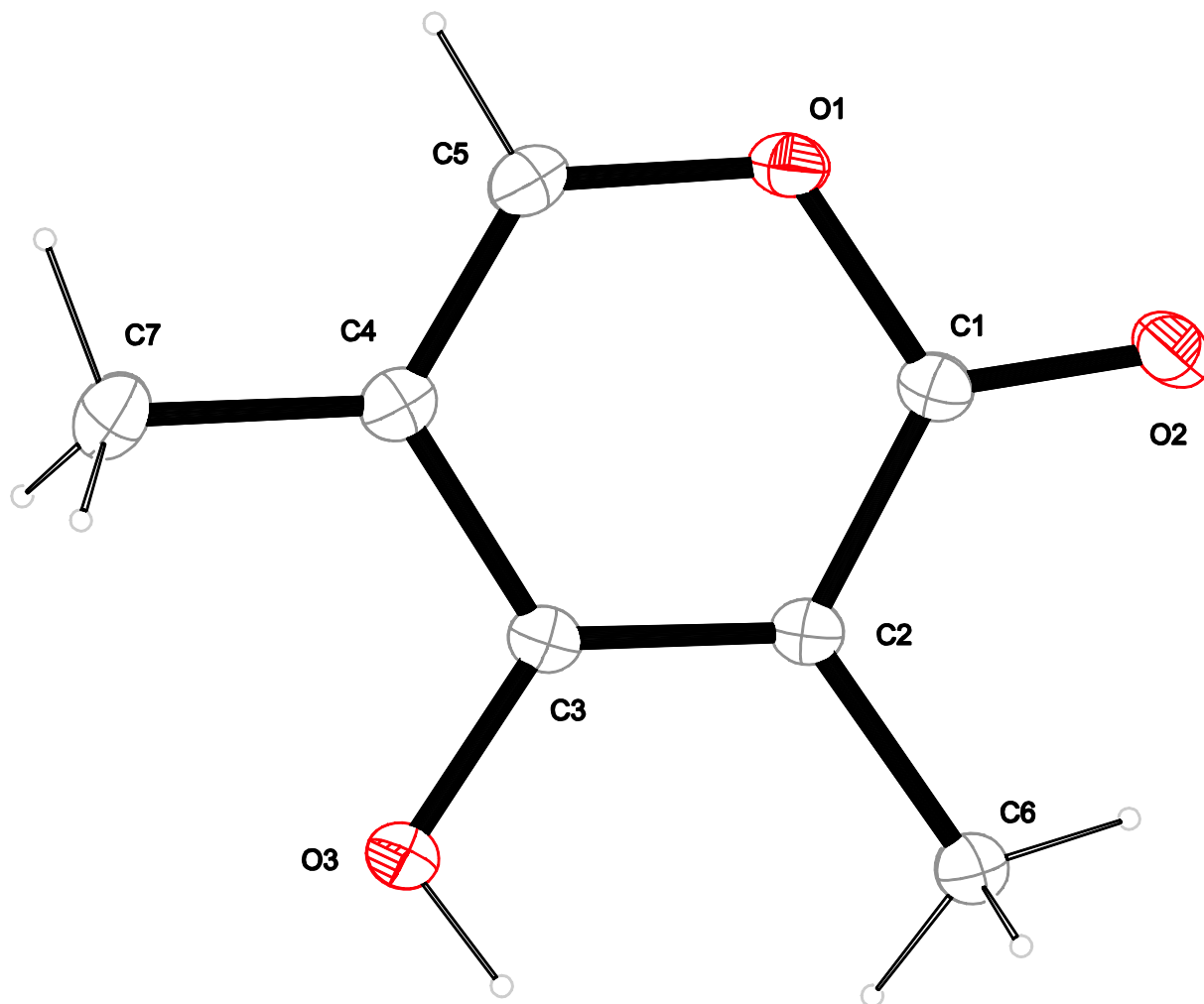
---

$R(F_{\text{obs}})$	0.0404
$R_w(F^2)$	0.0918
$S$	0.930
shift/error <sub>max</sub>	0.001
max electron density/ e Å <sup>-3</sup>	0.214
min electron density/ e Å <sup>-3</sup>	-0.130

---

4-hydroxy-3,5-dimethyl-2*H*-pyran-2-one

(82)



4-hydroxy-3,5-dimethyl-2*H*-pyran-2-one

82

---

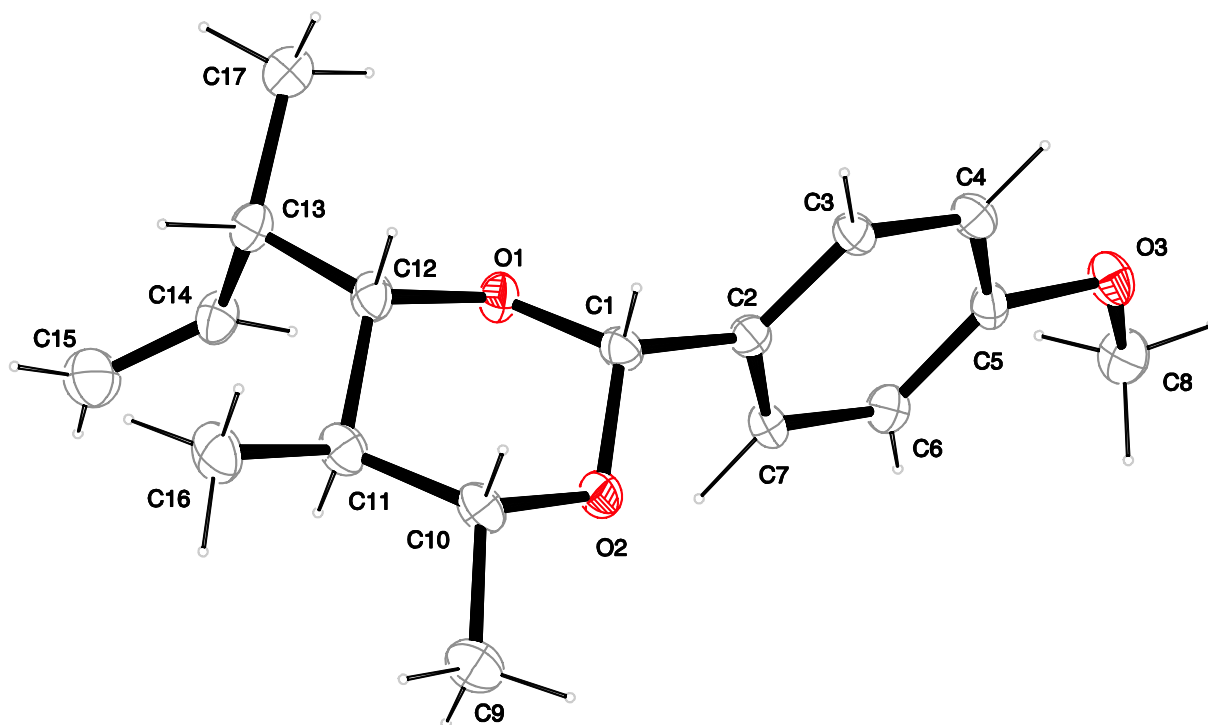
netto formula		$C_7H_8O_3$	
molecular mass/ g mol <sup>-1</sup>		140.137	
Crystal size/ mm		0.39 × 0.34 × 0.28	
temperature/ K		173(2)	
radiation		MoK $\alpha$	
diffractometer		'Oxford XCalibur'	
crystal system		orthorhombic	
space group		<i>Pccn</i>	
<i>a</i> / Å	9.6919(4)	$\alpha$ / °	90
<i>b</i> / Å	11.7002(5)	$\beta$ / °	90
<i>c</i> / Å	11.8300(5)	$\gamma$ / °	90
<i>V</i> /Å <sup>3</sup>		1341.49(10)	
<i>Z</i>		8	
calc. density/g cm <sup>-3</sup>		1.38774(10)	
$\mu$ /mm <sup>-1</sup>		0.109	
absorption correction		'multi-scan'	
transmission factor range		0.91693–1.00000	
refls. measured		8758	
$R_{int}$		0.0306	
mean $\sigma(I)/I$		0.0228	
$\theta$ range		4.21–26.35	
observed refls.		1012	
<i>x</i> , <i>y</i> (weighting scheme)		0.0758, 0	
hydrogen refinement		constr	
refls in refinement		1363	
parameters		94	
restraints		0	
$R(F_{obs})$		0.0381	

---

$R_w(F^2)$	0.1118
$S$	1.007
shift/error <sub>max</sub>	0.001
max electron density/e $\text{\AA}^{-3}$	0.225
min electron density/e $\text{\AA}^{-3}$	-0.218

---

## PMP-acetal (133)



PMP–acetal		133	
netto formula		$C_{17}H_{24}O_3$	
molecular mass/ $g\ mol^{-1}$		276.371	
Crystal size/ mm		0.46 × 0.39 × 0.08	
temperature/ K		173(2)	
radiation		MoK $\alpha$	
diffractometer		'Oxford XCalibur'	
crystal system		monoclinic	
space group		$P2_1$	
$a/ \text{\AA}$	8.3806(16)	$\alpha/ ^\circ$	90
$b/ \text{\AA}$	5.9084(14)	$\beta/ ^\circ$	90.224(19)
$c/ \text{\AA}$	16.099(4)	$\gamma/ ^\circ$	90
$V/ \text{\AA}^3$		797.2(3)	
$Z$		2	
calc. density/ $g\ cm^{-3}$		1.1514(4)	
$\mu/ mm^{-1}$		0.077	
absorption correction		'multi-scan'	
transmission factor range		0.12913–1.00000	
refls. measured		4256	
$R_{int}$		0.0597	
mean $\sigma(I)/I$		0.0705	
$\theta$ range		4.28–26.37	
observed refls.		1373	
$x, y$ (weighting scheme)		0.0584, 0	
hydrogen refinement		constr	
Flack parameter		–1(2)	
refls in refinement		1782	
parameters		185	
restraints		1	

EXPERIMENTAL

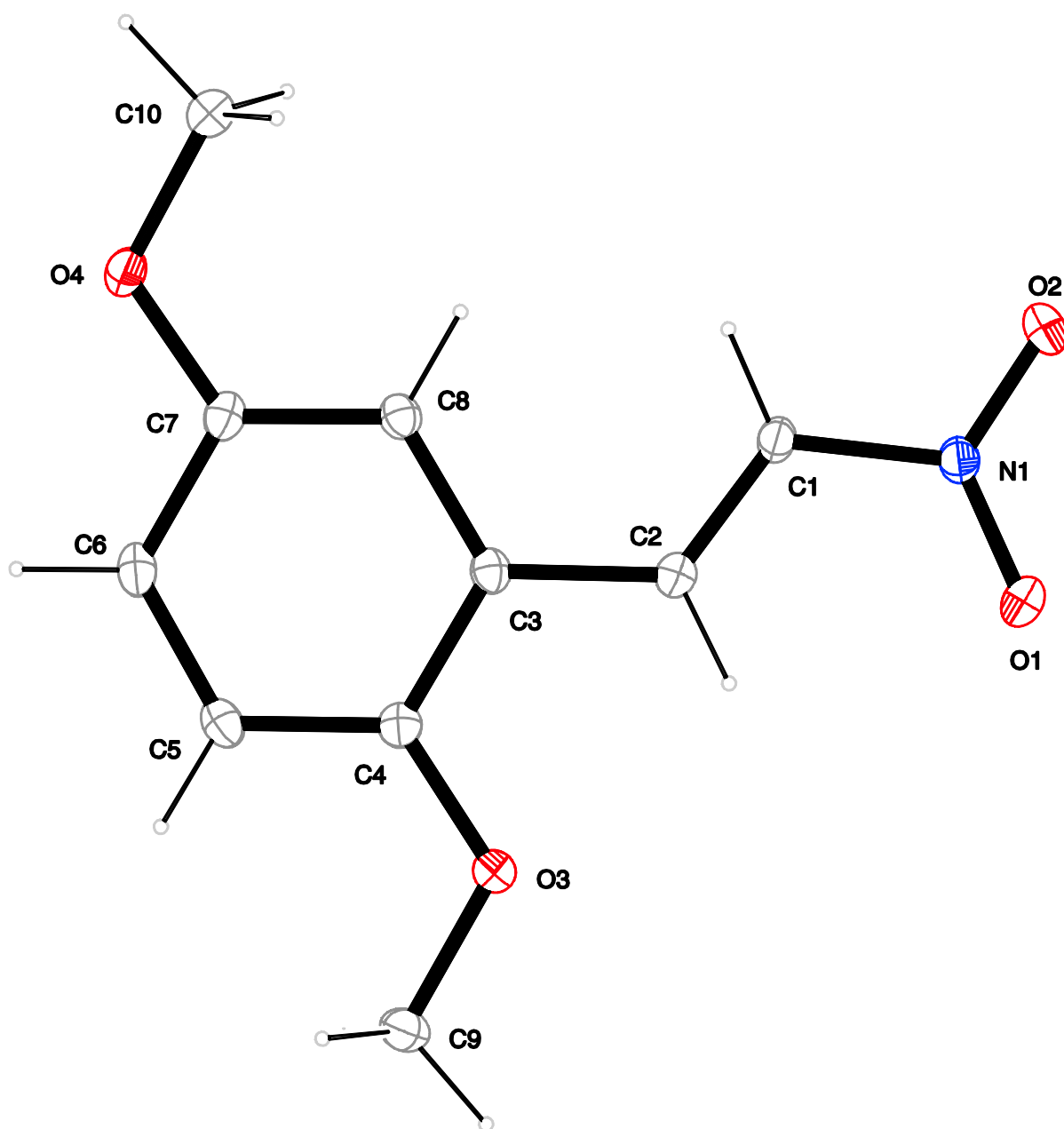
---

$R(F_{\text{obs}})$	0.0534
$R_w(F^2)$	0.1382
$S$	1.042
shift/error <sub>max</sub>	0.001
max electron density/e $\text{\AA}^{-3}$	0.215
min electron density/e $\text{\AA}^{-3}$	-0.216

---

Flack parameter meaningless, 393 Friedel pairs merged.

(*E*)-1,4-dimethoxy-2-(2-nitrovinyl)benzene (298)



---

*(E)*-1,4-dimethoxy-2-(2-nitrovinyl)benzene**298**

---

netto formula		$C_{10}H_{11}NO_4$	
molecular mass/ g mol <sup>-1</sup>		209.199	
Crystal size/ mm		0.25 × 0.20 × 0.12	
temperature/ K		173(2)	
radiation		MoKα	
diffractometer		'KappaCCD'	
crystal system		monoclinic	
space group		$P2_1/c$	
<i>a</i> / Å	3.90880(10)	$\alpha/^\circ$	90
<i>b</i> / Å	18.9082(5)	$\beta/^\circ$	94.6963(17)
<i>c</i> / Å	13.0295(3)	$\gamma/^\circ$	90
<i>V</i> /Å <sup>3</sup>		959.76(4)	
<i>Z</i>		4	
calc. density/g cm <sup>-3</sup>		1.44781(6)	
$\mu$ /mm <sup>-1</sup>		0.113	
absorption correction		none	
refls. measured		7436	
$R_{int}$		0.0275	
mean $\sigma(I)/I$		0.0254	
$\theta$ range		3.14–27.46	
observed refls.		1715	
<i>x</i> , <i>y</i> (weighting scheme)		0.0531, 0.3309	
hydrogen refinement		constr	
refls in refinement		2174	
parameters		138	
restraints		0	
$R(F_{obs})$		0.0418	
$R_w(F^2)$		0.1106	

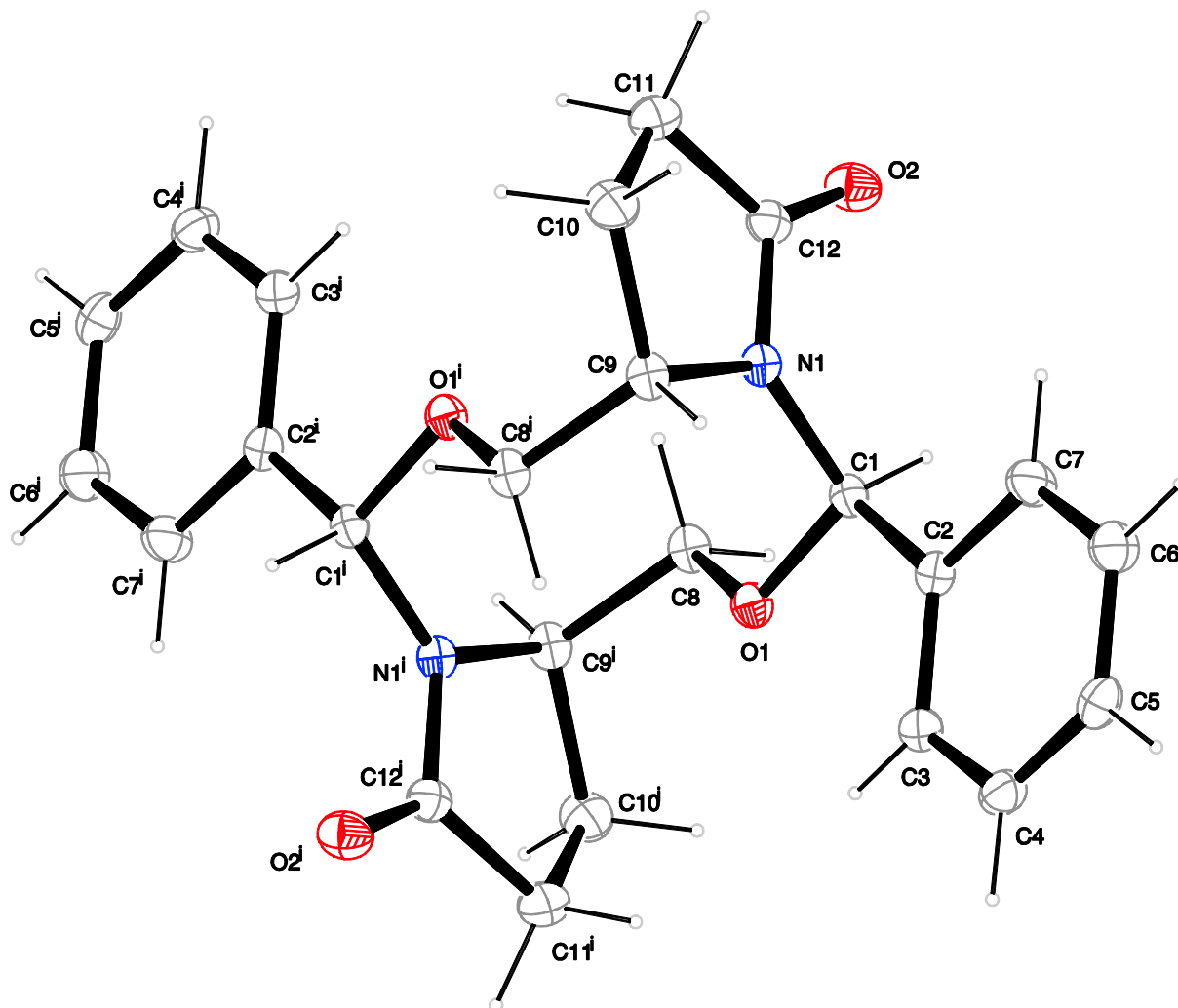
---

S	1.040
shift/error <sub>max</sub>	0.001
max electron density/e Å <sup>-3</sup>	0.217
min electron density/e Å <sup>-3</sup>	-0.295

---

(5*R*,7*aS*,12*R*,14*aS*)-5,12-diphenyloctahydrodipyrrolo[1,2-*c*:1',2'-*h*][1,6,3,8]dioxadiazecine-3,10(5*H*,12*H*)-dione

(249)



(5 <i>R</i> ,7 <i>aS</i> ,12 <i>R</i> ,14 <i>aS</i> )-5,12-diphenyloctahydrodipyrrolo[1,2- <i>c</i> :1',2'- <i>h</i> ][1,6,3,8]dioxadiazecine-3,10(5 <i>H</i> ,12 <i>H</i> )-dione		249	
netto formula		C <sub>24</sub> H <sub>26</sub> N <sub>2</sub> O <sub>4</sub>	
molecular mass/ g mol <sup>-1</sup>		406.474	
Crystal size/ mm		0.36 × 0.28 × 0.22	
temperature/ K		173(2)	
radiation		MoKα	
diffractometer		'KappaCCD'	
crystal system		monoclinic	
space group		<i>P</i> 2 <sub>1</sub> / <i>c</i>	
<i>a</i> / Å	8.0641(2)	α/ °	90
<i>b</i> / Å	14.8459(3)	β/ °	108.5480(10)
<i>c</i> / Å	8.8841(2)	γ/ °	90
<i>V</i> /Å <sup>3</sup>		1008.35(4)	
<i>Z</i>		2	
calc. density/g cm <sup>-3</sup>		1.33877(5)	
μ/mm <sup>-1</sup>		0.092	
absorption correction		none	
refls. measured		8142	
<i>R</i> <sub>int</sub>		0.0224	
mean σ( <i>I</i> )/ <i>I</i>		0.0182	
θ range		3.28–27.34	
observed refls.		1958	
<i>x</i> , <i>y</i> (weighting scheme)		0.0581, 0.3635	
hydrogen refinement		constr	
refls in refinement		2258	
parameters		136	
restraints		0	
<i>R</i> ( <i>F</i> <sub>obs</sub> )		0.0404	

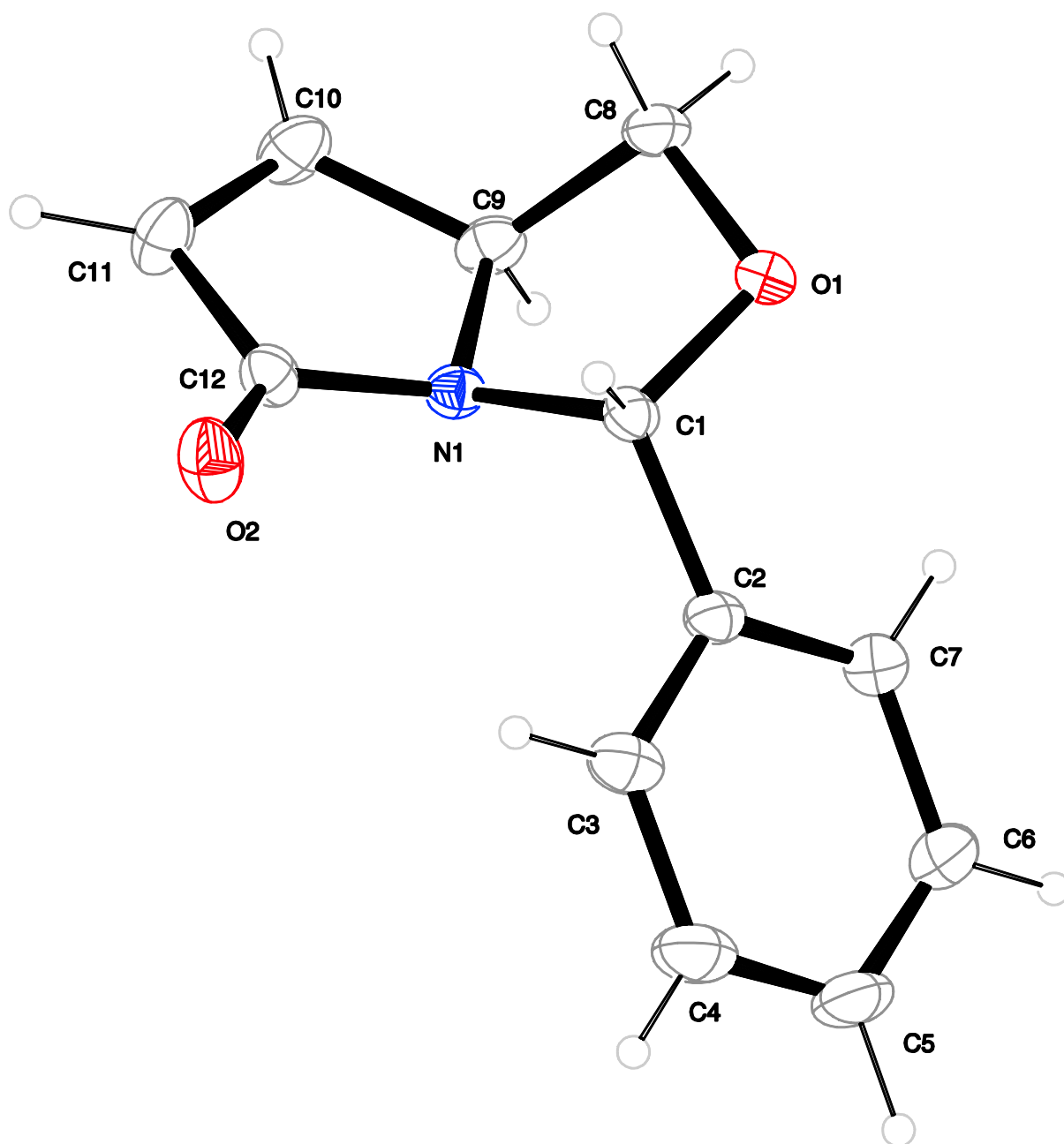
EXPERIMENTAL

---

$R_w(F^2)$	0.1164
$S$	1.045
shift/error <sub>max</sub>	0.001
max electron density/e $\text{\AA}^{-3}$	0.245
min electron density/e $\text{\AA}^{-3}$	-0.187

---

(3*R*,7*aS*)-3-phenyl-1,7*a*-dihydropyrrolo[1,2-*c*]oxazol-5(3*H*)-one (250)



**(3*R*,7*aS*)-3-phenyl-1,7*a*-dihydropyrrolo[1,2-*c*]oxazol-5(3*H*)-one****250**

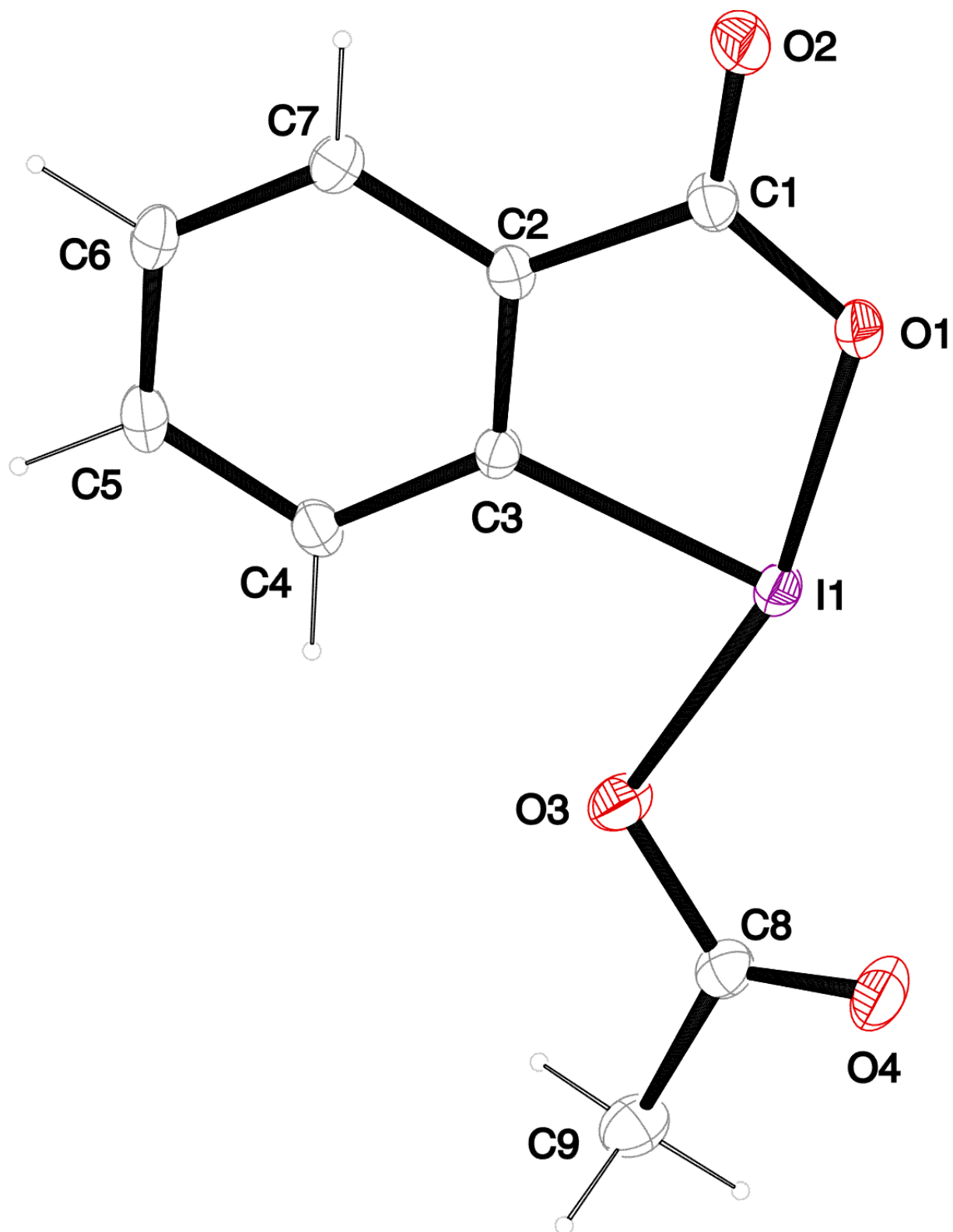
netto formula	C <sub>12</sub> H <sub>11</sub> NO <sub>2</sub>		
molecular mass/ g mol <sup>-1</sup>	201.221		
Crystal size/ mm	0.38 × 0.18 × 0.15		
temperature/ K	173(2)		
radiation	MoKα		
diffractometer	'KappaCCD'		
crystal system	trigonal		
space group	<i>P</i> 3 <sub>2</sub>		
<i>a</i> / Å	11.8691(4)	<i>α</i> / °	90
<i>b</i> / Å	11.8691(4)	<i>β</i> / °	90
<i>c</i> / Å	6.2589(2)	<i>γ</i> / °	120
<i>V</i> /Å <sup>3</sup>	763.60(4)		
<i>Z</i>	3		
calc. density/g cm <sup>-3</sup>	1.31276(7)		
<i>μ</i> /mm <sup>-1</sup>	0.090		
absorption correction	none		
refls. measured	6007		
<i>R</i> <sub>int</sub>	0.0294		
mean <i>σ</i> ( <i>I</i> )/ <i>I</i>	0.0180		
<i>θ</i> range	3.43–27.35		
observed refls.	1071		
<i>x</i> , <i>y</i> (weighting scheme)	0.0446, 0.1741		
hydrogen refinement	constr		
Flack parameter	–0.3(17)		
refls in refinement	1158		
parameters	137		
restraints	1		

---

$R(F_{\text{obs}})$	0.0360
$R_w(F^2)$	0.0936
$S$	1.069
shift/error <sub>max</sub>	0.001
max electron density/e $\text{\AA}^{-3}$	0.151
min electron density/e $\text{\AA}^{-3}$	-0.132

---

Flack parameter meaningless, 1154 Friedel pairs merged.



iodine(III) iodoxolone

**362**

netto formula	C <sub>9</sub> H <sub>7</sub> IO <sub>4</sub>		
molecular mass/ g mol <sup>-1</sup>	306.054		
Crystal size/ mm	0.31 × 0.26 × 0.20		
temperature/ K	173(2)		
radiation	MoKα		
diffractometer	'Oxford XCalibur'		
crystal system	monoclinic		
space group	<i>P</i> 2 <sub>1</sub> / <i>c</i>		
<i>a</i> / Å	7.5583(2)	α/ °	90
<i>b</i> / Å	7.81194(19)	β/ °	98.115(2)
<i>c</i> / Å	16.1529(4)	γ/ °	90
<i>V</i> /Å <sup>3</sup>	944.20(4)		
<i>Z</i>	4		
calc. density/g cm <sup>-3</sup>	2.15303(9)		
μ/mm <sup>-1</sup>	3.376		
absorption correction	'multi-scan'		
transmission factor range	0.98215–1.00000		
refls. measured	8132		
<i>R</i> <sub>int</sub>	0.0228		
mean σ( <i>I</i> )/ <i>I</i>	0.0247		
θ range	4.33–30.50		
observed refls.	2586		
<i>x</i> , <i>y</i> (weighting scheme)	0.0201, 0.2314		
hydrogen refinement	constr		
refls in refinement	2870		
parameters	128		
restraints	0		
<i>R</i> ( <i>F</i> <sub>obs</sub> )	0.0197		

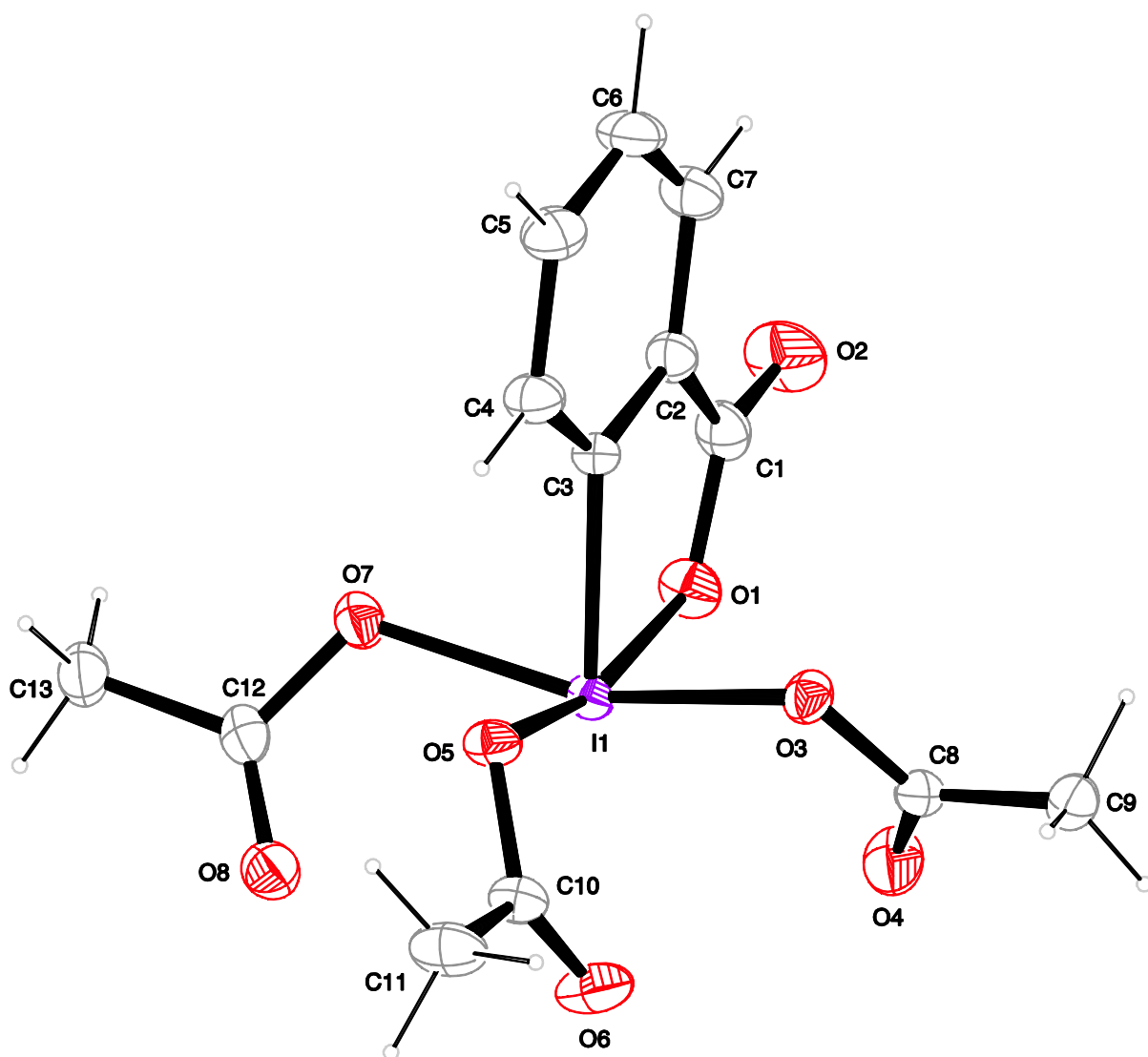
EXPERIMENTAL

---

$R_w(F^2)$	0.0471
$S$	1.057
shift/error <sub>max</sub>	0.002
max electron density/e $\text{\AA}^{-3}$	0.514
min electron density/e $\text{\AA}^{-3}$	-0.695

---

## DMP (270)



DMP		270	
netto formula		$C_{13}H_{13}IO_8$	
molecular mass/ g mol <sup>-1</sup>		424.142	
Crystal size/ mm		0.30 × 0.21 × 0.15	
temperature/ K		173(2)	
radiation		MoK $\alpha$	
diffractometer		'Oxford XCalibur'	
crystal system		triclinic	
space group		<i>P</i> 1bar	
<i>a</i> / Å	8.3829(4)	$\alpha$ / °	100.659(6)
<i>b</i> / Å	8.4906(6)	$\beta$ / °	99.289(5)
<i>c</i> / Å	11.6195(8)	$\gamma$ / °	111.040(5)
<i>V</i> /Å <sup>3</sup>		734.80(8)	
<i>Z</i>		2	
calc. density/g cm <sup>-3</sup>		1.9170(2)	
$\mu$ /mm <sup>-1</sup>		2.218	
absorption correction		'multi-scan'	
transmission factor range		0.611–0.717	
refls. measured		6431	
<i>R</i> <sub>int</sub>		0.0141	
mean $\sigma(I)/I$		0.0263	
$\theta$ range		4.29–30.50	
observed refls.		4154	
<i>x</i> , <i>y</i> (weighting scheme)		0.0244, 0.0931	
hydrogen refinement		constr	
refls in refinement		4411	
parameters		202	
restraints		0	
<i>R</i> ( <i>F</i> <sub>obs</sub> )		0.0187	

---

$R_w(F^2)$	0.0479
$S$	1.060
shift/error <sub>max</sub>	0.001
max electron density/e $\text{\AA}^{-3}$	0.548
min electron density/e $\text{\AA}^{-3}$	-0.590

---

## REFERENCES

- [1] D. J. Aberhart, K. H. Overton, S. Huneck, *J. Chem. Soc. D.* **1969**, 162–163.
- [2] W. Dieckmann, *Ber. Dtsch. Chem. Ges* **1894**, 102.
- [3] O. Diels, K. Alder, *Liebigs Ann. Chem.* **1928**, 460, 98–122.
- [4] O. Diels, K. Alder, *Ber. Dtsch. Chem. Ges.* **1929**, 62, 2081–2087.
- [5] O. Diels, K. Alder, *Ber. Dtsch. Chem. Ges.* **1929**, 62, 2087–2090.
- [6] O. Diels, K. Alder, *Liebigs Ann. Chem.* **1931**, 490, 257–266.
- [7] D. A. Evans, J. S. Clark, R. Metternich, V. J. Novack, G. S. Sheppard, *J. Am. Chem. Soc.* **1990**, 112, 866–868.
- [8] M. Chen, W. R. Roush, *J. Am. Chem. Soc.* **2012**, 134, 3925–3931.
- [9] N. Okamoto, O. Hara, K. Makino, Y. Hamada, *Tetrahedron: Asymmetry* **2001**, 12, 1353–1358.
- [10] D. B. Dess, J. C. Martin, *J. Org. Chem.* **1983**, 48, 4155–4156.
- [11] D. B. Dess, J. C. Martin, *J. Am. Chem. Soc.* **1991**, 113, 7277–7287.
- [12] A. Schröckeneder, D. Stichnoth, P. Mayer, D. Trauner, *Beilstein J. Org. Chem.* **2012**, 8, 1523–1527.
- [13] L. Fusaro, M. Luhmer, G. Cerioni, F. Mocci, *J. Org. Chem.* **2009**, 74, 8818–8821.
- [14] K. C. Nicolaou, T. Montagnon, S. A. Snyder, *Chem. Commun.* **2003**, 551–564.
- [15] E. Gravel, E. Poupon, *Eur. J. Org. Chem.* **2008**, 27–42.
- [16] S. Huneck, G. Follmann, *Z. Naturforsch., B: Chem. Sci.* **1967**, B 22, 1185–1188.
- [17] S. Huneck, A. Mathey, G. Trotet, *Z. Naturforsch., B: Chem. Sci.* **1967**, B 22, 1367–1368.
- [18] S. Huneck, G. Trotet, *Z. Naturforsch., B: Chem. Sci.* **1967**, B 22, 363.
- [19] S. Huneck, H. Ronneberg, S. Liaaenjenzen, *Pharmazie* **1982**, 37, 866.
- [20] W. Quillhot, J. A. Garbarino, V. Gambaro, *J. Nat. Prod.* **1983**, 46, 594–595.
- [21] G. R. Pettit, Q. W. Zhang, W. Pinilla, D. L. Herald, D. L. Doubek, J. A. Duke, *J. Nat. Prod.* **2004**, 67, 983–985.
- [22] D. J. Aberhart, K. H. Overton, S. Huneck, *J. Chem. Soc. C.* **1970**, 1612–1623.
- [23] G. Ferguson, I. R. Mackay, *J. Chem. Soc. D.* **1970**, 665–666.
- [24] H. Jayasuriya, Z. Guan, A. W. Dombrowski, G. F. Bills, J. D. Polishook, R. G. Jenkins, L. Koch, T. Crumley, T. Tamas, M. Dubois, A. Misura, S. J. Darkin-Ratray, L. Gregory, S. B. Singh, *J. Nat. Prod.* **2007**, 70, 1364–1367.
- [25] G. Lang, J. Wiese, R. Schmaljohann, J. F. Imhoff, *Tetrahedron* **2007**, 63, 11844–11849.
- [26] M. Mori, H. Morimoto, Y.-P. Kim, H. Ui, K. Nonaka, R. Masuma, K. Sakamoto, K. Kita, H. Tomoda, K. Shiomi, S. Omura, *Tetrahedron* **2011**, 67, 6582–6586.
- [27] H. Wei, T. Itoh, M. Kinoshita, N. Kotoku, S. Aoki, M. Kobayashi, *Tetrahedron* **2005**, 61, 8054–8058.
- [28] H. Wei, T. Itoh, N. Kotoku, M. Kobayashi, *Heterocycles* **2006**, 68, 111–123.
- [29] V. Sofiyev, G. Navarro, D. Trauner, *Org. Lett.* **2008**, 10, 149–152.
- [30] M. F. Jacobsen, J. E. Moses, R. M. Adlington, J. E. Baldwin, *Org. Lett.* **2005**, 7, 2473–2476.
- [31] J. A. Robinson, *Phil. Trans. R. Soc. Lond. B.* **1991**, 332, 107–114.
- [32] D. J. Aberhart, A. Corbella, K. H. Overton, *J. Chem. Soc. D.* **1970**, 664–665.
- [33] M. Jacolot, M. Jean, N. Levoine, P. van de Weghe, *Org. Lett.* **2012**, 14, 58–61.

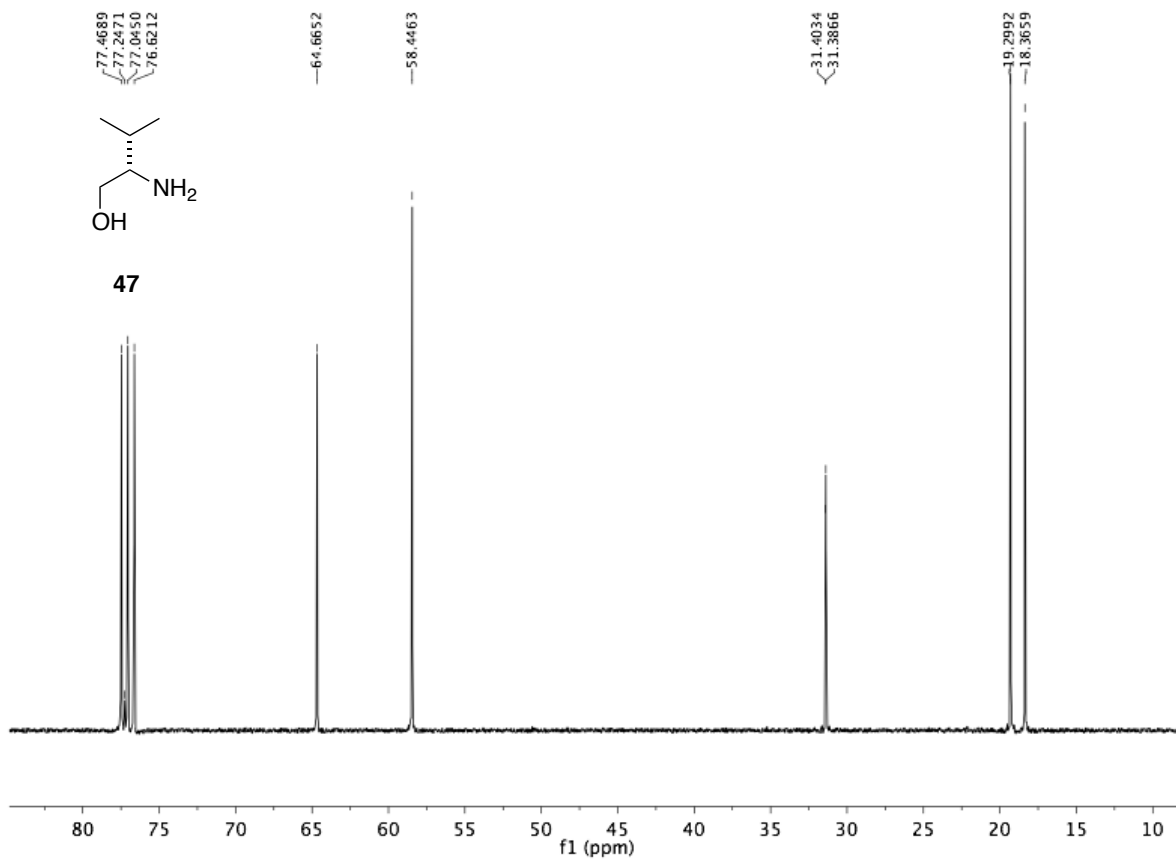
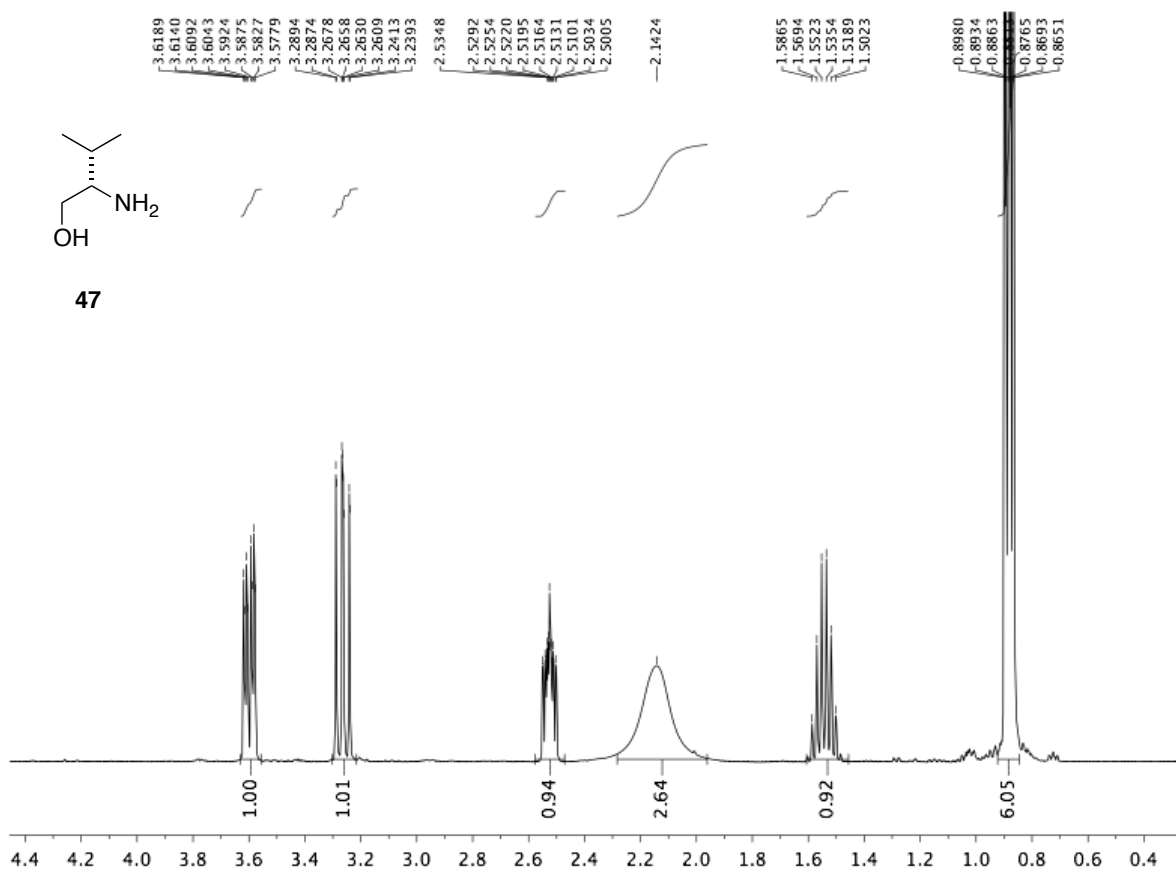
- [34] C. Olier, M. Kaafarani, S. Gastaldi, M. P. Bertrand, *Tetrahedron* **2010**, *66*, 413–445.
- [35] D. A. Evans, H. P. Ng, D. L. Rieger, *J. Am. Chem. Soc.* **1993**, *115*, 11446–11459.
- [36] D. A. Evans, H. P. Ng, *Tetrahedron Lett.* **1993**, *34*, 2229–2232.
- [37] D. A. Dickman, A. I. Meyers, G. A. Smith, R. E. Gawley, *Organic Syntheses* **1985**, *63*, 136.
- [38] J. R. Gage, D. A. Evans, *Organic Syntheses* **1990**, *68*, 77.
- [39] J. R. Gage, D. A. Evans, *Organic Syntheses* **1990**, *68*, 83.
- [40] B. C. Raimundo, C. H. Heathcock, *Synlett* **1995**, 1213–1214.
- [41] M. A. Walker, C. H. Heathcock, *J. Org. Chem.* **1991**, *56*, 5747–5750.
- [42] D. A. Evans, J. Bartroli, T. L. Shih, *J. Am. Chem. Soc.* **1981**, *103*, 2127–2129.
- [43] H. E. Zimmerman, M. D. Traxler, *J. Am. Chem. Soc.* **1957**, *79*, 1920–1923.
- [44] K. Hinterding, S. Singhanat, L. Oberer, *Tetrahedron Lett.* **2001**, *42*, 8463–8465.
- [45] F. Bennett, G. Fenton, D. W. Knight, *Tetrahedron* **1994**, *50*, 5147–5158.
- [46] N. Sakai, Y. Ohfuné, *J. Am. Chem. Soc.* **1992**, *114*, 998–1010.
- [47] H. H. Meyer, *Liebigs Ann. Chem.* **1984**, *1984*, 977–981.
- [48] R. H. Schlessinger, L. H. Pettus, *J. Org. Chem.* **1998**, *63*, 9089–9094.
- [49] H. P. Wessel, T. Iversen, D. R. Bundle, *J. Chem. Soc. Perkin Trans. 1* **1985**, 2247–2250.
- [50] A. B. Smith, T. J. Beauchamp, M. J. LaMarche, M. D. Kaufman, Y. Qiu, H. Arimoto, D. R. Jones, K. Kobayashi, *J. Am. Chem. Soc.* **2000**, *122*, 8654–8664.
- [51] W. R. Roush, A. E. Walts, L. K. Hoong, *J. Am. Chem. Soc.* **1985**, *107*, 8186–8190.
- [52] W. R. Roush, K. Ando, D. B. Powers, R. L. Halterman, A. D. Palkowitz, *Tetrahedron Lett.* **1988**, *29*, 5579–5582.
- [53] W. R. Roush, K. Ando, D. B. Powers, A. D. Palkowitz, R. L. Halterman, *J. Am. Chem. Soc.* **1990**, *112*, 6339–6348.
- [54] M. Chérest, H. Felkin, N. Prudent, *Tetrahedron Lett.* **1968**, *9*, 2199–2204.
- [55] N. T. Anh, O. Eisenstein, *New J. Chem.* **1977**, *1*, 61–70.
- [56] H. B. Bürgi, J. D. Dunitz, E. Shefter, *J. Am. Chem. Soc.* **1973**, *95*, 5065–5067.
- [57] H. B. Bürgi, J. D. Dunitz, J. M. Lehn, G. Wipff, *Tetrahedron* **1974**, *30*, 1563–1572.
- [58] T. Herold, R. W. Hoffmann, *Angew. Chem. Int. Ed.* **1978**, *17*, 768–769.
- [59] H. C. Brown, P. K. Jadhav, *J. Am. Chem. Soc.* **1983**, *105*, 2092–2093.
- [60] H. C. Brown, P. K. Jadhav, K. S. Bhat, *J. Am. Chem. Soc.* **1988**, *110*, 1535–1538.
- [61] H. C. Brown, R. S. Randad, *Tetrahedron Lett.* **1990**, *31*, 455–458.
- [62] H. C. Brown, K. S. Bhat, P. K. Jadhav, *J. Chem. Soc., Perkin Trans. 1* **1991**, 2633–2638.
- [63] U. S. Racherla, H. C. Brown, *J. Org. Chem.* **1991**, *56*, 401–404.
- [64] K. A. Scheidt, A. Tasaka, T. D. Bannister, M. D. Wendt, W. R. Roush, *Angew. Chem. Int. Ed.* **1999**, *38*, 1652–1655.
- [65] B. S. Bal, W. E. Childers Jr, H. W. Pinnick, *Tetrahedron* **1981**, *37*, 2091–2096.
- [66] M. Karplus, *J. Am. Chem. Soc.* **1963**, *85*, 2870–2871.
- [67] O. Diels, K. Alder, *Liebigs Ann. Chem.* **1926**, *450*, 237–254.
- [68] F. Effenberger, T. Ziegler, K.-H. Schönwälder, *Chem. Ber.* **1985**, *118*, 741–752.
- [69] K.-M. E. Ng, T. C. McMorris, *Can. J. Chem.* **1984**, *62*, 1945–1953.
- [70] R. Sustmann, *Pure Appl. Chem.* **1974**, *40*, 569–593.
- [71] I. E. Marko, P. Seres, T. M. Swarbrick, I. Staton, H. Adams, *Tetrahedron Lett.* **1992**, *33*, 5649–5652.
- [72] P. Yates, P. Eaton, *J. Am. Chem. Soc.* **1960**, *82*, 4436–4437.
- [73] I. E. Markó, G. R. Evans, *Synlett* **1994**, *1994*, 431–433.
- [74] G. H. Posner, J. C. Carry, T. E. N. Anjeh, A. N. French, *J. Org. Chem.* **1992**, *57*, 7012–7014.
- [75] L. Lombardo, *Tetrahedron Lett.* **1982**, *23*, 4293–4296.

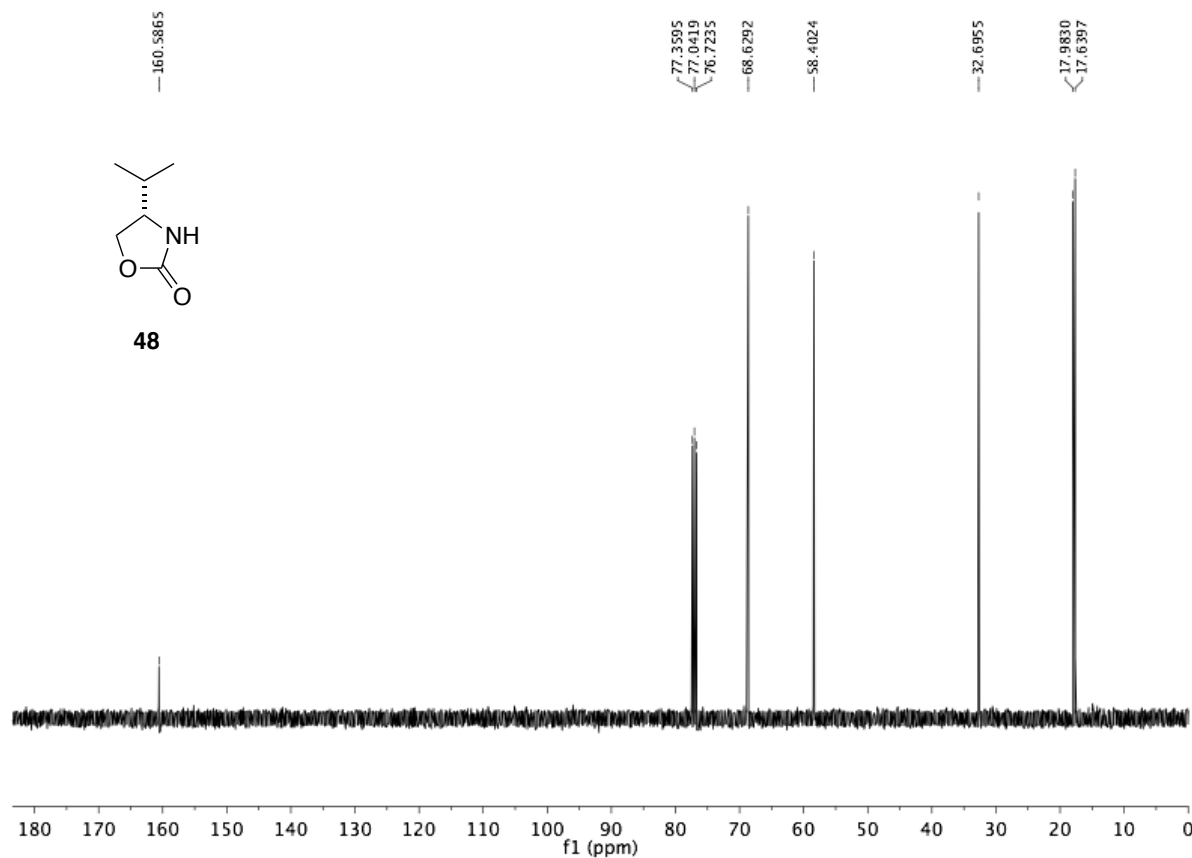
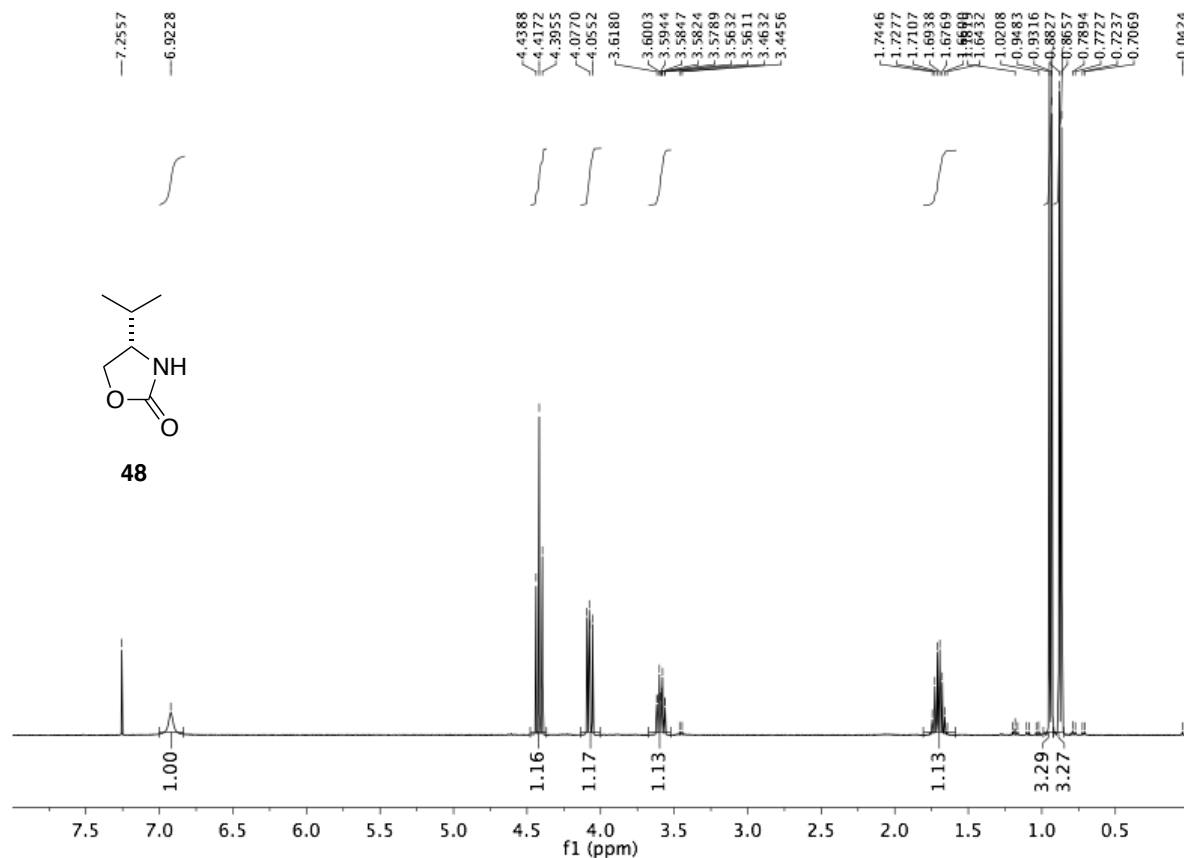
- [76] T. Okazoe, K. Takai, K. Oshima, K. Utimoto, *J. Org. Chem.* **1987**, *52*, 4410–4412.
- [77] T. Okazoe, K. Takai, K. Utimoto, *J. Am. Chem. Soc.* **1987**, *109*, 951–953.
- [78] W.-B. Yang, Y.-Y. Yang, Y.-F. Gu, S.-H. Wang, C.-C. Chang, C.-H. Lin, *J. Org. Chem.* **2002**, *67*, 3773–3782.
- [79] L. C. Dias, M. A. de Sousa, *Tetrahedron Lett.* **2003**, *44*, 5625–5628.
- [80] D. A. Evans, K. T. Chapman, E. M. Carreira, *J. Am. Chem. Soc.* **1988**, *110*, 3560–3578.
- [81] D. A. Evans, A. S. Kim, *Tetrahedron Lett.* **1997**, *38*, 53–56.
- [82] D. A. Evans, A. S. Kim, R. Metternich, V. J. Novack, *J. Am. Chem. Soc.* **1998**, *120*, 5921–5942.
- [83] A. B. Smith, B. M. Brandt, *Org. Lett.* **2001**, *3*, 1685–1688.
- [84] R. Kaiser, *J. Chem. Phys.* **1963**, *39*, 2435–2443.
- [85] T. Lister, M. V. Perkins, *Angew. Chem. Int. Ed.* **2006**, *45*, 2560–2564.
- [86] D. A. Evans, M. DiMare, *J. Am. Chem. Soc.* **1986**, *108*, 2476–2478.
- [87] M. Chen, W. R. Roush, *J. Am. Chem. Soc.* **2011**, *133*, 5744–5747.
- [88] P. S. Stewart, M. Chen, W. R. Roush, D. H. Ess, *Org. Lett.* **2011**, *13*, 1478–1481.
- [89] M. Chen, W. R. Roush, *Org. Lett.* **2011**, *14*, 426–428.
- [90] S. D. Rychnovsky, D. J. Skalitzky, *Tetrahedron Lett.* **1990**, *31*, 945–948.
- [91] L. I. Smith, *Chem. Rev.* **1938**, *23*, 193–285.
- [92] T. Curtius, *Ber. Dtsch. Chem. Ges.* **1883**, *16*, 2230–2231.
- [93] H. Wieland, L. Semper, *Liebigs Ann. Chem.* **1908**, *358*, 36–70.
- [94] H. Staudinger, K. Miescher, *Helv. Chim. Acta* **1919**, *2*, 554–582.
- [95] R. Huisgen, *Angew. Chem. Int. Ed.* **1963**, *2*, 565–598.
- [96] W. J. Middleton, *J. Org. Chem.* **1969**, *34*, 3201–3202.
- [97] A. P. Krapcho, D. R. Rao, M. P. Silvon, B. Abegaz, *J. Org. Chem.* **1971**, *36*, 3885–3890.
- [98] R. M. Kellogg, M. Noteboom, J. K. Kaiser, *J. Org. Chem.* **1975**, *40*, 2573–2574.
- [99] I. Kalwisch, L. Xingya, J. Gottstein, R. Huisgen, *J. Am. Chem. Soc.* **1981**, *103*, 7032–7033.
- [100] R. Huisgen, G. Mloston, K. Polborn, R. Sustmann, *Chem. Eur. J.* **2003**, *9*, 2256–2263.
- [101] T. B. Cameron, H. W. Pinnick, *J. Am. Chem. Soc.* **1980**, *102*, 744–747.
- [102] Y. Terao, M. Tanaka, N. Imai, K. Achiwa, *Tetrahedron Lett.* **1985**, *26*, 3011–3014.
- [103] A. Hosomi, Y. Matsuyama, H. Sakurai, *J. Chem. Soc., Chem. Commun.* **1986**, 1073–1074.
- [104] J. Choi, E. Imai, M. Mihara, Y. Oderaotoshi, S. Minakata, M. Komatsu, *J. Org. Chem.* **2003**, *68*, 6164–6171.
- [105] A. Zampella, M. V. D'Auria, L. G. Paloma, A. Casapullo, L. Minale, C. Debitus, Y. Henin, *J. Am. Chem. Soc.* **1996**, *118*, 6202–6209.
- [106] A. Zampella, M. V. D'Auria, L. G. Paloma, A. Casapullo, L. Minale, C. c. Debitus, Y. Henin, *Journal of the American Chemical Society* **1996**, *118*, 6202–6209.
- [107] C. M. Acevedo, E. F. Kogut, M. A. Lipton, *Tetrahedron* **2001**, *57*, 6353–6359.
- [108] P. W. Ford, K. R. Gustafson, T. C. McKee, N. Shigematsu, L. K. Maurizi, L. K. Pannell, D. E. Williams, E. Dilip de Silva, P. Lassota, T. M. Allen, R. Van Soest, R. J. Andersen, M. R. Boyd, *J. Am. Chem. Soc.* **1999**, *121*, 5899–5909.
- [109] B. Liang, P. J. Carroll, M. M. Joullié, *Org. Lett.* **2000**, *2*, 4157–4160.
- [110] S. Lesniak, G. Mloston, K. Urbaniak, P. Wasiak, A. Linden, H. Heimgartner, *Tetrahedron* **2006**, *62*, 7776–7782.
- [111] D. Seyferth, R. S. Marmor, P. Hilbert, *J. Org. Chem.* **1971**, *36*, 1379–1386.
- [112] J. C. Gilbert, U. Weerasooriya, *J. Org. Chem.* **1982**, *47*, 1837–1845.
- [113] L. Horner, H. Hoffmann, H. G. Wippel, *Chem. Ber.* **1958**, *91*, 61–63.

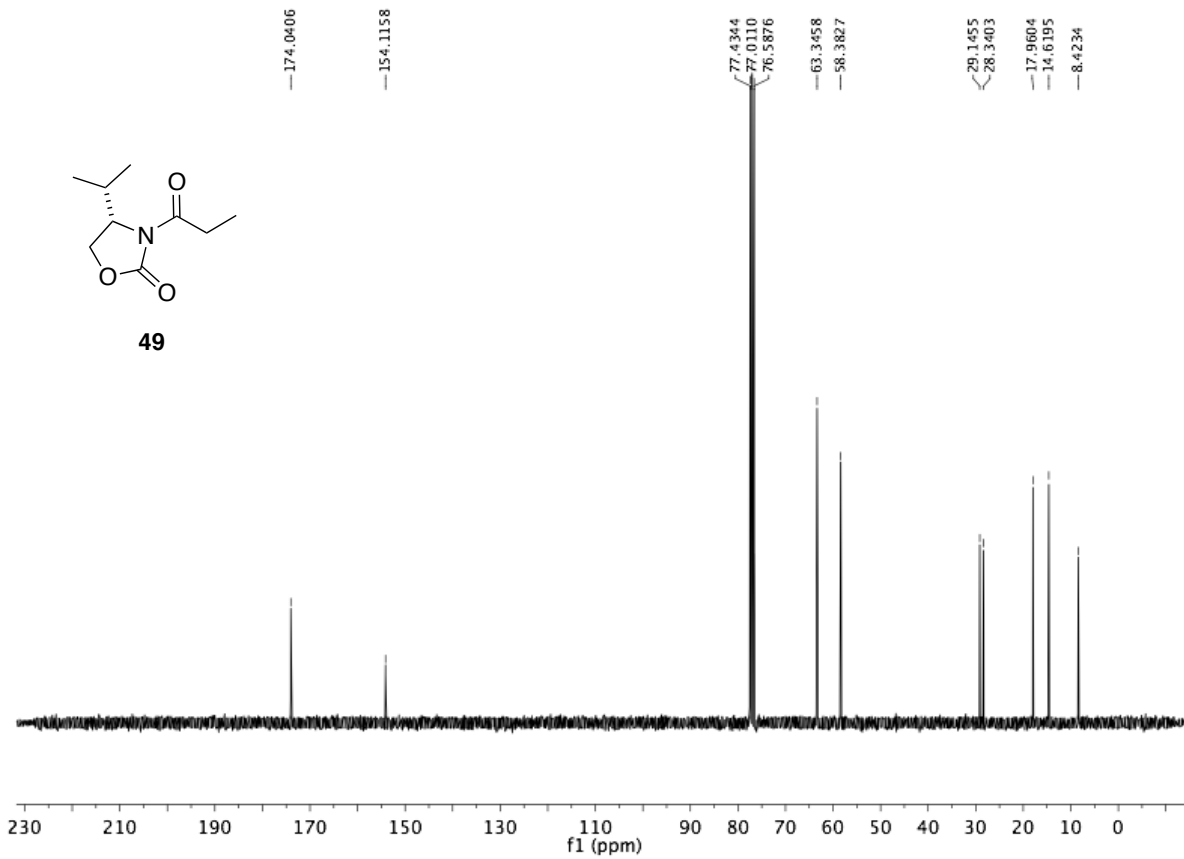
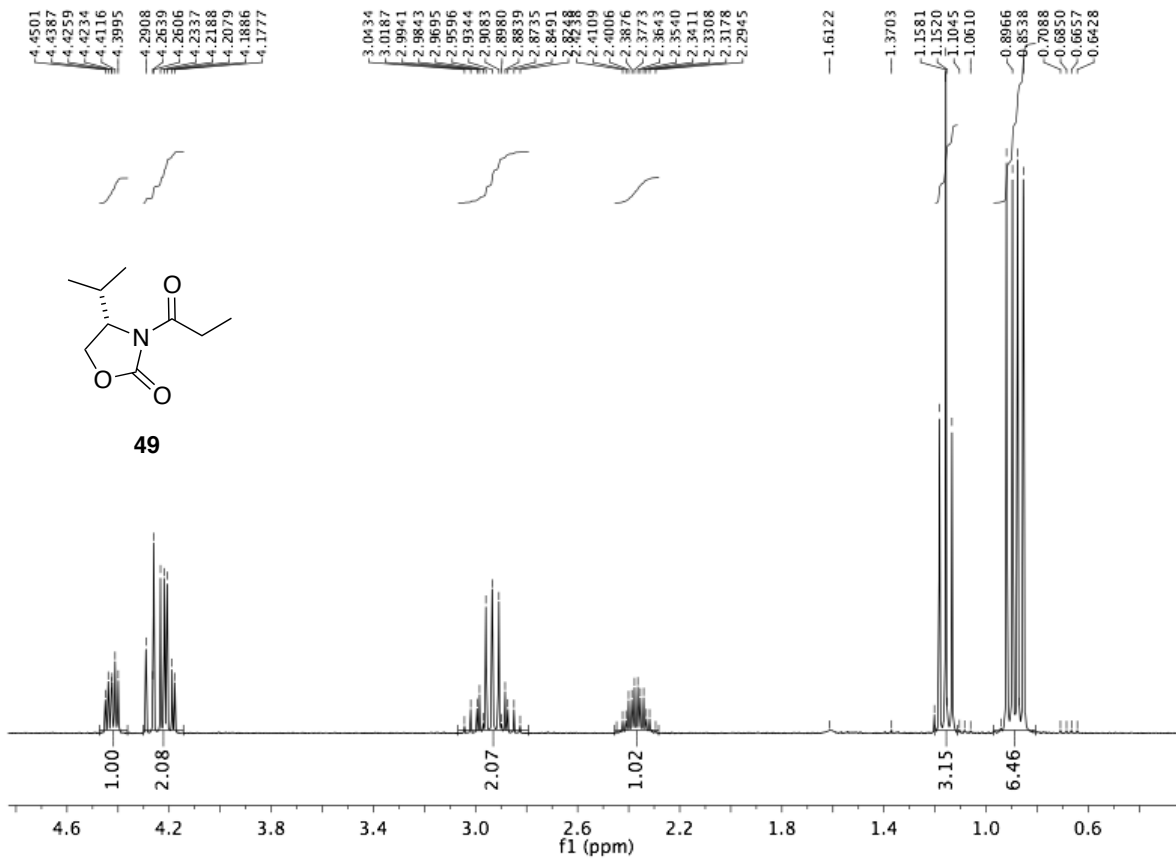
- [114] M. Mikolajczyk, S. Grzejszczak, A. Chefczynska, A. Zatorski, *J. Org. Chem.* **1979**, *44*, 2967–2972.
- [115] S. Brand, M. F. Jones, C. M. Rayner, *Tetrahedron Lett.* **1995**, *36*, 8493–8496.
- [116] M. Marigo, T. C. Wabnitz, D. Fielenbach, K. A. Jørgensen, *Angew. Chem. Int. Ed.* **2005**, *44*, 794–797.
- [117] K. A. Ahrendt, C. J. Borths, D. W. C. MacMillan, *J. Am. Chem. Soc.* **2000**, *122*, 4243–4244.
- [118] F. Löbermann, P. Mayer, D. Trauner, *Angew. Chem. Int. Ed.* **2010**, *49*, 6199–6202.
- [119] H. Irgartinger, B. Stadler, *Eur. J. Org. Chem.* **1998**, *1998*, 605–626.
- [120] H. Iwamoto, A. Takuwa, K. Hamada, R. Fujiwara, *J. Chem. Soc., Perkin Trans. 1* **1999**, 575–582.
- [121] W. E. Noland, B. L. Kedrowski, *J. Org. Chem.* **1998**, *64*, 596–603.
- [122] W. E. Noland, B. L. Kedrowski, *J. Org. Chem.* **2002**, *67*, 8366–8373.
- [123] M. A. Kienzler, S. Suseno, D. Trauner, *J. Am. Chem. Soc.* **2008**, *130*, 8604–8605.
- [124] D. M. Fort, R. P. Ubillas, C. D. Mendez, S. D. Jolad, W. D. Inman, J. R. Carney, J. L. Chen, T. T. Ianiro, C. Hasbun, R. C. Bruening, J. Luo, M. J. Reed, M. Iwu, T. J. Carlson, S. R. King, D. E. Bierer, R. Cooper, *J. Org. Chem.* **2000**, *65*, 6534–6539.
- [125] D. W. Laird, R. Poole, M. Wikstrom, I. A. van Altena, *J. Nat. Prod.* **2007**, *70*, 671–674.
- [126] G. M. da Costa, T. L. G. de Lemos, O. I. D. L. Pessoa, F. J. Q. Monte, R. Braz-Filho, *J. Nat. Prod.* **1999**, *62*, 1044–1045.
- [127] W. J. Robbins, F. Kavanagh, A. Hervey, *PNAS* **1947**, *33*, 171–176.
- [128] D. R. Appleton, C. S. Chuen, M. V. Berridge, V. L. Webb, B. R. Copp, *J. Org. Chem.* **2009**, *74*, 9195–9198.
- [129] Z. Zhang, J. Chen, Z. Yang, Y. Tang, *Org. Lett.* **2010**, *12*, 5554–5557.
- [130] H. Staudinger, J. Meyer, *Helv. Chim. Acta* **1919**, *2*, 635–646.
- [131] J. L. Collins, P. A. Grieco, J. K. Walker, *Tetrahedron Lett.* **1997**, *38*, 1321–1324.
- [132] P. A. Grieco, J. K. Walker, *Tetrahedron* **1997**, *53*, 8975–8996.
- [133] T. Dohi, Y. Hu, T. Kamitanaka, Y. Kita, *Tetrahedron* **2012**, *68*, 8424–8430.
- [134] T. Dohi, Y. Hu, T. Kamitanaka, N. Washimi, Y. Kita, *Org. Lett.* **2011**, *13*, 4814–4817.
- [135] R. F. Heck, *J. Am. Chem. Soc.* **1968**, *90*, 5518–5526.
- [136] R. F. Heck, J. P. Nolley, *J. Org. Chem.* **1972**, *37*, 2320–2322.
- [137] H. A. Dieck, R. F. Heck, *J. Am. Chem. Soc.* **1974**, *96*, 1133–1136.
- [138] T. M. Mizoroki, K.; Ozaki, A., *Bull. Chem. Soc. Jpn.* **1971**, *44*, 581.
- [139] S. Kobayashi, M. Araki, I. Hachiya, *J. Org. Chem.* **1994**, *59*, 3758–3759.
- [140] E. J. Corey, J. W. Suggs, *Tetrahedron Lett.* **1975**, *16*, 2647–2650.
- [141] A. K. Sharma, D. Swern, *Tetrahedron Lett.* **1974**, *15*, 1503–1506.
- [142] A. K. Sharma, T. Ku, A. D. Dawson, D. Swern, *J. Org. Chem.* **1975**, *40*, 2758–2764.
- [143] K. Omura, A. K. Sharma, D. Swern, *J. Org. Chem.* **1976**, *41*, 957–962.
- [144] S. L. Huang, K. Omura, D. Swern, *Synthesis* **1978**, *1978*, 297–299.
- [145] S. L. Huang, D. Swern, *J. Org. Chem.* **1978**, *43*, 4537–4538.
- [146] K. Omura, D. Swern, *Tetrahedron* **1978**, *34*, 1651–1660.
- [147] S. D. Meyer, S. L. Schreiber, *J. Org. Chem.* **1994**, *59*, 7549–7552.
- [148] S. De Munari, M. Frigerio, M. Santagostino, *J. Org. Chem.* **1996**, *61*, 9272–9279.
- [149] A. Hantzsch, *Liebigs Ann. Chem.* **1882**, *215*, 1–82.
- [150] J. K. Nelson, D. J. Burkhart, A. McKenzie, N. R. Natale, *Synlett* **2003**, *2003*, 2213–2215.
- [151] V. N. Telvekar, N. D. Arote, O. P. Herlekar, *Synlett* **2005**, *2005*, 2495–2497.
- [152] K. C. Nicolaou, C. J. N. Mathison, *Angew. Chem. Int. Ed.* **2005**, *44*, 5992–5997.
- [153] H. Ma, S. Wu, Q. Sun, H. Li, Y. Chen, W. Zhao, B. Ma, Q. Guo, Z. Lei, J. Yan, *Synthesis* **2010**, *2010*, 3295–3300.

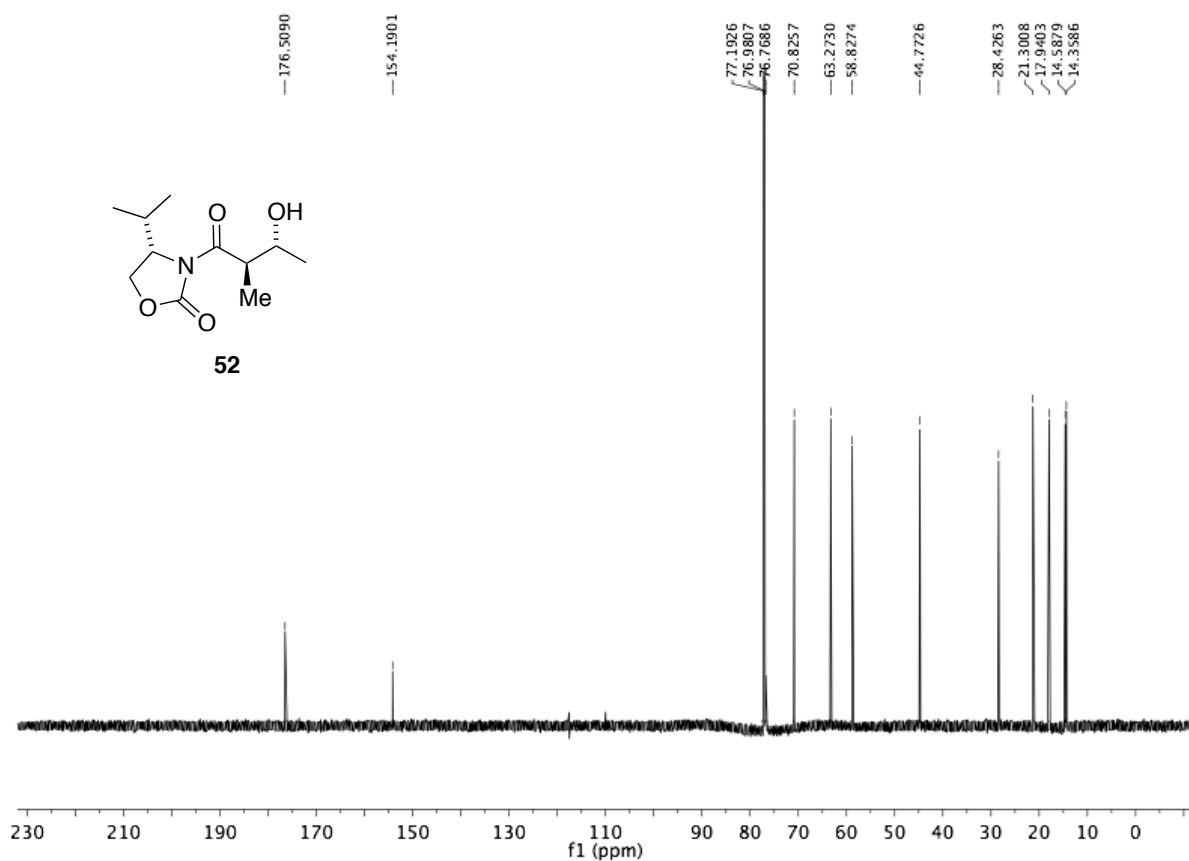
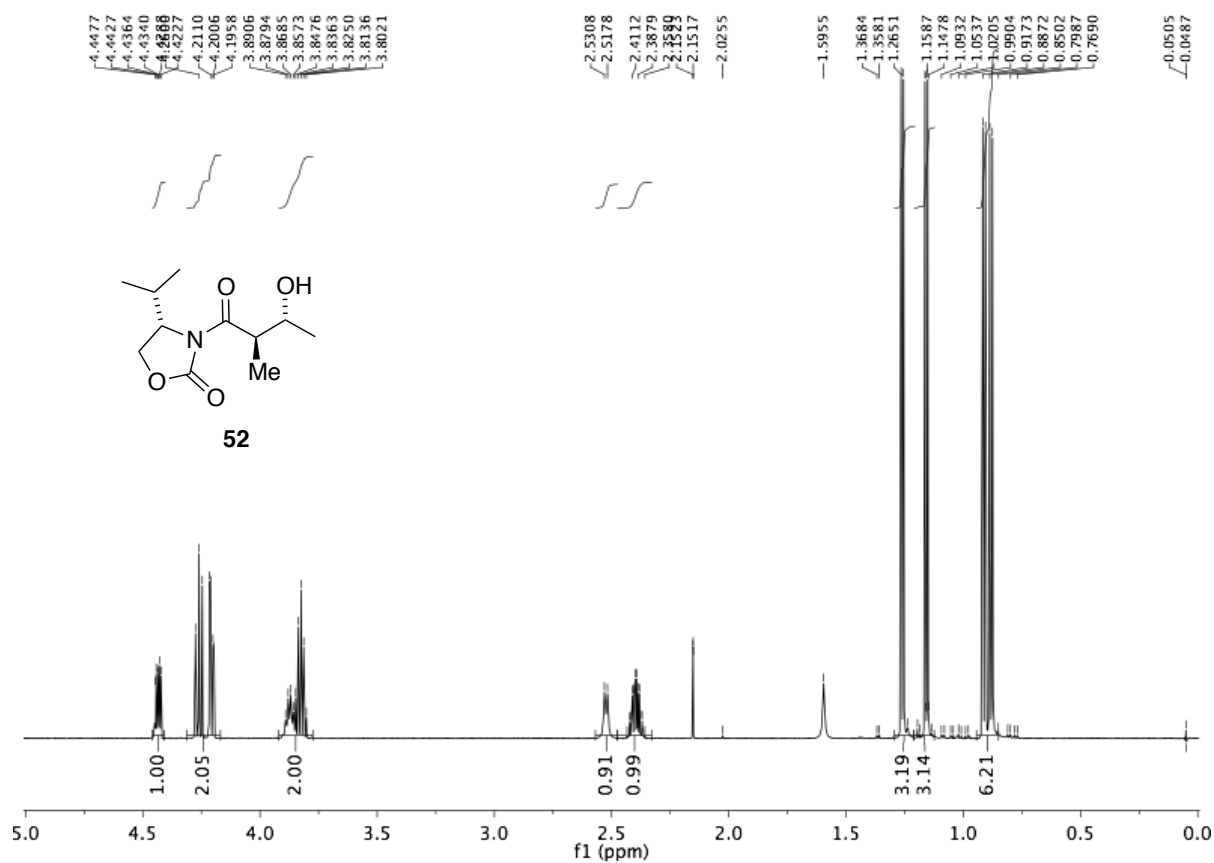
- [154] P. D. Salgaonkar, V. G. Shukla, K. G. Akamanchi, *Synth. Commun.* **2007**, *37*, 275–280.
- [155] M. Frigerio, M. Santagostino, S. Sputore, *J. Org. Chem.* **1999**, *64*, 4537–4538.
- [156] R. E. Ireland, L. B. Liu, *J. Org. Chem.* **1993**, *58*, 2899–2899.
- [157] J. Z. Gougoutas, J. C. Clardy, *J. Solid State Chem.* **1972**, *4*, 226–229.
- [158] P. J. Stevenson, A. B. Treacy, M. Nieuwenhuyzen, *J. Chem. Soc. Perkin Trans. 2* **1997**, 589–591.
- [159] L. Pauling, *The Nature of the Chemical Bond 3rd ed.*, 3 ed., Cornell University Press, New York, **1960**.
- [160] A. Bondi, *J. Phys. Chem.* **1964**, *68*, 441–451.
- [161] P. Politzer, P. Lane, M. C. Concha, Y. G. Ma, J. S. Murray, *J. Mol. Model.* **2007**, *13*, 305–311.
- [162] G. A. Stergioudis, S. C. Kokkou, A. P. Bozopoulos, P. J. Rentzeperis, *Acta Crystallogr. Sect. C: Cryst. Struct. Commun.* **1984**, *40*, 877–879.
- [163] N. W. Alcock, W. D. Harrison, C. Howes, *J. Chem. Soc. Dalton Trans.* **1984**, 1709–1716.
- [164] M. Ochiai, Y. Takaoka, Y. Masaki, Y. Nagao, M. Shiro, *J. Am. Chem. Soc.* **1990**, *112*, 5677–5678.
- [165] V. V. Zhdankin, O. Maydanovych, J. Herschbach, R. McDonald, R. R. Tykwinski, *J. Am. Chem. Soc.* **2002**, *124*, 11614–11615.
- [166] R. D. Richardson, J. M. Zayed, S. Altermann, D. Smith, T. Wirth, *Angew. Chem. Int. Ed.* **2007**, *46*, 6529–6532.
- [167] A. K. Miller, C. C. Hughes, J. J. Kennedy-Smith, S. N. Gradl, D. Trauner, *J. Am. Chem. Soc.* **2006**, *128*, 17057–17062.
- [168] P. Metrangolo, F. Meyer, T. Pilati, G. Resnati, G. Terraneo, *Angew. Chem. Int. Ed.* **2008**, *47*, 6114–6127.
- [169] M. C. Etter, J. C. Macdonald, J. Bernstein, *Acta Crystallogr. Sect. B: Struct. Sci.* **1990**, *46*, 256–262.
- [170] Gougouta, J. Z., J. C. Clardy, *J. Solid State Chem.* **1972**, *4*, 226–229.
- [171] W. C. Still, Still W C, United States, **1981**.
- [172] C.-D. Lu, A. Zakarian, *Organic Syntheses* **2008**, *85*, 158–171.
- [173] J. M. Hernández-Torres, J. Achkar, A. Wei, *J. Org. Chem.* **2004**, *69*, 7206–7211.
- [174] H. Sun, W. R. Roush, *Organic Syntheses* **2008**, *88*, 181–196.
- [175] M. Lautens, M. L. Maddess, E. L. O. Sauer, S. G. Ouellet, *Org. Lett.* **2001**, *4*, 83–86.
- [176] J. Marshall, A., H. Chobanian, *Organic Syntheses* **2005**, *82*, 43–54.

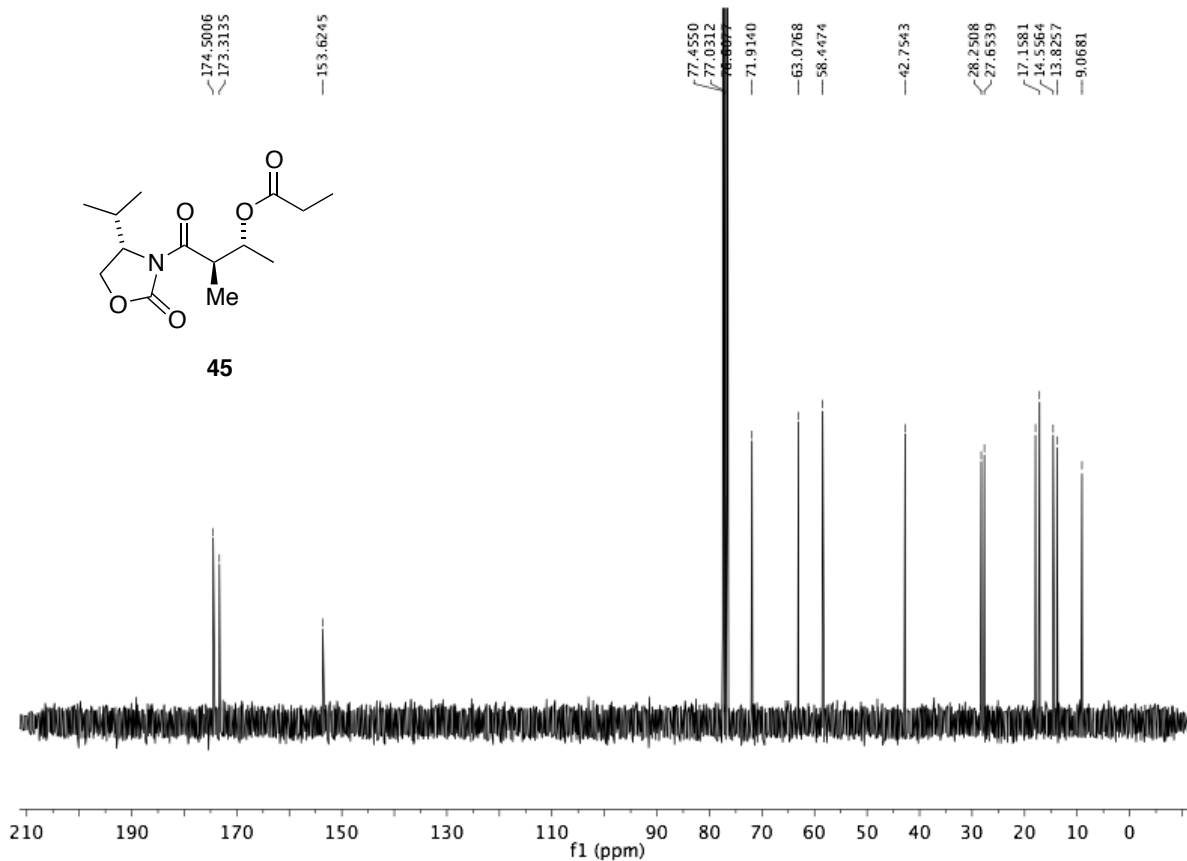
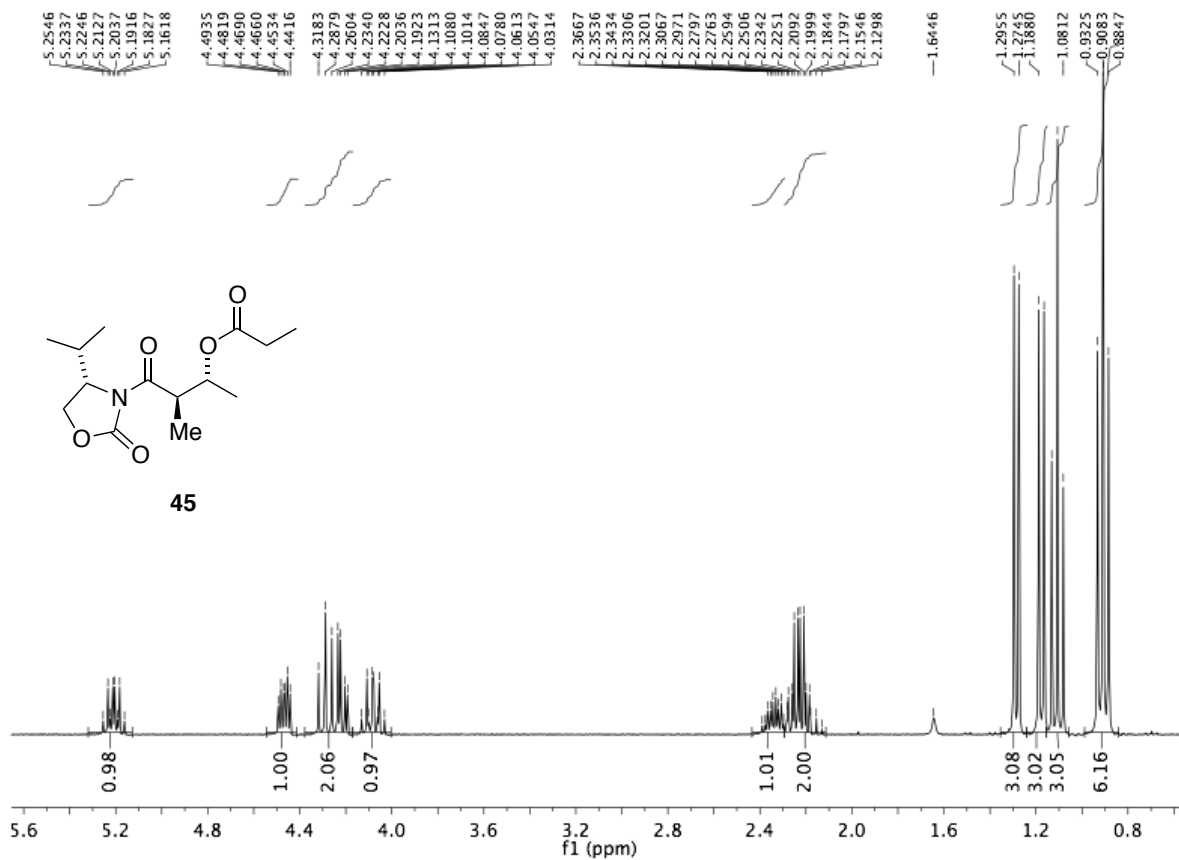
# APPENDIX

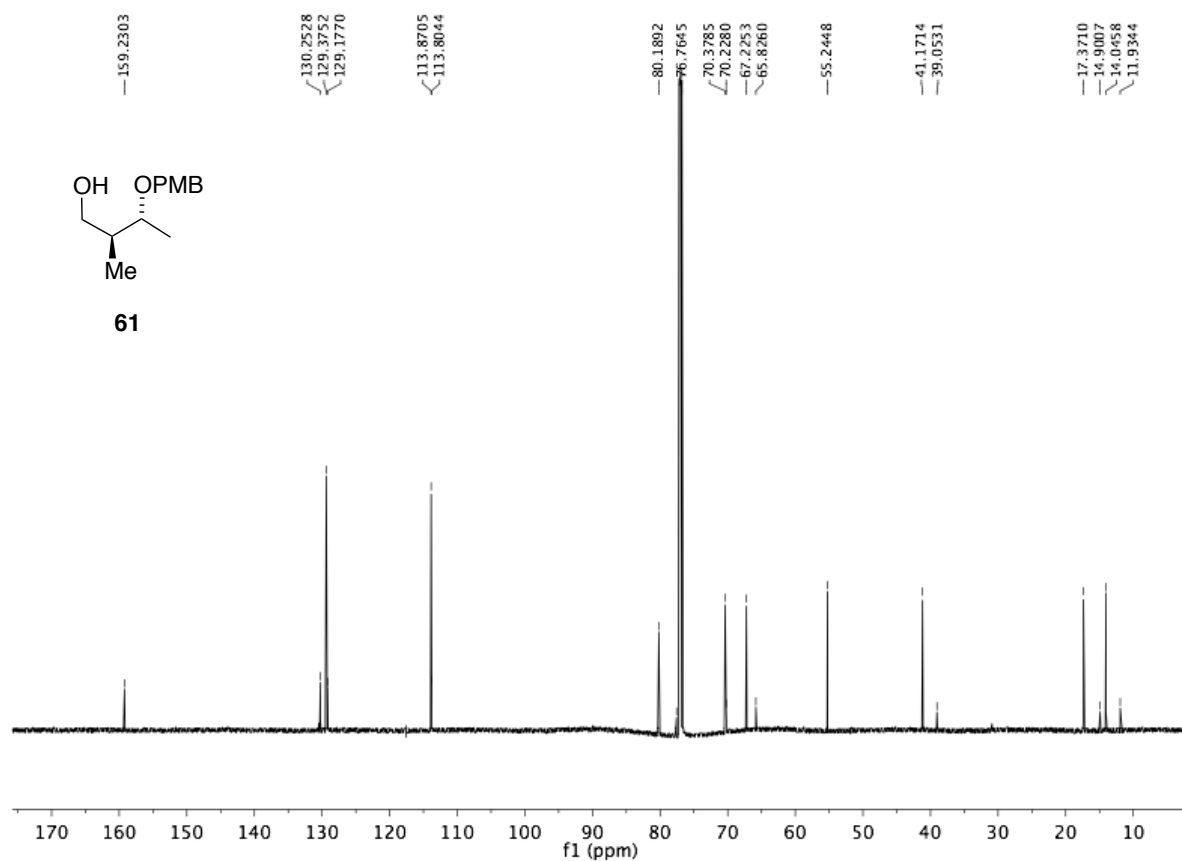
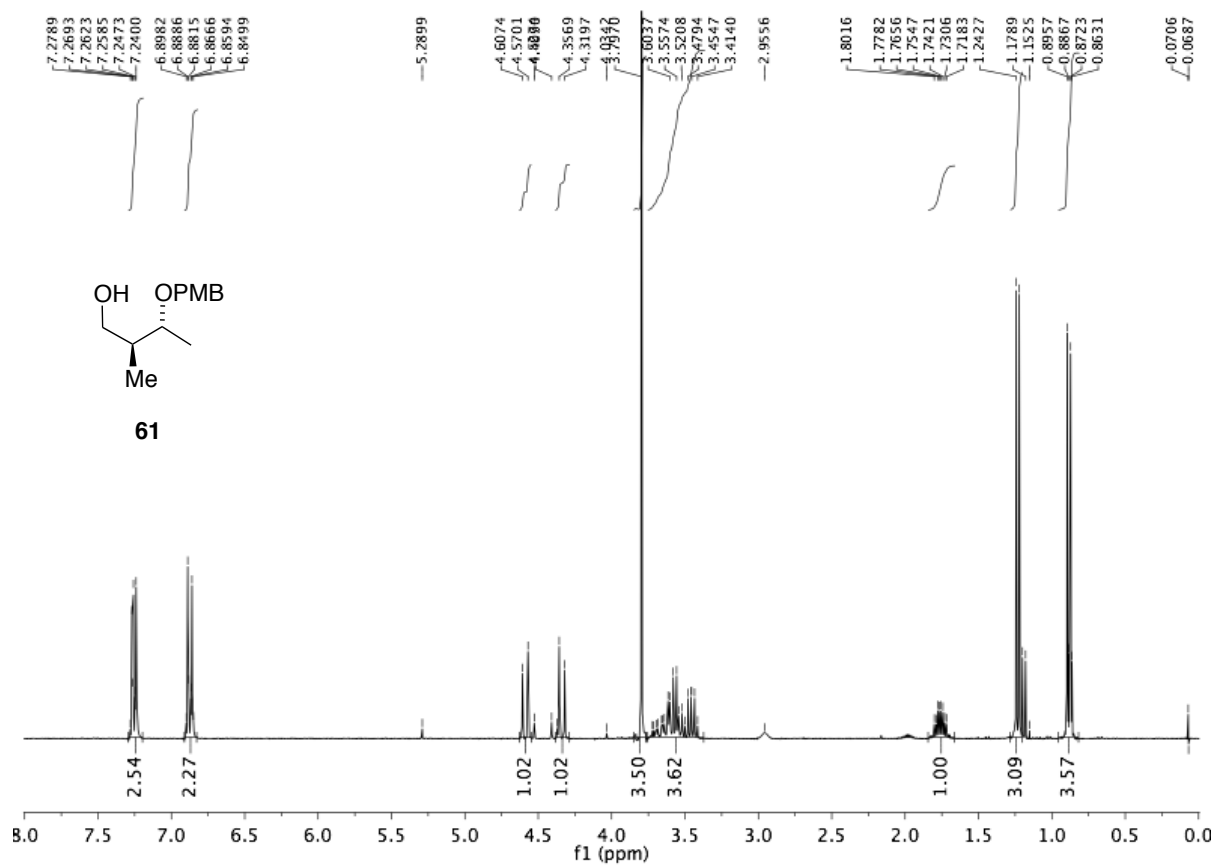


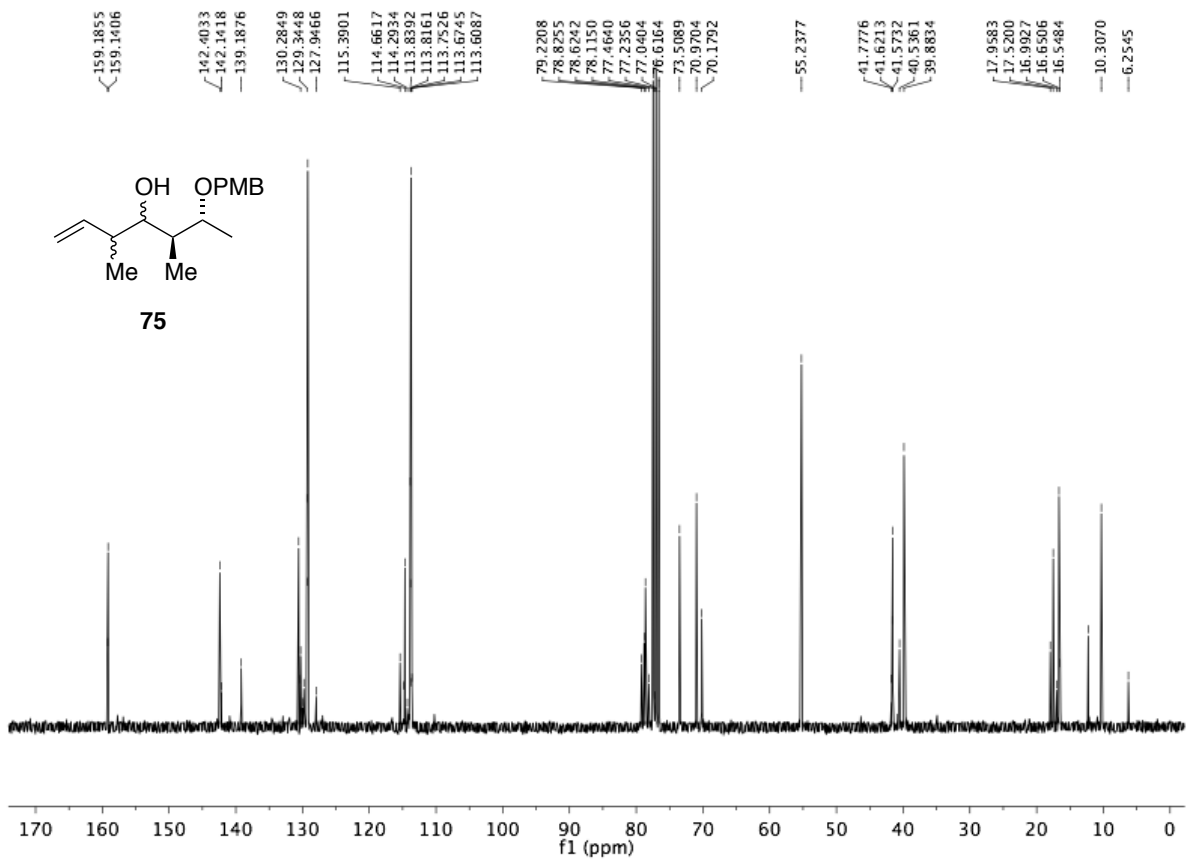
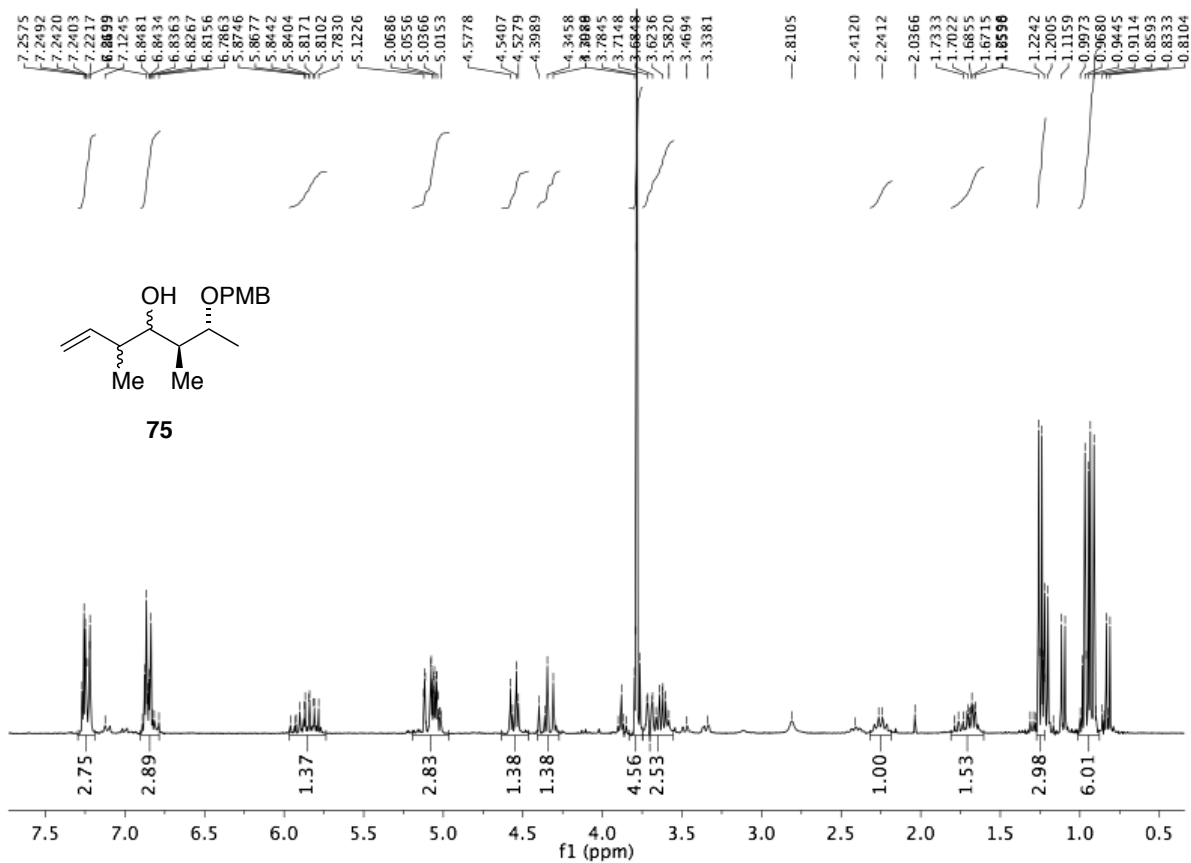


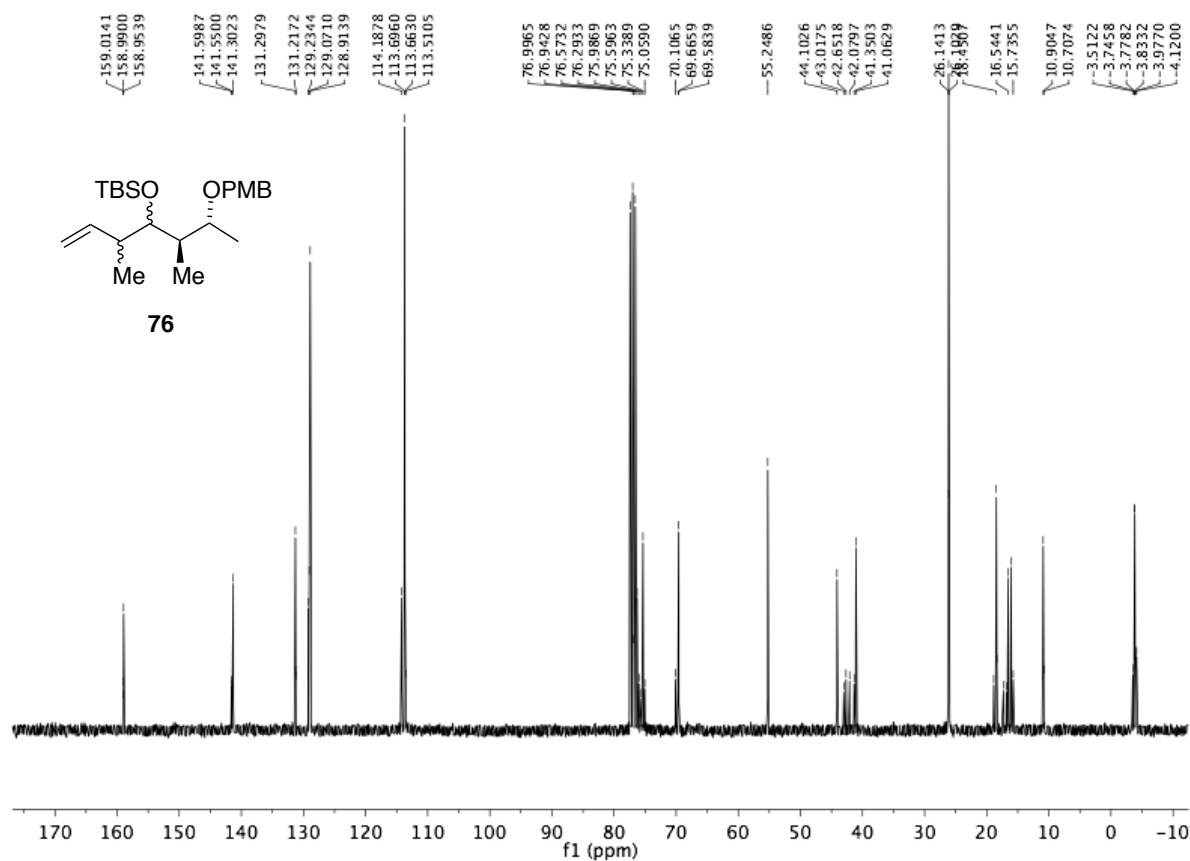
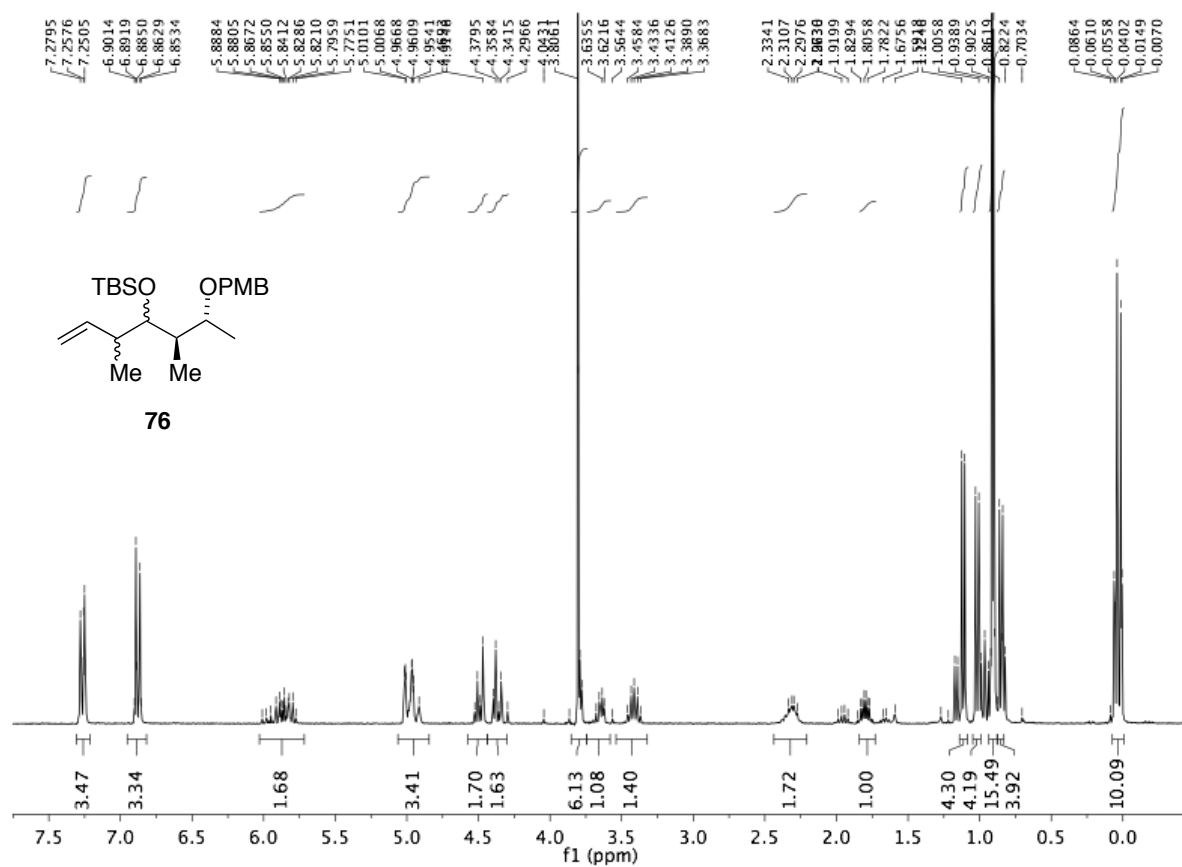


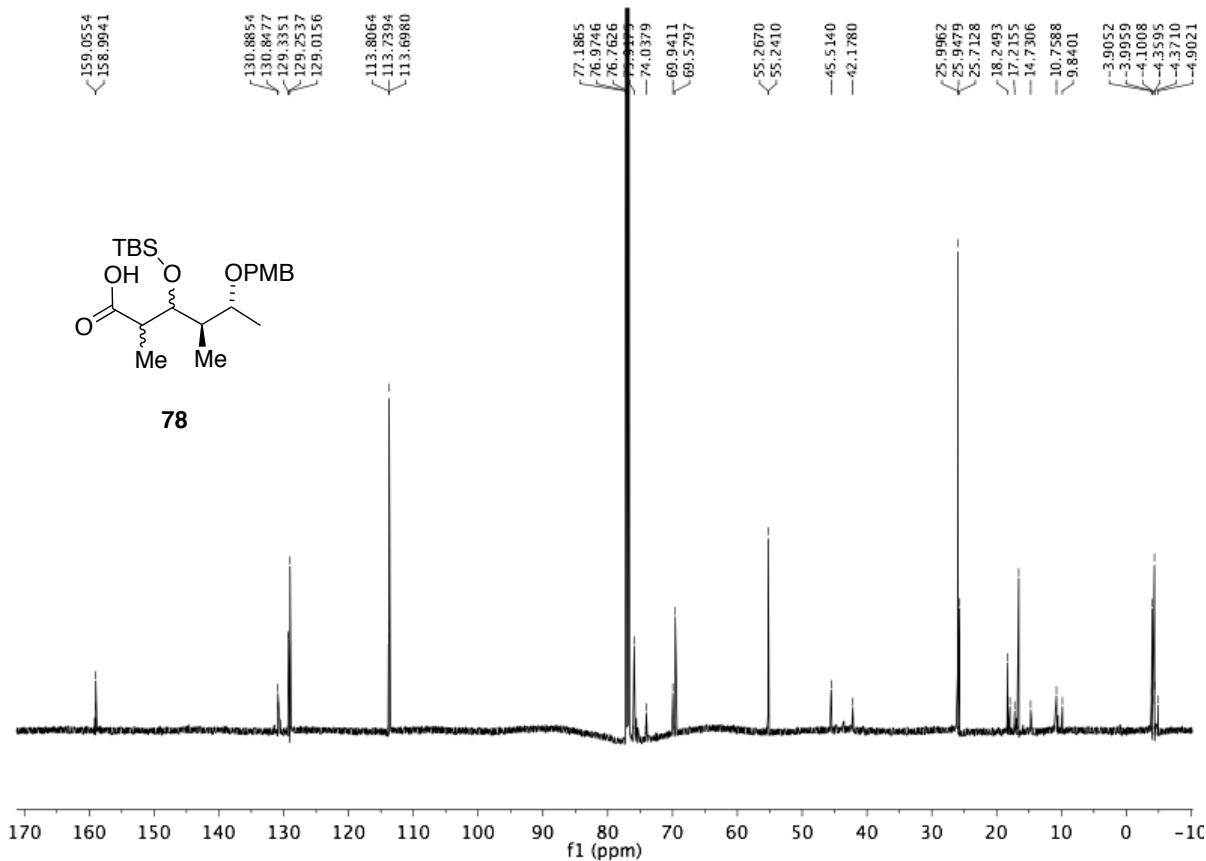
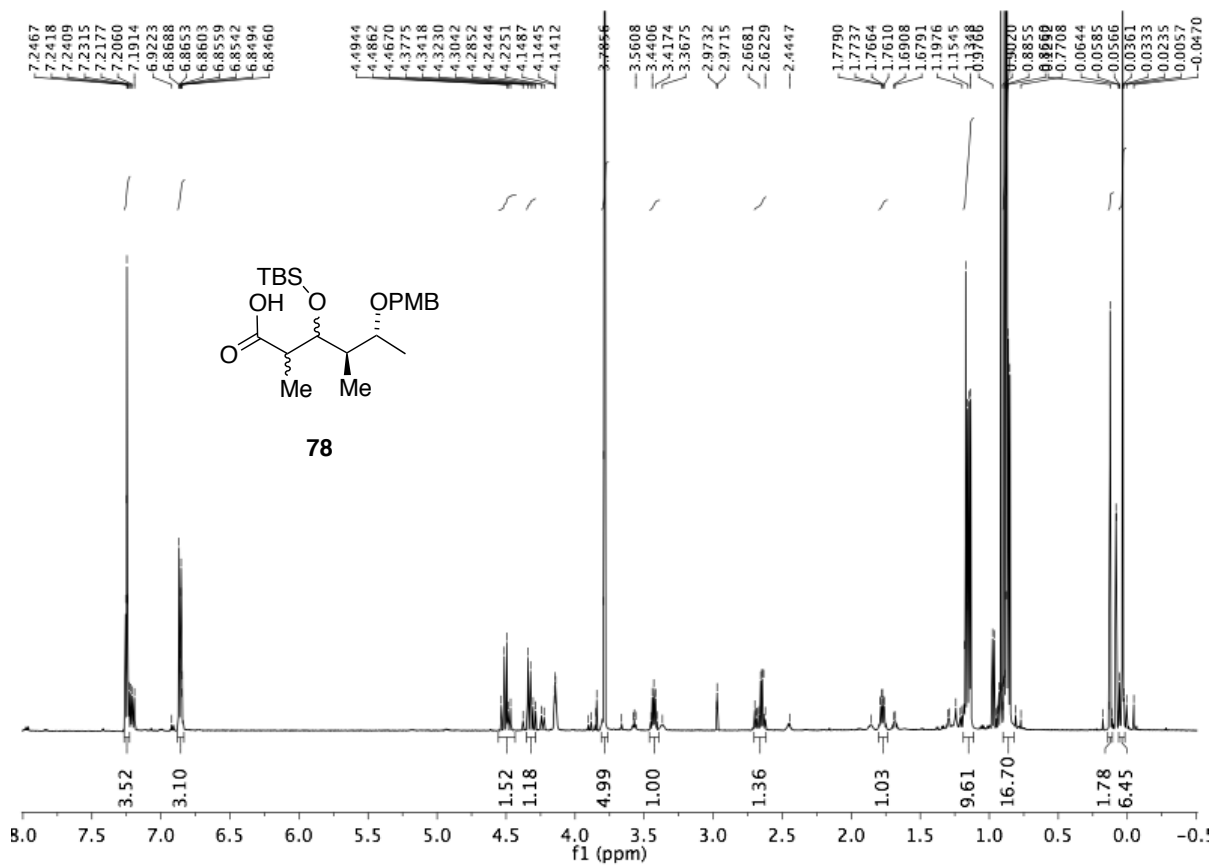


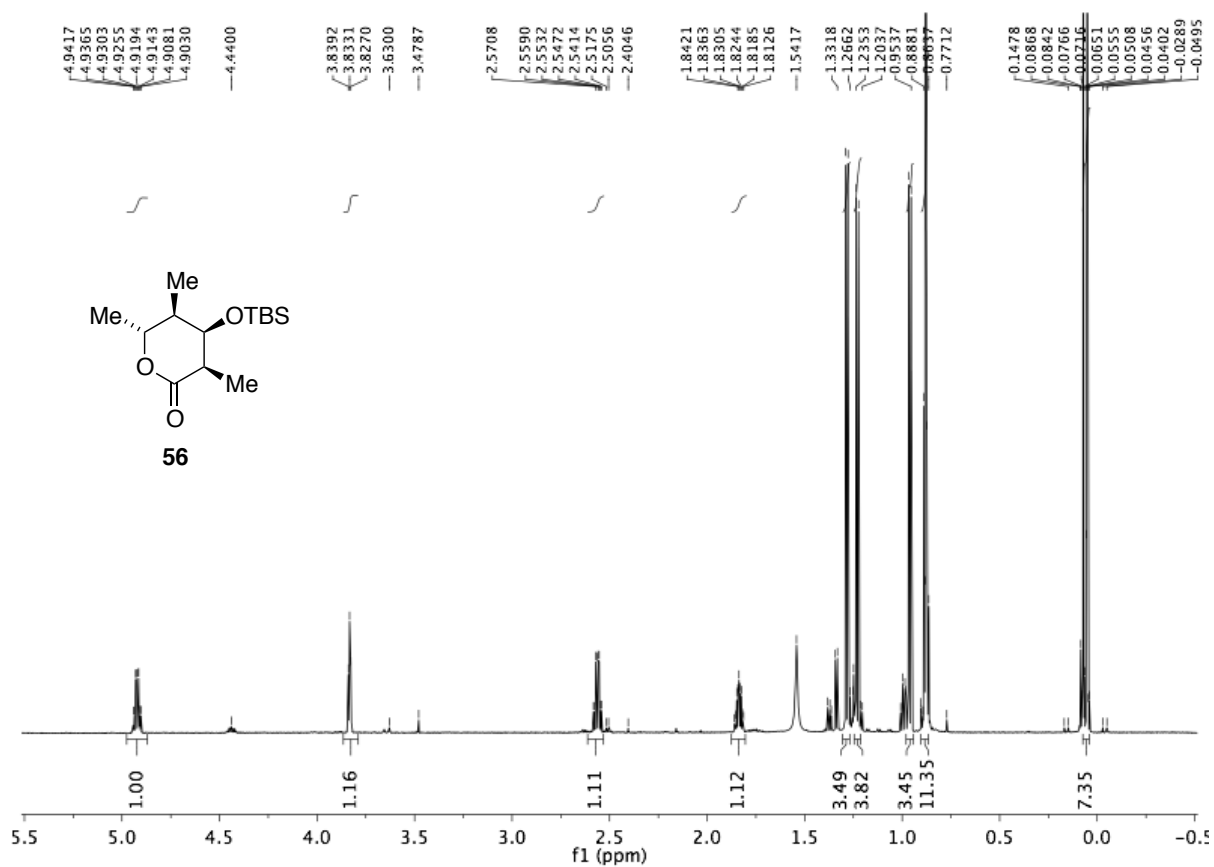


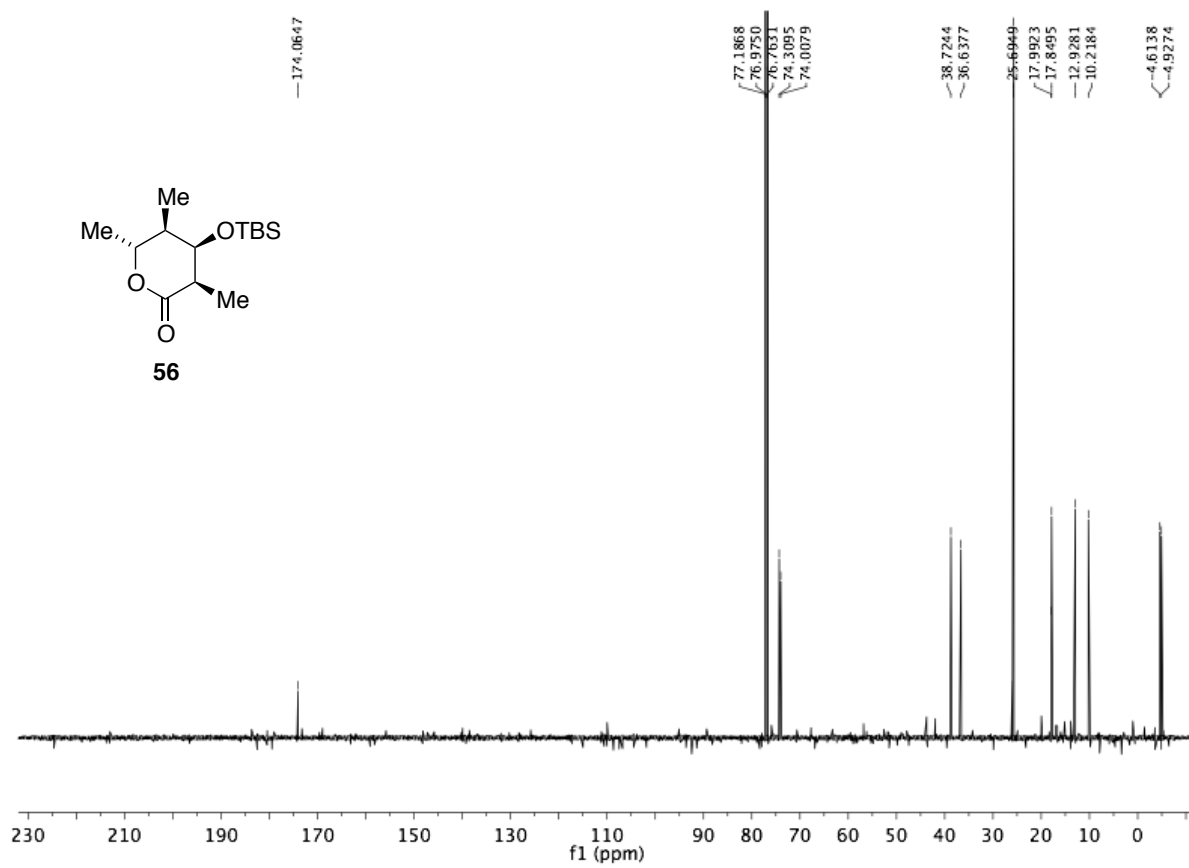


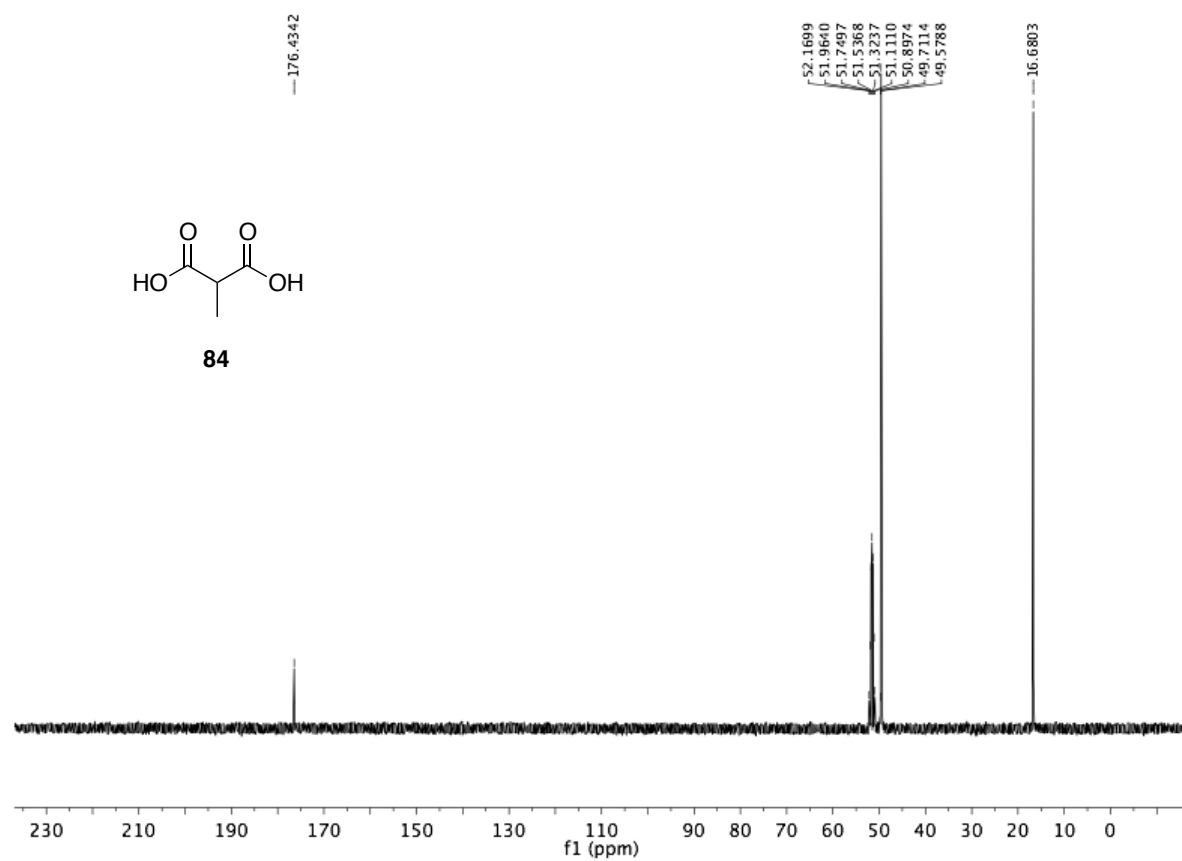
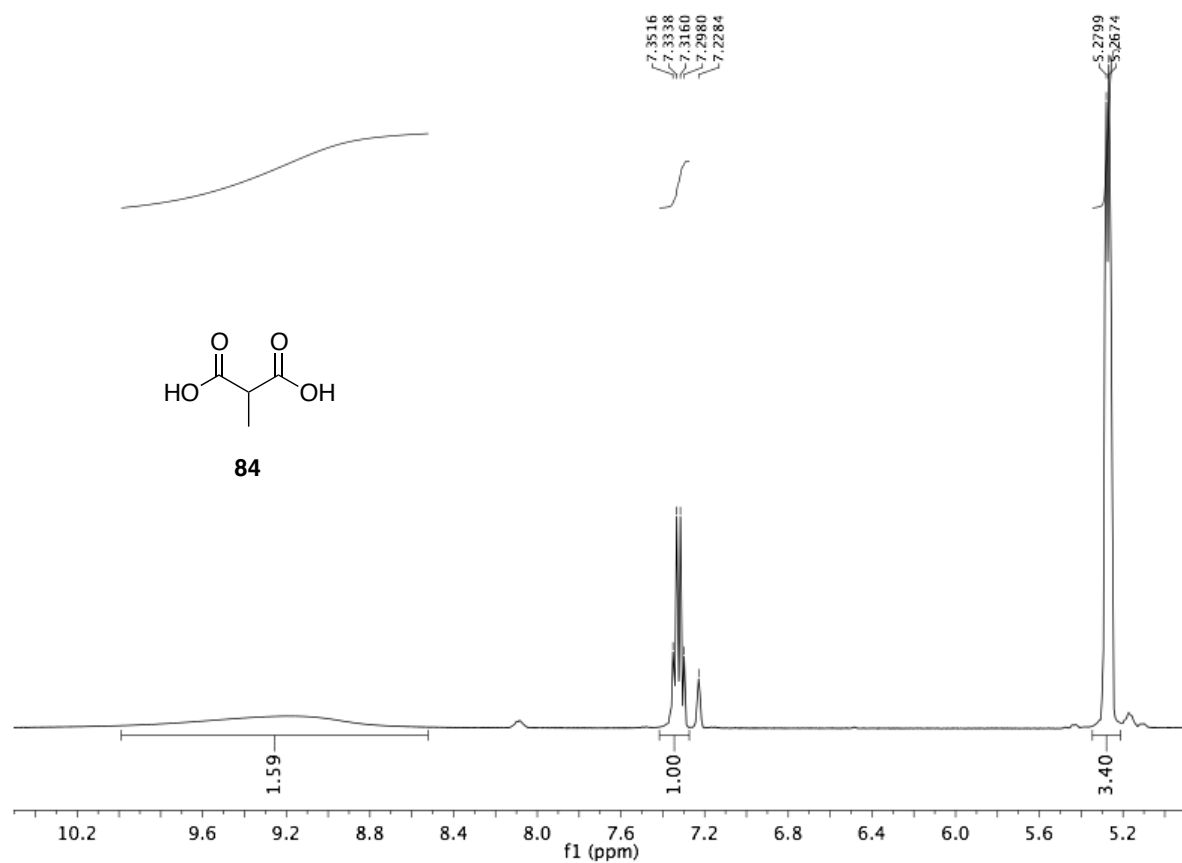


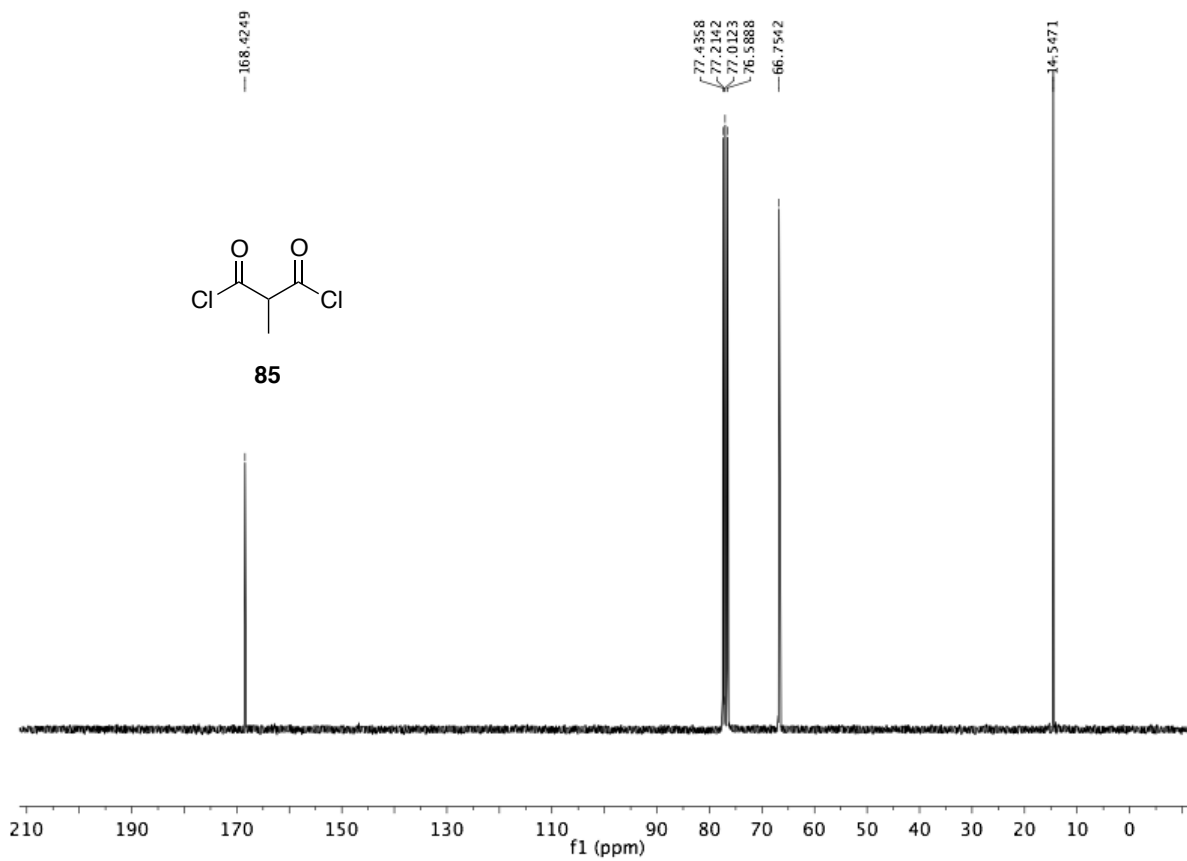
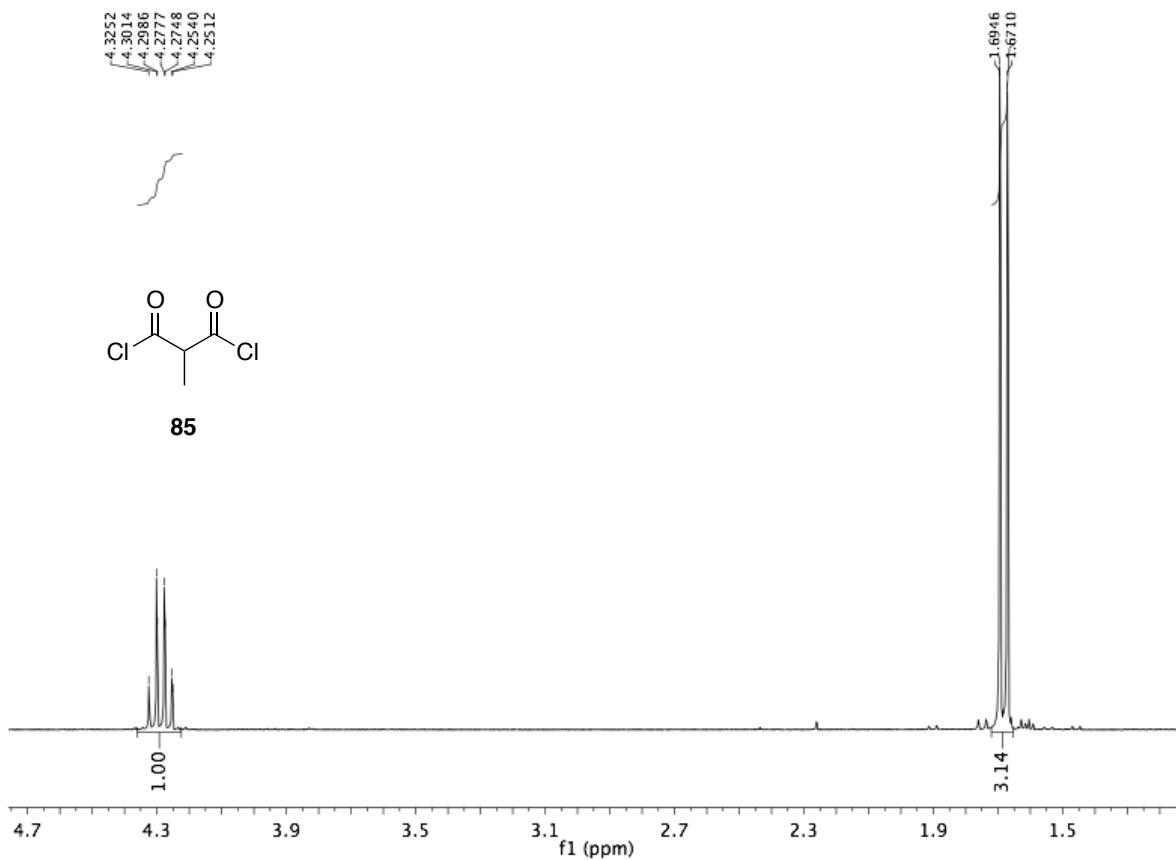


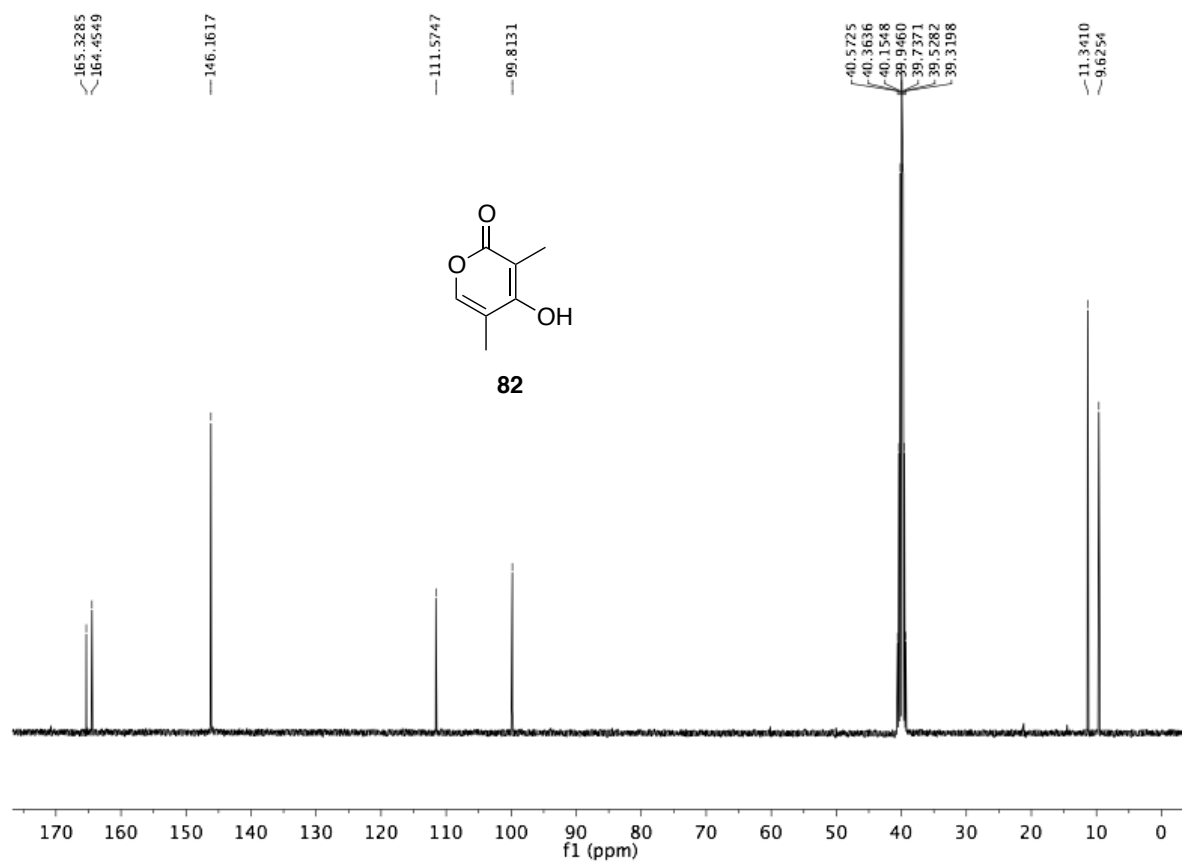
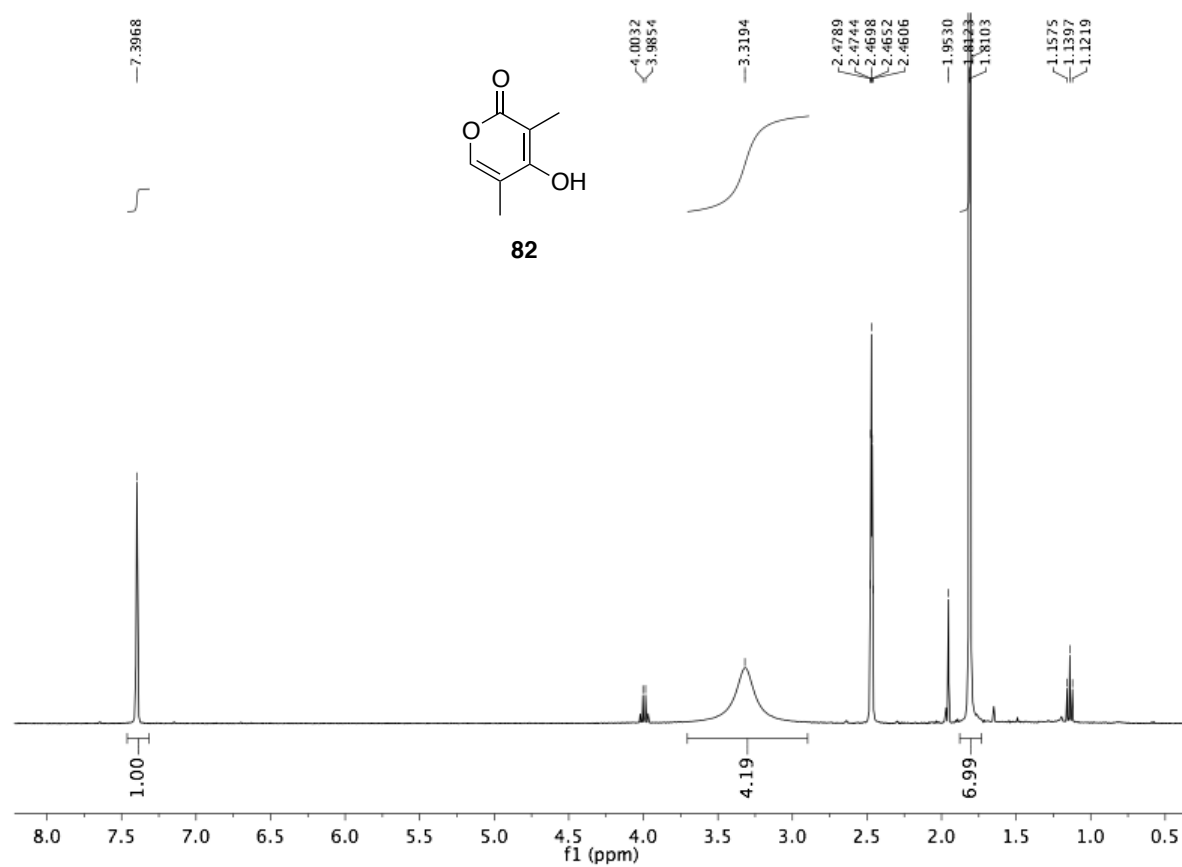


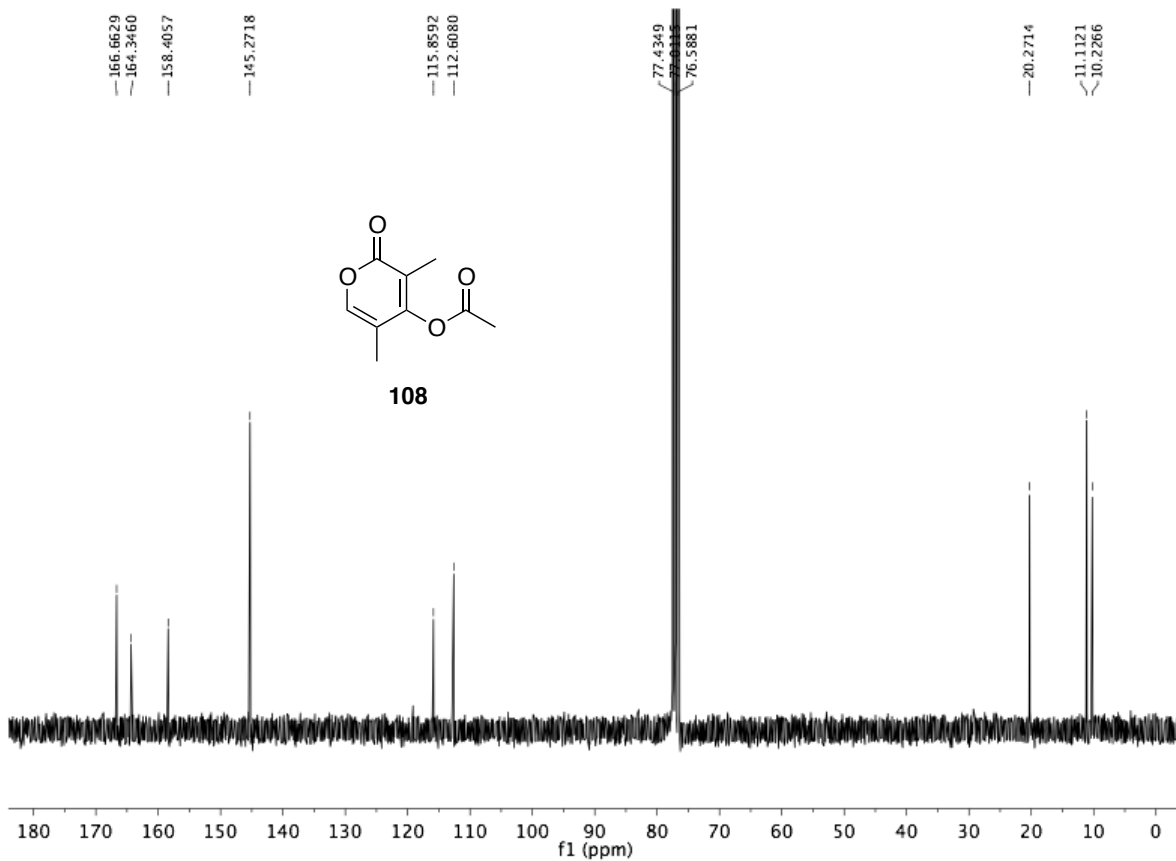
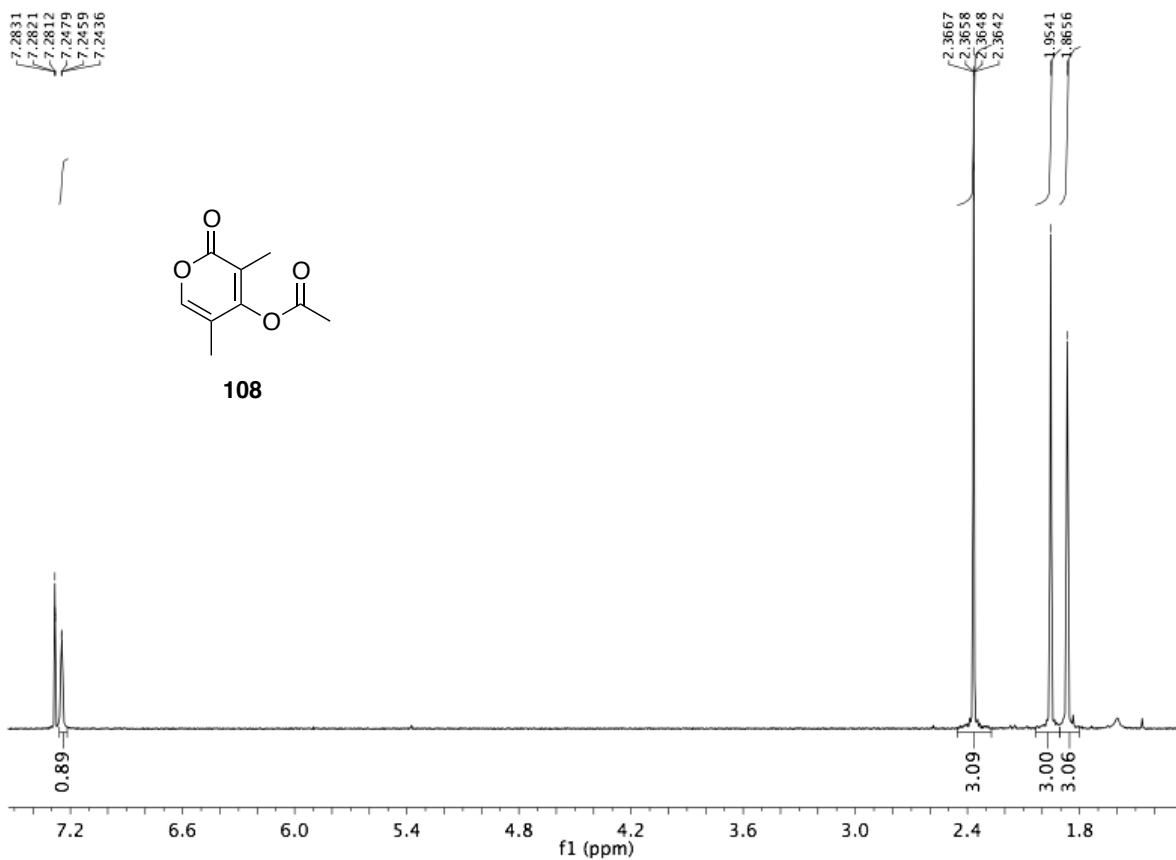


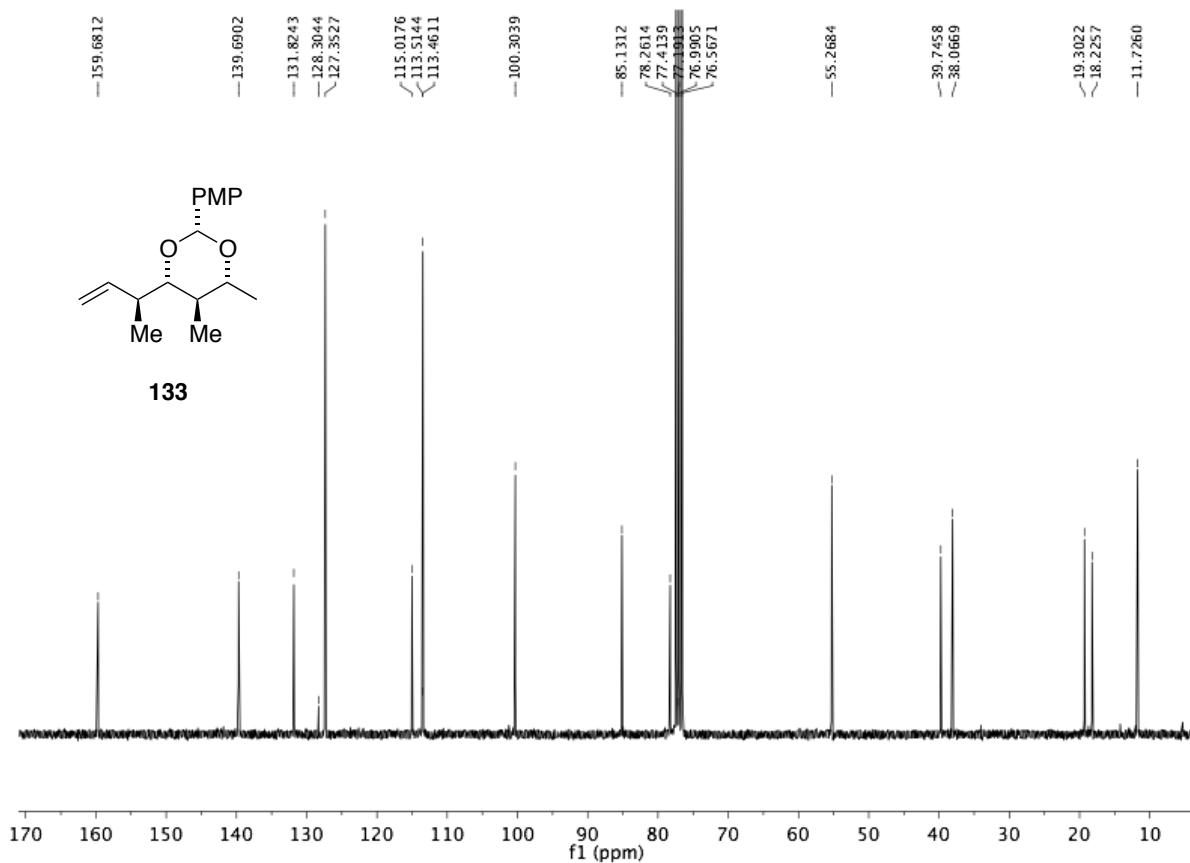
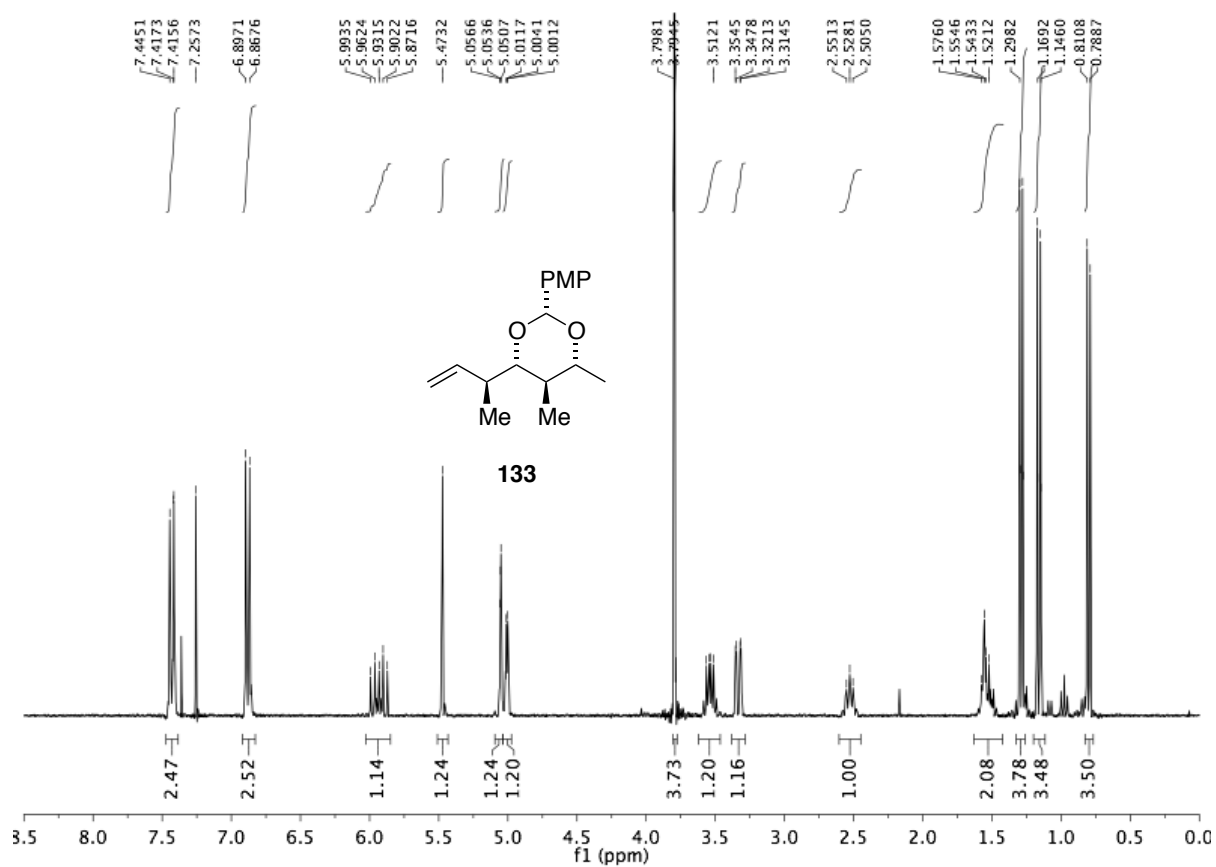


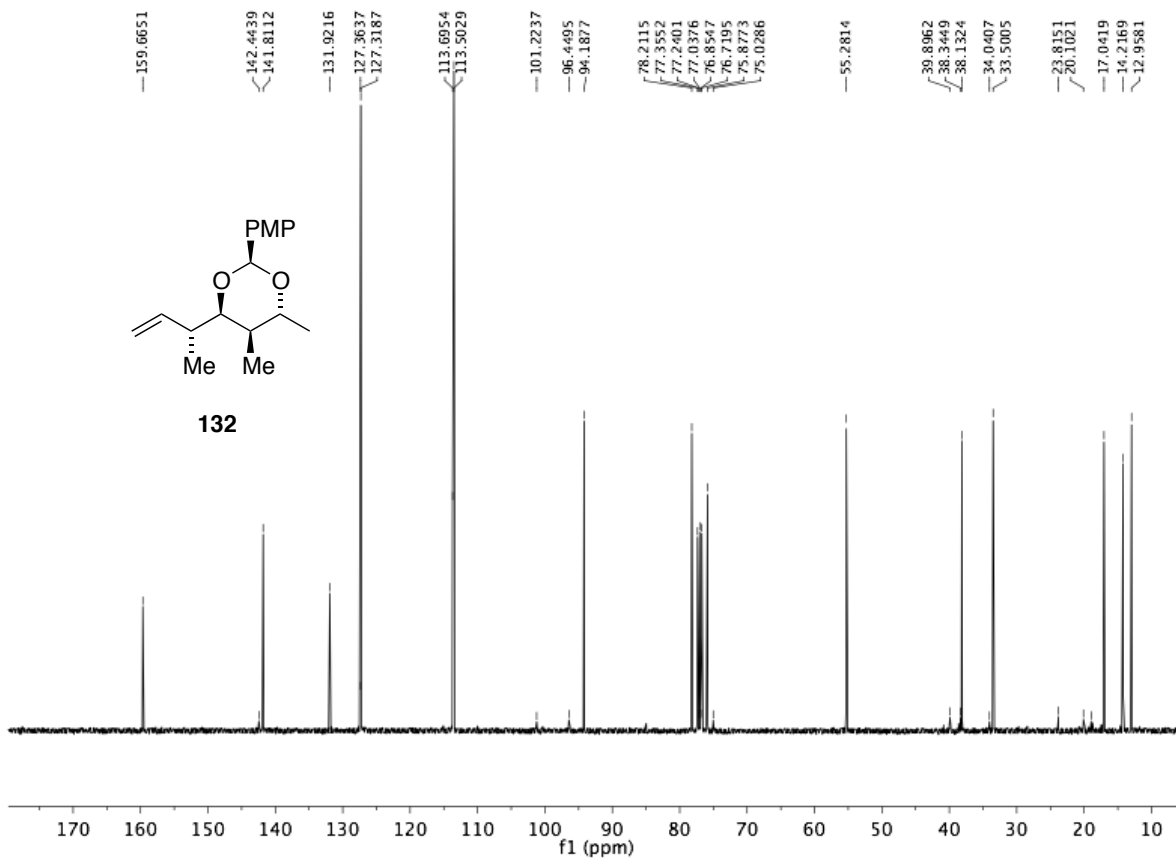
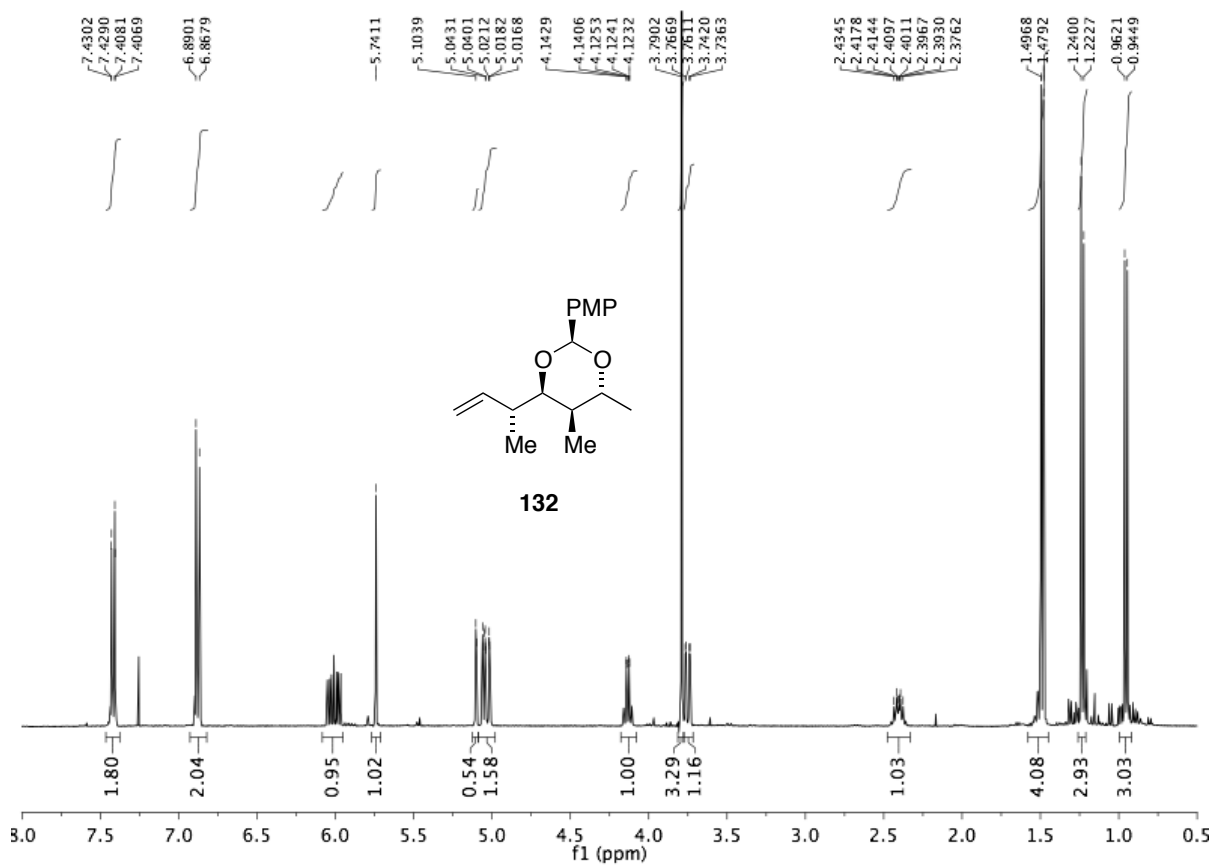


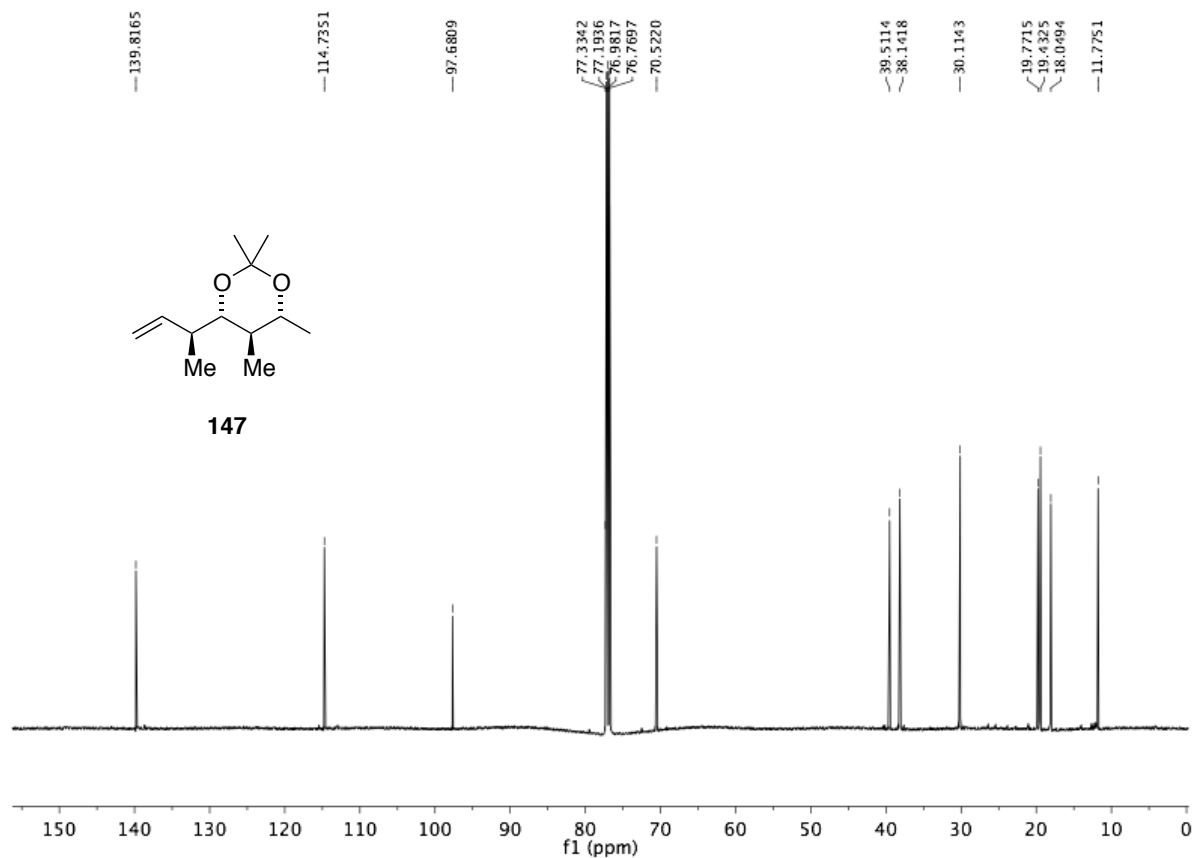
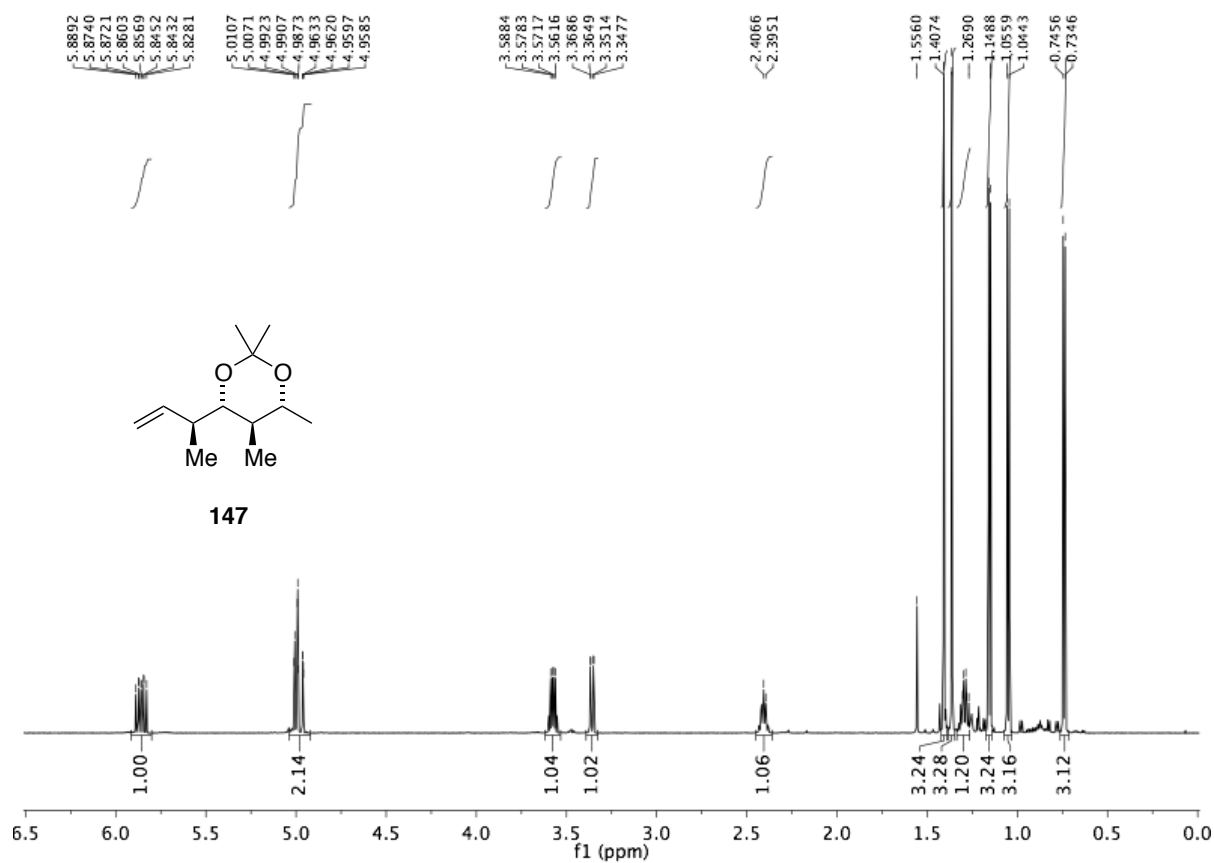


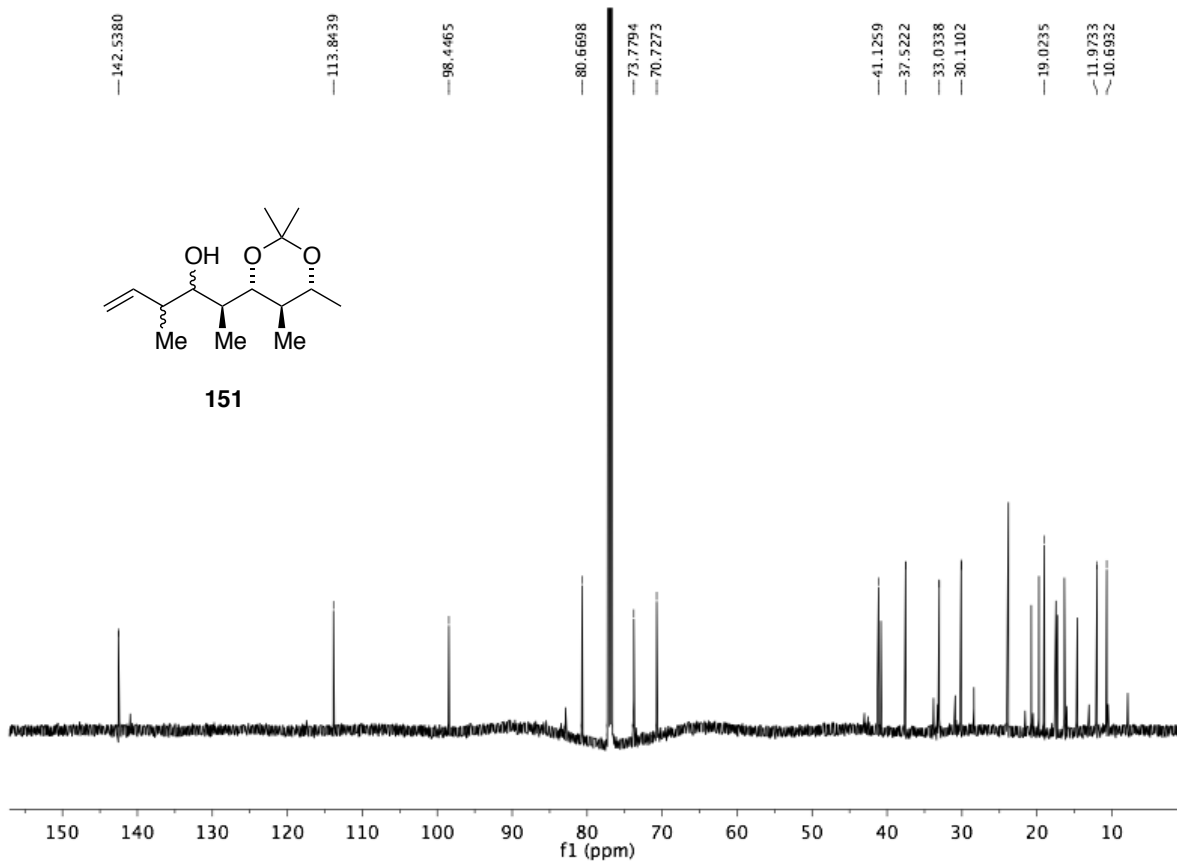
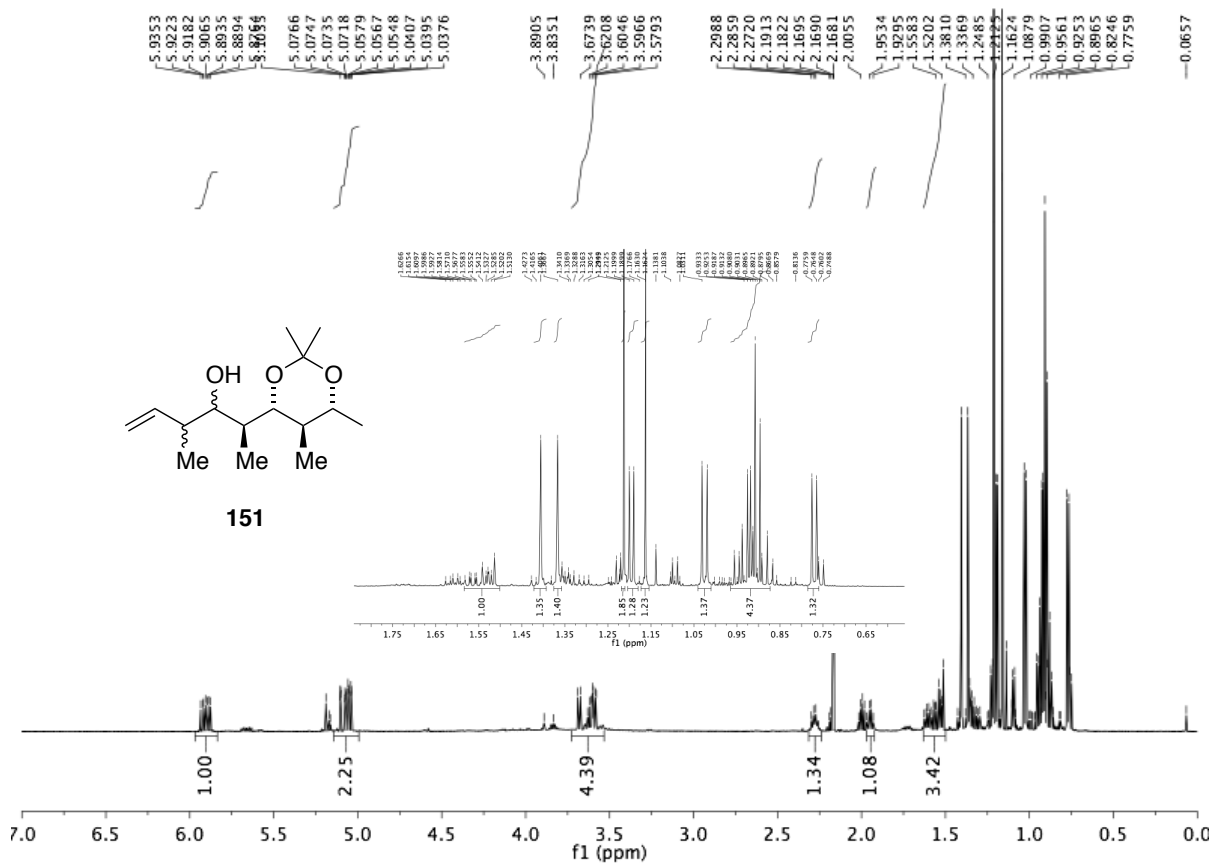


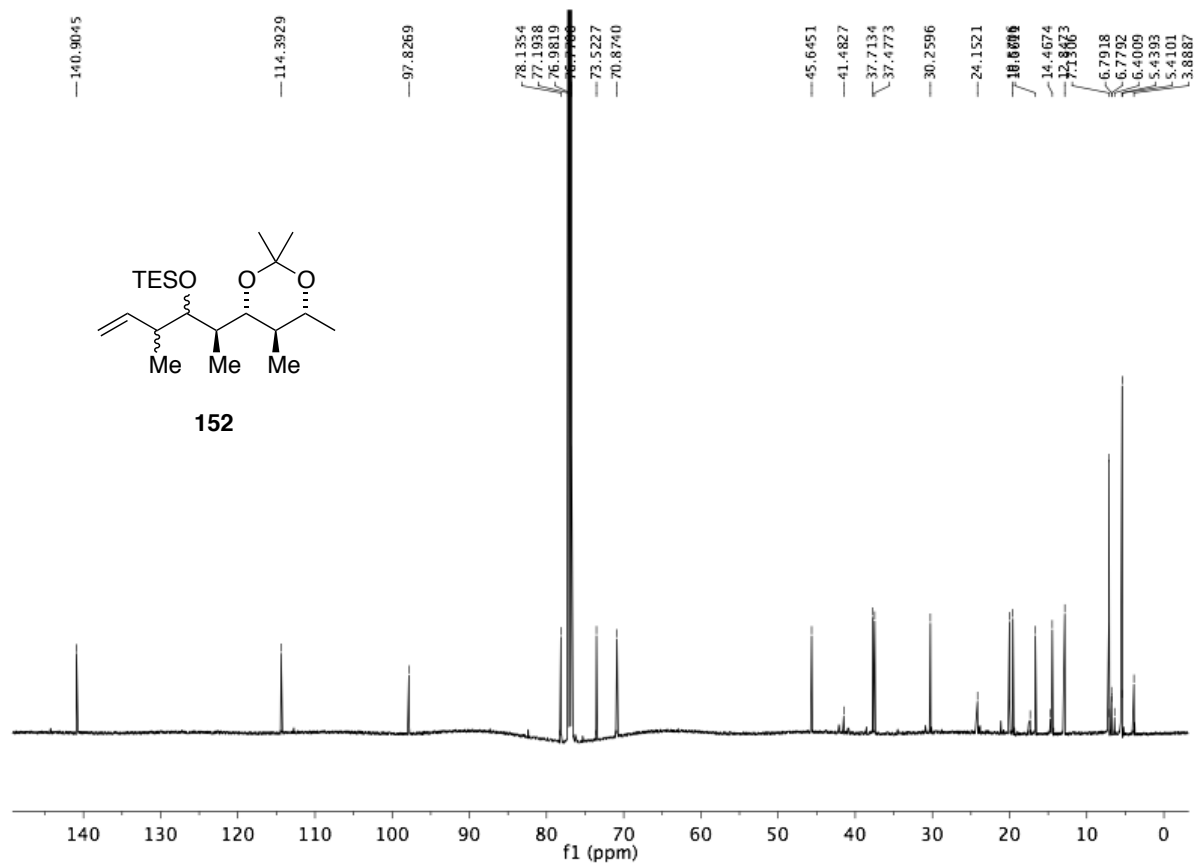
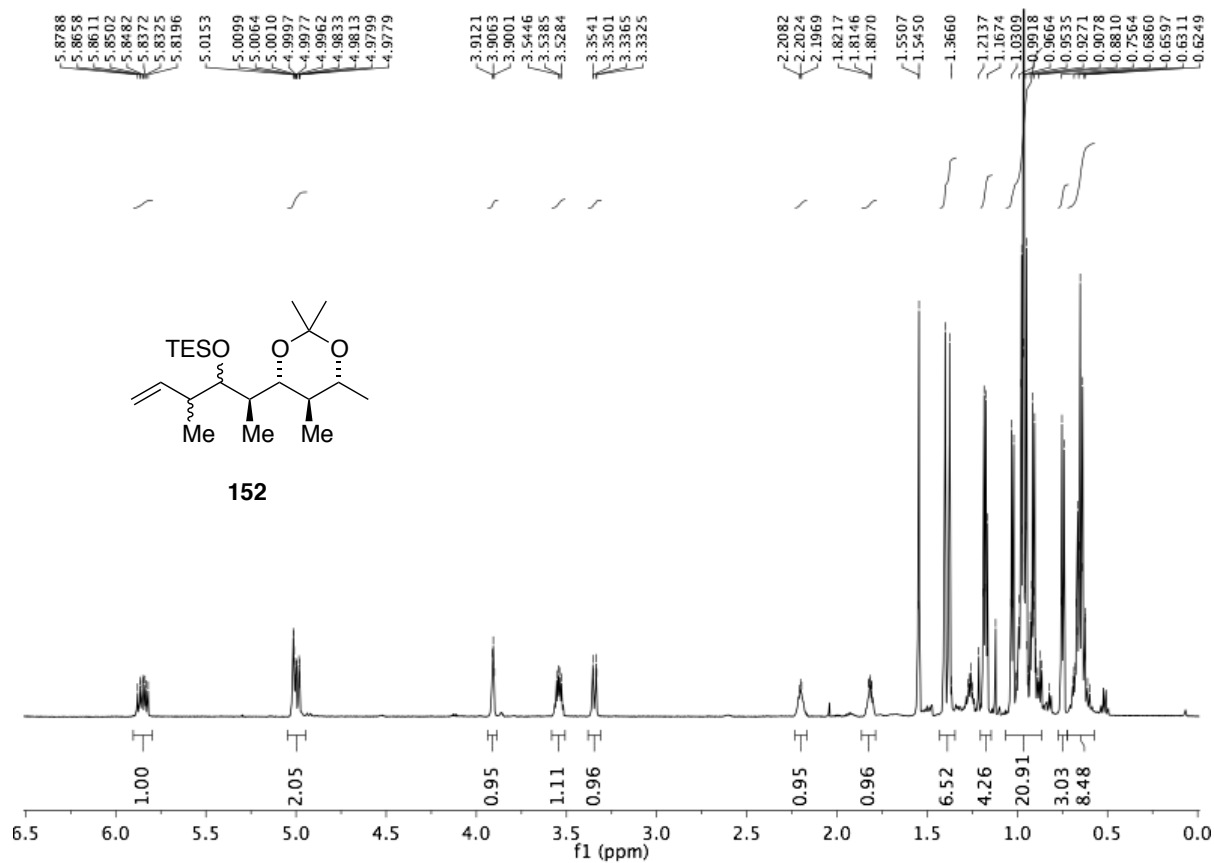


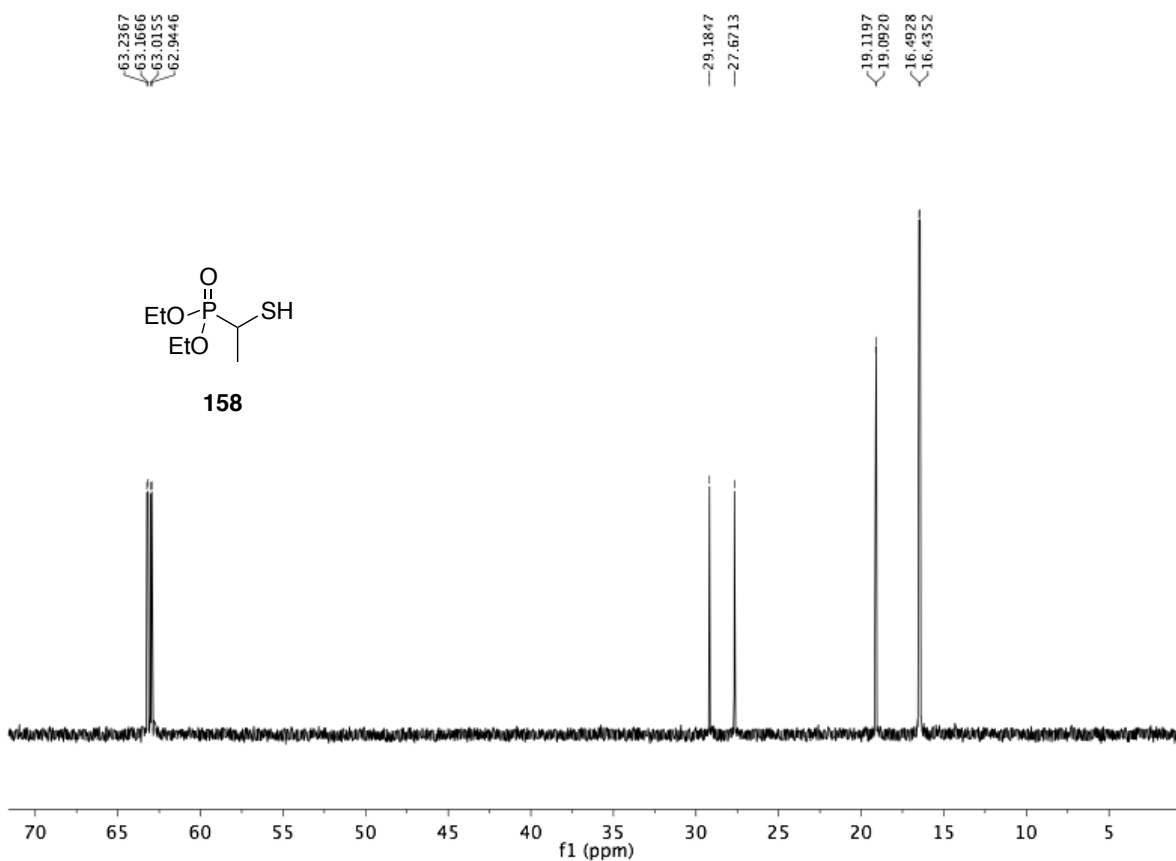
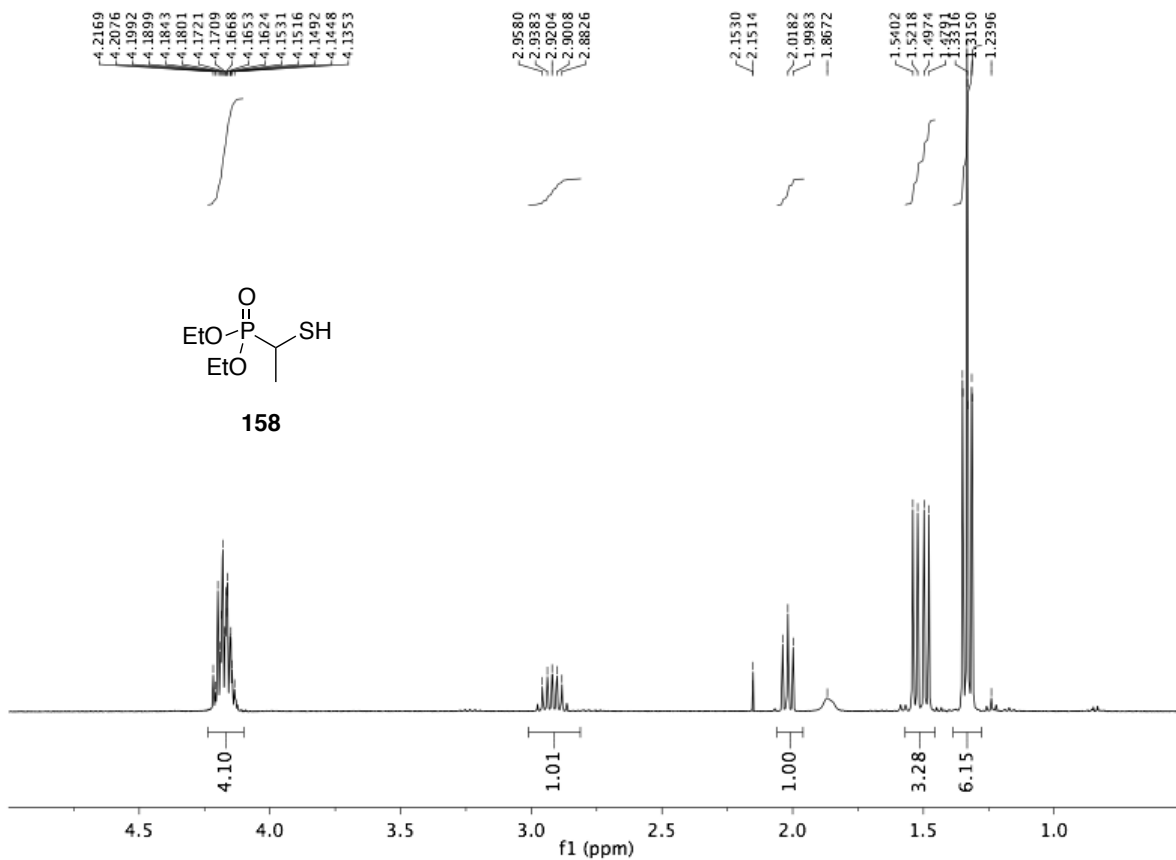


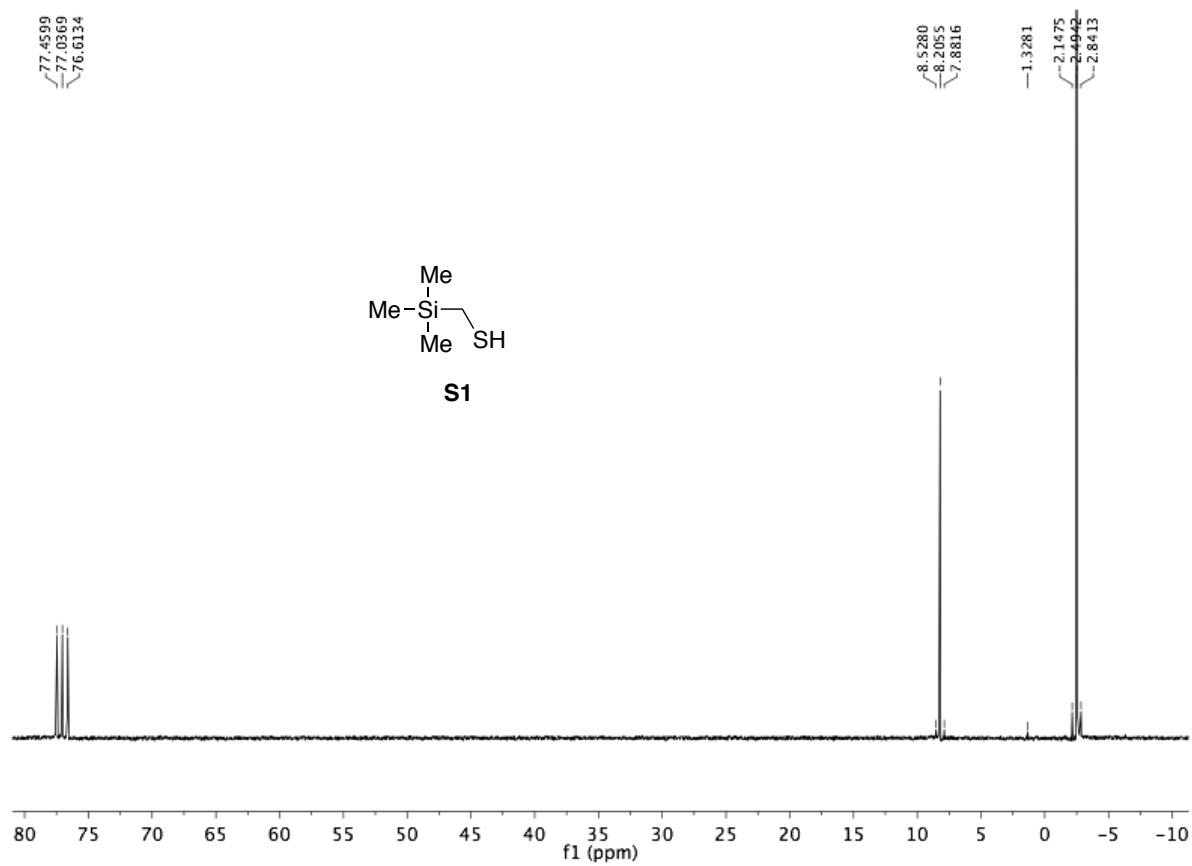
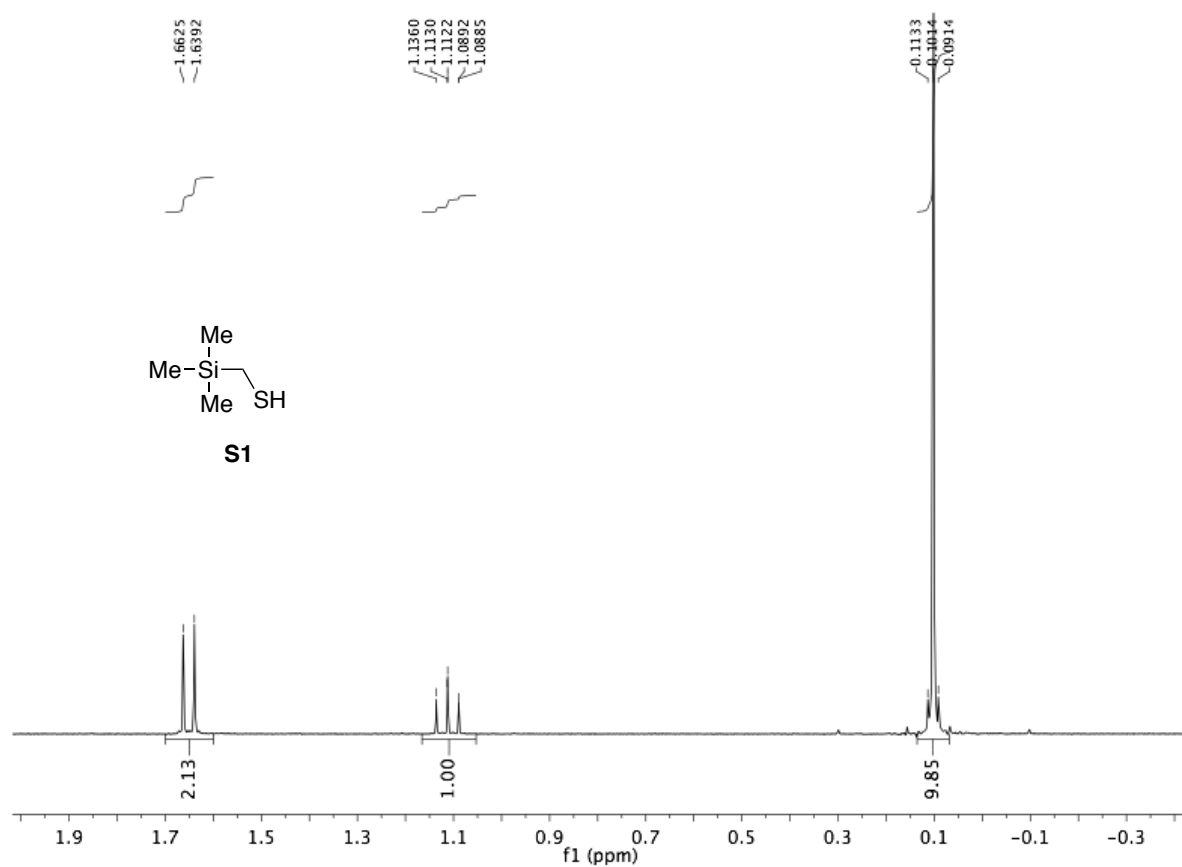


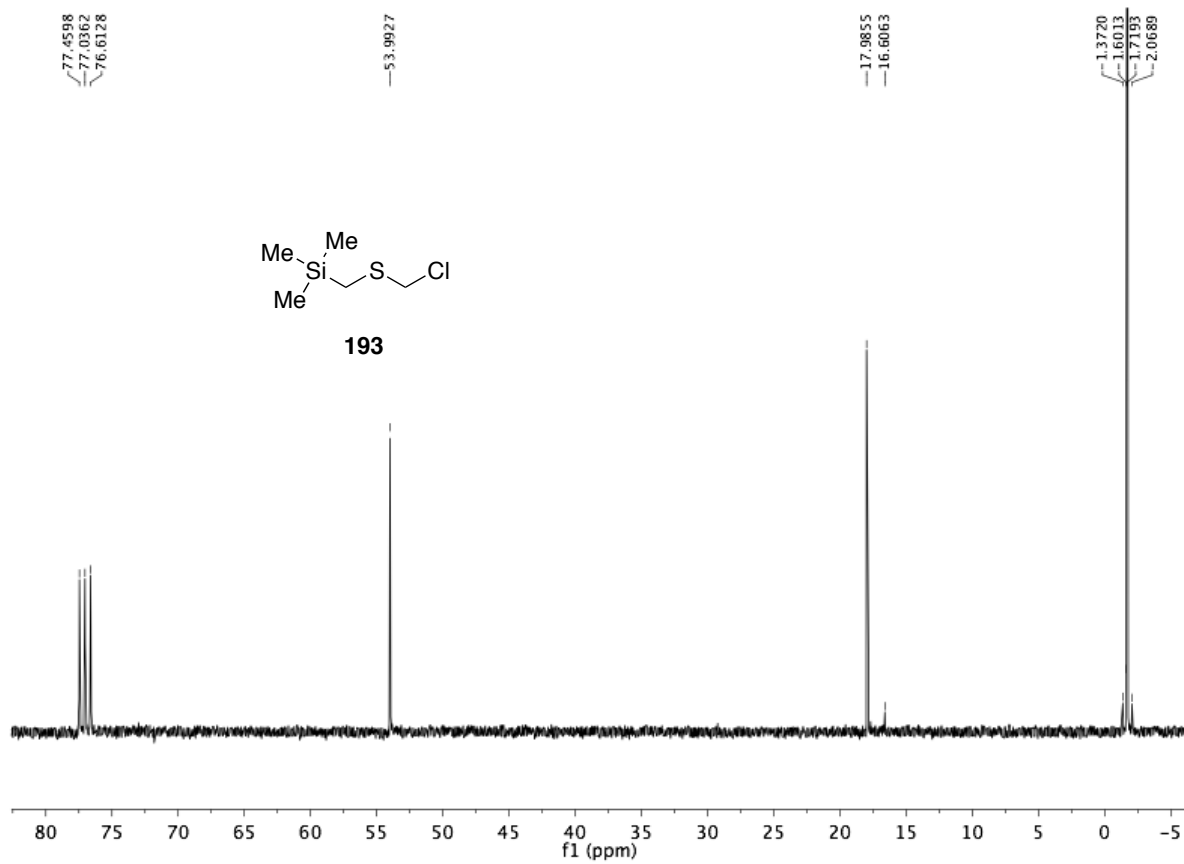
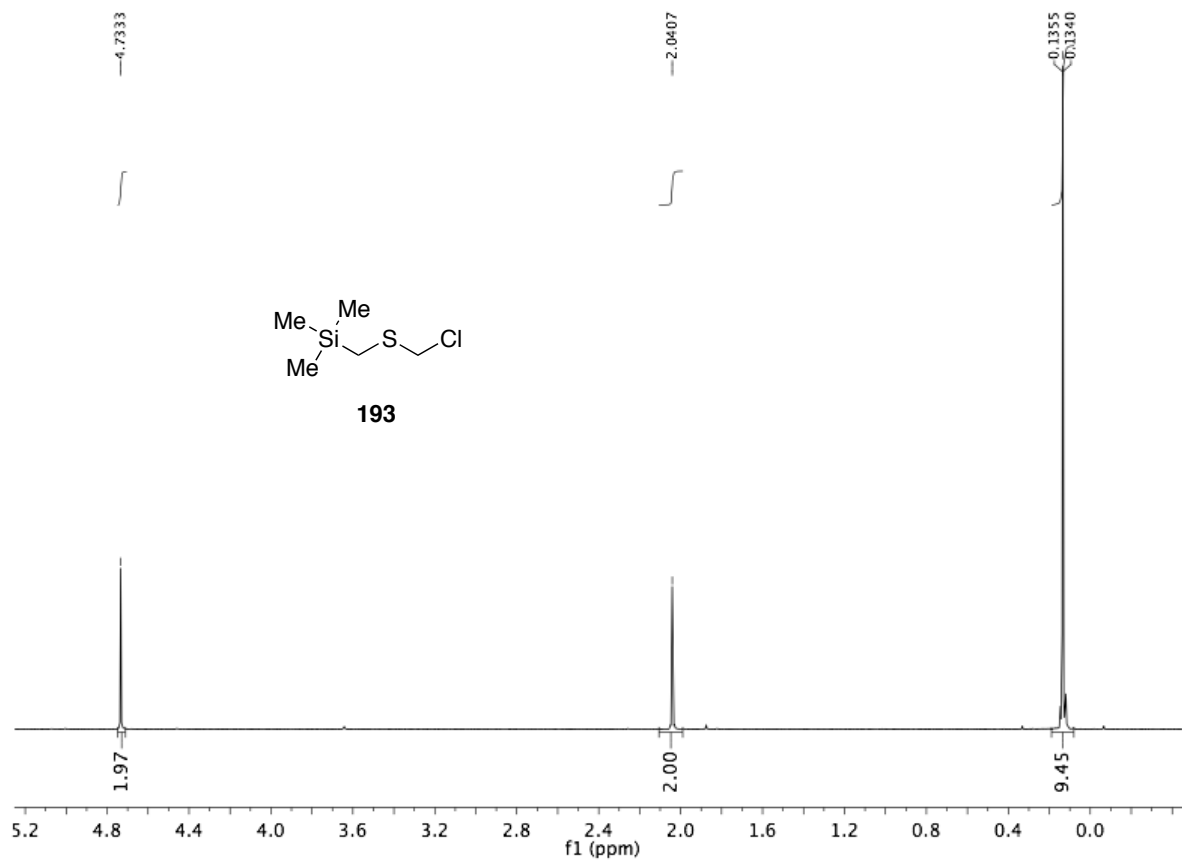


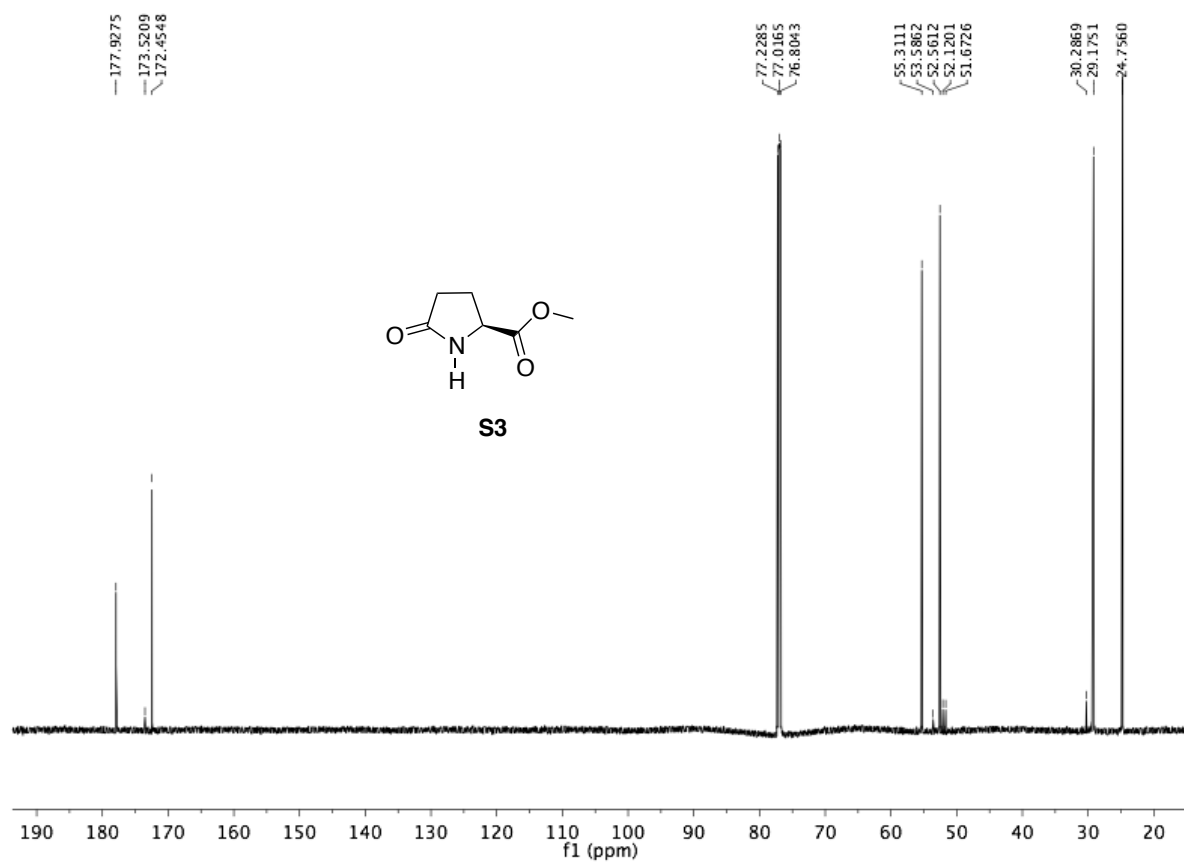
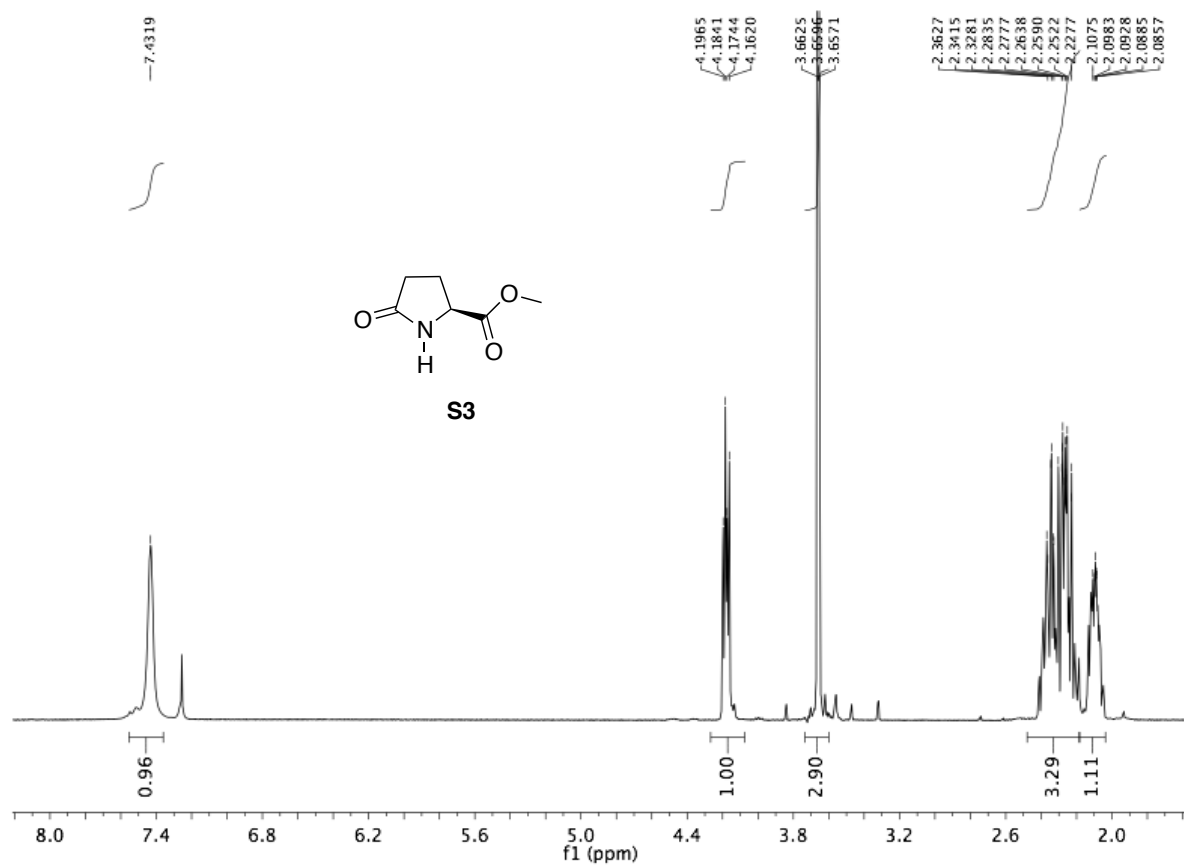


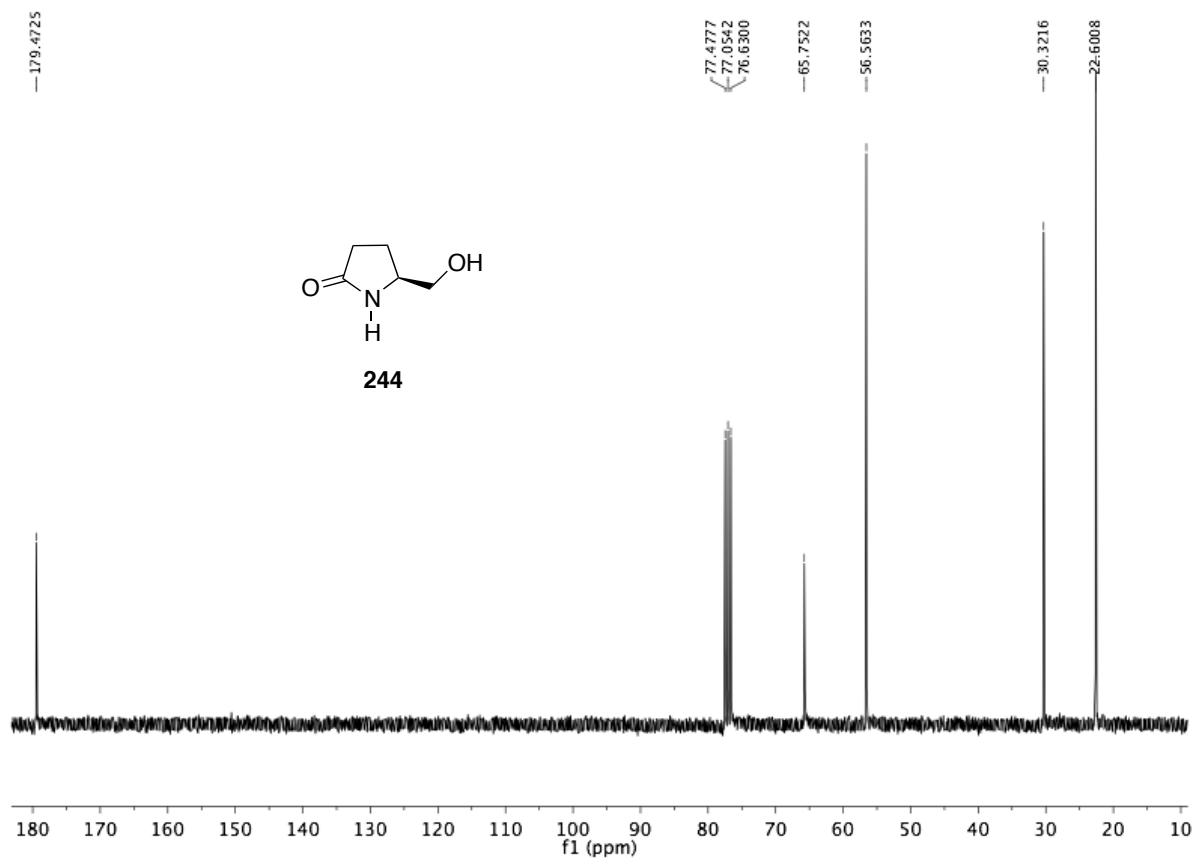
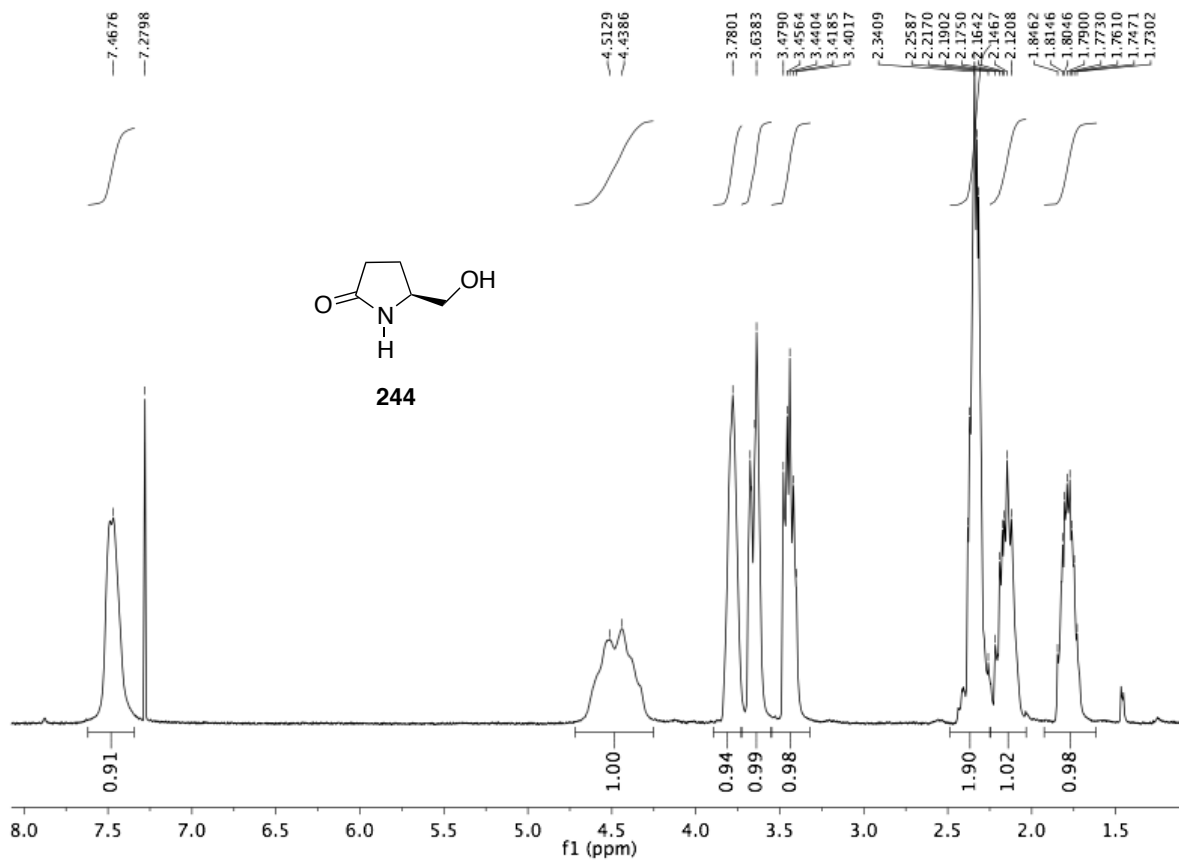


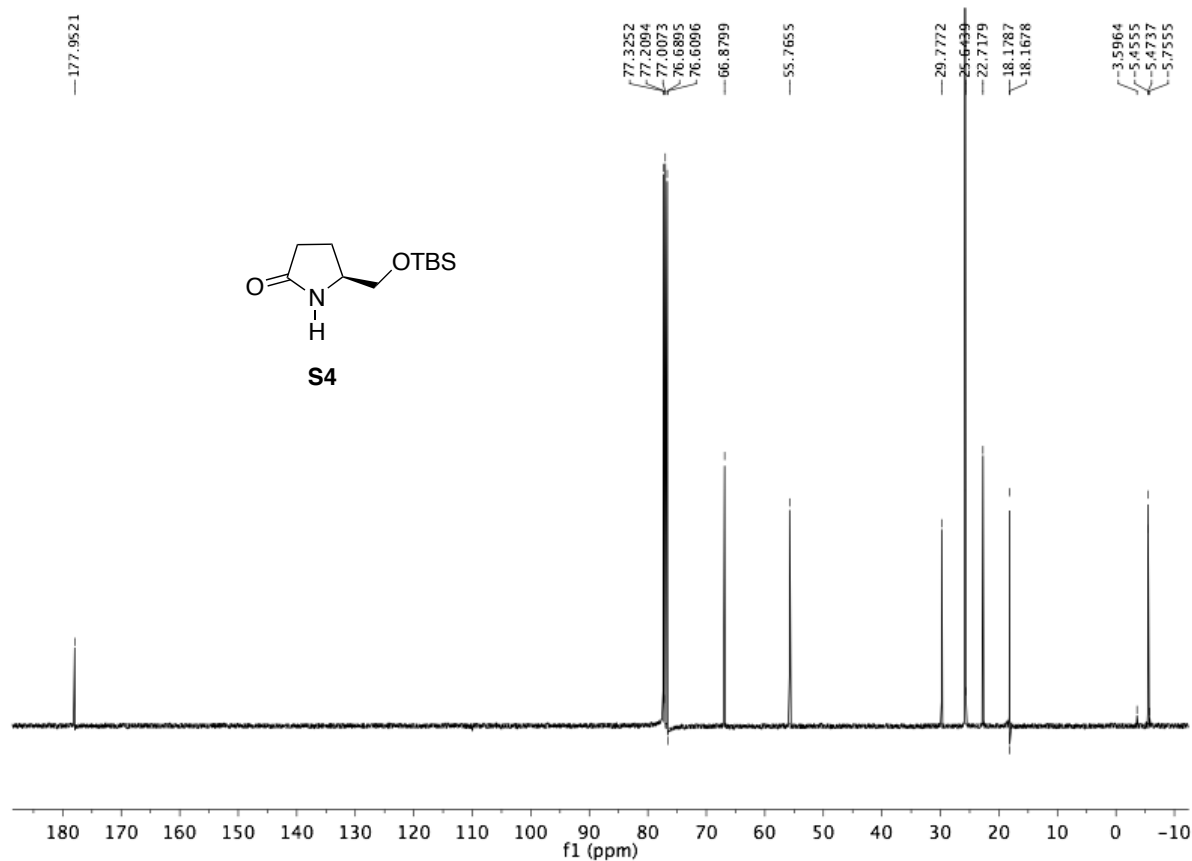
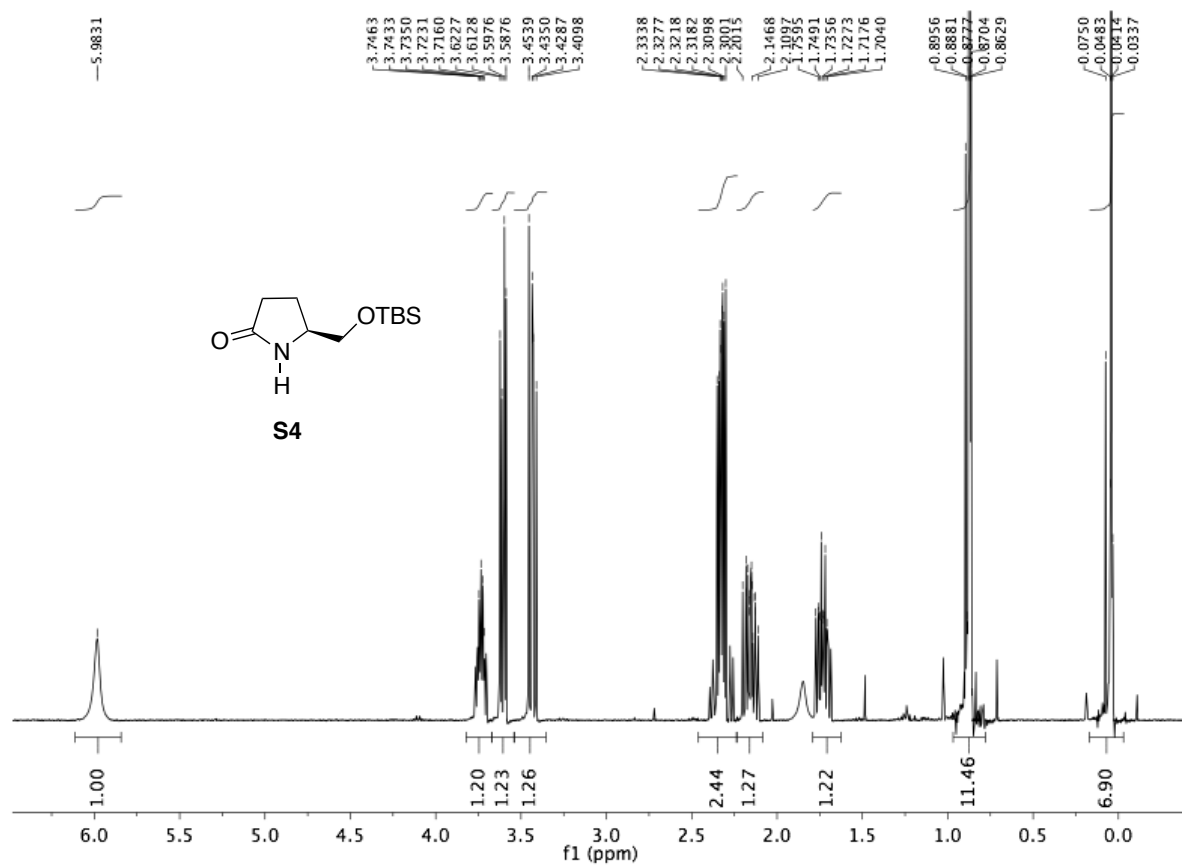


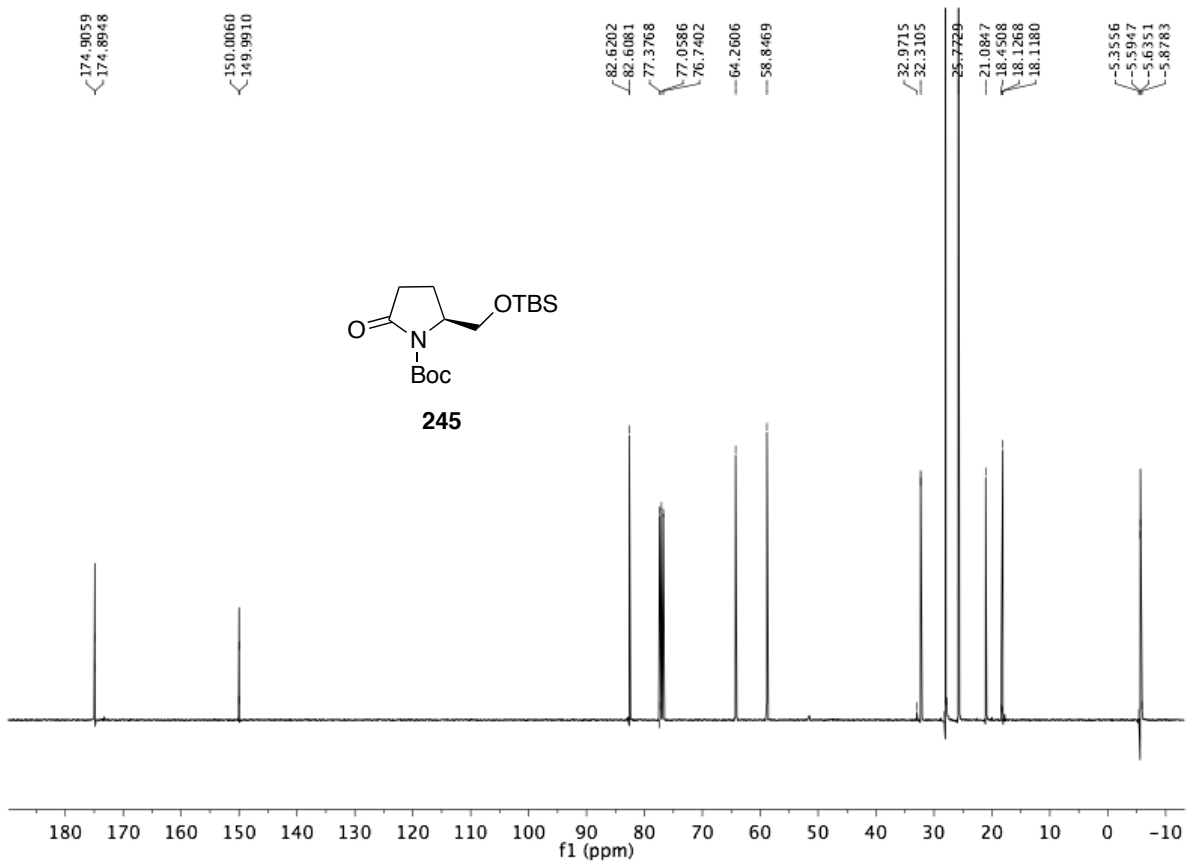
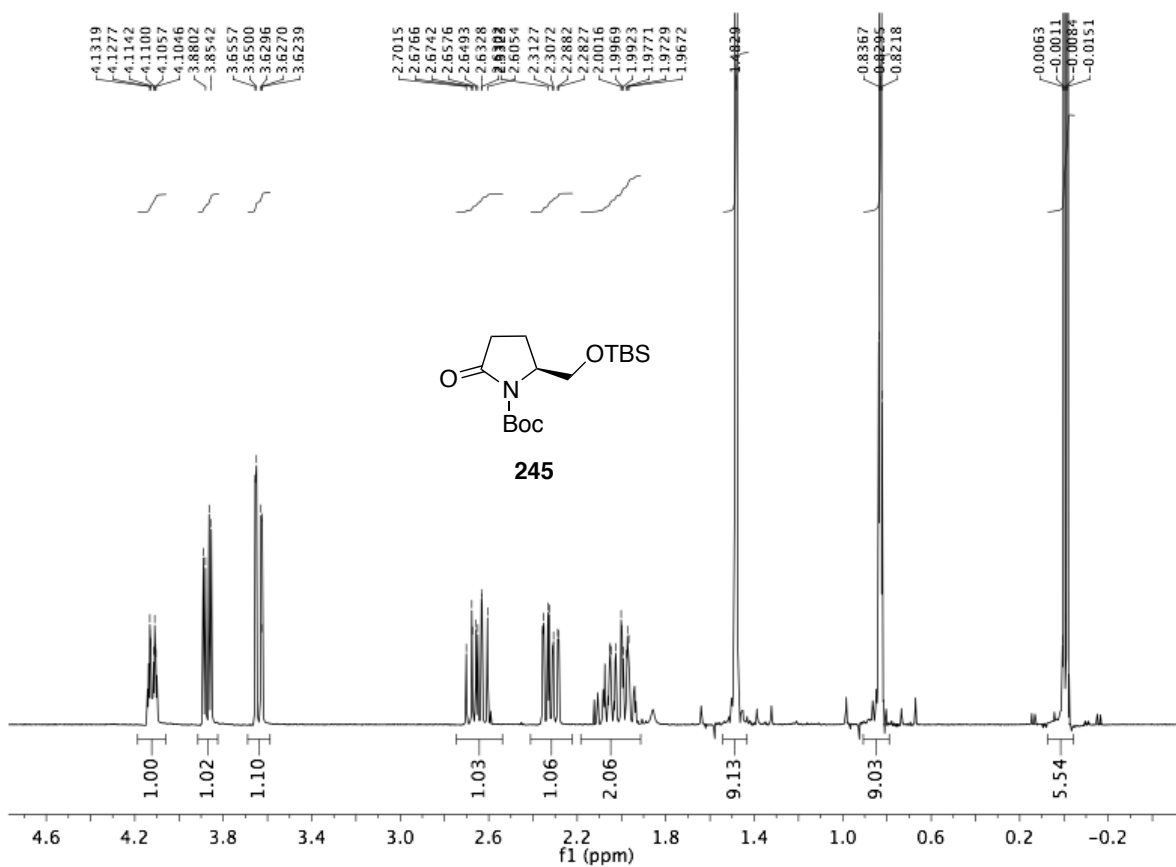




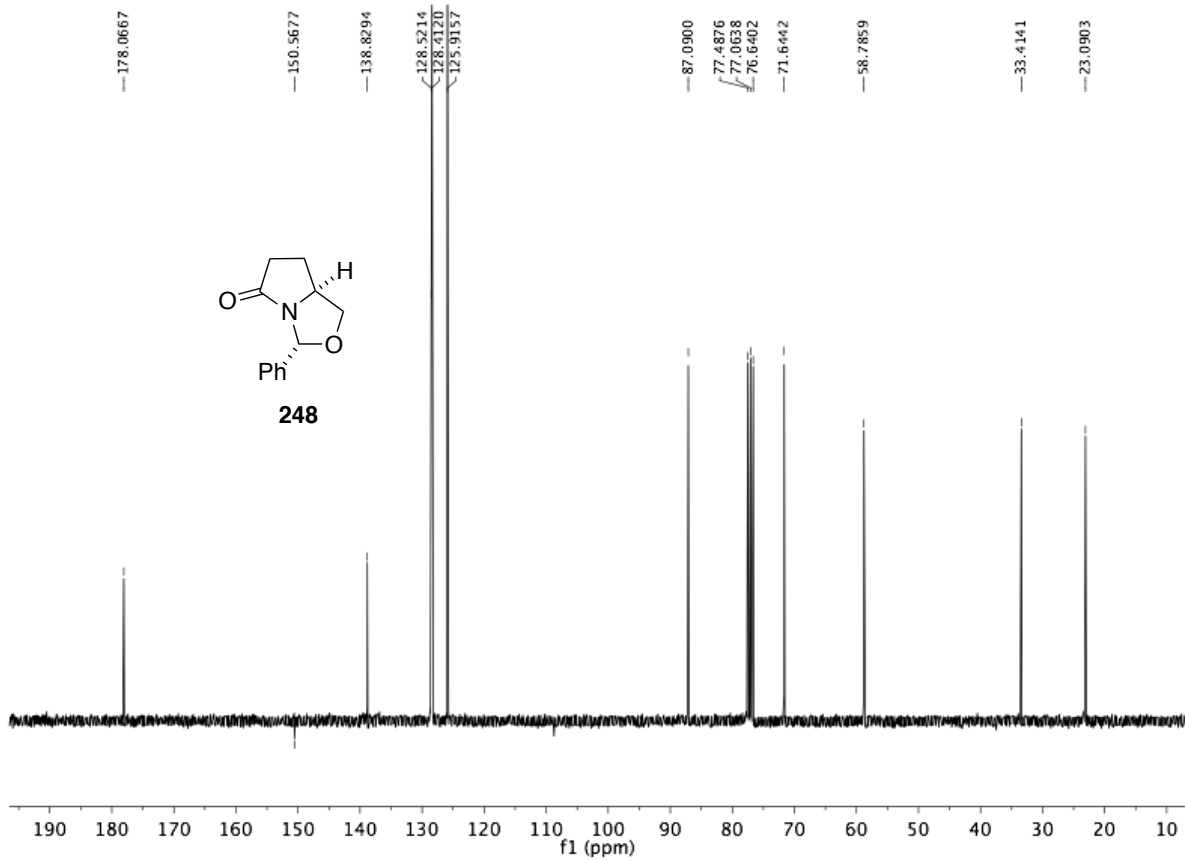
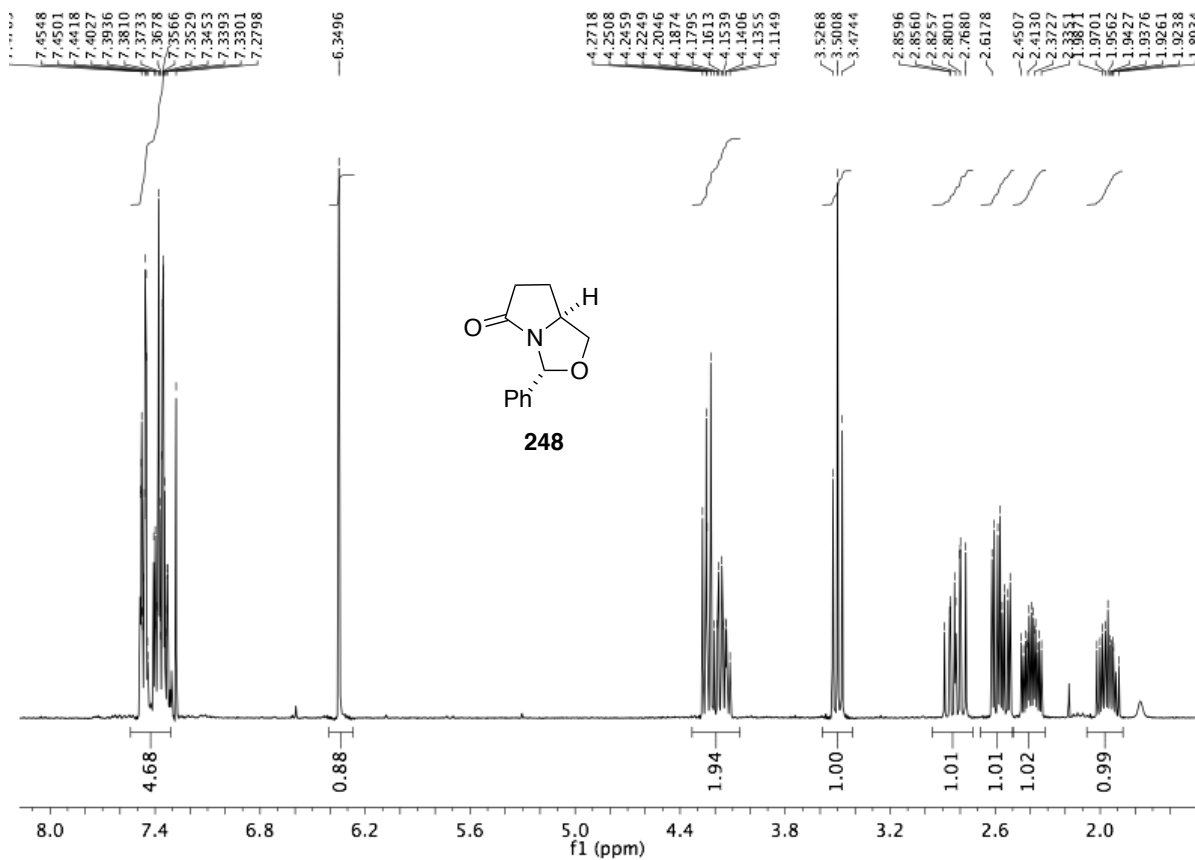


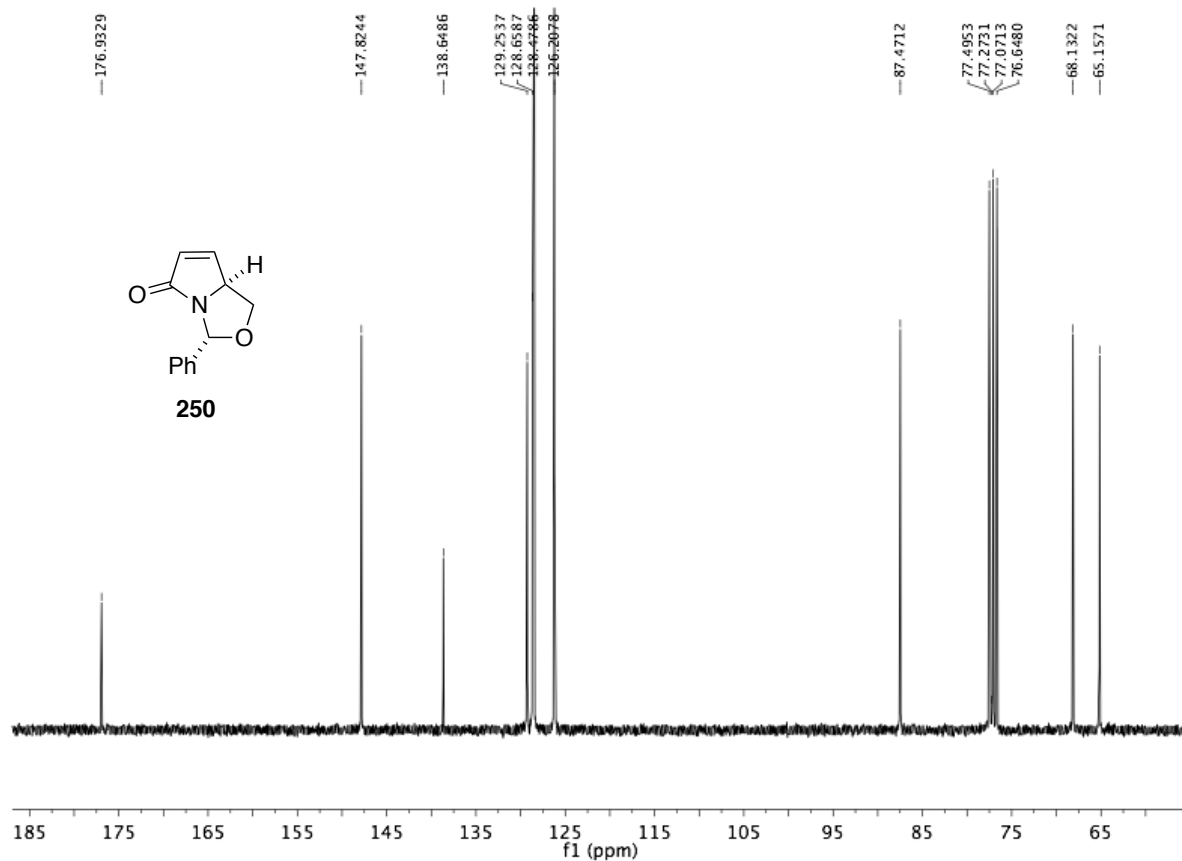
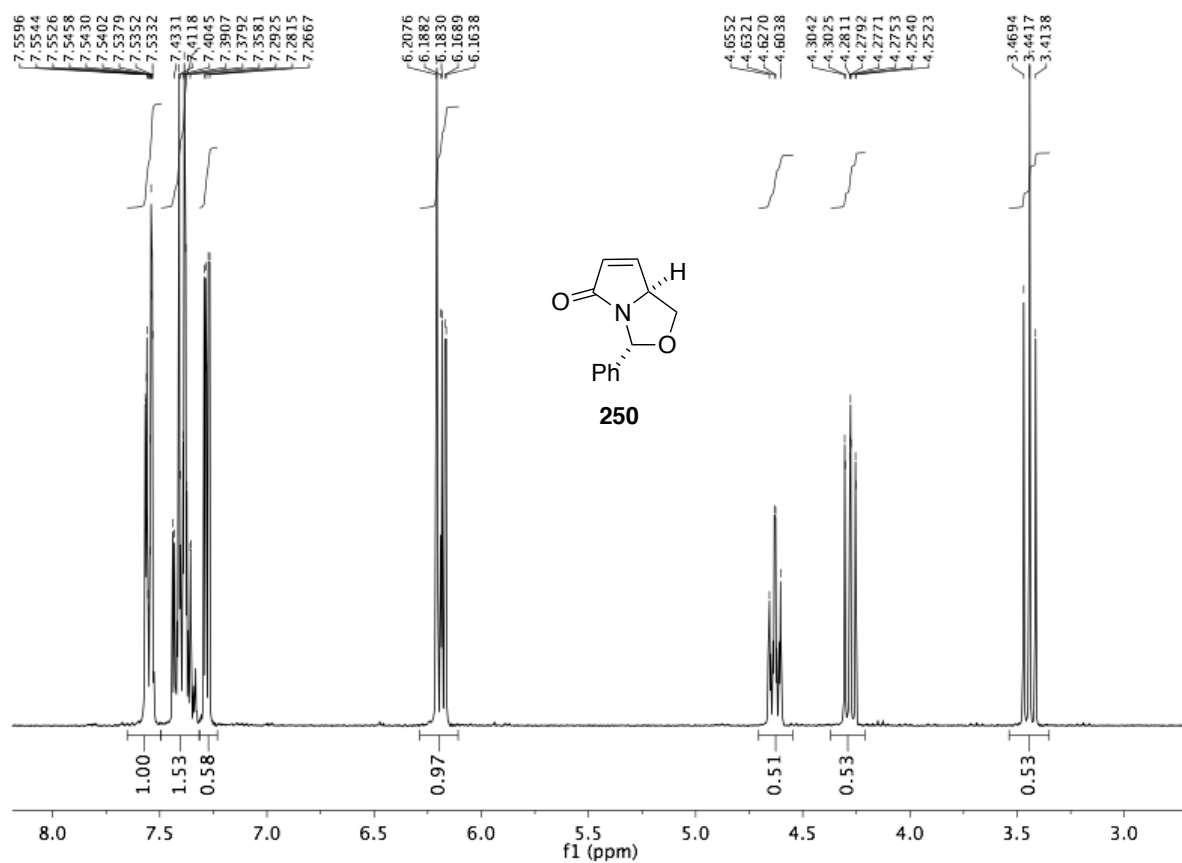


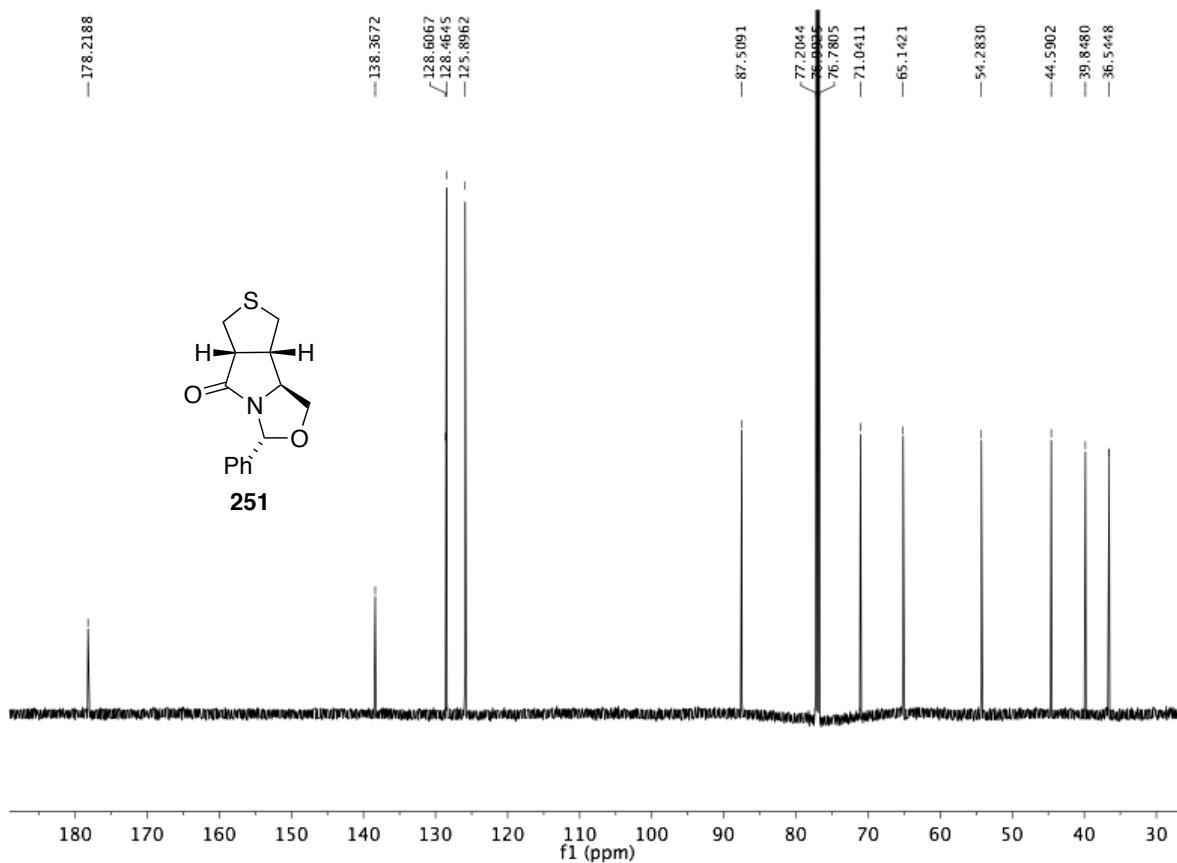
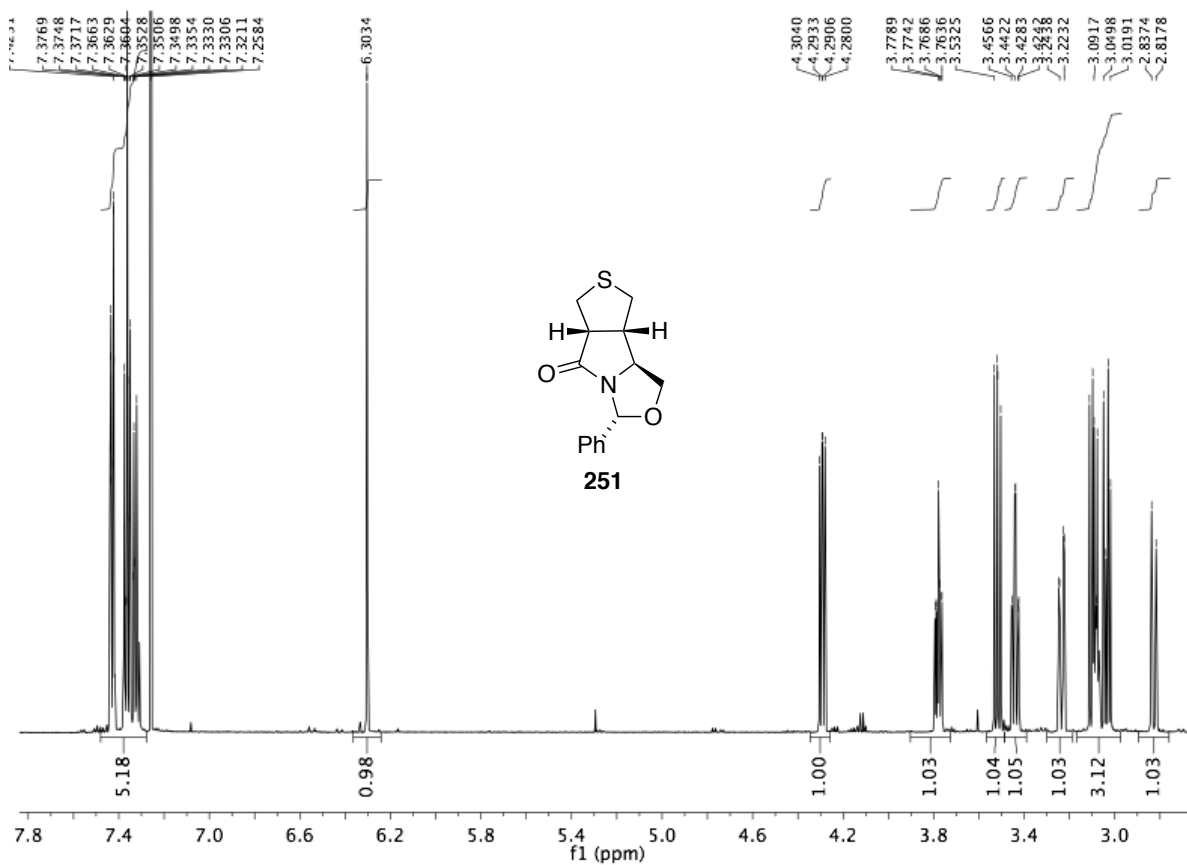


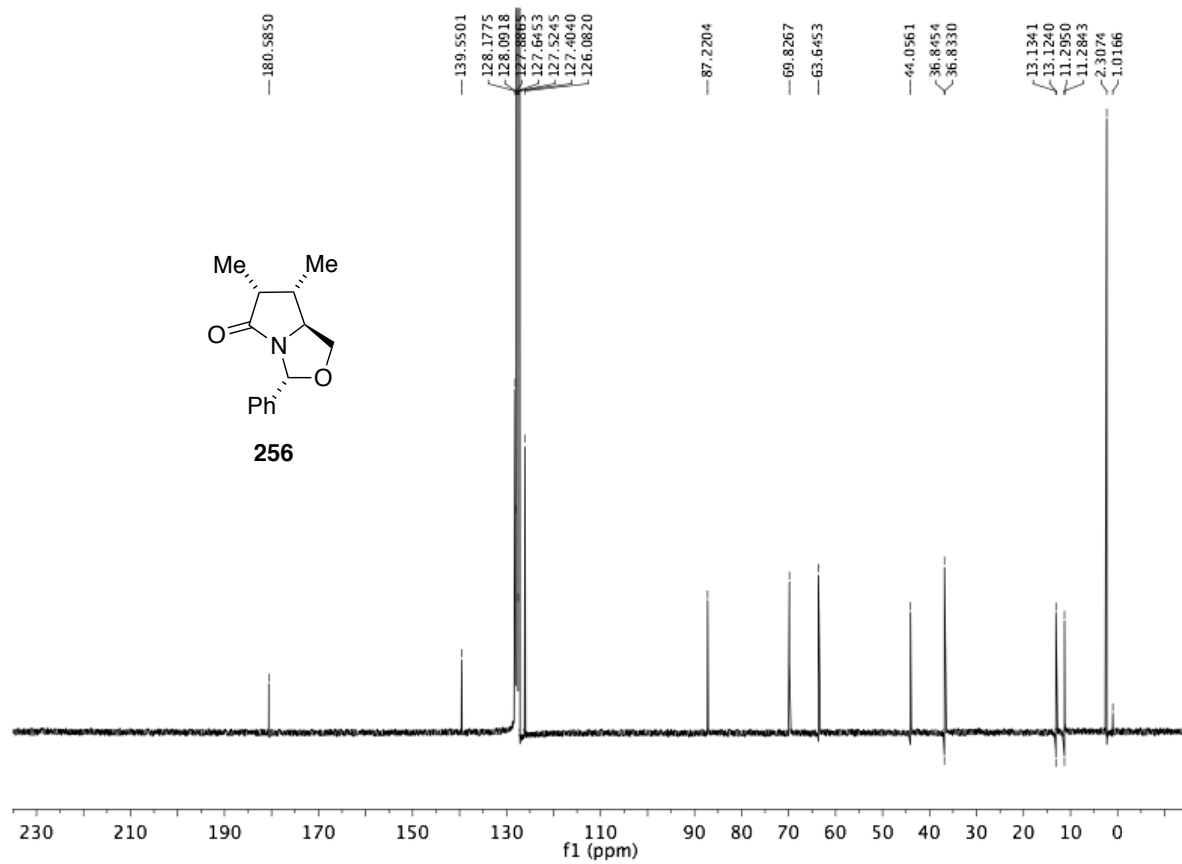
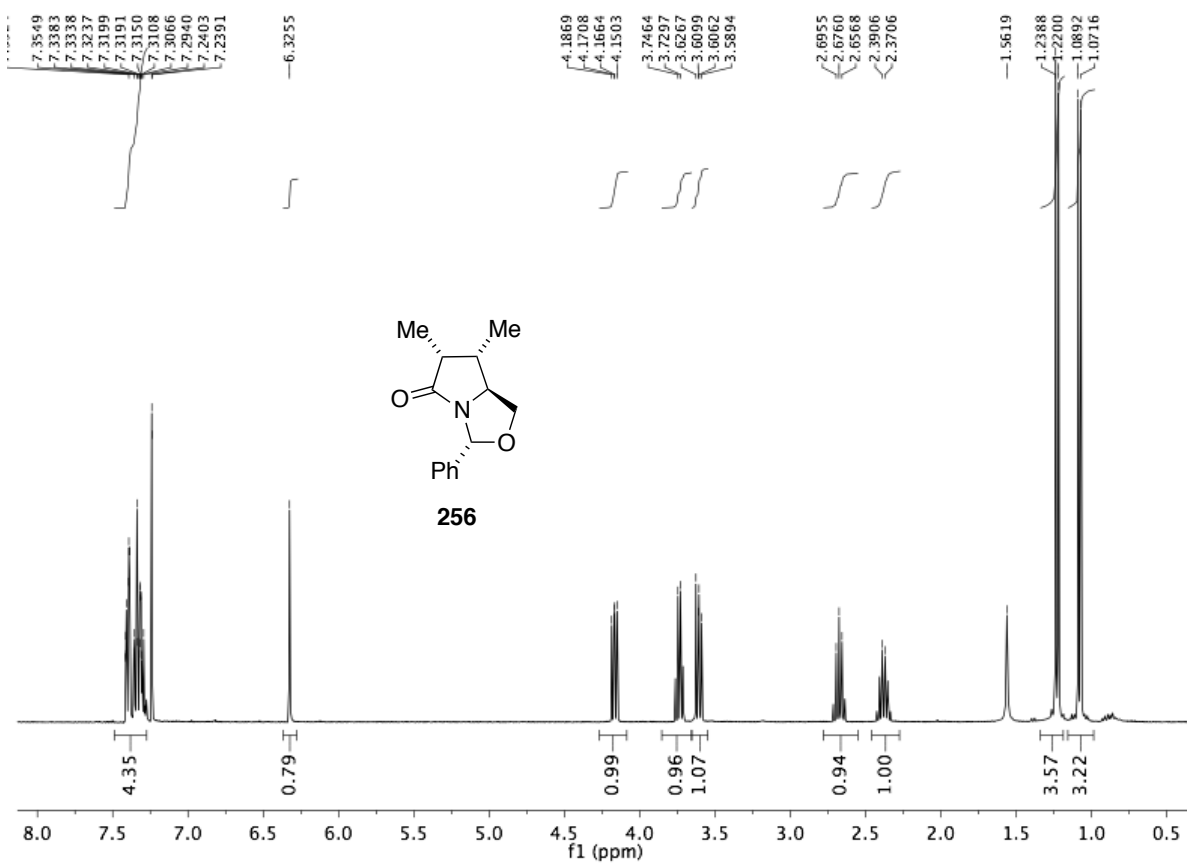


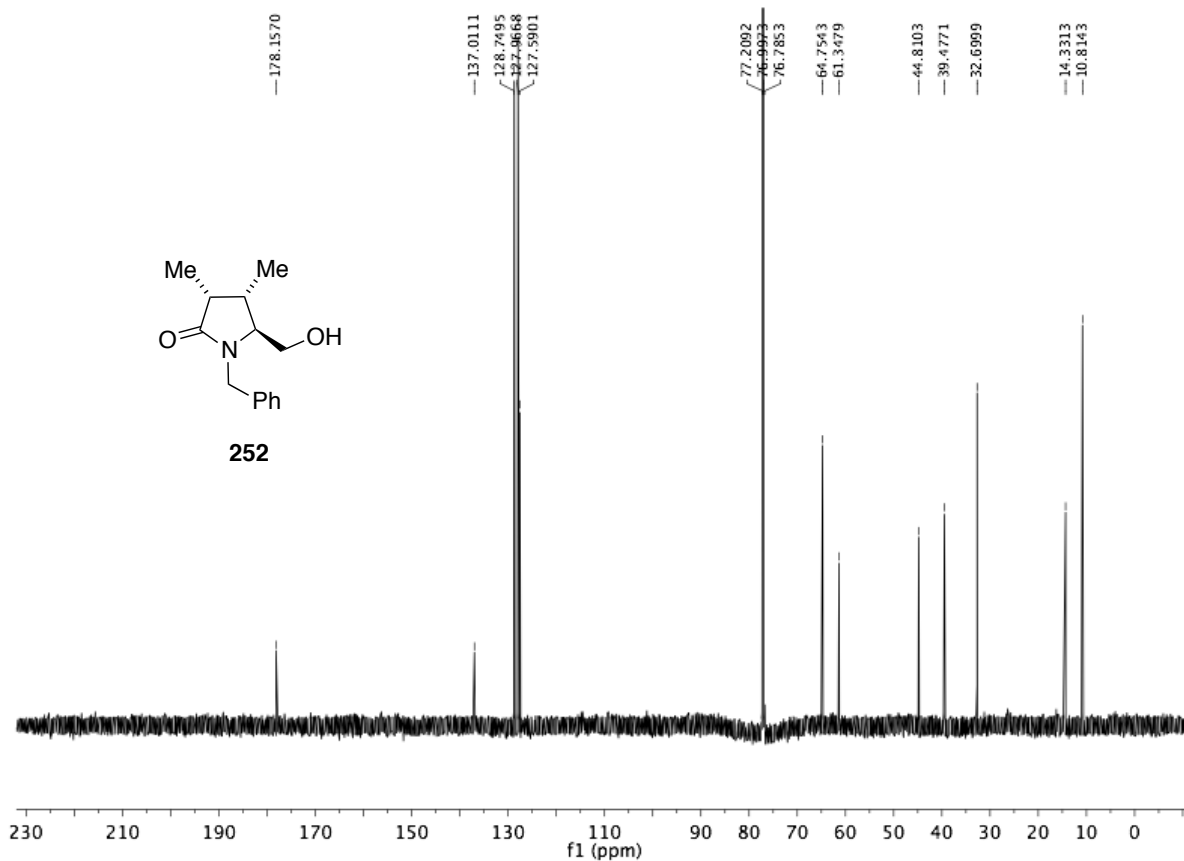
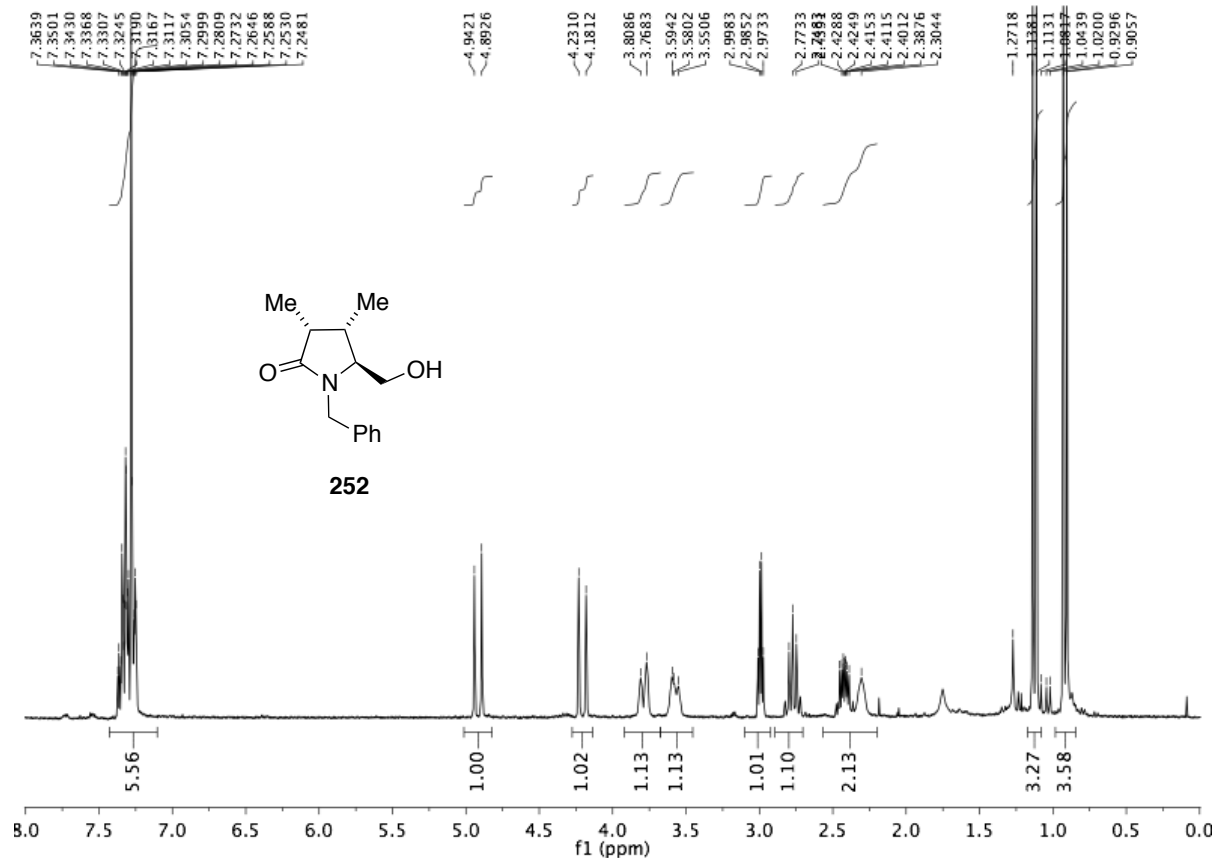


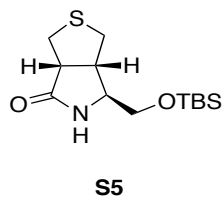
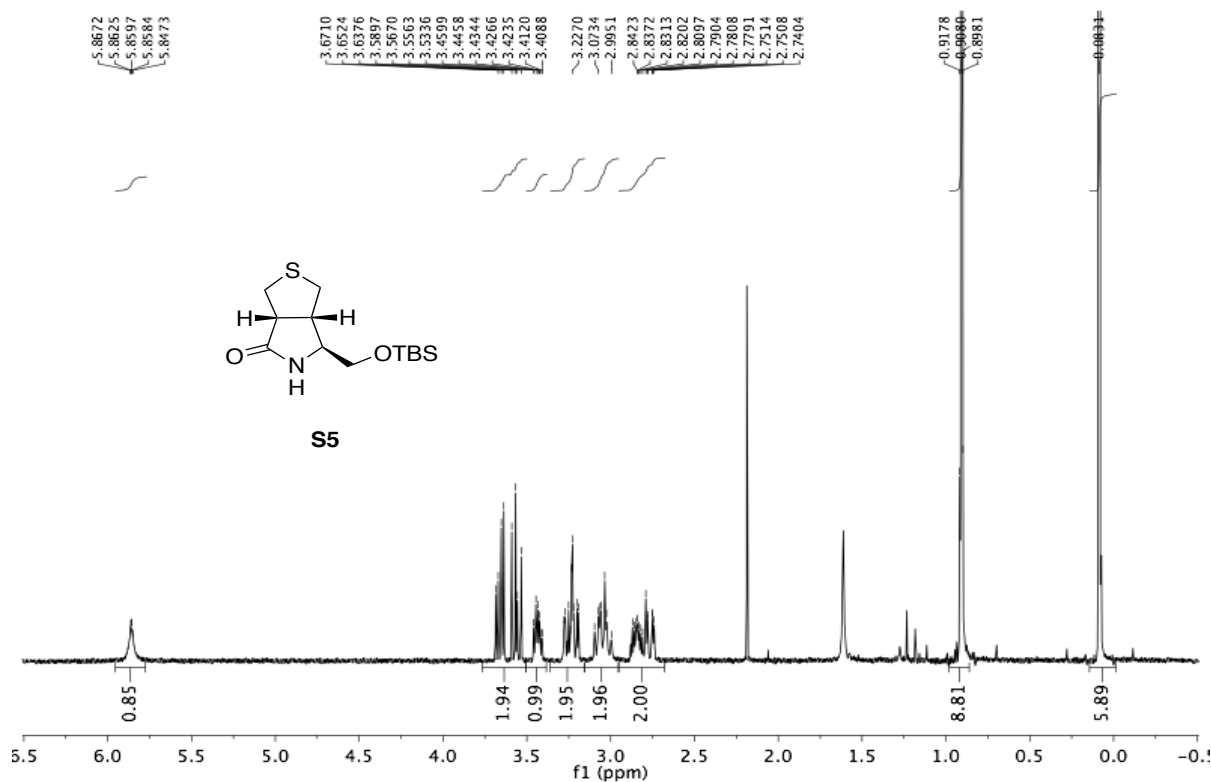












**S5**

